Hydrotreating model catalysts : from characterization to kinetics

Hydrotreating Model Catalysts:
from characterization to kinetics

PROEFSCHRIFT

ter verkrijging van de graad van doctor aan de
Technische Universiteit Eindhoven, op gezag van de
Rector Magnificus, prof.dr. R.A. van Santen, voor een
commissie aangewezen door het College voor Promoties
in het openbaar te verdedigen

op donderdag 11 oktober 2001 om 16.00 uur

door

Leon Coulier

geboren te Deventer

Dit proefschrift is goedgekeurd door de promotoren:

prof.dr. J.W. Niemantsverdriet
en
prof.dr. J.A.R. van Veen

The work described in this thesis has been carried out at the Schuit Institute of Catalysis within the Laboratory of Inorganic Chemistry and Catalysis, Eindhoven University of Technology, Eindhoven, The Netherlands. The Schuit Institute of Catalysis is part of the Netherlands School for Catalysis Research (NIOK).

Printed at the *University Press Facilities*, Eindhoven University of Technology

CIP-DATA LIBRARY TECHNISCHE UNIVERSITEIT EINDHOVEN

Coulier, Leon

Hydrotreating model catalysts: from characterization to kinetics / by Leon Coulier - Eindhoven : Technische Universiteit Eindhoven, 2001.
Proefschrift. –
ISBN 90-386-2992-3
NUGI 813
Trefwoorden: heterogene katalyse / oppervlakte onderzoek ; model katalysatoren / ontzwaveling ; kinetiek / ontzwaveling ; karakterisering / thiofeen / sulfides / XPS
Subject headings: heterogeneous catalysis / surface science ; model catalysts / hydrodesulfurization ; kinetics / hydrodesulfurization ; characterization / thiophene / sulfides / XPS

Contents

1

General Introduction

This chapter is a general introduction on the work described in this thesis. The first section will describe in general terms the principles, history and importance of catalysis. We will then focus on the principles and importance of hydrotreating and hydrotreating catalysts, which will be followed by a section on model catalysts. A short overview on the development of model catalysts and the advantages of these model systems will be given. Subsequently we will describe the main tools used in this thesis, i.e. X-ray Photoelectron Spectroscopy (XPS) and thiophene hydrodesulfurization (HDS). We summarize the current understanding of the topics and formulate our objectives. Finally, this chapter closes with an outline of this thesis.

1.1 Catalysis

A catalyst accelerates a chemical reaction. It does so by forming bonds with the reacting molecules (i.e. adsorption), such that they can react to a particular product, which detaches itself from the catalyst (i.e. desorption), and leaves the catalyst unaltered so that it is ready to interact with the next set of molecules. In fact, we can describe the catalytic reaction as a cyclic event in which the catalyst participates and is recovered in its original form at the end of the cycle. A catalyst cannot alter the chemical equilibrium of a given reaction; it only creates a favorable reaction pathway. This is done by decreasing the activation barrier ($E_{a,cat}$) compared to the gas phase reaction ($E_{a,gas}$) and thus increasing the reaction rate (see Figure 1.1). Consequently, the reaction can take place at lower temperatures and pressures, which decreases costs and amounts of energy for e.g. a chemical plant. Furthermore, if for a certain reaction different paths are possible that lead to various products, the catalyst can selectively decrease the activation energy of one of the possible reaction paths, thereby altering the selectivity of the reaction. In general a successful catalyst increases the yield of the desired product while decreasing that of other products, which has advantages for both economic and environmental reasons. [1]

The first introduction of the word ‘catalysis’ was by Berzelius in 1836, while Ostwald presented the first correct definition of a catalyst in 1895. He described a catalyst as a substance that changes the rate of a chemical reaction without itself appearing in the products. Since then catalysis has gained an increasing importance and has been closely related to our daily lives. Almost 80% of all chemicals produced in the chemical industry have been in contact with one or more catalysts. While only a very small portion of the world production is spent on catalysts, almost 25% of the world production is achieved with the aid of catalysts. Besides enabling well-known products as e.g. plastics, fuels, food or clothes, catalysis has become indispensable in environmental pollution control. The three-way

catalyst, which reduces pollution from car engines, is a well-known example of this. Another good example is hydrotreating of crude oils to circumvent the emission of SO_2 and NO_x, which contribute to acid rain. Hydrotreating catalysts will be the subject of this thesis.

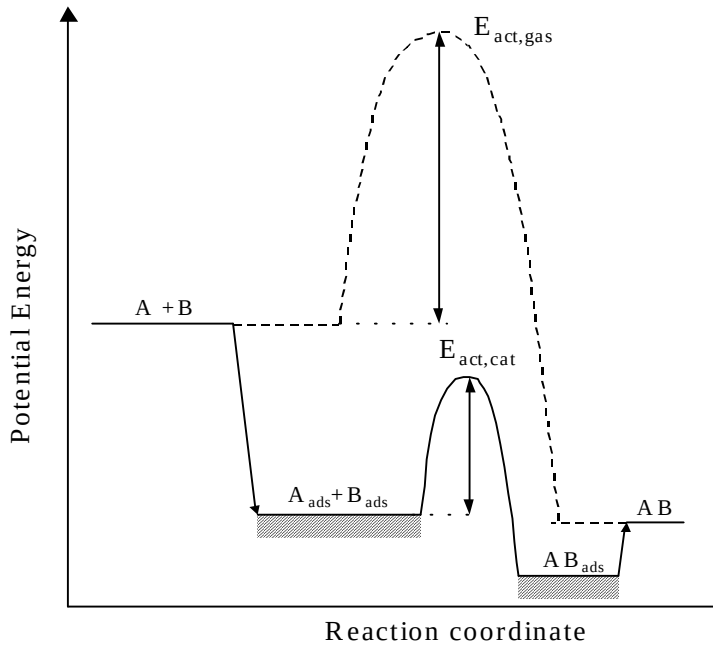

Figure 1.1 *Potential energy diagram for a heterogeneous catalytic reaction (solid line), i.e. reaction of A and B to form AB, compared with the non-catalytic gas-phase reaction (dashed line). The presence of a catalyst lowers the activation energy (E_{act}) considerably.*

One can divide the catalyst market into three main groups: i.e. petroleum refining (e.g. hydrotreating), environmental cleanup (e.g. automotive catalysts) and chemical production (e.g. polymerization, synthesis gas, oxidation etc.). Mainly due to the high activity and high costs (i.e. precious metals) of the automotive catalysts, the environmental cleanup catalysts dominate in terms of sales value, while in terms of physical volume the refinery catalysts dominate (see Figure 1.2A) [2].

1.2 Hydrotreating

One of the most important and large-scale chemical processes is oil refining. In an oil refinery, crude oil is converted into well-known products such as LPG, gasoline, kerosene and diesel oil. Figure 1.3 shows a schematic representation of a refinery [3]. The first step in oil refining is the separation of crude oil in different boiling fractions by atmospheric distillation. The resulting streams are further treated and purified by a variety of catalytic processes to meet the legal and environmental specifications for the various products. As can be seen in Figure 1.3, almost all product streams have to undergo hydrotreating. In hydrotreating, hetero-atoms, like S, N, O and metals, are removed from molecules and aromatic molecules are hydrogenated using hydrogen as a reactant. These processes use catalysts based on transition metal sulfides. Due to the large scale of these processes,

hydrotreating is one of the most important catalytic processes. To give an idea of its importance; hydrotreating catalysts represent 10% of the annual sales of the total market of catalysts. For example, the petroleum refining catalyst sales was $ 2.16 billion in 1998 [4]. Although fluid catalytic cracking catalysts contribute the largest part in sales value, hydrotreating catalysts hold the second place with a share of 35% (see Figure 1.2B). For the future, a growth of 1.9 % per year is expected between 1998 and 2003 for hydrotreating catalysts, showing the increasing demand and thus the importance of this field of catalysis [5].

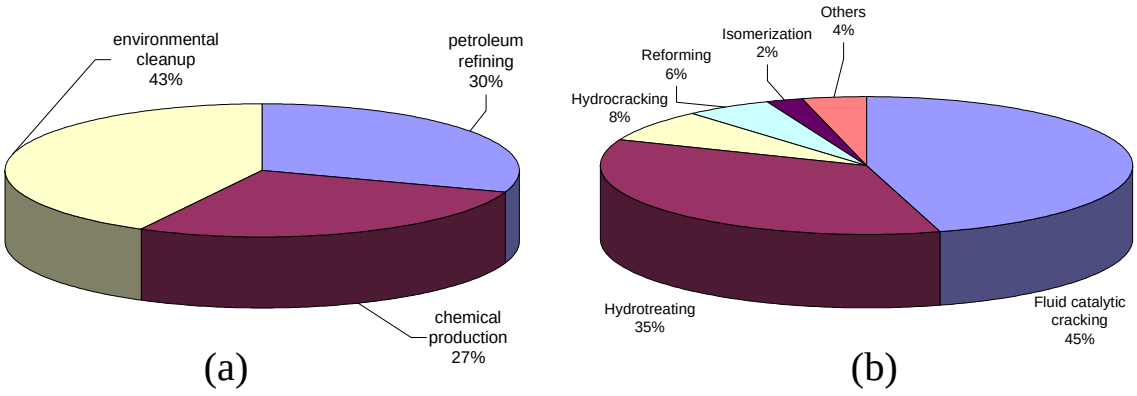

Figure 1.2 *a) Market share of main catalysts technology divisions in percentage in terms of sales value (USA, 1992), showing the importance of catalysts for petroleum refining. b) Percentage of world market share of petroleum refining catalyst (1998), showing the importance of hydrotreating catalysts.*

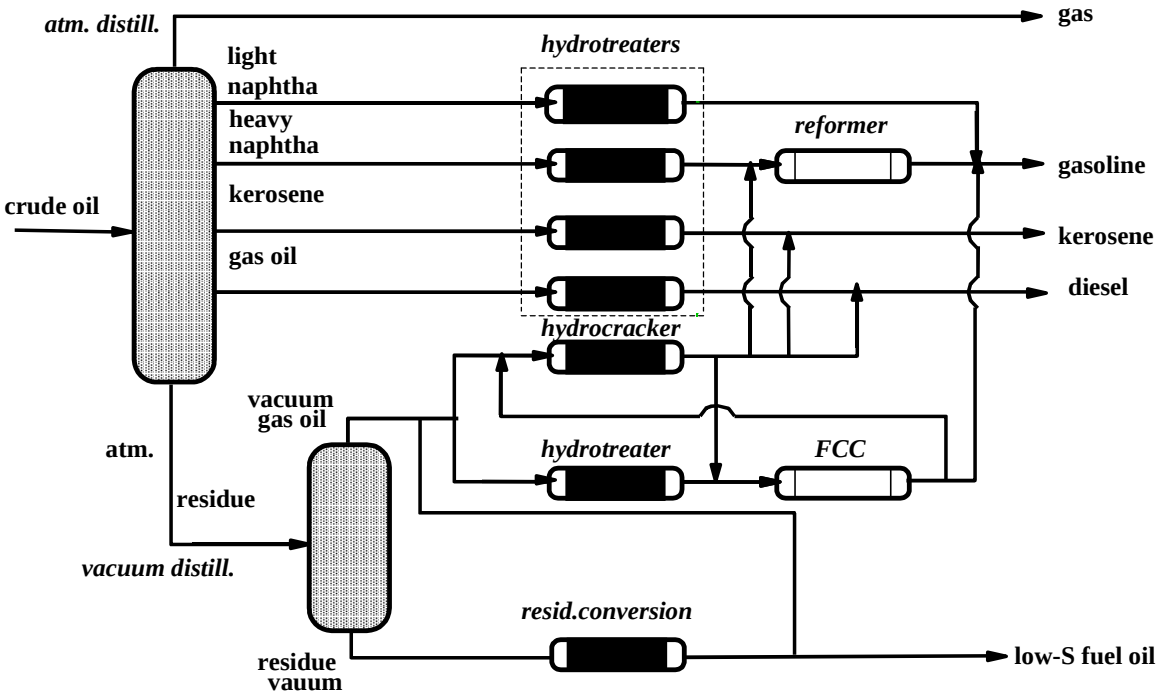

Figure 1.3 *Schematic representation of an oil refinery (adapted from [3]).*

Although hydrotreating processes are in use since 1930, improvement is still necessary due to economic and environmental reasons. Figure 1.4 shows that the continuous research in this field lead to an increase in HDS activity of commercial catalysts [6]. This catalyst improvement accelerated in the last few years, mainly driven by the stringent environmental legislation. Undoubtedly, scientific research has contributed to this improvement in catalyst performance. The environmental legislation for product specification is mainly focussing on reducing the amounts of sulfur oxide, nitrogen oxides, aromatics, vapor and soot particulate emissions. Especially the reduction of sulfur oxide and nitrogen oxides, molecules that cause acid rain, has gained global attention. Due to the enormous progress in reducing sulfur in fuels in the last decade, the problem of acid rain has almost been solved. However, it is known that sulfur declines the effectiveness of vehicle catalytic converters thereby increasing e.g. NO_x and hydrocarbon emissions. Table 1.1 shows the current and future standards for the amount of sulfur in transportation fuels as reported by the International Fuel Quality Center (IFQC). As can be seen, the sulfur level in both gasoline and diesel has to be decreased by a factor of 10 by 2005. However, it is very likely that the future will only bring more stringent environmental demands. For example, from January 2003 diesel and gasoline in Germany may only contain up to 10 ppm of sulfur. Most attention will thus be paid in the future to remove the minor amounts of remaining sulfur, so-called deep-HDS [3]. Besides the environmental legislation, economic reasons also induce increasing importance of hydrotreating. The main reason is the increasing demand for transportation fuel and decreasing demands for fuel oil [5]. To meet this change in demands, heavy fractions are cracked into lighter ones. However, catalysts used for this ‘cracking’ are poisoned by sulfur [7]. Therefore, highly active pre-FCC hydrotreating catalysts are also gaining importance. As shown already in Figure 1.4 hydrotreating catalysts are becoming increasingly active. Many oil industries are already capable to meet the required sulfur levels for 2005. However, it is expected that the sulfur levels will have to decrease even further in the future (<10 ppm) and therefore even more active catalysts are necessary to achieve this.

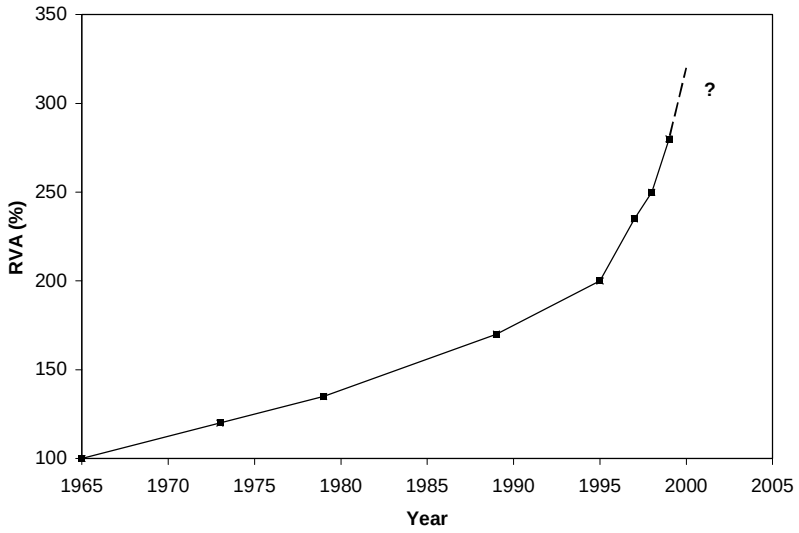

Figure 1.4 *Relative volume activity of Shell standard CoMo catalyst for HDS (1965 = 100) [6].*

Table 1.1. *Current and future standards for amounts of sulfur in transportation fuels in the European Union.*

Sulfur (ppm)	2000	2005	2010
Gasoline	150	50	10 ?
Diesel	350	50	10 ?

To show the complexity of oil refining, Table 1.2 shows the properties of crude oils in different places in the world [7]. Clearly the amounts of contamination vary widely, hence each crude oil has its own requirements for optimal catalyst performance. Despite the concerns about finite oil reserves and therefore the need for alternative energy sources, recent numbers indicate an increase in world oil supply for at least the first half of this century [8]. However, declining crude quality, proposed gasoline sulfur limits and a move to new, higher-value products result in an increasing demand for high performance hydrotreating catalysts [5]. For example, it is foreseen that the average sulfur content in crude oil will increase with 0.2% in the next decade [9]. This will put even higher demands on the performance of hydrotreating catalysts in the future and thus shows that also catalyst research will be highly necessary in the future. Catalysis is of course not the only way to improve the process efficiency, improving process conditions and reactor configurations are also tools to meet the requirements. Moreover, alternative technologies like adsorption or ultrasonic oxidation are also possibilities for process efficiency.

Table 1.2. *Typical composition of various crude oils [7].*

	Arabian light	Arabian heavy	Attaka	Boscan
Sulfur (wt%)	1.8	2.9	0.07	5.2
Nitrogen (wt%)	0.1	0.2	<0.1	0.7
Oxygen (wt%)	<0.1	<0.1	<0.1	<0.1
V (ppm)	18	50	<1	1200
Ni (ppm)	4	16	<1	150

1.3 Hydrotreating catalysts

The type of catalysts used for hydrotreating processes is mainly dependent on the specific reaction and process requirements. In general, catalysts for hydrotreating reactions consist of mixed sulfides of CoMo, NiMo, or NiW supported on high surface area carriers, like γ-alumina [7]. CoMo sulfide catalysts are preferred for hydrodesulfurization (HDS) reactions, while NiMo sulfide catalysts are excellent in hydrodenitrogenation (HDN) and hydrogenation (HYD) [7]. NiW sulfide catalysts are very promising for hydrocracking, aromatics hydrogenation at low H_2S concentrations and conversion of alkylated dibenzothiophenes, although the high costs of these catalysts makes industrial applications less attractive [10]. Noble metal catalysts, like e.g. Pd or Pt, have gained increasing attention due to their high hydrogenation activity [10]. However, these catalysts are sensitive towards poisoning by sulfur compounds. Interestingly, CoW sulfide catalysts seem somehow not to be a good combination for application in industrial hydrotreating processes. In general, the

specifications of the feed and the desired products will determine which catalyst (or combination of catalysts) will be used. As already mentioned hydrotreating catalysts are among the most applied catalysts in industry and hence research effort on these catalysts is tremendous. A number of excellent reviews summarize most of the literature on hydrotreating catalysts [7,11,12].

Despite the enormous amount of research, the structure of the active phase has been a matter of great debate. Although the presence of MoS_2- and WS_2-slabs has been generally accepted, the function and location of Co or Ni was the main subject of debate. In the past, various models were proposed for the role of the promoter; viz. the intercalation model of Voorhoeve [13], the pseudo-intercalation or decoration model of Farragher and Cossee [14] and the remote control or contact synergy model of Delmon [15]. However, at this time (almost) everyone supports the so-called 'CoMoS' model, in which Co atoms decorate the edges of MoS_2-slabs (see Figure 1.5). This model was first proposed by Ratnasamy and Sivanskar [16], but Topsøe and Topsøe [17] found the first experimental evidence for this on the basis of IR studies of adsorbed NO.

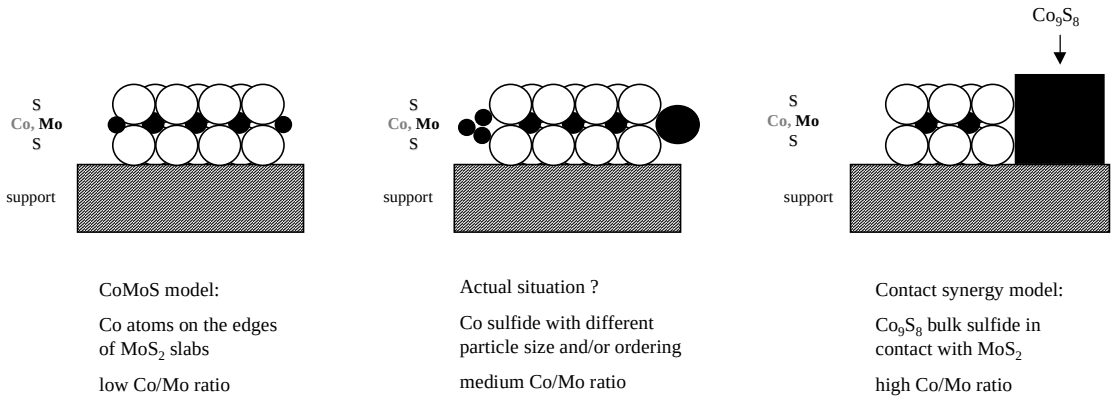

Figure 1.5 *Relation between different proposed models for the active phase in CoMo catalysts.*

Promoter atoms at the edges of MoS_2 crystals were directly observed with Analytical Electron Microscopy [18]. Recent STM work by Besenbacher and coworkers [19] showed atomic-scale images of the CoMoS structure. Evidence of CoMoS-like phases for Ni-promoted Mo- or W-based catalysts, i.e. NiMoS and NiWS, was found by Topsøe et al. [20] and Louwers and Prins [21], respectively. From combination of Mössbauer Emission Spectroscopy (MES) and HDS activity, Topsøe et al. [22-24] could identify a specific Co-signal to the CoMoS phase and showed a linear correlation between the amount of Co in CoMoS and the thiophene HDS activity. However, Crajé et al. [25] showed that the same Co-signal in MES was observed for Co/C and Co/Al_2O_3 and thus concluded that the CoMoS MES signal was not necessarily caused by the presence of a unique CoMoS phase. Van Veen et al. [26,27] confirmed this, by showing that there is no simple relation between amounts of CoMoS according to Mössbauer spectroscopy and HDS activity. Despite all these discussions, there is agreement on the CoMoS phase being the active phase in HDS.

A recent review by Eijsbouts [12] related the various structural models for CoMoS based on the fact that catalysts are dynamic and flexible (see Figure 1.5). At low Co/Mo ratio, Co atoms decorate the edges of MoS_2, while small Co-sulfide particles are present at higher

ratios. In the extreme case of very high Co/Mo ratios, Co_9S_8-like particles decorate the MoS_2-slabs, corresponding structurally to the contact synergy model [12]. For commercial catalysts the Co/Mo ratio lies between the two extreme cases, hence usually a distribution of Co sulfide particles with different particle size and ordering is present on these catalysts. Figure 1.6 shows that the CoMoS phase is not the only species present on commercial $CoMo/Al_2O_3$ catalysts [7]. The figure shows that besides the active phase, i.e. the CoMoS phase, bulk Co sulfide, unpromoted MoS_2 and $Co:Al_2O_3$ interacting species are likely to be present, indicating that characterizing these catalysts is not straightforward.

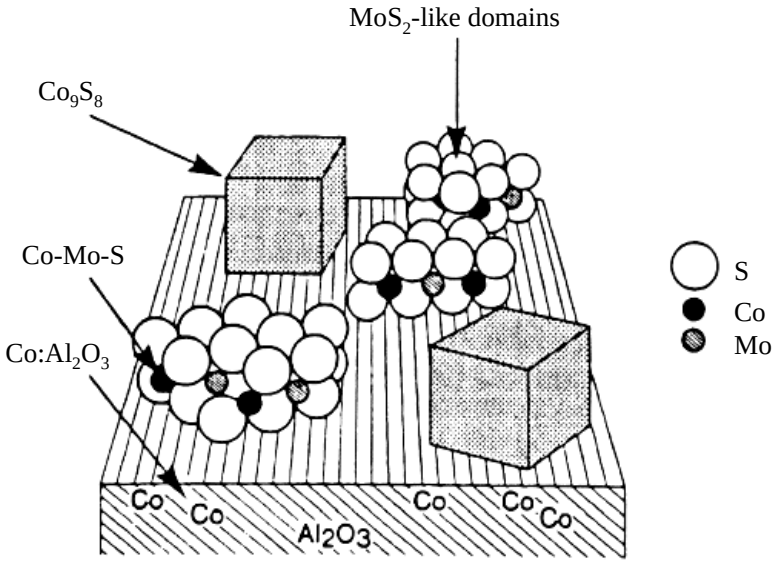

Figure 1.6 *Schematic picture of different phases present in a sulfided alumina-supported CoMo catalyst [7].*

To make things more complex, two different CoMoS structures on $CoMo/Al_2O_3$ were proposed by Candia et al. [28] and van Veen et al. [26,29]. The type I phase, i.e. CoMoS I, is thought to be incompletely sulfided and to consist mainly of MoS_2 monolayers interacting with the support via Mo-O-Al bonds. CoMoS II phases are thought to be fully sulfided and consist often of stacked MoS_2 particles that are only weakly interacting with the support via van der Waals interactions. Bouwens et al. [30] and Van Veen et al. [29] reported that the CoMoS II phase is twice as active than CoMoS I in gas phase thiophene HDS. These authors used a complexing agent, like nitrilo triacetic acid (NTA), to prepared the CoMoS II phase. The use of these complexing agents will be discussed later on. However, the difference in activity between CoMoS I and CoMoS II seems to be dependent on the type of reactant. For dibenzothiophene HDS in trickle flow, CoMoS I was found to be more active than CoMoS II [31].

For unpromoted catalysts the active sites are believed to be located at the MoS_2-edges and consist of coordinately unsaturated Mo sites (CUS), i.e. sulfur anion vacancies. These sites are also believed to be relatively more active in hydrogenation (HYD), than the active sites in promoted catalysts [28]. The rim edge model of Daage and Chianelli [32] states that

for stacked MoS_2 layers, the top and bottom layer, i.e. rim sites, are responsible for both HYD and HDS, whereas the intermediate layers, i.e. edge sites, are only responsible for HDS. The high activity of promoted catalysts may be explained by IR measurements by Topsøe et al. [17]. These results suggest that the metal-sulfur bond strength in CoMoS is lower than that in MoS_2, which could be the reason of the promoting effect of Co [17]. Recent theoretical calculations confirm a weakening of the Mo-S bond by Co enabling the easy creation of surface vacancies [33].

The activity of HDS catalysts is strongly affected by the dispersion and morphology of the active phase [7]. The interaction of the transition metal sulfide with the support has a large influence on the final dispersion and morphology of the active phase. Al_2O_3 is the most commonly applied support because of its strong interaction with Mo, which results in a high dispersion and high stability of the active phase [7]. Other supports, like SiO_2 and TiO_2, have also been studied and reviewed by various authors [7,34,35]. In general, SiO_2 leads to poor dispersion of MoS_2 due to a weak Mo-support interaction and hence it results in a low HDS activity [7]. TiO_2 has a stronger interaction with Mo than Al_2O_3 and has proven to be a promising support for HDS catalysts (see e.g. [36]). Especially, the relatively high activity of Mo/TiO_2 vs. Mo/Al_2O_3 is interesting, and has been attributed to differences in morphology, dispersion or sulfidability [34,35]. Recent reports by Ramirez [37] and Vissenberg [38] propose that Ti-species, sulfided and/or reduced during heat treatment, act as promoter and thus increase the activity. However, this has not been proven yet. Another interesting aspect is the relative small promotion effect for TiO_2-promoted catalysts compared to Al_2O_3 [36]. Literature on (promoted) TiO_2-supported catalysts and comparison with other supports are however not abundant and a good explanation for the observations has not been found yet.

Despite the enormous amount of research in the past decades, many questions still remain. A complicating factor is the large number of variables in preparation, pretreatment and activity measurement conditions. Differences in these conditions can (partially) explain the contradictory results found in literature. As a consequence it is sometimes very difficult to compare results from different studies. For example, a consistent comparison between the four 'possible' systems, i.e. CoMo, NiMo, NiW and CoW, prepared under identical conditions is hard to find. Comparing the characterization and HDS activities of these four systems supported on various supports is even more difficult to find and is therefore one of the subjects of this thesis.

1.4 Use of complexing agents in HDS catalysts

As mentioned earlier, complexing agents (or chelating agents), like nitrilo triacetic acid (NTA), have been used to prepare the so-called CoMoS II phase. An European patent of Shell by Thompson [39] describes the preparation of highly active SiO_2-supported CoMo and NiMo catalysts using a nitrogen-containing organic ligand such as NTA, ethylene diamine tetraacetic acid (EDTA) or diethylene triamine (DT). A paper by Van Veen et al. [26] showed that NTA-containing catalysts show equally high HDS activity for both SiO_2 and Al_2O_3. It was furthermore shown that $CoMoNTA/Al_2O_3$ was twice as active as conventionally impregnated $CoMo/Al_2O_3$, hence it was concluded that CoMoS II was twice as active as CoMoS I [26,30,31]. The same was observed for NiMo catalysts [29]. However, it was shown for dibenzothiophene (DBT) HDS, that Co(Ni)MoS II was less active than

Co(Ni)MoS I [29]. Remarkably, it has also been claimed that for carbon supports, NTA leads to a higher thiophene HDS activity than Al_2O_3 or SiO_2 [26,30].

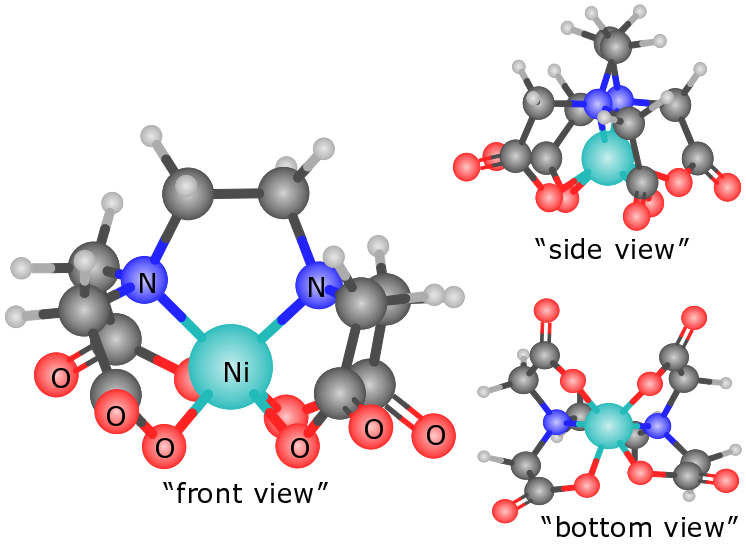

Figure 1.7 *Visual representation of the complexation of a Ni atom by a complexing agent, i.e. ethylene diamine tetraacetic acid (EDTA).*

The work of Medici and Prins [40] focussed on NiMo/SiO_2 catalysts using complexing agents. These authors showed that both Ni and Mo could complex to NTA [40]. Figure 1.7 shows an example of such a complex of Ni with EDTA. They concluded that the MoS_2 dispersion was independent of the presence of NTA and that NTA mainly had a dramatic influence on the sulfidation of Ni. The role of NTA and similar complexing agents is to prevent the sulfidation of Ni at low temperature, and thus increase the formation of the NiMoS phase leading to higher HDS activity [40]. De Jong et al. [41] concluded more precisely that NTA retards the sulfidation of Co to such an extent that the order of sulfidation of Co and Mo changes. As a result the sulfidation of Co is retarded to temperatures where MoS_2 is already formed [41]. Shimizu et al. [42,43] extended the use of complexing agents to other complexing agents, e.g. cyclohexane diamine tetraacetic acid (CyDTA), and other catalysts, e.g. NiW. They concluded that by using complexing agents the (di)benzothiophene HDS activity of CoMo/Al_2O_3 and NiW/Al_2O_3 increases in the order NTA < EDTA < CyDTA [42,43]. It was also found that the complexing agents had little effect on the activity of NiMo/Al_2O_3 [42,43]. The authors concluded that complexing agents interact strongly with Co (or Ni), thereby preventing Co (or Ni) from interacting with Mo (or W) or Al_2O_3 [43]. Furthermore, it was concluded that pre-formation of a MoS_2-like structure was necessary to induce the promoting effect [43]. However, these authors could not explain the small effect of complexing agents on NiMo/Al_2O_3. Table 1.3 shows the complex formation constants in literature for the various complexing agents with the different metal-ions in water [44]. It can be seen that these numbers, which represent the stability of the metal-agents complex, are only slightly higher for Ni than for Co. Hence, one would expect similar effects of these complexing agents on Co- and Ni-promoted catalysts. Reports by Cattaneo et al. [45,46] confirmed this, by showing that EDTA, which retards the sulfidation of Ni to somewhat higher temperatures than NTA, leads to a higher activity than NTA for NiMo/SiO_2 catalysts.

They found also that using ethylene diamine (ED) as complexing agent results in highly active catalysts [45,46]. However, the Ni-ED complexes were found to be highly unstable, which resulted in sulfidation of Ni at very low temperature, which seems in contradiction with all results described above [45,46].

Medici and Prins [40] showed that chelating agents, like NTA, prefer complexation with Ni^{2+} and MoO_4^{2-} does only form complexes when all Ni-ions are complexed to NTA. The same accounts for EDTA. CyDTA does not form complexes with either Mo or W [43].

Table 1.3. *Complex formation constants for Co^{2+} and Ni^{2+} with various chelating agents in water [44].*

	Co^{2+}	Ni^{2+}
NTA	10.38	11.54
EDTA	16.31	18.62
CyDTA	18.92	19.40

Catalysts containing complexing agents should be treated carefully during experiments. Some authors used NTA and calcined these catalysts before use. Activity measurements showed that the enhancement in activity due to NTA disappeared due to the calcination step [47]. There is also some debate concerning the heating rate during sulfidation. While Van Veen et al. [26,29,30,31] use a heating rate of 2 ^{0}C/min to prevent early decomposition of the complexes, Prins and coworkers [40,44,46] use a heating rate of 6 ^{0}C/min and report no differences in sulfidation. A recent paper by Cattaneo et al. [48] on $NiMo/Al_2O_3$ reports some very contradictory effects of complexing agents. Not only do they observe that calcined $NiMo/Al_2O_3$ catalysts are as active in thiophene HDS as $NiMoEDTA/Al_2O_3$, catalysts containing NTA show even a lower activity than conventional $NiMo/Al_2O_3$ [48].

From the above it can be concluded that there are still many unresolved questions and a lot of contradictions concerning the use and role of complexing agents. One of the questions concerns the exact role of the complexing agent; is the increase in activity due retardation of Co and Ni only or is the dispersion also altered by the complexing agents? Furthermore, a clear and consistent comparison of the effect of complexing agents on CoMo, NiMo, NiW and CoW catalysts on different supports is lacking in the literature.

1.5 Thiophene hydrodesulfurization (HDS)

Among all molecules used for activity studies in HDS, thiophene is one of the most simple and (maybe therefore) one of the most often used molecules to model sulfur containing compounds in hydrodesulfurization of crude oil. Many studies dealt with the reaction kinetics and mechanism of thiophene HDS, as reviewed by several authors [49-51]. Despite the amount of research there is still debate on both the kinetics and the mechanism. Various possibilities of reaction paths for thiophene HDS have been proposed as shown in Figure 1.8. Lipsch and Schuit [52] were one of the first to study the kinetics of thiophene HDS and reported that the thiophene HDS occurs via direct C-S bond cleavage to form butadiene. Kraus and Zdrazil [53] and Markel et al. [54] proposed intermediates like tetrahydrothiophene (THT) or dihydrothiophene (DHT). However, these intermediates are

very difficult to observe under standard reaction conditions [55]. Because these species are very reactive, readsorption in the pores of the catalysts will convert the main part of these species to C_4-species. For standard reaction conditions, only the main products are found, i.e. n-butane, 1-butene, c-2-butene and t-2-butene. Recently, low temperature experiments by Hensen et al. [56] showed evidence for DHT as intermediates in thiophene HDS.

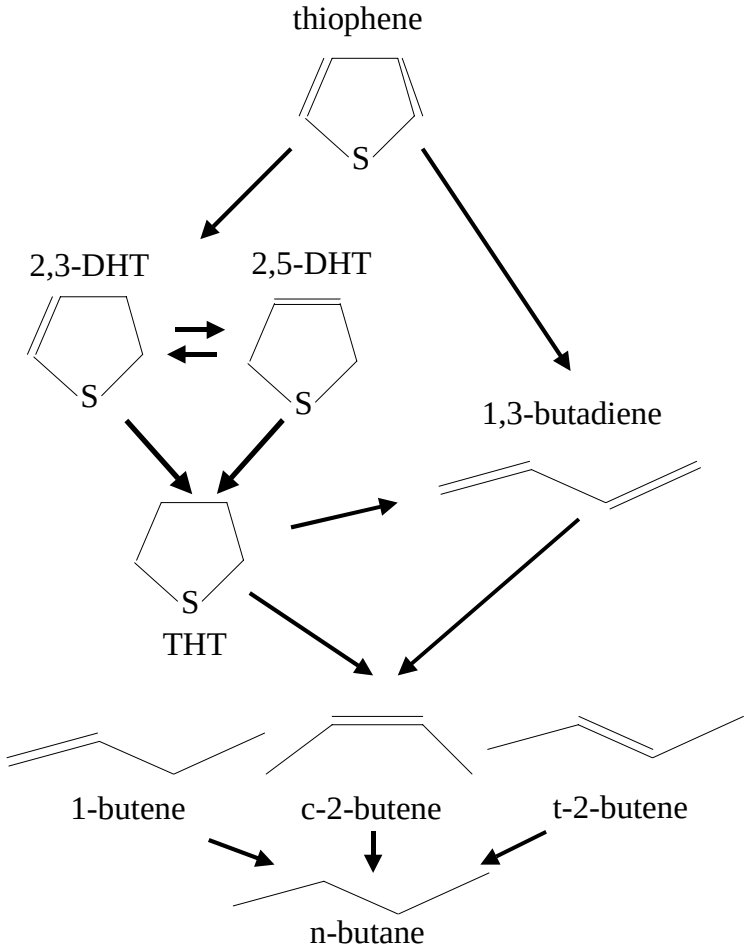

Figure 1.8 *Possible reaction paths for the hydrodesulfurization of thiophene.*

In general, thiophene HDS kinetics is described by Langmuir-Hinshelwood type of reaction equations with the surface reaction between adsorbed thiophene and adsorbed hydrogen as rate limiting step. H_2S is usually taken as an inhibitor in competition with thiophene for the same adsorption sites, although some authors conclude that S removal can also be rate limiting in some cases. Perpendicular end-on adsorption of thiophene is thought to be the precursor for direct desulfurization, whereas π-complexation may lead to hydrogenation of the aromatic ring, leading to hydrothiophenes as intermediates before C-S bond cleavage. The adsorption of H_2 is assumed to take place on separate sites, although some authors report competition between H_2 and thiophene for the same type of site. Van Parijs and Froment [57] reported the existence of two types of active sites on HDS catalysts, i.e. one for hydrogenolysis and one for hydrogenation. This is in agreement with the Rim Edge model of Daage and Chianelli [32], as described earlier. Another debate concerns the adsorption mode of hydrogen being either molecularly or dissociatively adsorbed.

Due to all these uncertainties and contradictory results, various (empirical) kinetic models have been proposed. Kinetic studies by Leliveld et al. [58] and Hensen et al. [56] showed that at low temperatures the reaction rate could be described with pseudo first order kinetics. At higher temperatures the conversion curve deviated from pseudo first order kinetics and a strong decrease in apparent activation energy with temperature was observed, indicating a change in steady state coverage by thiophene as function of temperature [58]. Hensen [56] further concluded that carbon-sulfur bond cleavage is rate limiting, although for CoMo catalysts hydrogenative sulfur removal may be the rate-limiting step. A strong interaction between metal sulfide and thiophene was found to be important for a high HDS activity [56]. While most kinetic studies are carried out in a small temperature range, Leliveld et al. [58] used for the first time a broad temperature range (T=200-550 ^{0}C) for their kinetic study. At temperatures above 400 ^{0}C they observed an exponential increase of the reaction rate. This was ascribed to the presence of a second type of active sites that are only active at high temperature [58].

The above shows that thiophene HDS may look like a simple reaction at first sight, but in fact is very complex. Although the literature gives some clues regarding the mechanism and kinetics, little has been established with certainty. Especially the limited pressure- and temperature-range used for kinetic studies and the large differences in pretreatment and reaction conditions causes the contradictory results. Any comparison of different catalysts in kinetic studies is virtually absent. The absence of pores in our model catalysts, as will be explained in the next section, makes it possible to study intrinsic kinetics in flow, while the chance for readsorption of intermediates is also minimized. In combination with a broad temperature range, this approach can throw some new light on this 'well-known' reaction.

1.6 Surface science models (of hydrotreating catalysts)

Industrial catalysts are generally highly complex systems. Various phases and elements are present and the active phase is mostly present as very small particles hidden inside the pores of the support. This porous support is used to increase the active surface area and to stabilize the active phase. The main goal of catalyst characterization in fundamental catalysis research is to determine the structure and composition of the catalytically active surface in atomic detail under the conditions where it does its work, because this is the only way in which catalytic behaviour can be related to surface properties. Due to the porous structure of industrial catalysts most of the active material is hidden and not visible for most surface-sensitive spectroscopic techniques. Furthermore, the catalyst often consists of a non-conducting, oxidic support, possibly leading to charging problems and accompanied by deterioration or loss of spectroscopic information. Finally, using porous catalysts one should always be aware of intrinsic diffusion limitations, complicating the elucidation of intrinsic kinetics.

Models of catalysts are used to circumvent the disadvantages of industrial catalysts. The ultimate, i.e. most simple, model is a well-defined single crystal surface. These single crystals have been used successfully in ultra high vacuum (UHV) to study fundamental adsorption behaviour of molecules on metal surfaces and its dependence on surface geometry and composition. Even lateral interactions of (co)adsorbates and elementary surface reactions are currently investigated on single crystal surfaces [59]. A major drawback of single crystal

surfaces is the so-called pressure- and material-gap with respect to industrial catalysts. UHV conditions and infinitely extended surfaces of single crystals are a totally different world than high pressure and small particles supported on a porous substrate. Furthermore, single crystal studies are dominated by metallic catalysts, while literature on e.g. oxides or sulfides is less abundant.

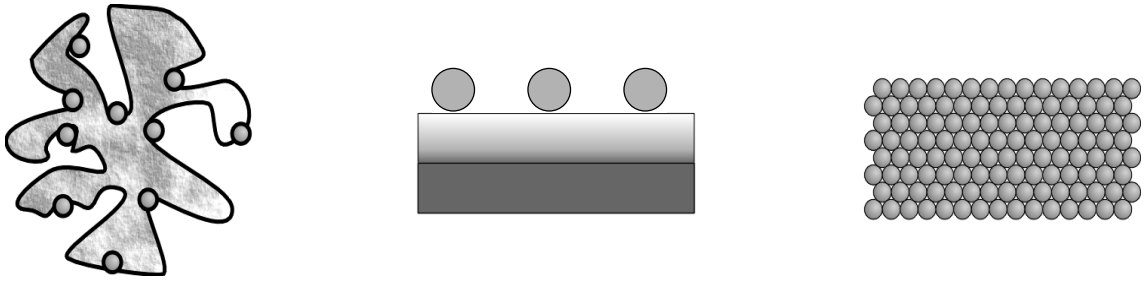

Industrial catalyst on porous support | model catalyst on flat support | unsupported single crystal model catalyst

Figure 1.9 *Schematic drawing of a porous catalyst (left), a flat supported model catalyst (middle) and a single crystal.*

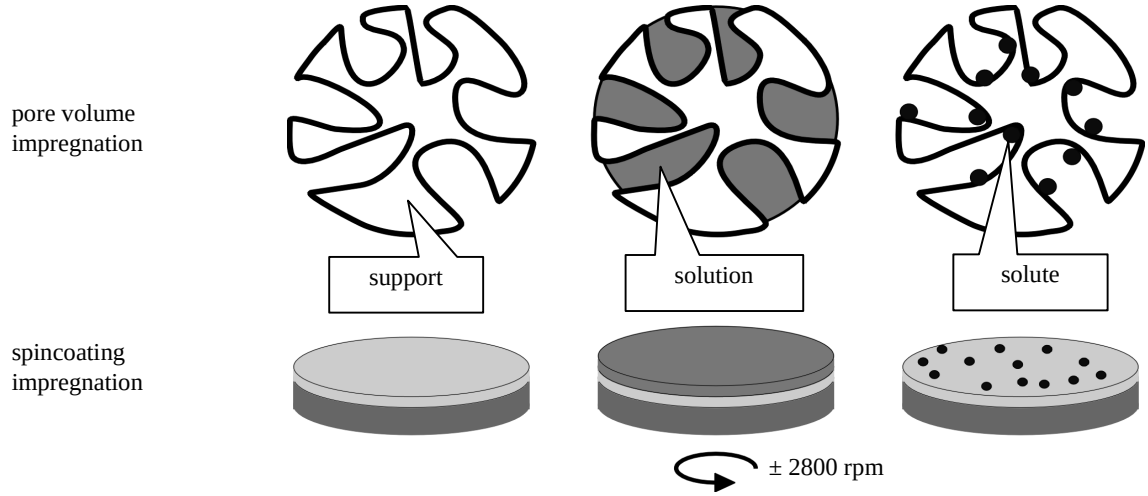

Figure 1.10 *Analogy between the spincoating technique used for model catalysts in this thesis and impregnation of a porous catalyst.*

More realistic models, so-called model catalysts, are used to bridge the gap between well-defined single crystal surfaces and industrial catalysts. These model catalysts consist of a flat 'model' support, covered by the precursor material (see Figure 1.9). The 'model' support is made of a thin layer of SiO_2 or Al_2O_3 on a conducting substrate. The precursor material can be applied by evaporation, electron beam lithography or wet chemical preparation [60]. Especially the latter method has gaining increasing importance. The so-called spincoating technique introduced by Kuipers et al. [61] mimics the widely applied pore-volume impregnation used on industrial catalysts and gives full control over the loading (see Figure 1.10) [62]. Due to the non-porous conducting support all active particles are on

top of the substrate and are thus 'visible' for various surface sensitive techniques and charging during electron- or ion-spectroscopies is largely eliminated. Furthermore, the absence of pores means no internal diffusion limitation is possible and hence intrinsic kinetics can be measured. The majority of studies on model catalysts concern the 'classic' metals on oxidic supports. However, recently model catalysts have also been applied in different fields of catalysis like e.g. polymerization [63] or oxide/sulfide catalysts [41]. An excellent review on the preparation and applications of model supports and catalysts has been published by Gunter et al. [60].

Model catalysts have also been used for research in HDS. The early literature was mainly based on single crystals, as reviewed by various authors [11,64]. These authors used preadsorbed sulfur on e.g. Mo-surfaces in their adsorption and desulfurization studies of sulfur-containing molecules, therefore it is difficult to say if such studies are really looking at sulfides or at metallic surfaces. Furthermore, these studies use large surfaces and no particles are present which seems a major drawback, especially with the CoMoS phase in mind. Of course, the influence of the support is also a subject that can not be studied using these single crystal studies. However these studies have given some insight into the bonding of sulfur with Co, Ni and Mo.

McIntyre and Spevack and coworkers [65-68] were the first to use flat supported model catalysts in HDS. These authors, however, prepared their model catalysts by evaporation of metallic Mo and Co onto an alumina film [67,68]. Although they calcined their samples before sulfidation, to make oxides, the chemistry of cluster formation and interaction with the support is totally different from that of the industrial catalyst. Despite this, they showed that their HDS model catalysts are active in thiophene HDS [65,66].

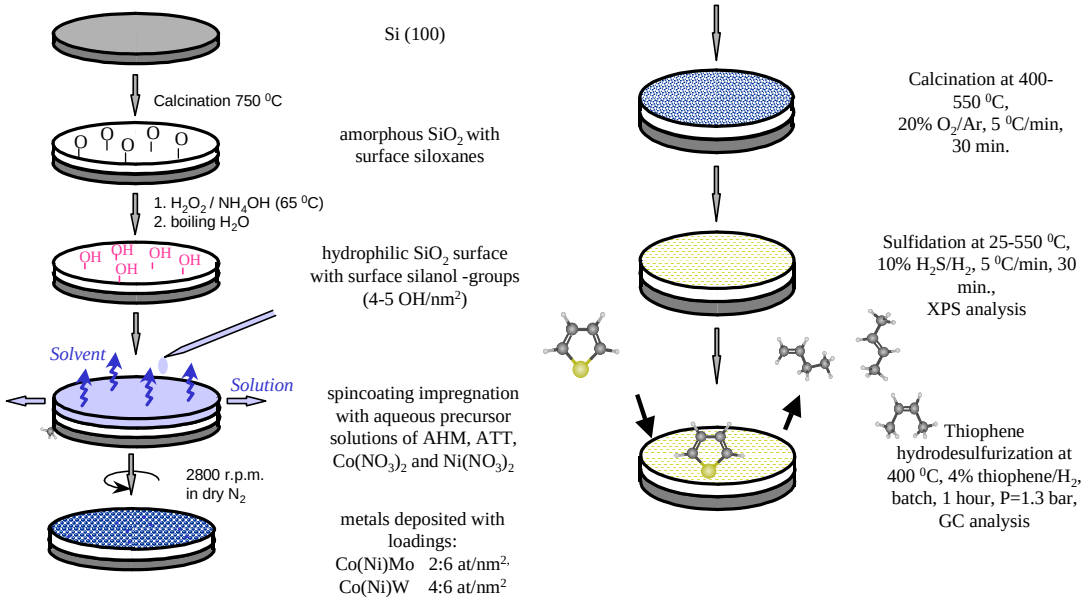

Figure 1.11 *Preparation, pretreatment and testing of HDS model catalysts, as described in this thesis.*

The discovery of Kuipers et al. [61] to use the spincoating technique for preparing model catalysts in a wet chemical way, lead to the preparation of HDS model catalysts prepared in a similar way as that for industrial catalysts. The group of Niemantsverdriet et al.

[69,70] started to use this approach to study the sulfidation of SiO_2-supported MoO_3 in great detail. XPS studies [69,70] showed that the sulfidation of Mo occurred via Mo^{5+}-oxysulfides and that no MoO_2 or elemental sulfur was involved, as proposed by Arnoldy et al. [71]. More recently, de Jong et al. [41] prepared $CoMoNTA/Al_2O_3$ and $CoMoNTA/SiO_2$ model catalysts and concluded that these catalysts exhibit activities and product distributions for thiophene HDS similar to those of their high surface area counterparts.

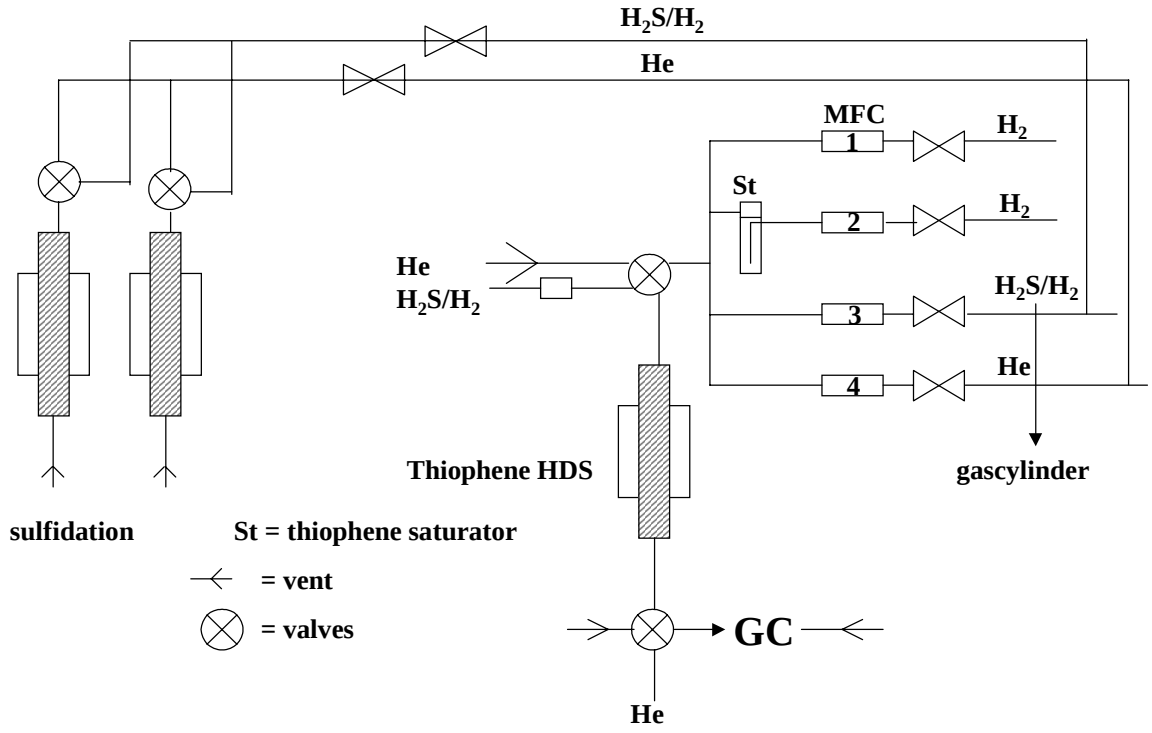

Figure 1.12 *Schematic picture of the used for sulfidation and thiophene hydrodesulfurization of our model catalysts. The same equipment has been used for porous catalysts [72].*

In this thesis we will use this same approach to make HDS model catalysts. The objective is to make the model catalysts as realistic as possible. This means that all preparation and pretreatment conditions must be similar to that of porous HDS catalysts. Figure 1.11 shows schematically the preparation and pretreatment of our model catalysts and clearly shows that all conditions are similar to that of high surface area HDS catalysts [38,72]. The ultimate test to show that our model catalysts are realistic is of course to test them in a reaction. Figure 1.12 shows a picture of the equipment used for sulfidation and thiophene HDS. The same equipment and conditions have been used for high surface area HDS catalysts [38,72]. Demonstrating that we can make our model catalysts as realistic as possible and that they are catalytically active in thiophene HDS is only the first step. The second step is to use these model catalysts in HDS catalyst research, thereby using the advantages of the flat model systems, and to contribute some scientifically added value to the field of HDS catalysis.

1.7 X-ray Photoelectron Spectroscopy (XPS)

X-ray Photoelectron Spectroscopy (XPS) is amongst the most frequently used characterization techniques in catalysis [73]. It is also the main tool in the present work. The technique yields information on the elemental composition, the oxidation state of the elements and in favorable cases on the dispersion of one phase over another. XPS is based on the photoelectric effect, in which an atom absorbs a photon of energy hν; next a core or valence electron with binding energy E_b is ejected with kinetic energy (see Figure 1.13):

$$E_k = h\nu - E_b - \varphi \qquad (1.1)$$

with
E_k: the kinetic energy of the photoelectron
h: Planck's constant
ν: the frequency of the exciting radiation
E_b: the binding energy of the photoelectron with respect to the Fermi level of the sample
φ: the work function of the spectrometer.

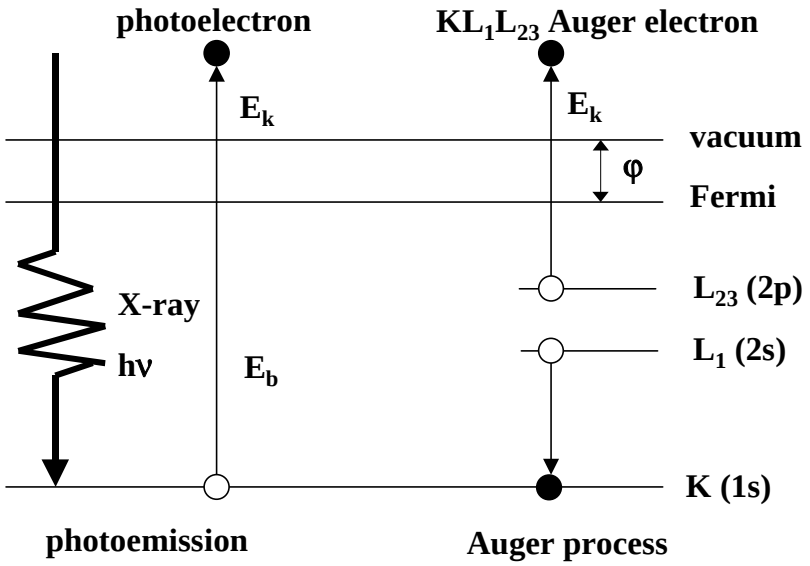

Figure 1.13 *Schematic representation of the principle of X-ray Photoelectron Spectroscopy (XPS). An incident X-ray photon is adsorbed and a photoelectron with a certain kinetic energy is emitted. The binding energy, which is element specific, can be calculated using the measured kinetic energy.*

Commonly used X-ray sources are Mg-Kα (1253.6 eV) and Al-Kα (1486.3 eV). In XPS one measures the intensity of photoelectrons N(E) as a function of their kinetic energy but is usually plotted as N(E) vs. the binding energy (E_b). In addition to the expected photoelectron peaks, the spectrum also contains peaks due to Auger electrons (see Figure 1.13). Although Auger electrons have fixed kinetic energies, which are independent of the X-ray energy, Auger peaks are nevertheless plotted on the binding energy scale, which has of course no physical significance. Almost all photoelectrons used in XPS have kinetic energies

in the range of 0.2-1.5 keV. The accompanying inelastic mean free paths (i.e. 0.5-2 nm) result in a probing depth (usually taken as 3λ) between 1.5 and 6 nm.

Binding energies are not only element specific but contain chemical information as well, because the energy levels of core electrons depend slightly on the chemical state of the atom. Chemical shifts are typically in the range of 0-3 eV. For example, during the sulfidation of $Mo^{VI}O_3$ to $Mo^{IV}S_2$, the Mo $3d_{5/2}$ binding energy shifts from 232.5 eV to 228.9 eV, which can be clearly seen in the XPS spectra [74]. The same accounts for W, Co and Ni [75-78]. Table 1.4 shows the binding energies of bulk compounds relevant for this thesis [74-78]. Figure 1.14 shows the XPS spectra of fully oxidic and sulfidic Co, Ni, Mo and W. The XPS spectra of elements like Co and Ni are extra complicated by the presence of so-called shake-up features. These shake-up features arise when the photoelectron imparts energy to another electron of the atom. This electron ends up in a higher unoccupied state (shake-up). As a consequence, the photoelectron loses kinetic energy and appears at a higher binding energy in the spectrum. Figure 1.14 shows large differences in binding energy and peak shape between the fully oxidic and sulfidic compounds. This makes XPS a perfect technique to follow the transition from oxide to sulfide during thermal treatment. However, in most XPS studies reported in literature, only the begin state and end state of the catalysts are used and the transition is not followed as a function of temperature. Using this approach one loses a lot of potentially used information about e.g. intermediate states.

Table 1.4. *XPS binding energies (B.E.), sensitivity factors (S) and spin orbit splitting (Δ) of bulk compounds relevant for this thesis [74-78].*

Element	compounds	B.E. (eV) (±0.2 eV)	Δ (eV)	S
Co $2p_{3/2}$	Co_2O_3	780.0	15.2	3.590
	Co_9S_8	778.4		
Ni $2p_{3/2}$	Ni_2O_3	856.5	17.49	4.044
	Ni_3S_2	854.1		
	NiS	854.9		
Mo $3d_{5/2}$	MoO_3	232.5	3.13	3.321
	MoS_2	228.9		
W $4f_{7/2}$	WO_3	35.2	2.18	3.523
	WS_2	31.7		
S 2p	S^{2-}	162.0	1.18	0.666
Si 2p	SiO_2	103.3	-	0.339
Al 2p	Al_2O_3	74.4	-	0.234
Ti 2p	TiO_2	458.8	5.54	2.001

An experimental problem in XPS is that electrically insulating samples may charge during measurements, because photoelectrons leave the sample. Due to the positive charge on the samples, all XPS peaks in the spectrum shift by the same amount to higher binding energy. Calibration is necessary for comparing XPS binding energies. This is always done by using the binding energy of a known compound. In the past the C 1s binding energy at 284.6 eV of the almost always-present carbon contamination was used as a reference binding energy for catalysts. However, the origin of these species is unknown and often several C

species are present, which makes it difficult to use it. More recently, the Si 2p or Al 2p of SiO_2 and Al_2O_3, respectively, are used as a reference. Because both SiO_2 and Al_2O_3 are insulators, the charging for porous catalysts can be up to 10 eV, while for model catalysts, with a conducting substrate, this can be reduced to <1 eV. The use of different references for correcting for charging and the use of different binding energies for the same reference compounds makes it sometimes very difficult to compare binding energies with literature values.

If one assumes a homogeneous distribution of two elements in a sample, one can calculate the atomic ratio of these elements:

$$n_1/n_2 = (I_1/S_1)/(I_2/S_2) \qquad (1.2)$$

with
n_1/n_2: atomic ratio of n_1 and n_2
I_1,I_2: intensity of the XPS peaks of element 1 and 2
S_1,S_2: sensitivity factors as tabulated in Table 1.4 [74]

In the case of catalysts, i.e. particles spread over a support, differences in the ratio can give information on changes in dispersion.

1.8 Scope of this thesis

The subject of this thesis is the preparation, characterization and application of hydrotreating model catalysts prepared by spincoating. The main characterization technique is XPS and the catalysts are tested in thiophene hydrodesulfurization (HDS) activity measurements. As explained earlier the first objective is to prepare realistic models of hydrotreating catalysts and to test these catalysts in thiophene HDS. The second objective is to use these model catalysts in HDS catalyst research. In general, we will combine information on the sulfidation behaviour, as obtained with XPS, with thiophene HDS activity measurements. This combination gives us a chance to study the formation of the active phase and the influence of e.g. support and complexing agents.

The first part of the thesis (Chapter 2 to 5) is about SiO_2-supported HDS catalysts. All known catalytic systems (e.g. CoMo, NiMo, NiW and CoW) will be studied to gain knowledge of the formation of the active phase. Especially the influence of complexing agents will be important. Although all four systems show similarities, significant differences arise with respect to the sulfidation behaviour and HDS activity. This part will prove that XPS can be a useful technique for characterization of catalysts and that our model catalysts are indeed realistic models of industrial HDS catalysts.

Chapter 6 and 8 will extend the work to other supports, e.g. Al_2O_3 and TiO_2. The influence of the interaction with the support on the sulfidation behaviour and HDS activity will be the main focus. In combination with Chapters 2 to 5 it will give a broad overview of different HDS catalysts, something that is lacking in the current literature on HDS. However, support interactions do complicate the interpretation of the results and make things less straightforward than for SiO_2-supported catalysts.

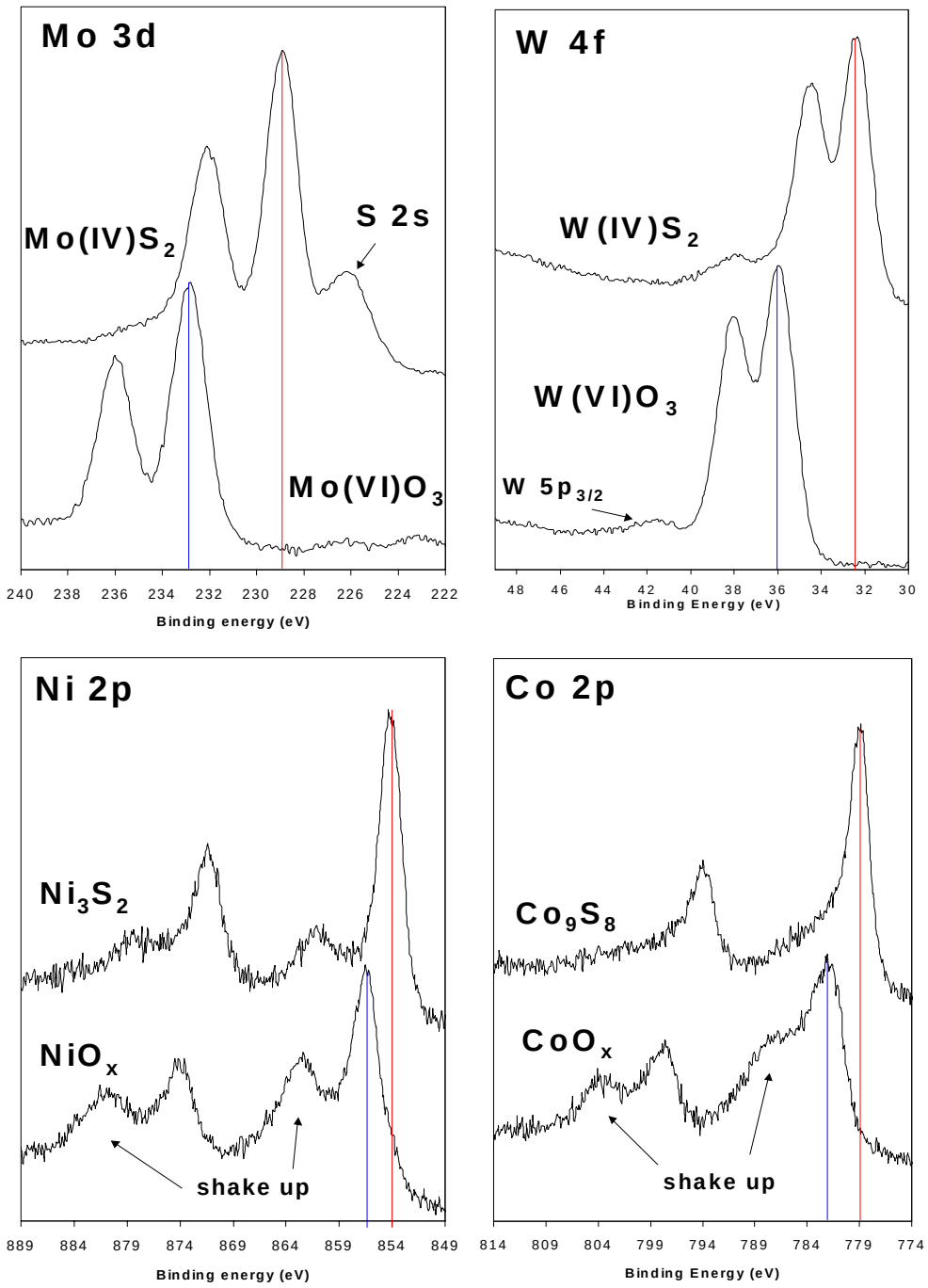

Figure 1.14 *a) Mo 3d, b) W 4f, c) Ni 2p and d) Co 2p XPS spectra of fully oxidic and sulfidic SiO_2-supported model catalysts. Large differences in binding energy and peak shape between the oxides and sulfides are visible, indicating that XPS is a good technique to follow the transition from oxide to sulfide.*

Chapter 7 will go into more detail on the properties of TiO_2-supports. It will be seen that the TiO_2-support is not inert to reducing atmospheres and can act as a promoter, thereby increasing the HDS activity.

The last chapter (Chapter 9) will deal with the kinetics of thiophene HDS on various catalysts. Temperature dependent activity measurements show Volcano-plot behaviour for the first time. Although more measurements are necessary, it is possible, by using kinetic expressions from literature, to find a possible explanation for this Volcano-behaviour and the subsequent effect on the (apparent) activation energy. We will also compare the activities of the various catalytic systems studied in this thesis.

In the last chapter we will summarize our most important findings, determine if our results satisfy our objectives and give our comments and recommendations on future research.

References

[1] R.A. van Santen and J.W. Niemantsverdriet, "Chemical Kinetics and Catalysis", Plenum, New York, 1995.
[2] R.J. Farrauto and C.H. Bartholomew, "Fundamentals of Industrial Catalytic Processes", Blackie Academic & Professional, London, 1997.
[3] J.W. Gosselink, *Cattech* **4**, 127 (1998).
[4] S.K. Moore, K. Walsh and P. Fairley, *Chemical Week,* **March 17***, 32 (1999).*
[5] *Oil and Gas Journal,* **Oct. 9**, 64 (2000).
[6] J.A.R. van Veen, private communication.
[7] H. Topsøe, B.S. Clausen and F.E. Massoth, "Hydrotreating Catalysis", Springer, Berlin, 1996.
[8] M. Radler, *Oil and Gas Journal*, **Dec. 18**, 121 (2000).
[9] S.F. Venner, *Hydrocarbon Processing* **79**, May (2000).
[10] A. Stanislaus and B.H. Cooper, *Catal. Rev.–Sci. Eng.* **36**, 75 (1994).
[11] R. Prins, V.H.J. de Beer and G.A. Somorjai, *Catal. Rev.-Sci. Eng.* **31**, 1 (1989).
[12] S. Eijbouts, *Appl. Catal. A.* **158**, 53 (1997).
[13] R.J.H. Voorhoeve and J.C.M. Stuiver, *J. Catal.* **23**, 228 (1971).
[14] A.L. Farragher and P. Cossee, *Proc. 5th Int. Congress on Catalysis* (J.W. Hightower, Ed.), Elsevier, Amsterdam, 1301 (1973).
[15] B. Delmon, *Bull. Soc. Chim. Belg.* **88**, 979 (1979).
[16] P. Ratnasamy and S. Sivasanker, *Catal. Rev.-Sci. Eng.* **22**, 401 (1980).
[17] N.-Y. Topsøe and H. Topsøe, *J. Catal.* **84**, 386 (1983).
[18] O. Sørensen, B.S. Clausen, R. Candia and H. Topsøe, *Appl. Catal.* **13**, 363 (1985).
[19] J.V. Lauritsen, S. Helveg, E. Laegsgaard, I. Stensgaard, B.S. Clausen, H. Topsøe and F. Besenbacher, *J. Catal.* **197**, 1 (2001).
[20] N.-Y. Topsøe, H. Topsøe, O. Sørensen, B.S. Clausen and R. Candia, *Bull. Soc. Chim. Belg.* **93**, 727 (1984).
[21] S.P.A. Louwers and R. Prins, *J. Catal.* **139**, 525 (1993).
[22] H. Topsøe, B.S. Clausen, R. Candia, C. Wivel and S. Mørup, *J. Catal.* **68**, 433 (1981).
[23] C. Wivel, R. Candia, B.S. Clausen, S. Mørup and H. Topsøe, *J. Catal.* **68**, 453 (1981).
[24] C. Wivel, B.S. Clausen, R. Candia, S. Mørup and H. Topsøe, *J. Catal.* **87**, 497 (1984).

[25] M.W.J. Crajé, V.H.J. de Beer, J.A.R. van Veen and A.M. van der Kraan, *J. Catal.* **143**, 601 (1993).
[26] J.A.R. van Veen, E. Gerkema, A.M. van der Kraan and A. Knoester, *J. Chem. Soc. Chem. Comm.*, 1684 (1987).
[27] M.W.J. Crajé, V.H.J. de Beer, J.A.R. van Veen and A.M. van der Kraan, *Appl. Catal. A* **100**, 97 (1993).
[28] R. Candia, O. Sørensen, J. Villadsen, N.-Y. Topsøe, B.S. Clausen and H. Topsøe, *Bull. Soc. Chim. Belg.* **93**, 763 (1984).
[29] J.A.R. van Veen, H.A. Colijn, P.A.J.M. Hendriks and A.J. van Welsenes, *Fuel. Proc. Technol.* **35**, 137 (1993).
[30] S.M.A.M. Bouwens, F.B.M. van Zon, M.P. van Dijk, A.M. van der Kraan, V.H.J. de Beer, J.A.R. van Veen and D.C. Koningsberger, *J. Catal.* **146**, 375 (1994).
[31] J.A.R. van Veen, E. Gerkema, A.M. van der Kraan, P.A.J.M. Hendriks and H. Beens, *J. Catal.* **133**, 112 (1982).
[32] M. Daage and R.R. Chianelli, *J. Catal.* **149**, 414 (1994).
[33] L. Byskov, B. Hammer, J.K. Nørskov, B.S. Clausen and H. Topsøe, *Catal. Lett.* **47**, 177 (1997).
[34] F. Luck, *Bull. Soc. Chim. Belg.* **100**, 781 (1991).
[35] M. Breysse, J.L. Portefaix and M. Vrinat, *Catal. Today* **10**, 489 (1991).
[36] J. Ramirez, S. Fuentes, G. Diaz, M. Vrinat, M. Breysse and M. Lacroix, *Appl. Catal.* **52**, 211 (1989).
[37] J. Ramirez, L. Cedeno and G. Busca, *J. Catal.* **184**, 59 (1999).
[38] M.J. Vissenberg, Ph.D. thesis, Eindhoven University of Technology, The Netherlands, 1999.
[39] M.S. Thompson, European patent application 0.181.031.A2 (1986); US Patent 4.574.120 (1986).
[40] L. Medici and R. Prins, *J. Catal.* **163**, 38 (1996).
[41] A.M. de Jong, V.H.J. de Beer, J.A.R. van Veen and J.W. Niemantsverdriet, *J. Phys. Chem.* **100**, 17722 (1996).
[42] T. Shimizu, K. Hiroshima, T. Honma, T. Mochikuzi and M. Yamada, *Catal. Today* **45**, 271 (1998).
[43] Y. Ohta, T. Shimizu, T. Honma and M. Yamada, *Stud. Surf. Sci. Catal.* **127**, 161 (1999).
[44] L.G. Silen and A.E. Martell, "Stability constants of metal-complexes", Vol. 2, Chemical Society, London, 1964.
[45] R. Cattaneo, T. Shido and R. Prins, *J. Catal.* **185**, 199 (1989).
[46] R. Cattaneo, Th. Weber, T. Shido and R. Prins, *J. Catal.* **191**, 225 (2000).
[47] W.R.A.M. Robinson, J.A.R. van Veen, V.H.J. de Beer and R.A. van Santen, *Fuel. Proc. Technol.* **61**, 89 (1999).
[48] R. Cattaneo, F. Rota and R. Prins, *J. Catal.* **199**, 318 (2001).
[49] A.N. Startsev, *Catal. Rev.-Sci. Eng.* **37**, 353 (1995).
[50] M.L. Vrinat, *Appl. Catal.* **6**, 137 (1983).
[51] H. Schulz, M. Schon and N. Rahman, *Stud. Surf. Sci. Catal.* **27**, 201 (1986).
[52] J.M.J.G. Lipsch and G.C.A. Schuit, *J. Catal.* **15**, 179 (1969).
[53] J. Kraus and M. Zdrazil, *React. Kinet. Catal. Lett.* **6**, 475 (1977).
[54] E.J. Markel, G.L. Schrader, N.N. Sauer and R.J. Angelici, *J. Catal.* **116**, 11 (1989).
[55] B.T. Carvill and M.J. Thompson, *Appl. Catal.* **75**, 249 (1991).

[56] E.J.M. Hensen, M.J. Vissenberg, V.H.J. de Beer, J.A.R. van Veen and R.A. van Santen, *J. Catal.* **163**, 429 (1996).
[57] I.A. van Parijs and G.F. Froment, *Ind. Eng. Chem. Prod. Res. Dev.* **25**, 431 (1986).
[58] R.G. Leliveld, A.J. van Dillen, J.W. Geus and D.C. Koningsberger, *J. Catal.* **175**, 108 (1998).
[59] M.J.P. Hopstaken, Ph.D. thesis, Eindhoven University of Technology, The Netherlands, 2000.
[60] P.L.J. Gunter, J.W. Niemantsverdriet, F.H. Ribeiro and G.A. Somorjai, *Catal. Rev.-Sci. Eng.* **39**, 77 (1997).
[61] E.W. Kuipers, C. Laszlo and W. Wieldraaijer, *Catal. Lett.* **17**, 71 (1993).
[62] R.M. van Hardeveld, P.L.J. Gunter, L.J. van IJzendoorn, W. Wieldraaijer, E.W. Kuipers and J.W. Niemantsverdriet, *Appl. Surf. Sci.* **84**, 339 (1995).
[63] P.C. Thüne, Ph.D. thesis, Eindhoven University of Technology, The Netherlands, 2000.
[64] G.A. Somorjai, *Catal. Lett.* **15**, 25 (1992).
[65] N.S. McIntyre, T.C. Chan, P.A. Spevack and J.R. Brown, in "Advances in Hydrotreating Catalysts", M.L. Occelli and R.G. Anthony (Eds.), Elsevier, Amsterdam, 187 (1989).
[66] N.S. McIntyre, T.C. Chan, P.A. Spevack and J.R. Brown, *Appl. Catal.* **63**, 391 (1990);
[67] P.A. Spevack and N.S. McIntyre, *Appl. Catal.* **64**, 191 (1990);
[68] P.A. Spevack and N.S. McIntyre, *J. Phys. Chem.* **97**, 11031 (1993).
[69] A.M. de Jong, H.J. Borg, L.J. van IJzendoorn, V.G.M.F. Soudant, V.H.J. de Beer, J.A.R. van Veen and J.W. Niemantsverdriet, *J. Phys. Chem.* **97**, 6477 (1993).
[70] J.C. Muijsers, Th. Weber, R.M. van Hardeveld, H.W. Zandbergen and J.W. Niemantsverdriet, *J. Catal.* **157**, 698 (1995).
[71] P. Arnoldy, J.A.M. van den Heijkant, G.D. de Bok and J.A. Moulijn, *J. Catal.* **92**, 35 (1985).
[72] E.J.M. Hensen, Ph.D. thesis, Eindhoven University of Technology, The Netherlands, 2000.
[73] J.W. Niemantsverdriet, "Spectroscopy in Catalysis: An Introduction", VCH, Weinheim, 1993.
[74] J.F. Moulder, W.F. Stickle, P.E. Stobol and K.D. Bombden, "Handbook of XPS", Perkin-Elmer, Eden Prairie, 1992.
[75] I. Alstrup, I. Chorkendorff, R. Candia, B.S. Clausen and H. Topsøe, *J. Catal.* **77**, 397 (1982).
[76] T.A. Patterson, J.C. Carver, D.E. Leyden and D.M. Hercules, *J. Phys. Chem.* **80**, 1700 (1976).
[77] K.T. Ng and D.M. Hercules, *J. Phys. Chem.* **80**, 2094 (1976).
[78] L. Salvati Jr., L.E. Makovsky, J.M. Stencel, F.R. Brown and D.M. Hercules, *J. Phys. Chem.* **85**, 3700 (1981).

2

On the formation of cobalt-molybdenum sulfides in silica-supported hydrotreating model catalysts*

Abstract

Model catalysts, consisting of a conducting substrate with a thin SiO_2 layer on top of which the active catalytic phase is deposited by spincoating impregnation, were applied to study the formation of the active phase (CoMoS) in hydrodesulfurization (HDS) catalysts. The catalysts thus prepared showed representative activity in thiophene HDS, confirming that these models of HDS catalysts are realistic. Combination of the sulfidation behaviour of Co and Mo, studied by XPS, and HDS activity measurements shows that the key step in the formation of the CoMoS phase is the retardation of the sulfidation of Co. Complexing Co to nitrilo triacetic acid (NTA) retarded the Co sulfidation, resulting in the most active catalyst. Due to the retardation of Co in these catalysts, the sulfidation of Mo precedes that of Co, thereby creating the ideal conditions for CoMoS formation. In the CoMo catalyst without NTA the sulfidation of Co is also retarded due to a Co-Mo interaction. However the sulfidation of Mo still lags behind that of Co, resulting in less active phase and a lower activity in thiophene HDS.

* This chapter is published as: L. Coulier, V.H.J. de Beer, J.A.R. van Veen, and J.W. Niemantsverdriet, *Topics in Catal.* **13** (2000) 99.

2.1 Introduction

Hydrotreating, the catalytic removal of S, N, and O from heavy oil fractions, is one of the largest applications of heterogeneous catalysis. Molybdenum based catalysts make up the larger part of the materials used for hydrodesulfurization (HDS), i.e. the removal of sulfur [1-3]. In the past, detailed structural information concerning these catalysts, which mostly included alumina-supported Co(Ni) promoted MoS_2, was difficult to obtain due to their structural complexity. However, studies by Topsøe et al. [1,3] on alumina-supported CoMo catalysts recently revealed evidence concerning the structure of the active phase. This active phase, commonly referred to as CoMoS, consists of MoS_2 slabs with the edges decorated by Co, which is also in the sulfidic state [1,3]. Van Veen et al. [4,5] have demonstrated that the CoMoS II phase, the highly active cobalt-promoted MoS_2, can be synthesized by sulfiding cobalt and molybdenum complexes of nitrilo triacetic acid (NTA). Although the existence and structure of the CoMoS phase has found widespread acceptance, many questions still exist concerning the formation of the active phase. It is, for example, not clear what the influence of the sulfidation order of Mo and Co is on the formation of the active phase. It is known that Co already sulfides at low temperatures and forms large and stable bulk sulfides, while Mo starts to sulfide at moderate temperatures. Hence, it is not immediately apparent how a phase in which cobalt decorates the edges of MoS_2 slabs can form in stead of the thermodynamically expected mixture of Co_9S_8 and MoS_2.

Silica-supported CoMo catalysts, prepared by conventional impregnation from aqueous solutions of Co and Mo salts, exhibit low HDS activity compared to the γ-Al_2O_3-supported catalysts [5,6]. This has been attributed to the low dispersion of Co and Mo after calcination and consequently to the low concentration of the active phase, caused by the weak interaction with the support [5,6]. Adding chelating agents, like nitrilo triacetic acid (NTA), and thereby leaving out the calcination step, proved to be a way to prepare HDS catalysts on any support with similar HDS activity as their γ-Al_2O_3 supported counterparts [4-6].

Model catalysts, consisting of a flat conducting substrate with a thin SiO_2 or Al_2O_3 layer on top of which the active phase is deposited, have been very successful in the field of catalysis [7]. In the field of HDS catalysis several groups have used model systems for their research [8-12]. One of the main advantages of using conducting supports is that sample charging in electron and ion spectroscopy is largely eliminated [7], resulting in excellent resolution of XPS spectra. Another advantage is the absence of pores, which makes it possible to measure intrinsic kinetics. The absence of pores also implies that all active particles are on top of the surface, i.e. that all active particles are visible with XPS. This is in contrast with porous catalysts in which most active material is hidden inside pores.

To compare results obtained on model catalysts with those on high surface area catalysts it is important that systems are realistic. This means that preparation, pretreatment and activity tests should be done under conditions equal to those used for 'real' catalysts. Furthermore these systems should possess representative catalytic activity, to qualify as a realistic model of a catalyst. In our study the model catalysts are prepared by spincoating, a technique mimicking the impregnation technique used for porous catalysts, which offers full control over the loading [13,14]. In this paper, we use the model catalyst approach to investigate the formation of the active phase in SiO_2-supported (Co)MoS catalysts. All conditions used for preparation, pretreatment and activity are identical to those used for high surface area catalysts; hence we believe that we deal with realistic model equivalents of the

industrial HDS catalyst. We will show that these 'realistic' model catalysts show indeed catalytic activity in thiophene HDS. By comparing the stepwise sulfidation of these systems studied with XPS and the catalytic activity and selectivity in HDS it becomes clear that the key step in the formation of the CoMoS phase is the retardation of the sulfidation of Co.

2.2 Experimental

Model Catalysts. A silica model support was prepared by oxidizing a Si (100) wafer with a diameter of 75 mm in air at 750 ^{0}C for 24 h. RBS measurements indicated that the SiO_2 layer is 90 nm thick. AFM measurements indicated that the roughness of the SiO_2 surface was below 5 Å. After oxidation the wafer was cleaned in a solution of ammonia and hydrogen peroxide at 65 ^{0}C for 10 min. The surface was rehydroxylated by boiling in water for 30 min. Cobalt and molybdenum were applied by spin coating the SiO_2/Si (100) wafers at 2800 rpm in N_2 with aqueous solutions of cobalt nitrate ($Co(NO_3)_2 \cdot 6H_2O$; Merck) and ammonium heptamolybdate ($(NH_4)_6Mo_7O_{24} \cdot 4H_2O$; Merck), respectively. The concentration of Co and Mo in the aqueous solutions was adjusted to result in a loading of 2 Co atoms/nm^2 and 6 Mo atoms/nm^2 after spincoating, as determined by RBS. The mixed phase model catalysts were prepared by spincoating with aqueous solutions containing Co and Mo with an atomic ratio of 1:3, respectively. Catalysts containing nitrilo triacetic acid (NTA) were prepared by spincoating ammoniacal solutions containing MoO_3 (Merck), cobalt nitrate and NTA (Acros Organics) as described by van Veen et al. [5]. The NTA solutions contained Co:Mo:NTA ratios of 1:3:4 with an excess 10 mol% of NTA.

Calcination was carried out in a glass reactor under a 20% O_2/Ar flow at 1.5 bar. The catalysts were heated to 500 ^{0}C at a rate of 5 ^{0}C/min and kept at the desired temperature for 30 min.

Sulfidation of the model catalysts was carried out in a glass tube reactor with a mixture of 10% H_2S/H_2 at a flow rate of 60 mL/min. The catalysts were heated at a rate of 5 ^{0}C/min (NTA-containing samples: 2 ^{0}C/min) to the desired temperature and kept there for 30 min. After sulfidation, the reactor was cooled to room temperature under a helium flow and brought to the glovebox, where the model catalyst was mounted in a transfer vessel for transport to the XPS under N_2 atmosphere.

XPS. XPS spectra were measured on a VG Escalab 200 MK spectrometer equipped with an Al Kα source and a hemispherical analyzer connected to a five-channel detector. Measurements were done at 20 eV pass energy. Energy correction was performed by using the Si 2p peak of SiO_2 at 103.3 eV as a reference.

Thiophene HDS. Atmospheric gas phase thiophene HDS was used as a test reaction for the model catalysts. The measurements were carried out in a microflow reactor under standard conditions (1.5 bar, 400 ^{0}C, 4% thiophene/H_2). About 3 cm^2 of model catalysts was placed inside a glass reactor. First the model catalysts were sulfided at 400 ^{0}C for 1 h as described above. Then a mixture of 4% thiophene/H_2 was passed through the reactor at a rate of 50 mL/min and at 400 ^{0}C. After 3 min the reactor was closed and operated as a batch reactor. After the desired reaction time a sample was taken from the reactor with a valved syringe for GC analysis of the reaction products. When a sample was taken, the reactor is flushed with thiophene/H_2 for 5 min and closed again for the next analysis. Blank runs of the empty reactor and bare model support were also performed. The activity of the model catalysts is expressed as conversion (%) per 5 cm^2 of catalyst.

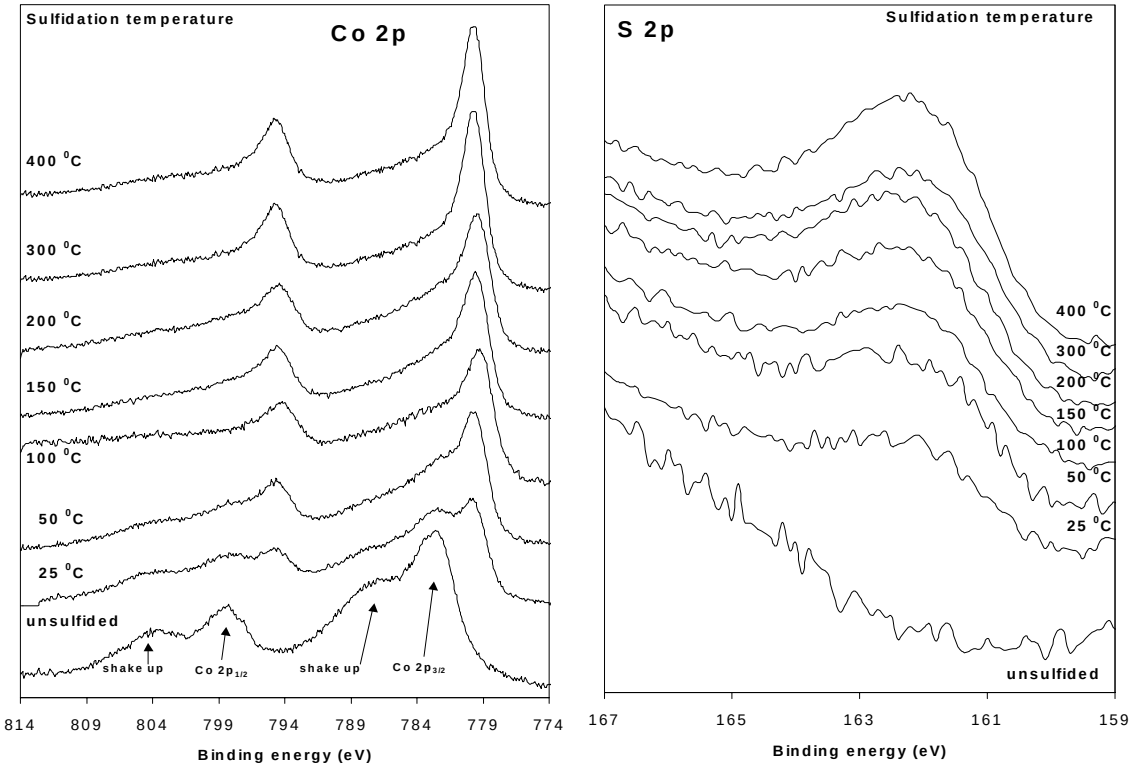

Figure 2.1 *Co 2p (left) and S 2p (right) XPS spectra of calcined $CoO_x/SiO_2/Si(100)$ model catalysts as a function of sulfidation temperature, show that cobalt oxide, having little interaction with the support, sulfided at low temperatures.*

2.3 Results

2.3.1 XPS measurements

Co/SiO_2. Figure 2.1 shows Co 2p and S 2p XPS spectra of a $Co/SiO_2/Si(100)$ model catalysts, prepared by spincoating impregnation from an aqueous solution of cobalt nitrate and calcined at 500 ^{0}C, after sulfidation in 10% H_2S/H_2 for 30 min with a heating rate of 5 ^{0}C/min at different temperatures. The cobalt loading corresponds to 2 at/nm^2. The Co 2p spectrum of the unsulfided catalysts shows the characteristic pattern of oxidic cobalt in a 2+ oxidation state, with the Co $2p_{3/2}$ peak at 782.3 eV and a shake up feature at higher binding energy [15]. Sulfidation of the catalysts at room temperature shows the appearance of a second Co $2p_{3/2}$ peak at 779.1 eV, which corresponds to the binding energy of bulk cobalt sulfide, Co_9S_8 [15]. At higher temperatures (T>50 ^{0}C) the peak at 782.3 eV disappears and only the one at 778.9 eV remains, which means that cobalt has completely transformed into the sulfidic state. The S 2p spectra show a broad envelope in which the components of the doublet can not be resolved. The binding energy of the S 2p doublet is 161.7 eV, in agreement with sulfur in the S^{2-} state. The S 2p spectra show that the sulfidation of Co starts at 25 ^{0}C and is completed around 100 ^{0}C.

Similar series were measured for catalysts that were not calcined and with a higher loading of 6 Co atoms per nm^2. These spectra (not shown) do not differ from the ones showed

in Figure 2.1; hence also in these cases the sulfidation of cobalt takes place at low temperatures.

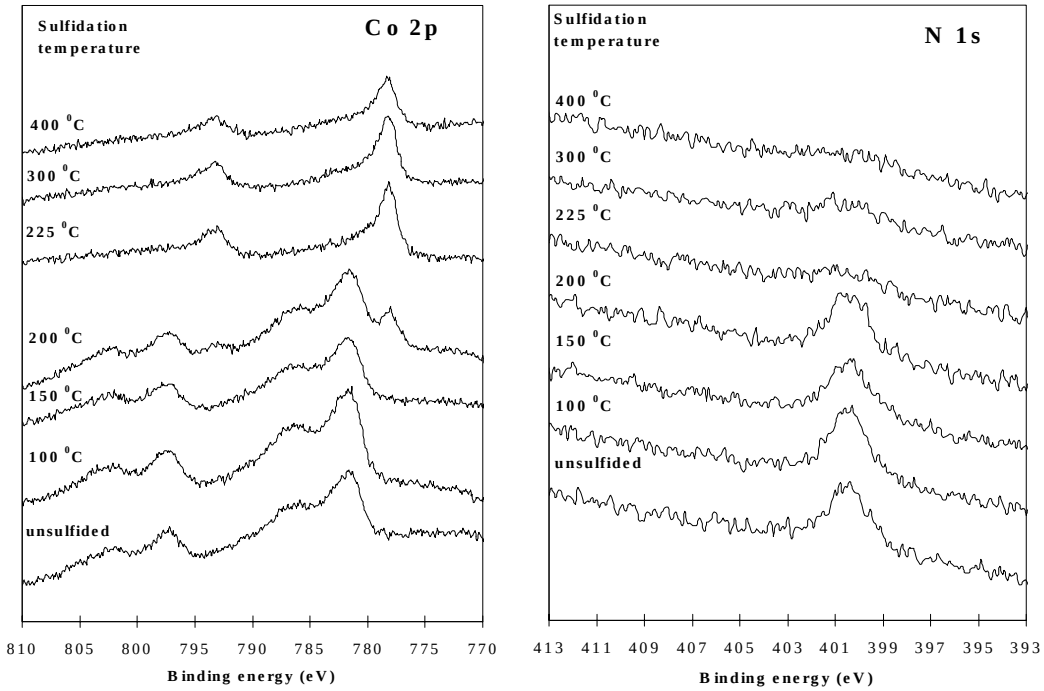

Figure 2.2 *Co 2p (left) and N 1s (right) XPS spectra of CoNTA/SiO_2/Si(100) model catalysts sulfided at various temperatures show that the NTA agent retards the sulfidation of Co.*

The XPS spectra of cobalt model catalysts, prepared by spin-coating an aqueous solution of cobalt nitrate and NTA, are shown in Figure 2.2. The loading of the model catalysts was 4 at/nm^2. As can be seen from Figure 2.2 the transformation of cobalt to the sulfidic state does not start until temperatures above 150 ^{0}C and is complete at 225 ^{0}C. At temperatures below 150 ^{0}C the Co 2p spectra show the characteristic spectrum of oxidic cobalt, while at higher temperatures the doublet of sulfidic cobalt appears. The N 1s spectra, resulting from the NTA agent, are also shown in Figure 2.2. At temperatures where the sulfidation of cobalt starts, the N 1s peak at 400.4 eV starts to decrease, while at temperatures where the sulfidation of cobalt is complete the N 1s peak has completely disappeared. Due to the decomposition of NTA, visible by the decrease of the N 1s peak, Co is available for sulfidation; therefore the disappearance of the nitrogen peak coincides with the start of the Co sulfidation.

Mo/SiO_2. The sulfidation of molybdenum oxide on SiO_2, calcined at 500 ^{0}C, proceeds at higher temperatures than that of cobalt, as the XPS spectra in figure 5 indicate. Figure 2.3 shows the Mo 3d spectra during sulfidation at different temperatures. The Mo 3d spectrum of oxidic molybdenum consists of a single Mo 3d doublet with a Mo $3d_{5/2}$ binding energy of 232.7 eV. This value, although characteristic of molybdenum with a formal charge of 6+ in an oxidic surrounding, is slightly higher than that of crystalline MoO_3, 232.3 eV [9] but

agrees well with the binding energy of $MoO_3 \cdot H_2O$, which equals 232.6 eV [8,9]. Although molybdenum is calcined at 500 ^{0}C it may still be in a hydrated form.

The Mo 3d doublet after sulfidation at high temperatures (T> 175 ^{0}C) has a Mo $3d_{5/2}$ binding energy of 228.8 eV, which is typical for molybdenum with a formal charge state of 4+ as in MoS_2. The spectra also show a shoulder at low binding energy, which can be attributed to the S 2s electrons. The S 2p spectra in Figure 2.3 can be fitted with a single doublet with a S 2p binding energy of 161.8 eV, consistent with the S^{2-}-type ligands present in MoS_2, although terminal S_2^{2-} would appear at the same value [8]. The presence of the latter can therefore not be excluded. The S 2p doublet appears at temperatures where the sulfidation of Mo starts and remains constant at higher temperatures indicating that the sulfidation of Mo is complete.

The Mo 3d spectra of the catalysts sulfided at intermediate temperatures can all be interpreted in terms of the Mo^{6+} and Mo^{4+} doublets described above and one additional doublet with a Mo $3d_{5/2}$ binding energy of 231.5-232.0 eV. This doublet, already present after sulfidation at 50 ^{0}C, can be assigned to molybdenum having a formal charge of 5+, possibly in an oxysulfidic surrounding [9]. The contribution of Mo^{6+} disappears from the spectra of samples sulfided at 150 ^{0}C and higher, while the Mo^{4+} starts to form in substantial amounts at sulfidation temperatures above 150 ^{0}C.

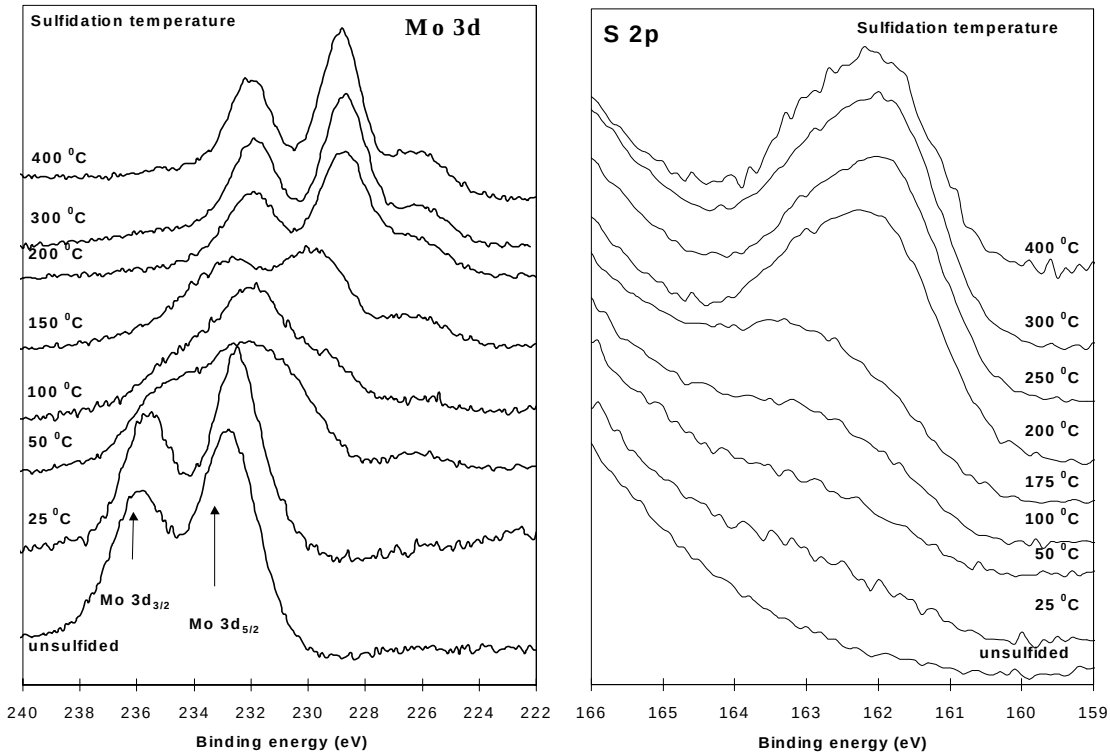

Figure 2.3 *Mo 3d (left) and S 2p (right) XPS spectra of $MoO_3/SiO_2/Si(100)$ model catalysts as a function of sulfidation temperature indicating that the sulfidation of Mo start at moderate temperatures and occurs through different intermediate states.*

XPS spectra of uncalcined Mo/SiO_2 catalysts and catalysts with a loading of 2 Mo at/nm^2 showed the same results. This indicates that these factors do not influence the sulfidation behaviour of Mo. For more extensive studies of the sulfidation of Mo model catalysts with XPS measurements with higher resolution, we refer to de Jong et al. [9] and Muijsers et al. [8]. A mechanistic description has been given by Weber et al. [16,17].

$CoMo/SiO_2$. A mixed phase catalyst, i.e. with Co and Mo, was prepared by spincoating the model support with a solution containing both Co and Mo with an atomic ratio of 1/3. Figure 2.4 shows the Co 2p spectra and Mo 3d spectra of a $CoMo/SiO_2$ catalyst with a loading of 2 Co at/nm^2, 6 Mo at/nm^2 and calcined at 500 ^{0}C. The Mo 3d spectrum of the unsulfided catalyst shows a Mo 3d doublet at a binding energy of 232.7 eV. This doublet is characteristic of oxidic Mo in an oxidation state of 6+, in agreement with the single phase Mo catalyst. The Mo 3d doublet observed after sulfidation at high temperatures (T> 175 ^{0}C) with a Mo $3d_{5/2}$ binding energy at 228.7 eV is characteristic for MoS_2. The sulfidation of Mo starts at temperatures above 50 ^{0}C and is completed above 175 ^{0}C. At temperatures between 50 and 175 ^{0}C the sulfidation of Mo goes through intermediates, which can be interpreted in terms of the Mo^{6+}, Mo^{5+} and Mo^{4+} doublets as described earlier in this paper. The Mo^{4+} starts to form around 150 ^{0}C, while the Mo^{6+} contribution disappears completely at temperatures above 175 ^{0}C.

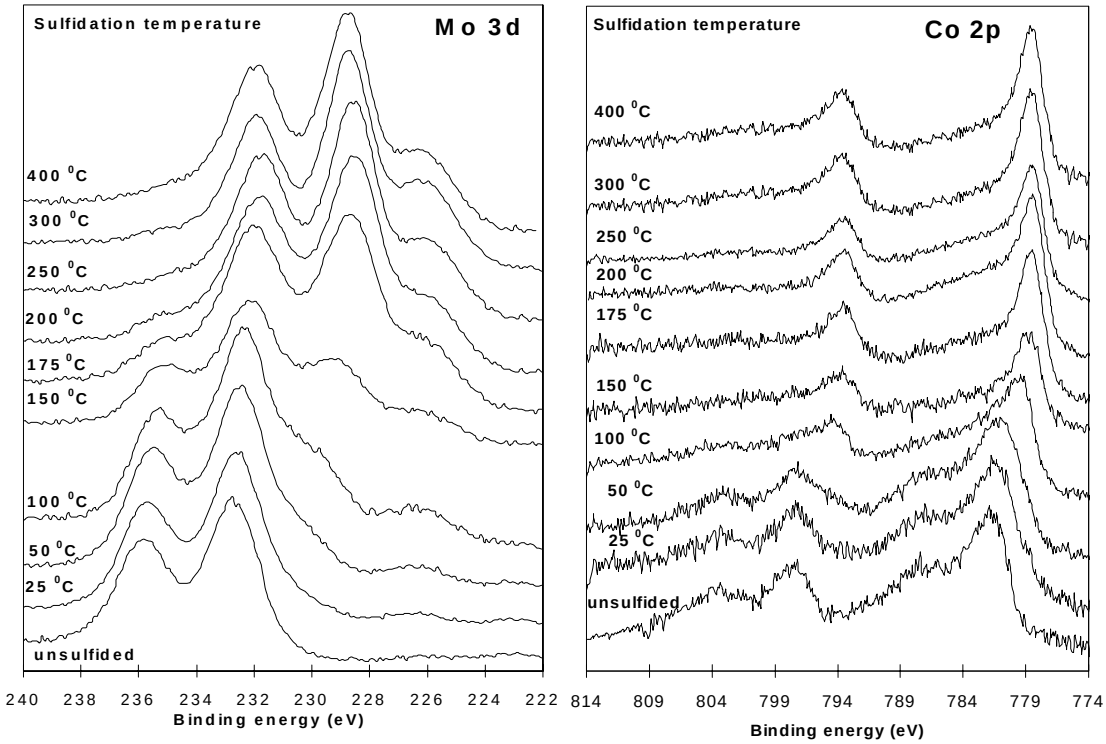

Figure 2.4 *Mo 3d and Co 2p XPS spectra of a calcined $CoO_x/MoO_3/SiO_2$ catalyst during sulfidation at different temperatures. The spectra show that the sulfidation of Co is retarded in the presence of Mo, while the sulfidation of Mo remains unchanged compared to the single-phase catalysts.*

Figure 2.4 shows the sulfidation behaviour of Co in the mixed phase catalyst. The unsulfided Co 2p spectrum shows a Co $2p_{3/2}$ peak at 781.8 eV with shake up features at higher binding energy, which is characteristic for oxidic Co in an 2+ oxidation state. At sulfidation temperatures above 175 ^{0}C the Co 2p spectrum shows Co $2p_{/2}$ peak at a binding energy of 779.3 eV, which is characteristic for Co in a sulfidic environment. The asymmetric features at higher binding energy are caused by shake up features which are less pronounced compared to oxidic Co. Figure 6b shows that the sulfidation of Co does not start until temperatures above 50 ^{0}C, while the sulfidation is completed around 150 ^{0}C.

The same spectra (not shown) for the uncalcined CoMo/SiO_2 model catalyst showed the same features, as did CoMo/SiO_2 with lower loading (1:3 at/nm^2). Hence we conclude that in a mixed CoMo/SiO_2 catalyst, cobalt sulfide between 50 and 150 ^{0}C and molybdenum between 100 and 200 ^{0}C. Note that these temperature regions overlap to an appreciable extent, although sulfidation of cobalt proceeds faster than that of molybdenum.

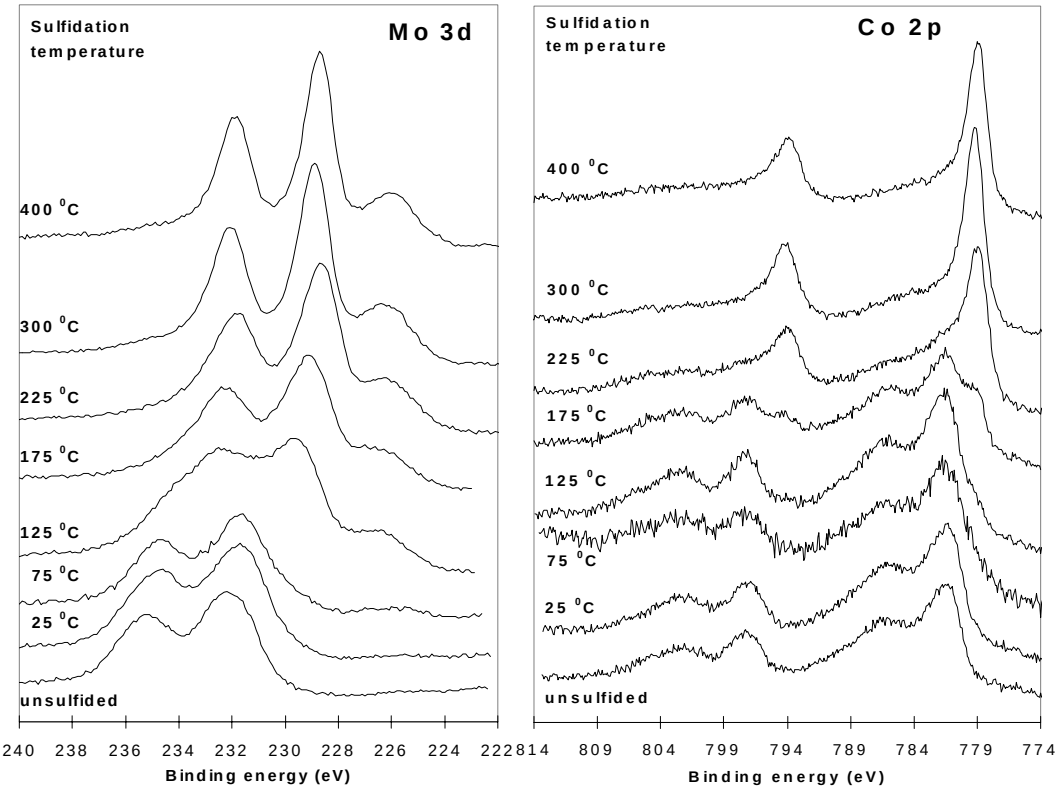

Figure 2.5 *Mo 3d and Co 2p XPS spectra of CoMoNTA/SiO_2/Si(100) model catalysts as a function of sulfidation temperature. The NTA agent retards the sulfidation of Co even more, while Mo still sulfides at the same temperature.*

CoMoNTA/SiO_2. Figure 2.5 shows the Mo 3d and Co 2p spectra of the silica-supported CoMo model catalysts prepared with the NTA-complex. The Mo 3d spectra of the freshly prepared model catalyst reveal only a Mo 3d doublet with a Mo $3d_{5/2}$ binding energy of 232.4 eV, corresponding to a Mo^{6+} species. At 175 ^{0}C a shoulder at higher binding energy appears indicating that the sulfidation of Mo has started. At temperatures around 225 ^{0}C and higher Mo is transformed to a species with a Mo $3d_{5/2}$ binding energy of 228.8 eV, which

agrees well with the binding energy of MoS_2. For a detailed description of the changes in Mo XPS spectra during sulfidation we refer to XPS studies of Mo/SiO_2 and $CoMo/SiO_2$ model catalysts described earlier in this paper.

The Co 2p spectra of the freshly impregnated catalysts as well of these after sulfidation at temperatures up to 125 ^{0}C show again the characteristic pattern of oxidic cobalt, with a single Co $2p_{3/2}$ peak at 781.5 eV and a shake up feature at higher binding energies. At 175 ^{0}C a second Co $2p_{3/2}$ peak appears at 779.5 eV, which can be assigned to sulfided cobalt [15]. Sulfidation at temperatures above 175 ^{0}C only show the Co $2p_{3/2}$ peak at 779.5 eV, indicating that Co is completely sulfided. The decomposition of the NTA complex could be followed by the decrease in the N 1s and C 1s XPS intensity (not shown). The temperature at which the decomposition of NTA takes places coincides with the start of the sulfidation of Co and Mo. These results are in agreement with a previous study by de Jong et al. [10].

Hence, NTA complexation retards the sulfidation of cobalt to temperatures where molybdenum is converted to the sulfidic state.

2.3.2 HDS activity measurements

Measuring the catalytic activity of these model systems provides the most convincing test for the validity of our model approach. Therefore batch thiophene HDS activity measurements were performed on the model catalysts. An example of such an activity test is shown in Figure 2.6, where the conversion of thiophene (%) into the different products, over a $CoMo/SiO_2$ model catalyst have been plotted. Because the number of active sites is unknown, it is impossible to express the activity as a turnover frequency. If the conversion is scaled to a 'pseudo'-turnover number per Mo atom activities on our model systems, e.g. for the $CoMoNTA/SiO_2$ model catalyst, of ~10^{-2} s^{-1} averaged over 1 h reaction time are obtained. This value agrees well with turnover frequencies measured on alumina and silica supported CoMoS catalysts [1]. The sample shown in Figure 2.6 was taken after one hour of batch reaction at 400 ^{0}C in 4% thiophene/H_2. The conversions are based on 5 cm^2 of catalyst and corrected for conversions obtained in blank experiments. The blank experiments, i.e. the empty reactor, also showed some conversion of thiophene. The main products were methane, ethane and propane. This activity is thought to be due to thermal decomposition of the thiophene, which may be assisted by the reactor wall. The product distribution in Figure 2.6 shows that the main product is 1-butene. Also the two secondary products, i.e. trans-2-butene and cis-2-butene, are present, as well as the cracking products, methane, ethane and propane. The figure shows that our $CoMo/SiO_2$ model catalyst is active in thiophene hydrodesulfurization. The product distribution is similar to that of a high surface area catalyst at low conversion. The conversions obtained seem to be low, but significant and on a per molybdenum basis similar to those of high-surface area catalysts.

Figure 2.7 compares the activity in thiophene HDS of the different model catalysts discussed in this paper. The activity is expressed as yield (%) of the different products, for 1 hour of batch reaction based on 5 cm^2 of catalyst and corrected for the blank samples. All activities presented are averages of at least six different measurements. It is clear that the silica-wafer has very low activity, as expected, with relatively large amounts of cracking products. The Co/SiO_2 also shows low activity, although the relative amount of primary product 1-butene increases. The Mo/SiO_2 model catalyst really shows an increase in activity with a factor of 2 to 3 compared with SiO_2 and Co/SiO_2. The promotion effect of Co is

clearly visible from the high activity of the CoMo/SiO_2 catalysts. The calcined CoMo sample has a somewhat lower activity than the uncalcined one, which we tentatively attribute to loss of dispersion. As expected the CoMoNTA catalyst has the highest activity, because it is known that 100% of CoMoS forms in the presence of NTA [5]. For this sample the relative amount of secondary products is higher, this is also observed for high surface area catalysts at higher conversion.

Activity tests measured as a function of time showed a linear increase of conversion with time, even after 12 hours. This indicates that the model catalysts do not deactivate, although it is possible that this can happen in the first minutes of the reaction. The product distribution of the CoMoNTA/SiO_2 sample after 12 hours showed a shoulder in the C_4-region, which could be assigned to n-butane. It is known that this is only formed at higher conversions, because it can only be formed by hydrogenation of butenes [1].

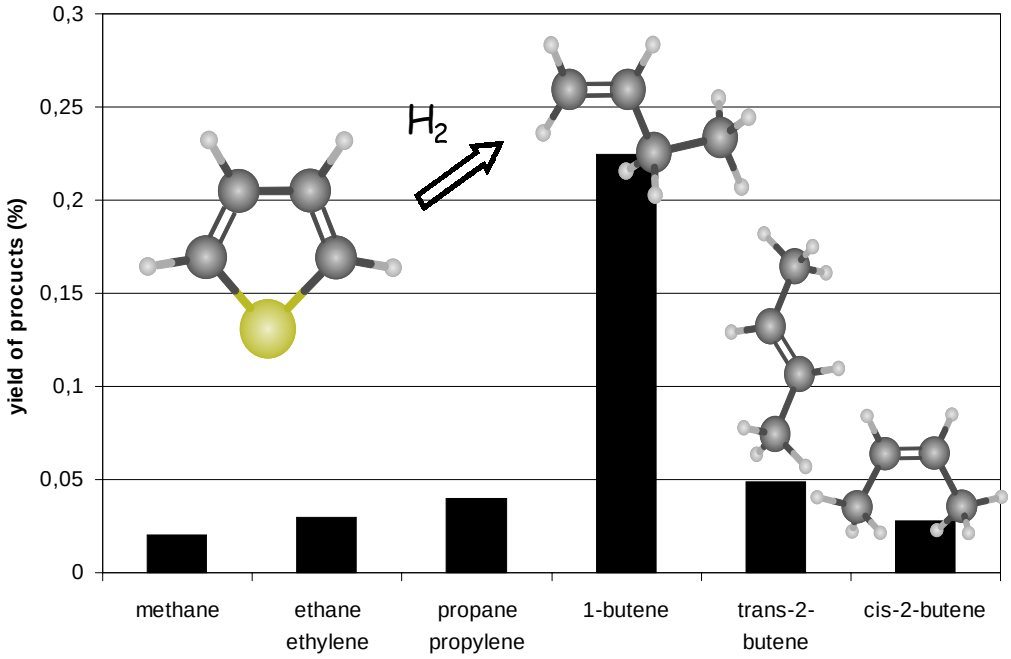

Figure 2.6 *Example of a thiophene hydrodesulfurization experiment on a CoMo/SiO_2/Si(100) model catalysts. The figure shows the product distribution after 1 hour of batch reaction at 400 ^{0}C analyzed by GC.*

2.4 Discussion: correlating XPS results with HDS activity measurements

Co/SiO_2. The XPS spectra described in the previous section reveal how the states of molybdenum and cobalt change during sulfidation at different temperatures. The Co 2p spectra in Figure 2.1 show that the sulfidation of Co occurs through oxygen-sulfur exchange resulting in the disappearance of the shake up features characteristic for oxidic cobalt. A shift in Co $2p_{3/2}$ binding energy to lower values is also visible during sulfidation. The binding energy value after sulfidation of 779.1 eV agrees well with the binding energy of bulk cobalt sulfide, i.e. Co_9S_8 [15]. The sulfidation starts already at room temperature while the sulfidation is complete around 100 ^{0}C. It is known that bulk cobalt sulfide is not active in

HDS, which is clearly visible in the product distributions shown in Figure 2.7. As stated earlier calcination of the Co model catalysts and higher Co loading did not show any visible change in sulfidation behaviour of Co. The indifference of calcination suggests that the interaction of Co with the support is very low. No evidence of sintering or spreading during calcination was found. Increasing the loading has also no effect on the sulfidation behaviour. Figure 2.2 shows the effect of complexing Co with a NTA complex. It is clearly visible that due to the complexation the sulfidation of Co is retarded. While in the absence of NTA Co already starts sulfiding at room temperature and is completed at 100 ^{0}C, the NTA retards the sulfidation of Co to temperatures above 150 ^{0}C. Around 250 ^{0}C the sulfidation is complete. The N 1s spectra in Figure 2.2 confirm that sulfidation of Co starts when the N 1s signal starts to decrease. The decrease of the N 1s signal is due to the decomposition of the NTA agent. While NTA should start to decompose around 270 ^{0}C, it can be seen in Figure 2.2 that in our case the decomposition of NTA starts at a much lower temperature, indicating that the decomposition is driven by the sulfidation reaction. At temperatures where the sulfidation of Co is complete the N 1s signal is disappeared, confirming that no Co is attached to NTA. Although the Co sulfidation is retarded by complexation with NTA, Co_9S_8 is expected to form after complete sulfidation. Hence the HDS activity of the $CoNTA/SiO_2$ is expected to be low.

Mo/SiO_2. The sulfidation behaviour of Mo shown in Figure 2.3 indicates that the sulfidation occurs at higher temperatures as compared to that of Co. The sulfidation starts above 50 ^{0}C and is completed at 175 ^{0}C. The mechanism of sulfidation is by O-S exchange transforming MoO_3 into MoS_2, while in the intermediate temperature range Mo^{5+} and oxysulfide species are present [16,17]. Our results are in agreement with earlier work of de Jong et al. [9] and Muijsers et al. [8]. Calcination and varying the Mo loading had no influence on the sulfidation behaviour of Mo on SiO_2. The same explanation obtains as for Co: the low interaction of Mo with the silica support is not changed by calcination, hence it does not affect the sulfidation behaviour. Due to the absence of interaction with the support Mo particles can be treated as isolated MoO_3 particles, independent of loading. If we compare the sulfidation of Co in Figure 2.1 and that of Mo in Figure 2.2 we conclude that the sulfidation of Mo has just started at temperatures where Co is almost completely sulfided. This result confirms the expectation stated earlier that it is difficult to understand how the CoMoS phase in HDS catalysts, in which Co atoms are situated on the edges of MoS_2 slabs, will form as Co forms stable and bulk sulfides at low temperatures while Mo sulfides at higher temperatures.

It is known that supported Mo particles are active in HDS, which agrees well with the activity observed in Figure 2.7 for the Mo/SiO_2 model catalysts calcined at 500 ^{0}C. No observable difference in activity was found for uncalcined and calcined catalysts on silica, indicating that no sintering or spreading occurred during calcination.

$CoMo/SiO_2$. The Co 2p and Mo 3d XPS spectra of the $CoMo/SiO_2$ model catalysts in Figure 2.4 show some interesting features. The Mo 3d spectra of Mo/SiO_2 in Figure 2.3 and of $CoMo/SiO_2$ in Figure 2.4 show that the sulfidation of Mo starts at the same temperature, i.e. 50 ^{0}C. However in the case of Mo/SiO_2 the sulfidation is complete around 175 ^{0}C, while it is complete above 200 ^{0}C for the CoMo catalyst. Furthermore the Co 2p spectra show an even larger difference. The sulfidation of Co/SiO_2 starts already at room temperature and is complete above 50 ^{0}C, as shown in Figure 2.1. The Co 2p spectra of the $CoMo/SiO_2$ model catalyst in Figure 2.4 show that in this case the sulfidation of Co does not start until

temperatures above 50 ^{0}C and is complete around 150 ^{0}C. Hence the presence of Mo retards the sulfidation of Co by 50 to 100 ^{0}C. The sulfidation of Mo also shows some delay due to the presence of Co, but not as much as vice versa. We attribute this retardation to a Co-Mo interaction, although there is no clear independent evidence for this. From XPS measurements on reference samples of $CoMoO_4$ it could not be excluded that the $CoMoO_4$ was present in the model catalyst. It is known that $CoMoO_4$ cannot be transformed into the CoMoS phase, hence the presence of this phase in our catalysts should result in a low activity after sulfidation. However Figure 2.7 shows that the $CoMo/SiO_2$ catalysts is (relatively) active, so we conclude that bulk $CoMoO_4$ is not present.

The interaction between Co and Mo has consequences for the rate at which both components form sulfides. For the single-phase catalysts the two separated phases, Co and Mo sulfide, form in different temperature regimes, as Figure 2.1 and 2.2 clearly show. When mixed, however there is a temperature range where Co and Mo convert to the sulfidic form simultaneously. Here it is conceivable Co partially ends up on the edges of MoS_2, hence it is likely that these catalysts have a substantial fraction of Co and Mo in the CoMoS form.

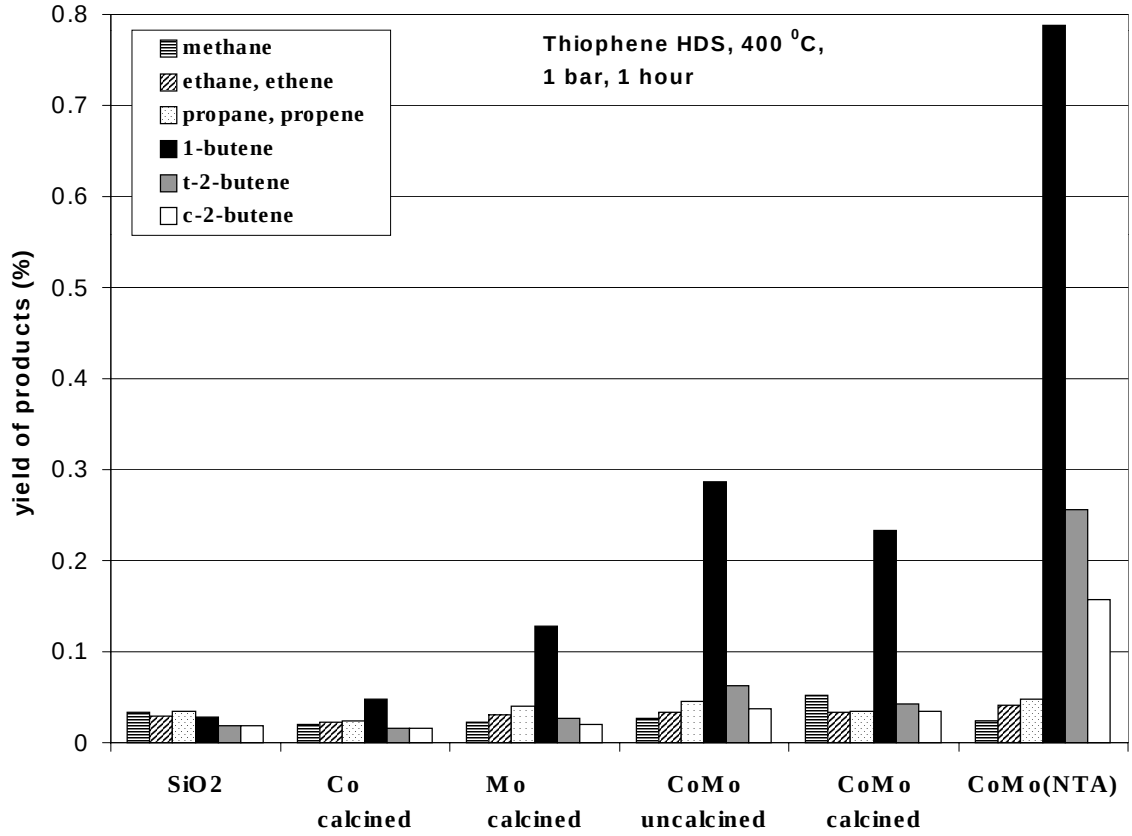

Figure 2.7 *Product distribution after 1 h of thiophene HDS batch reaction for silica-supported model catalysts.*

The activity measurements in figure 9 show clearly the promotion effect of Co. Especially the primary product 1-butene show a large increase compared to the Mo/SiO_2. This is evidence for the presence of the CoMoS phase on the catalyst. The promotion factor, i.e. activity CoMo/activity Mo, is about 2, which agrees well with promotion factors found in

high surface area catalysts [18]. The calcined CoMo/SiO_2 catalyst has a somewhat lower activity. Although the XPS spectra of both uncalcined and calcined catalysts showed no visible difference, the activities are different. A plausible explanation is that during calcination to 500 ^{0}C some sintering occurs, resulting in larger MoS_2 slabs. Larger MoS_2 slabs expose less edge sites available for Co, and posses less active sites. The influence of calcination on the particle size and spreading will be studied with TEM and AFM in the future.

CoMoNTA/SiO_2. Figure 2.5 shows that complexing Co and Mo with the NTA agent retards the sulfidation behaviour of Co significantly, while that of Mo remains more or less unchanged. This has a drastic influence on the sulfidation order of Co vs. Mo. Looking at the XPS spectra after sulfidation at 175 ^{0}C in Figure 2.5 it is seen that the sulfidation of Mo is almost completed at the temperature when Co has just started. Due to the presence of NTA, the sulfidation of Co now lags behind that of Mo and thus occurs in the presence of preformed MoS_2.

The activity measurements in Figure 2.7 show that the CoMoNTA/SiO_2 model catalysts, expected to consist exclusively of the highly active CoMoS phase [5], is indeed by far the most active one. Especially the relative amounts of secondary products, trans-2-butene and cis-2-butene, are large. The activity of the CoMoNTA catalysts is a factor 2 to 3 higher than the CoMo catalyst. Both results agree well with activity measurements on high surface area catalysts [18].

The picture that emerges from XPS and activity measurements is thus that CoMo catalysts in which molybdenum sulfidation precedes that of cobalt yield the highest activity. The order of sulfidation makes it possible to first form MoS_2 slabs after which Co can sulfide and can move to the edges, which result in the formation of the CoMoS phase. Hence, retardation of cobalt sulfidation during the activation of CoMo catalysts is the key for making active hydrodesulfurization catalysts. This is only partially achieved in silica-supports impregnated with an aqueous mixture of common precursors such as cobalt nitrate and ammonium heptamolybdate. The effect is optimally utilized when a complexing agent such as NTA is present, which releases the cobalt at a stage where molybdenum sulfide particles have already been (partially) formed. Similar observations were made for high surface area NiMo-NTA/SiO_2 studied with EXAFS and TPS [19].

2.5 Conclusions

The present paper illustrates that flat, conducting supports are useful tools in studies of catalyst preparation. Such model studies can indeed have industrial relevance, provided it is taken care that

- The model support is sufficiently thick to be representative for industrial carriers. According to Gunter et al. [7] the thickness of silica and alumina should be at least 3 nm to this end.
- The support is fully hydroxylized. For silica this implies that the number of OH groups should be around 4-5 per nm^2.
- The catalytically active materials are applied via wet chemical impregnation procedure as used by industry. Anchoring reactions, such as between negative molybdate ions in

solution and positive OH_2^+ entities on the surface can straightforwardly be applied. Pore volume impregnation is successfully mimicked by spincoating [13,14].

In this paper it was shown that SiO_2-supported CoMo model catalysts have representative activity in the hydrodesulfurization of thiophene. This confirms that these models of HDS catalysts are indeed realistic. From the sulfidation behaviour of Mo and Co, as studied by XPS, and the HDS activity of the catalysts, it was concluded that the key step in the active phase formation is the retardation of the sulfidation of Co. Chelating agents, e.g. nitrilo triacetic acid (NTA), form stable complexes with Co thereby retarding the sulfidation of Co to temperatures where Mo is already (partially) sulfided. This change in order of sulfidation, i.e. sulfidation of Mo preceding that of Co, is the ideal condition for CoMoS formation. In CoMo catalysts without chelating agents the sulfidation of Co is also retarded compared to Co catalysts due to a Co-Mo interaction. Despite this interaction the sulfidation of Co still precedes that of Mo, resulting in less active phase.

References

[1] H. Topsøe, B.S. Clausen and F.E. Massoth, "Hydrotreating Catalysis", Springer-Verlag, Berlin, 1996.

[2] R. Prins, V.H.J. de Beer and G.A. Somorjai, *Catal. Rev.-Sci. Eng.* **31** (1989) 1.

[3] H. Topsøe and B.S. Clausen, *Catal. Rev.-Sci. Eng.* **26** (1984) 395.

[4] S.M.A.M. Bouwens, F.B.M. van Zon, M.P. van Dijk, A.M. van der Kraan, V.H.J. de Beer, J.A.R. van Veen and D.C. Koningsberger, *J. Catal.* **146** (1994) 375.

[5] J.A.R. van Veen, E. Gerkema, A.M. van der Kraan and A. Knoester, *J. Chem. Soc., Chem. Commun.* **22** (1987) 1684.

[6] M.S. Thompson, European patent application 0.181.031.A2 (1986).

[7] P.L.J. Gunter, J.W. Niemantsverdriet, F.H. Ribeiro and G.A. Somorjai, *Catal. Rev.-Sci. Eng.* **39** (1997) 77.

[8] J.C. Muijsers, Th. Weber, R.M. van Hardeveld, H.W. Zandbergen and J.W. Niemantsverdriet, *J. Catal.* **157** (1995) 698.

[9] A.M. de Jong, H.J. Borg, L.J. van IJzendoorn, V.G.M.F. Soudant, V.H.J. de Beer, J.A.R. van Veen and J.W. Niemantsverdriet, *J. Phys. Chem.* **97** (1993) 6477.

[10] A.M. de Jong, V.H.J. de Beer, J.A.R. van Veen and J.W. Niemantsverdriet, *J. Phys. Chem.* **100** (1996) 17722.

[11] P.A. Spevack and N.S. McIntyre, *J. Phys. Chem.* **97** (1993) 11031.

[12] N.S. McIntyre, T.C. Chan, P.A. Spevack and J.R. Brown, *Appl. Catal.* **63** (1990) 391.

[13] E.W. Kuipers, C. Laszlo and W. Wieldraaijer, *Catal. Lett.* **17** (1993) 71.

[14] R.M. van Hardeveld, P.L.J. Gunter, L.J. van IJzerdoorn, W. Wieldraaijer, E.W. Kuipers and J.W. Niemantsverdriet, *Appl. Surf. Sci.* **84** (1995) 339.

[15] Alstrup, I. Chorkendorff, R. Candia, B.S. Clausen and H. Topsøe, *J. Catal.* **77** (1982) 397.

[16] Th. Weber, J.C. Muijsers and J.W. Niemantsverdriet, *J. Phys. Chem.* **99** (1995) 9194.

[17] Th. Weber, J.C. Muijsers, J.H.M.C. van Wolput, C.P.J. Verhagen and J.W. Niemantsverdriet, *J. Phys. Chem.* **100** (1996) 14144.

[18] M.J. Vissenberg, Ph.D. thesis, Schuit Institute of Catalysis, Eindhoven University of Technology, Eindhoven, The Netherlands (1999).

[19] L. Medici and R. Prins, *J. Catal.* **163** (1996) 38

3

Correlation between hydrodesulfurization activity and order of Ni and Mo sulfidation in planar silica-supported NiMo catalysts: the influence of chelating agents*

Abstract

Surface science models of silica-supported NiMo catalysts have been prepared to study the formation of the active phase (NiMoS) in hydrotreating catalysts. Combination of XPS and thiophene hydrodesulfurization (HDS) measurements shows that the key step in the formation of the NiMoS phase is the order in which Ni- and Mo-precursors transfer to the sulfidic state. In NiMo systems prepared by conventional methods the sulfidation of Ni precedes that of Mo. However, complexing Ni to chelating agents like nitrilo triacetic acid (NTA), ethylene diamine tetraacetic acid (EDTA) and 1,2-cyclohexane diamine tetraacetic acid (CyDTA) retard the sulfidation of Ni. For EDTA and CyDTA the Ni sulfidation is delayed to temperatures where MoS_2 is already completely formed. These catalysts show the highest activity in thiophene HDS, indicating that complete sulfidation of Mo preceding that of Ni provides the ideal circumstances for NiMoS formation.

* This chapter was published as: L. Coulier, V.H.J. de Beer, J.A.R. van Veen, and J.W. Niemantsverdriet, *J. Catal.* **197** (2001) 26.

3.1 Introduction

Catalysts used in hydrotreating of oil fractions consist of sulfides of molybdenum or tungsten, promoted with cobalt or nickel supported on alumina. In catalysts based on molybdenum, the active phase is the so-called CoMoS phase, which consists of sulfided Co decorating the edges of MoS_2 slabs [1-3]. Van Veen et al. [4,5] showed that the highly active CoMoS II phase can be synthesized by using nitrilo triacetic acid (NTA) in the case of Al_2O_3-supported catalysts. For molybdenum-based catalysts with Ni as promoter a NiMoS phase analogous to the CoMoS phase has been reported [6-8].

Silica-supported CoMo catalysts exhibit low hydrotreating activity compared to the γ-Al_2O_3-supported catalysts [5]. Adding chelating agents, like NTA, proved to be a way to prepare hydrotreating catalysts on any support with similar hydrotreating activity as their γ-Al_2O_3 supported counterparts [4,5,9].

Prins and coworkers [10-12] have shown that addition of chelating agents, such as NTA, ethylene diamine tetraacetic acid (EDTA) and ethylene diamine (ED) has a similarly favorable effect on high surface area NiMo/SiO_2 catalysts. TPS and EXAFS studies show that adding chelating agents to the impregnating solutions prevents the sulfidation of Ni at low temperature, thereby increasing the formation of the NiMoS phase, as was deduced from the increased activity in thiophene HDS [10]. De Jong et al. [13] and Coulier et al. [14] showed that the same effect, i.e. stabilization of cobalt against sulfidation, explains the role of NTA in enabling the formation of CoMoS in silica- and alumina-supported CoMo catalysts. Shimizu et al. [15,16] reported that adding chelating agents in the preparation also has a beneficial effect for the dibenzothiophene (DBT) HDS activity of Al_2O_3-supported CoMo catalysts, although a little effect was observed for NiMo catalysts. Van Veen et al. [8] found that NiMo-NTA/Al_2O_3 catalysts are even less active in DBT HDS than NiMo/Al_2O_3 catalysts. Both studies were carried out at high pressures (3-5 MPa).

Model catalysts, consisting of a flat conducting substrate with a thin SiO_2 or Al_2O_3 layer on top of which the active phase is deposited by spincoating [17,18], have been successful in the field of HDS catalysis research [13,14,19]. The advantage of these model systems, having a conducting substrate, is that sample charging is largely eliminated, resulting in much better resolution of XP spectra with respect to high surface area catalysts [20]. In an earlier publication it was concluded that in the case of CoMo supported on flat SiO_2/Si(100) supports, these model catalysts showed representative activity in thiophene HDS, confirming that these are realistic models of HDS catalysts [13,14].

In this article SiO_2-supported NiMo model catalysts are used to study the formation of the active phase during sulfidation and the influence of various chelating agents. By comparing the stepwise sulfidation studied by semi in-situ X-ray Photoelectron Spectroscopy and the thiophene hydrodesulfurization activity we show that the extent to which chelating agents retard the conversion of nickel to sulfides with respect to that of molybdenum correlates directly with the activity of the catalysts for thiophene HDS. By using the appropiate chelating agent, the HDS activity of NiMo/SiO_2 model catalysts can be optimized. A parallel comparison of the role of chelating agents on CoMoS formation in CoMo/SiO_2 catalysts has been published elsewhere [14].

3.2 Experimental

$NiMo/SiO_2/Si$ model catalysts were prepared in the same way as the CoMo system described in detail earlier [14]. Briefly, a silica model support was prepared by oxidizing a Si(100) wafer in air at 750 ^{0}C for 24 hr. After oxidation the wafer was cleaned in a mixture of H_2O_2 and NH_4OH at 65 ^{0}C. The surface was rehydroxylated by boiling in water for 30 min. Next this model support was covered with the impregnation solution, containing the catalyst precursor compounds, and dry-spinned in a homemade spincoat apparatus in N_2 atmosphere with 2800 rpm. The catalyst precursors were nickel nitrate ($Ni(NO_3)_2 \cdot 6H_2O$, Merck) and ammonium heptamolybdate. The concentration of Ni and Mo were adjusted to obtain loadings of 2 Ni and 6 Mo atoms/nm^2 after spincoating, as calculated according to reference [18]. After spincoating the catalysts were calcined in 20% O_2/Ar at 500 ^{0}C for 60 min at a rate of 5 ^{0}C/min. For comparison, uncalcined samples were measured as well; these will be indicated as $NiMo/SiO_2$ uncalc.

Catalysts containing chelating agents were prepared by spincoating the support with ammoniacal solutions containing MoO_3, nickel nitrate and the chelating agent as described by Van Veen et al. [4]. The amount of chelating agents was adjusted as to complex both Ni and Mo, except for ethylene diamine (ED) where a Ni:ED ratio of 1:4 was taken [11,12]. Chelating agents used were nitrilo triacetic acid (NTA) (Acros Organics), ethylene diamine tetraacetic acid (EDTA) (Merck, p.a.), ethylene diamine (ED) (Fluka, p.a.) and 1,2-cyclohexane diamine tetraacetic acid (CyDTA) (Fluka, p.a.). The notation NiMo-NTA/SiO_2/Si(100) refers to a catalyst to which NTA was added in the preparation.

Sulfidation of the catalysts was carried out in a glass tube reactor in 10% H_2S/H_2. The catalysts were heated at a rate of 5 ^{0}C/min (chelating agents: 2 ^{0}C/min) to the desired temperature and kept there for 30 min. After sulfidation, the reactor was cooled to room temperature under a helium flow and brought to the glovebox, where the model catalyst was mounted in a transfer vessel for transport to the XPS under N_2 atmosphere.

XPS spectra were measured on a VG Escalab 200 MK spectrometer equipped with an Al Kα source and a hemispherical analyzer connected to a five-channel detector. Measurements were done at 20 eV pass energy. Energy correction was performed by using the Si 2p peak of SiO_2 at 103.3 eV as a reference. Binding energies were determined with a precision of ± 0.2 eV. In a few cases a shift in binding energy of Ni and Mo was observed at high sulfidation temperature due to the increased conductivity of the sulfide phase. XPS spectra have been corrected for this.

Thiophene HDS activity measurements were carried out in batch mode under standard conditions (1.5 bar, 400 ^{0}C) after presulfidation at 400 ^{0}C, for details see [14].

3.3 Results

3.3.1. Sulfidation of nickel and molybdenum

Ni/SiO_2. Figure 3.1 shows the Ni 2p and the S 2p XPS spectra of a Ni/SiO_2 model catalyst, after sulfidation at various temperatures. The Ni 2p spectrum of the unsulfided catalyst shows the characteristic pattern of oxidic nickel with the Ni $2p_{3/2}$ peak at 856.8 eV and a shake up feature at higher binding energy [21]. The binding energy of 856.8 eV

corresponds well with that of Ni_2O_3 [21]. Sulfidation at room temperature shows the appearance of a second doublet at lower binding energy. At higher temperatures this doublet increases in intensity, while the doublet with Ni $2p_{3/2}$ at 856.8 eV decreases and disappears at temperatures above 50 ^{0}C. The Ni $2p_{3/2}$ peak at 853.8 eV after sulfidation at high temperatures corresponds well with that of bulk nickel sulfide, Ni_3S_2 [21]. The Ni 2p doublet of nickel sulfide also shows shake up features at higher binding energy, but the intensity of the peaks is less than in the case of oxidic nickel. The binding energy of the S 2p doublet in Figure 3.1 is 161.8 eV, which agrees with that of sulfur in the S^{2-} state. The S 2p spectra confirm that the sulfidation of nickel oxide starts already at room temperature and is completed at 100 ^{0}C. Sulfidation of uncalcined Ni/SiO_2 and Ni/SiO_2 with different Ni loadings yielded similar XPS spectra as in Figure 3.1.

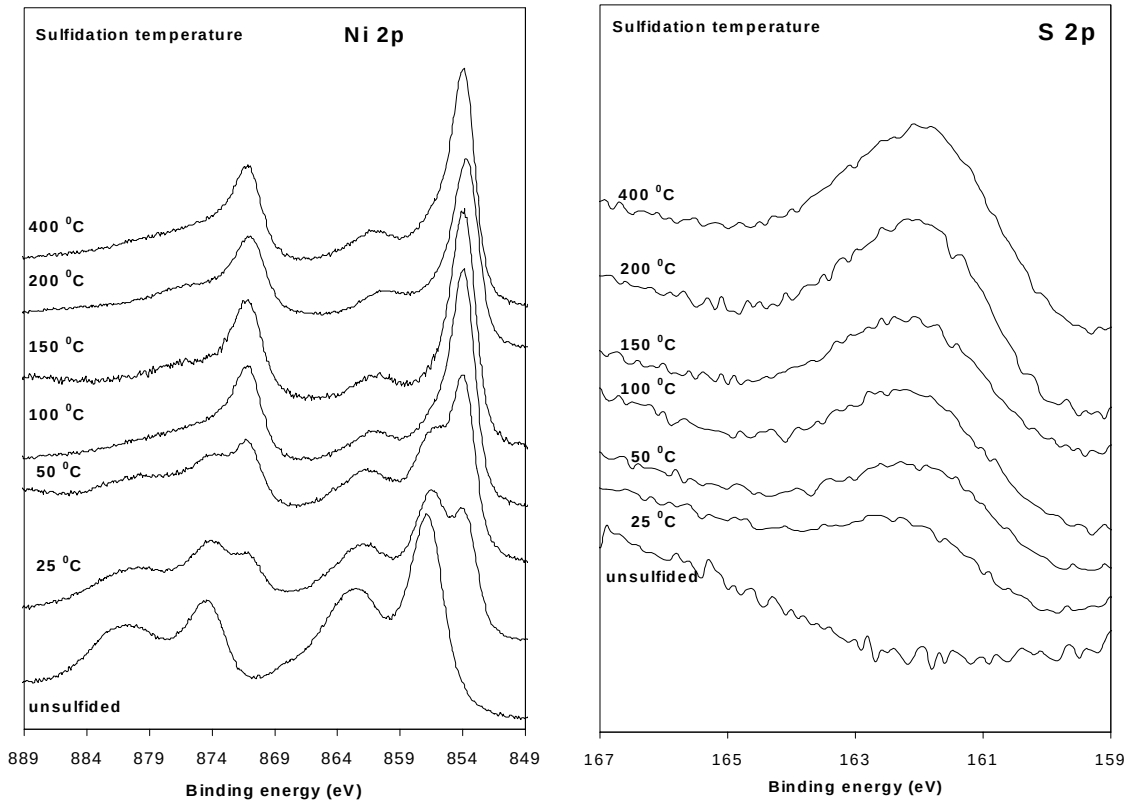

Figure 3.1 *Ni 2p (left) and S 2p (right) spectra of calcined $NiO_x/SiO_2/Si(100)$ model catalysts sulfided in 10% H_2S/H_2 for 30 min at various temperatures, showing that nickel oxide is already converted to bulk nickel sulfide at low temperatures.*

Figure 3.2 shows the Ni 2p and N 1s XPS spectra of Ni-EDTA/SiO_2/Si(100) catalysts as a function of sulfidation temperature. The Ni 2p spectra show that the sulfidation of Ni is retarded to temperatures above 200 ^{0}C. The sulfidation is complete at 300 ^{0}C. The Ni $2p_{3/2}$ binding energy of the fully sulfided Ni-EDTA catalysts of 853.8 eV indicates that Ni_3S_2 is formed at high sulfidation temperatures, despite the retardation (see Table 2). The N 1s spectra, resulting from the EDTA agent, show the decrease of the N 1s peak intensity at temperatures above 200 ^{0}C, which results from the decomposition of the Ni-EDTA complexes. This coincides well with the sulfidation of Ni observed from the Ni 2p spectra.

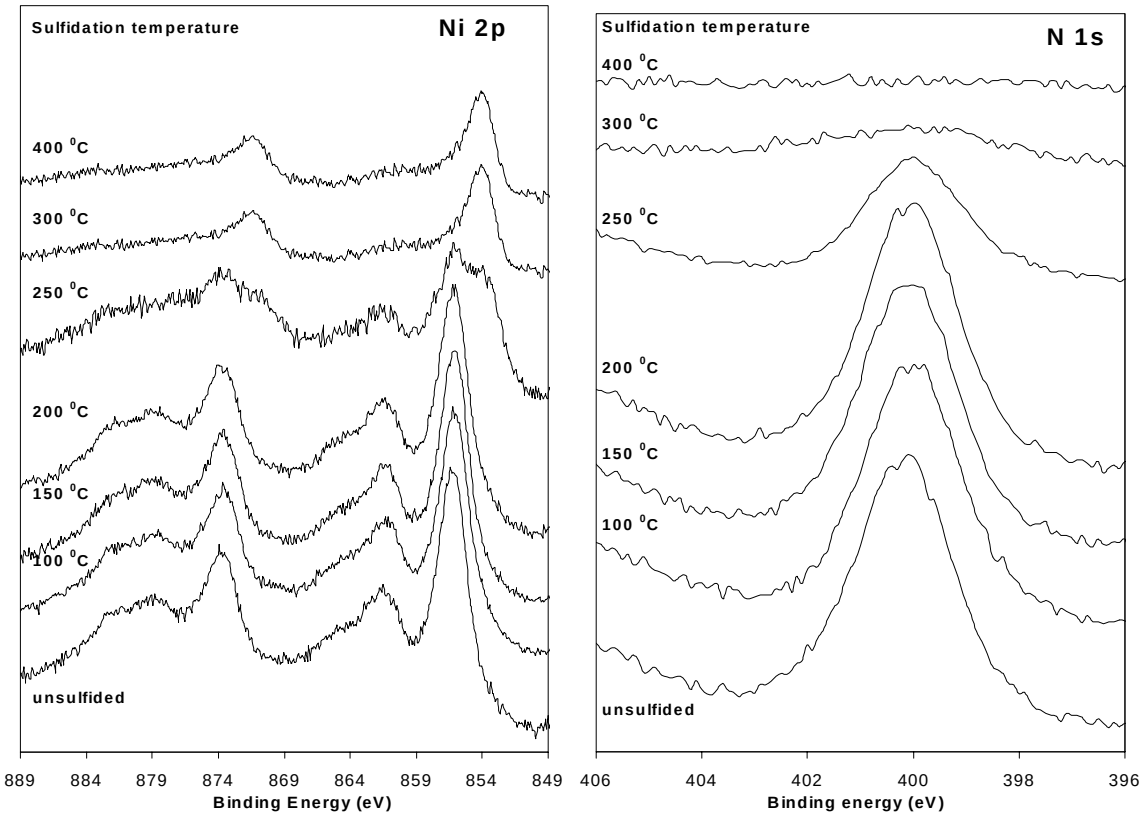

Figure 3.2 *Ni 2p (left) and N 1s (right) XPS spectra of Ni-EDTA/SiO_2/Si(100) model catalysts sulfided at various temperatures show that sulfidation of Ni is retarded to high temperatures due to the presence of the EDTA agent.*

Mo/SiO_2. The sulfidation behavior of molybdenum was described in earlier papers [13,14,19,22-24]. Briefly, the sulfidation of Mo proceeds at moderate temperatures, starting around 50 ^{0}C. Complete transformation to MoS_2 occurs at temperatures above 150 ^{0}C. Note that these temperatures are significantly higher than for the sulfidation of Ni/SiO_2 in Figure 3.1. The Mo 3d spectra of the catalysts sulfided at intermediate temperatures can be all interpreted in terms of Mo^{6+}, Mo^{5+} and Mo^{4+} doublets as described in an earlier paper [13,19]. Addition of chelating agents in the preparation stage did not affect the sulfidation behaviour of Mo significantly, except for an almost 1 eV decrease in the binding energy of the unsulfided catalyst as compared to standard MoO_3 due to complexation (see the example of Mo-NTA in Table 3.1). Sulfidation of Mo at high temperatures leads to complete transition to MoS_2, as in Mo/SiO_2 without chelating agents.

NiMo/SiO_2. Figure 3.3 shows the Ni 2p and Mo 3d spectra of NiMo/SiO_2 in different stages of sulfidation. The Mo 3d spectra are identical to those of Mo/SiO_2 [14]. However, the Ni 2p spectra reveal slower conversion of nickel to the sulfidic state than in Ni/SiO_2 (see Figure 3.1). The sulfidation of Ni starts at temperatures around 100 ^{0}C, which is 75^{0}C higher than for the calcined Ni/SiO_2 catalyst. At these temperatures a second doublet with small shake up features appears at a Ni $2p_{3/2}$ binding energy of 854.2 eV. Above 150 ^{0}C the sulfidation is complete. The binding energy of the sulfided Ni is 0.4 eV higher than that of

sulfided Ni/SiO_2. Comparing Ni and Mo, one observes that the rates of sulfidation are similar, with the start around 50 ^{0}C and completion between 150 ^{0}C and 200^{0}C.

The XPS spectra of uncalcined NiMo/SiO_2 catalysts (not shown) are similar to those of the single-phase catalysts. Sulfidation of Ni precedes that of Mo, although the temperature regime where sulfidation occurs shows some overlap. Noteworthy is that the binding energy of sulfided Ni in uncalcined NiMo/SiO_2 equals that of the sulfided Ni-only catalysts.

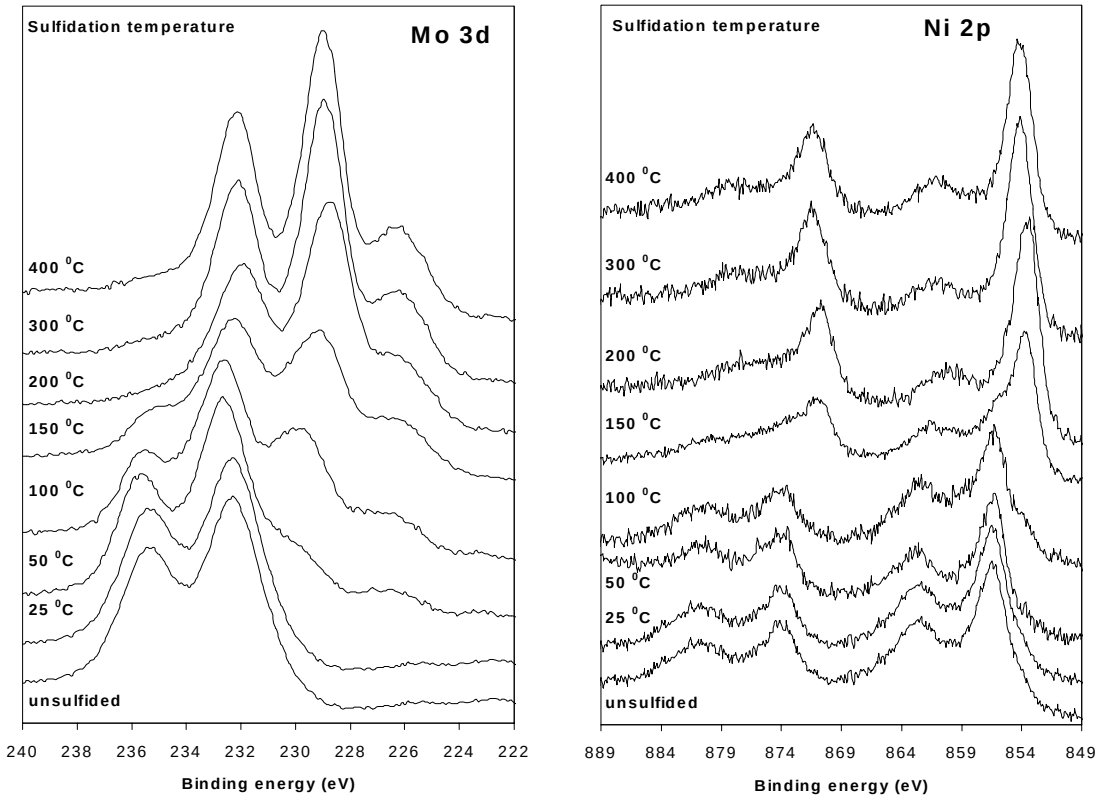

Figure 3.3 *Mo 3d (left) and Ni 2p (right) XPS spectra of a calcined $NiO_x/MoO_3/SiO_2/Si(100)$ model catalyst during sulfidation at different temperatures. The spectra show that the sulfidation of Ni is retarded due to a Ni-Mo interaction, resulting in simultaneous sulfidation of Ni and Mo.*

3.3.2 Influence of chelating agents on the sulfidation behaviour of Ni and Mo

NiMo-EDTA/SiO_2. Figure 3.4 shows the Ni 2p and Mo 3d spectra of a NiMo-EDTA/SiO_2 sulfided at various temperatures. The Mo 3d spectrum of the fresh catalyst shows one doublet with a Mo $3d_{5/2}$ binding energy of 232.2 eV characteristic of molybdenum complexed to chelating agents, as discussed above. The sulfidation behaviour of Mo is identical to that of Mo/SiO_2 and NiMo/SiO_2, with conversion to sulfides starting around 50 ^{0}C and being complete above 150 ^{0}C. The doublet with Mo $3d_{5/2}$ binding energy at 229.0 eV is characteristic for MoS_2.

The Ni 2p spectra show that EDTA retards the sulfidation of Ni significantly. The spectrum of the fresh catalyst shows a single doublet with Ni $2p_{3/2}$ at 856.1 eV, corresponding to Ni complexed to EDTA, and shake up features at higher binding energy. Sulfidation does

not start until temperatures around 200 ^{0}C where a second doublet at lower binding energy appears. The sulfidation is complete at 300 ^{0}C. The same sulfidation behaviour was observed for Ni-EDTA/SiO_2 catalysts as described earlier. Note however that the Ni $2p_{3/2}$ binding energy of the sulfided Ni in NiMo-EDTA/SiO_2, i.e. 854.1 eV, is 0.3 eV higher than that of the fully sulfided Ni-EDTA/SiO_2 catalyst (853.8 eV).

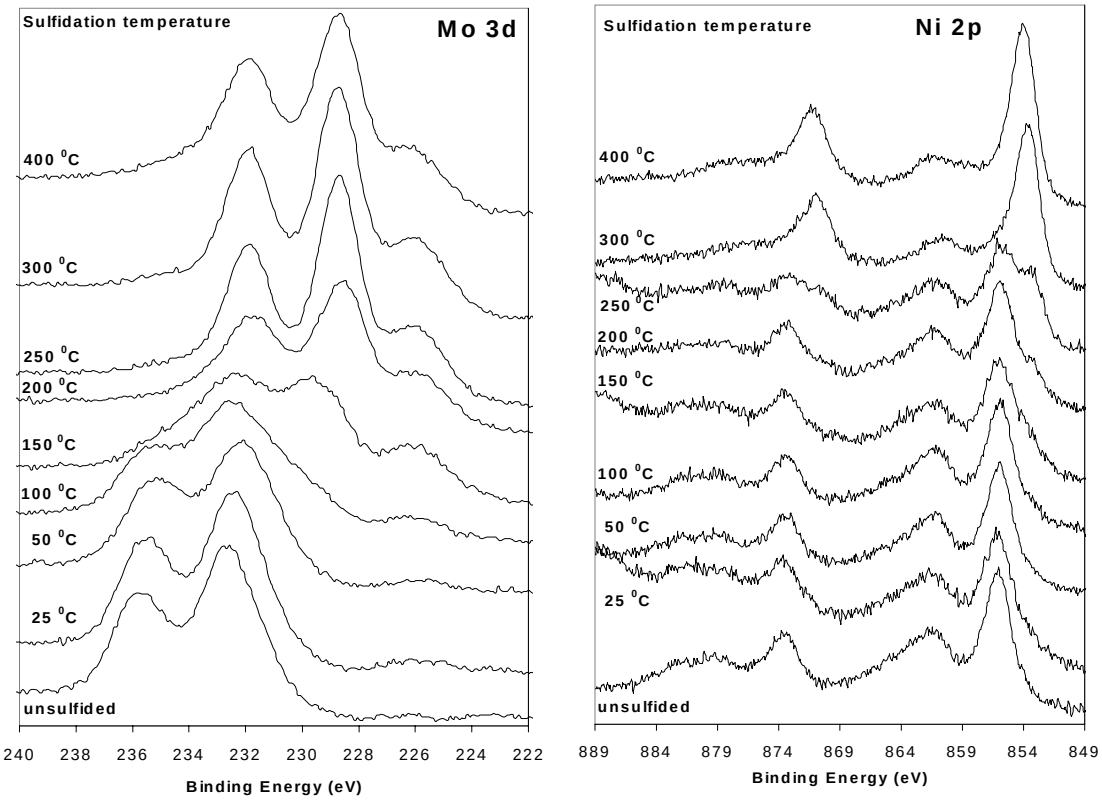

Figure 3.4 *Mo 3d (left) and Ni 2p (right) XPS spectra of NiMo-EDTA/SiO_2/Si(100) model catalysts. EDTA retards the sulfidation of Ni to high temperatures, where Mo is already completely sulfided.*

XPS studies on NiMo-CyDTA/SiO_2 catalysts revealed that CyDTA retards the sulfidation of Ni to even higher temperatures than EDTA does. The situation is very similar to that in the NiW-CyDTA system, as we published recently [25].

NiMo-NTA/SiO_2. The XPS spectra of the sulfided NiMo-NTA/SiO_2/Si(100) model catalysts are shown in Figure 3.5. While the Mo 3d spectra are similar to that in Figure 3.4, the Ni 2p spectra differ. It is clearly visible that the sulfidation of Ni is retarded to temperatures above 125 ^{0}C due to the presence of the NTA complex. This corresponds well with the sulfidation of CoMo-NTA/SiO_2 as published earlier [14]. However the retarding effect is not as strong as in the case of EDTA. As a result, there exists some overlap in temperature regime in which Ni and Mo convert to the sulfidic state, whereas with EDTA as chelating agent Ni and Mo convert to sulfides in fully separated temperatures regions. The Ni $2p_{3/2}$ binding energy of the nickel in the sulfidic state (854.2 eV) equals that in NiMo-EDTA/SiO_2 and differs from that of bulk nickel sulfide (see Table 3.2).

NiMo-ED/SiO_2. Figure 3.6 shows the effect of ethylene diamine (ED) on the sulfidation of nickel in the Ni 2p and N 1s (containing also the Mo $3p_{3/2}$) spectra of NiMo-ED/SiO_2. The Mo 3d spectra are not shown because they are similar to that of NiMo/SiO_2 in Figure 3.3. The Ni $2p_{3/2}$ peak in the spectrum of the fresh catalyst has a binding energy of 856.0 eV (Table 3.1), which is significantly lower than that of oxidic Ni and therefore can be attributed to Ni complexed to ED. Sulfidation is revealed by the Ni 2p spectra, while the N 1s spectra monitor the presence of ED in the catalyst. Sulfidation of Ni starts already at room temperature and appears complete at 100 ^{0}C. The N 1s peak at 400 eV decreases in intensity but remains visible to temperatures up to 200^{0}C, indicating that ED is still present in small amounts. The Ni $2p_{3/2}$ binding energy is 853.8 eV after sulfidation up to 200^{0}C but increases to 854.3 eV after sulfidation at 400^{0}C. The sulfidation of Mo is complete above 150^{0}C. Hence, the Ni sulfide assumes its final form at temperatures above those where Mo is fully sulfided.

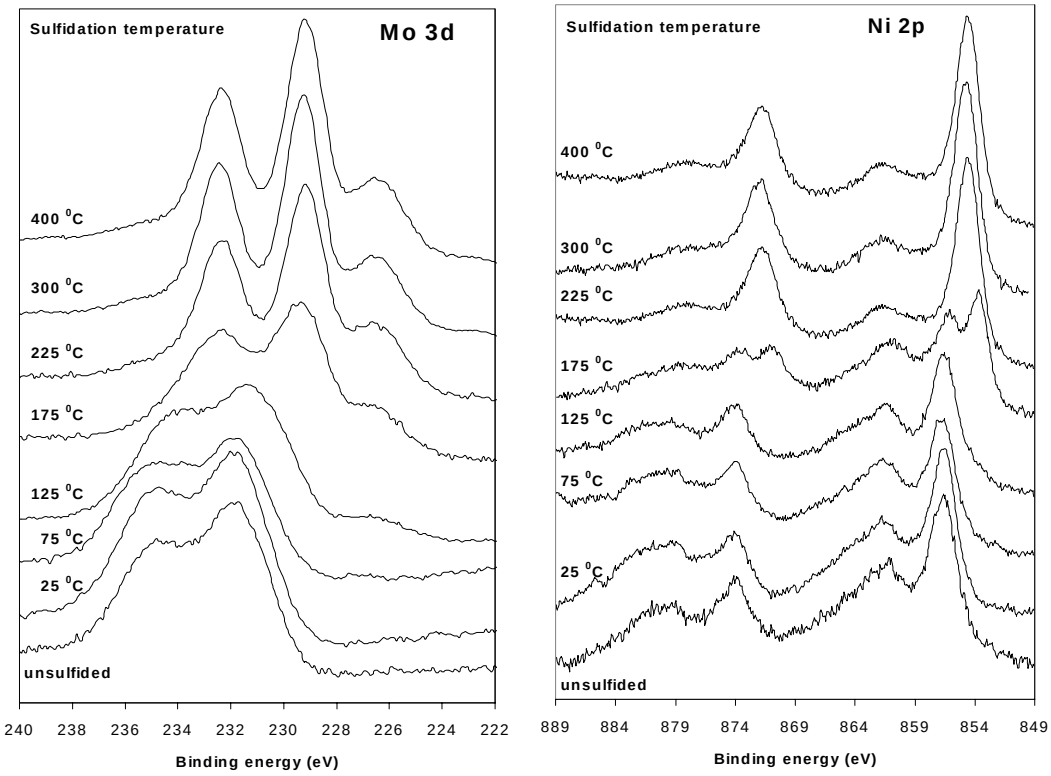

Figure 3.5 *Mo 3d and Ni 2p XPS spectra of NiMo-NTA/SiO_2/Si(100) model catalysts during sulfidation at various temperatures. The spectra show that NTA retards the sulfidation of Ni, but to a lesser extent than EDTA.*

Table 3.1 *Mo 3d and Ni 2p XPS binding energies of fresh NiMo/SiO_2 catalysts*

Catalyst prepared	Mo $3d_{5/2}$ (eV)	Ni $2p_{3/2}$ (eV)
Without chelating agents	232.8 ± 0.2	856.6 ± 0.2
With ethylene diamine (ED)	232.5 ± 0.2	856.0 ± 0.2
With NTA, EDTA or CyDTA	232.2 ± 0.2	856.2 ± 0.2

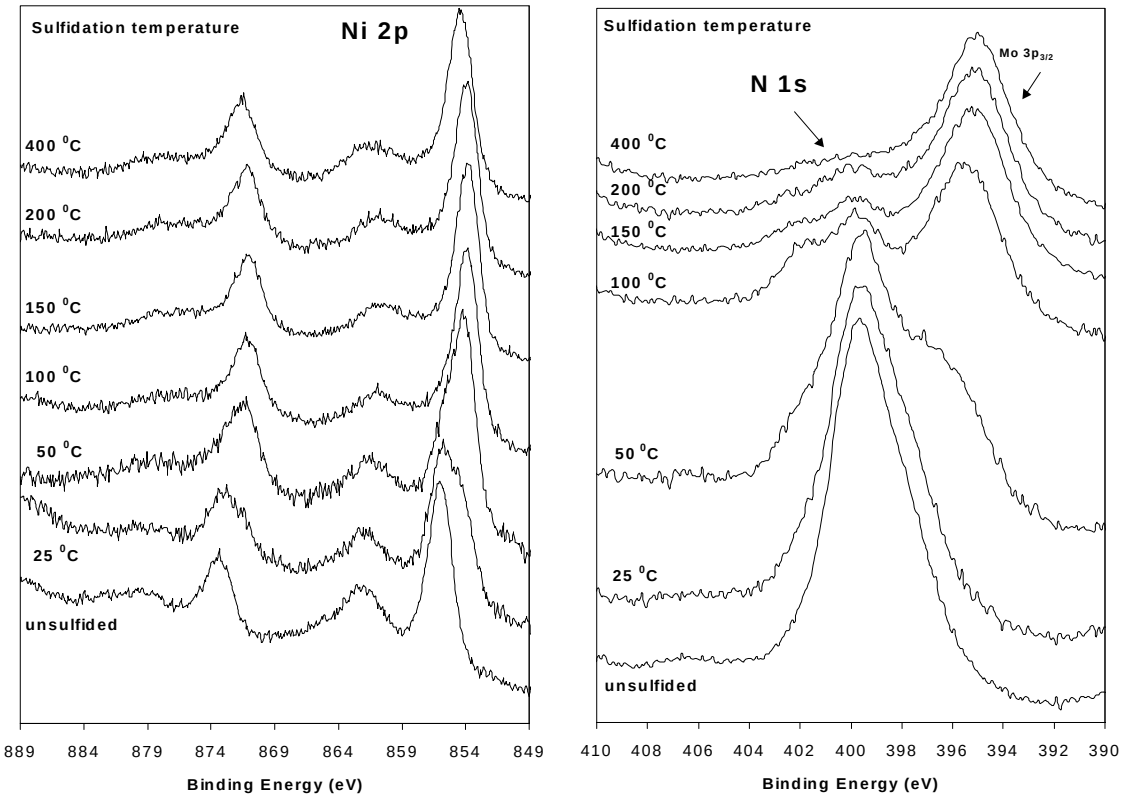

Figure 3.6 *Ni 2p and N 1s XPS spectra of NiMo-EN/SiO_2/Si(100) model catalysts sulfided in 10% H_2S/H_2 for 30 min at various temperatures.*

3.3.3 HDS activity measurements

Demonstrating that the planar model systems are catalytically active in hydrodesulfurization is the most convincing test for the validity of the model approach and enables us to make correlations between sulfidation and catalytic behavior. To this end, batch thiophene HDS activity measurements were performed on all model systems.

Figure 3.7 shows an example of such an experiment on a NiMo-NTA/SiO_2/Si(100) model catalysts. The figure shows the yield of C_4-products and the total conversion as a function of reaction time. It is clearly visible that the conversion increases linearly with time, indicating that no significant deactivation occurs. The product distribution in Figure 3.7 shows the most important products, 1-butene, trans-2-butene, and cis-2-butene. We also observed some minor quantities of C_1-C_3 cracking products (not shown).

Figure 3.8 compares the activity of the different model catalysts in thiophene HDS discussed in this paper. The activity is expressed as yield of products per 5 cm^2 of catalyst after 1 hour of batch reaction at 400 ^{0}C and has been corrected for blank measurements (bare silica support and empty reactor).

The activity of Ni/SiO_2 is low, although noticeably and corresponds to a pseudo turnover frequency of $1.8*10^{-3}$ thiophene per Ni atom per second. Low activities were also found for uncalcined Ni/SiO_2 and Ni-NTA/SiO_2 (not shown). Mo/SiO_2 shows a somewhat higher activity than Ni/SiO_2, but the yield is still low (< 0.5 %). For Mo-NTA/SiO_2 the same

activity was observed as for Mo/SiO_2. The synergistic effect of Ni and Mo is clearly visible from the large increase in activity of e.g. NiMo/SiO_2 compared to Mo/SiO_2. The activity of calcined NiMo/SiO_2 is higher then that of uncalcined NiMo/SiO_2, which we attribute to an increase in Ni-Mo interaction due to calcination, as will be explained in the discussion.

The highest activities are observed in NiMo/SiO_2 catalysts prepared with chelating agents, as Figure 3.8 shows. The relative amount of secondary products, i.e. t-2-butene and c-2-butene, becomes appreciably higher than in the product distribution of the less active catalysts. The inset in Figure 3.8 shows a selectivity plot of the total yield of 2-butenes (%) against the total conversion. The straight line confirms that the variations in product distribution observed with the different catalysts are caused by a kinetic effect. The same trend could be observed in Figure 3.7 for NiMo-NTA/SiO_2. At short reaction times, i.e. low conversions, 1-butene was the dominant product while at longer reaction times, i.e. higher conversions, the relative amount of trans-2-butene and cis-2-butene increased. After a reaction time of 60 min c-2-butene became even the dominant product. NiMo-EDTA/SiO_2 and NiMo-CyDTA/SiO_2, for which the sulfidation of Mo precedes that of Ni and sulfidation takes place in separate temperature regimes, appears to be the most active catalyst. The thiophene conversion into C_4-olefins is roughly a factor of 6-10 higher than that of the standard NiMo/SiO_2 catalyst.

If we arrange the catalysts into groups with low, standard and enhanced HDS activity, we find a correlation between HDS activity and state of Ni in the sulfided catalyst as expressed by the Ni $2p_{3/2}$ binding energy, see Table 3.2.

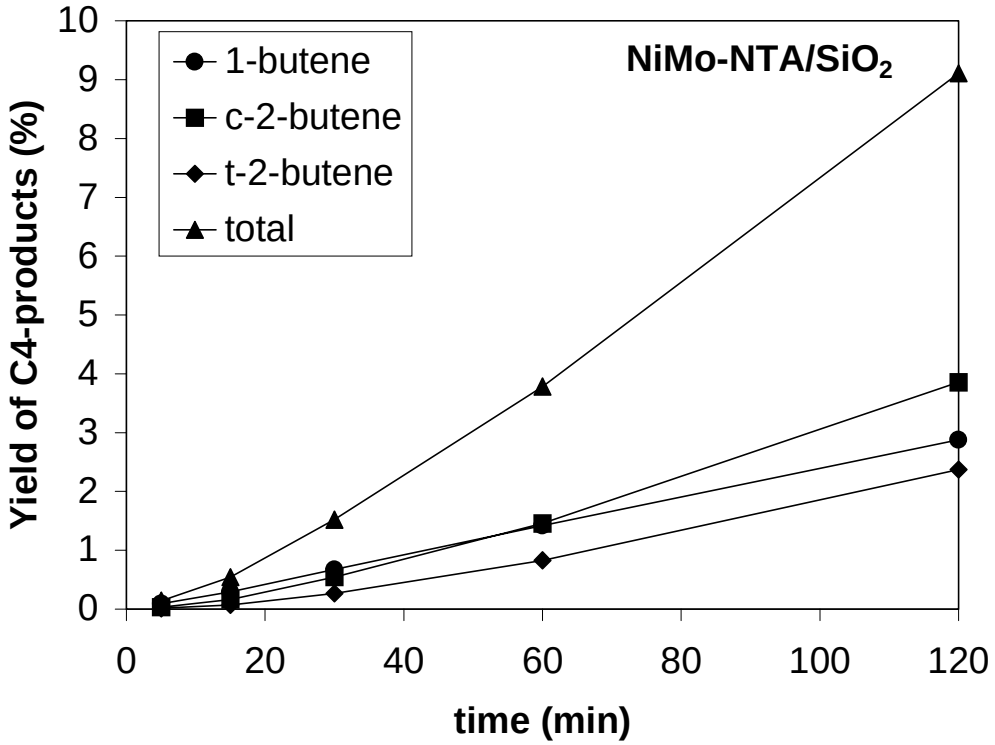

Figure 3.7 *Thiophene hydrodesulfurization experiment on a NiMo-NTA/SiO_2 model catalyst. The figure shows the yield of C_4-products and the total conversion in a batch reaction at 400^0C as a function of reaction time.*

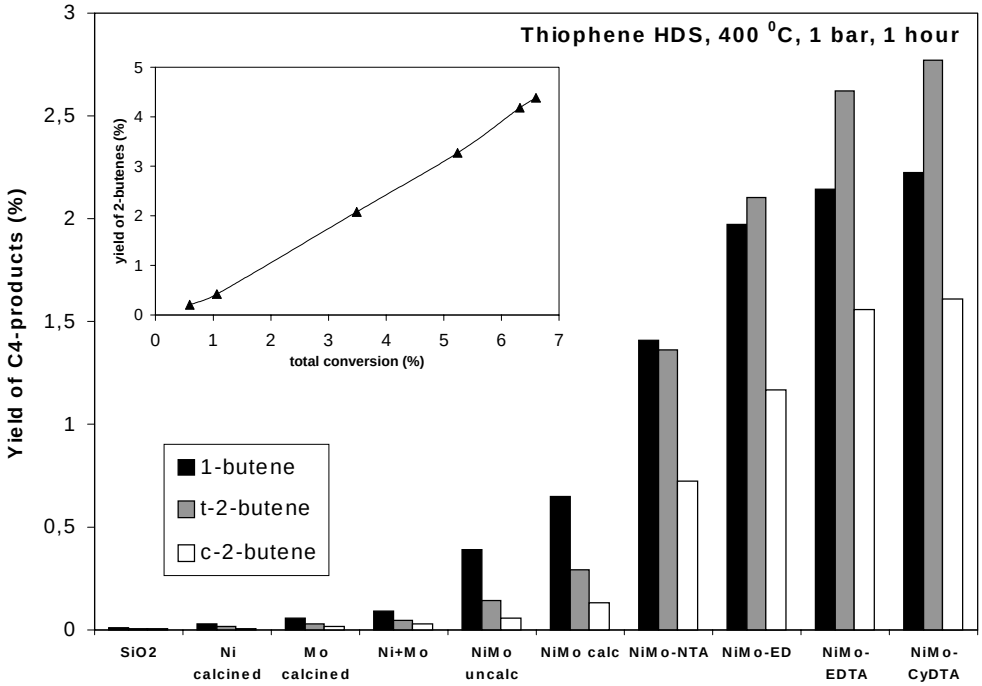

Figure 3.8 *Thiophene HDS product distribution measured for various SiO_2-supported sulfided Ni, Mo, and NiMo catalysts.*

Table 3.2 Mo 3d and Ni 2p *XPS binding energies of various sulfided NiMo/SiO_2 catalysts.*

	Mo $3d_{5/2}$ (eV)	Ni $2p_{3/2}$ (eV)
Low HDS activity		
Ni/SiO_2, Ni-NTA/SiO_2, Mo/SiO_2, Mo-NTA/SiO_2	228.9 ± 0.2	853.8 ± 0.2
Standard HDS activity		
NiMo-uncalc/SiO_2	228.9 ± 0.2	853.8 ± 0.2
NiMo-calc/SiO_2	229.0 ± 0.2	854.0 ± 0.2
Enhanced HDS activity		
All catalysts prepared with chelating agents	229.0 ± 0.2	854.2 ± 0.2

3.5 Discussion

The major conclusion from this work is that a clear correlation exists between the thiophene HDS activity of NiMo/SiO_2 model catalysts and the order in which the initially oxidic nickel and molybdenum convert into the sulfidic state during presulfidation in H_2S/H_2. Topsøe's CoMoS model [1-3], applied to the Ni-Mo system (NiMoS) offers a good basis for explaining the differences between the differently prepared catalysts dealt with in this paper. The observation of a NiMoS phase analogue to CoMoS has been proposed by others [6-8]. The structure of the NiMoS phase consists of sulfided nickel decorating MoS_2-slabs. The most favorable order for converting a mixture of nickel oxide and molybdenum oxide to the NiMoS phase would be to let molybdenum form MoS_2 slabs, after which nickel can decorate

the most reactive sites of the MoS_2, viz. those situated at the edges. This reversed order of sulfidation is best realized in the systems where CyDTA and EDTA are used as ligands for nickel, and the corresponding catalysts yield the most active NiMo combinations for thiophene HDS.

Below, the relation between sulfidation and activity properties will be briefly discussed for all catalysts studied.

Ni/SiO_2. The Ni 2p and S 2p spectra in Figure 3.1 show that the sulfidation of Ni/SiO_2 proceeds through oxygen-sulfur exchange. The transformation of nickel from the oxidic state to the sulfidic state is clearly visible from the shift in the binding energy to lower values (see also Table 3.1). The sulfidation starts already at room temperature and is completed around 100 ^{0}C. Comparing the binding energy at high sulfidation temperatures with binding energies of reference compounds, it appears that most probably Ni_3S_2 is present [21].

It is known that bulk nickel sulfide has low activity for thiophene HDS [3], which is confirmed by the low activity shown in Figure 3.8. As stated earlier, neither calcination nor the application of a higher nickel loading caused any measurable changes in sulfidation behavior of Ni. Sulfidation of these samples result in the formation of bulk nickel sulfide and yields catalysts with a low HDS activity (experiments not shown). A similar formation of bulk sulfides at low temperatures and thus a low HDS activity in the case of Co/SiO_2 model catalysts was reported in earlier paper [14].

Chelating agents have no effect on the HDS activity of Ni/SiO_2. Although EDTA retards the sulfidation of Ni to higher temperatures as was observed in Figure 3.2, it was concluded from the Ni $2p_{3/2}$ binding energy (Table 3.2) of the fully sulfided catalysts that bulk nickel sulfide was formed. Therefore the HDS activity of Ni-EDTA/SiO_2 is of the same order as that of Ni/SiO_2, as we indeed observed. Other chelating agents, e.g. NTA, probably have the same effect as was observed for Co-NTA/SiO_2 in earlier work [14].

Mo/SiO_2. As described earlier, the sulfidation of Mo takes place at moderate temperatures and through different intermediates [14,19]. The sulfiding mechanism proceeds by O-S exchange transforming oxidic Mo into MoS_2. In the intermediate temperature range Mo^{5+} and oxysulfide species are present [23,24]. It is known that supported MoS_2 slabs are active in HDS, which agrees with the observed thiophene HDS activity (Figure 3.8). No significant differences in activity were found between uncalcined and calcined Mo catalysts, as expected in view of their similar sulfidation behaviour. The same accounts for Mo-NTA/SiO_2. Although the fresh Mo-NTA catalyst contains Mo-atoms complexed to NTA (see Table 3.1), sulfidation at high temperature will form MoS_2-slabs independent of the initial state of Mo.

NiMo/SiO_2. The Ni 2p and Mo 3d XPS spectra of uncalcined NiMo/SiO_2 are similar to those of the single phase Ni and Mo catalysts. We therefore conclude that in an uncalcined catalyst the two elements Mo and Ni do not influence each other's sulfidation behavior. As a result, Ni sulfidation almost entirely precedes that of Mo, apart from some overlap. Hence, unless redispersion of nickel sulfide is invoked, at most only a minor part of the Ni atoms will be able to migrate to MoS_2 to form the NiMoS phase. The moderate increase in HDS activity of NiMo/SiO_2 compared to that of Mo/SiO_2 (see Figure 3.8) is in agreement with these ideas.

Calcination NiMo/SiO_2 has a beneficial effect on the HDS activity of the sulfided system, as seen in Figure 3.8. Interestingly, the XPS spectra show that due to calcination Ni sulfidation is retarded to higher temperatures: it starts at 100 ^{0}C (instead of 25^{0}C in Ni/SiO_2) and is completed around 200 ^{0}C (100 ^{0}C in Ni/SiO_2; see Figure 3.3). We attribute this to a Ni-

Mo interaction, although no clear proof is available at present. We encountered the same situation in the case of CoMo/SiO_2 model catalysts [14]. Comparison with XPS spectra of reference samples indicates that the presence of $NiMoO_4$, which has been suggested [26] to be an ineffective precursor of NiMoS formation, can be excluded. The interaction between Ni and Mo has consequences for the rate at which both components form sulfides. Although Mo sulfidation still lags behind that of Ni, there is a significantly larger temperature range where Ni and Mo sulfide simultaneously, with a greater chance to form the desired NiMoS phase. This explains the higher activity of the calcined NiMo/SiO_2 catalyst.

NiMo-NTA/SiO_2. Adding NTA to the impregnating solution leads to complexation of Ni and stabilizes Ni against sulfidation, whereas Mo sulfidation is not affected by the NTA ligands. As a result the sulfidation of Mo now partially precedes that of Ni as could be seen from Figure 3.5. This should be sufficient to enable formation of a relatively large amount of NiMoS phase. Indeed, the activity of sulfided NiMo-NTA/SiO_2, shown in Figure 3.8, is rather high. In earlier publications the same effect of NTA was observed for CoMo/SiO_2 model catalysts [13,14].

The high activity of sulfided NiMo-NTA/SiO_2 is in agreement with the work of Prins and coworkers [10-12]. These authors concluded from EXAFS data that NTA retards the sulfidation of Ni. However, differently as in our work, they found that Ni sulfidation still precedes that of Mo. We wonder if the difference may be due to the rate of H_2O removal, which is extremely efficient in the present planar model catalysts, but is considerably slower in porous catalysts. According to Arnoldy et al. [27] and Weber et al [24], sulfur uptake by the oxide proceeds by oxygen-sulfur exchange according to the reaction:

$$MO_n + H_2S = MO_{n-1}S + H_2O$$

Hence, a higher partial pressure of H_2O in the pores of a high surface area catalyst will slow the sulfidation reaction down. Medici and Prins [10] also used a higher heating rate during sulfidation, which can also influence the sulfidation behavior of Ni and Mo. The difference in HDS activity between NiMo/SiO_2 and NiMo-NTA/SiO_2 is in our case much larger than that found by Prins et al. [10,11]. This suggests that the present planar models derived from NiMo-NTA/SiO_2 contain more Ni in the NiMoS phase than the corresponding high surface area catalysts used in [10,11].

NiMo-ED/SiO_2. The complexation of ethylene diamine (ED) to Ni in NiMo/SiO_2 catalysts was also studied by Prins et al. [11,12]. The authors found that a high Ni/ED ratio was required to complex all Ni. Using EXAFS they showed that while NTA and EDTA retarded the sulfidation Ni, ED decreased the sulfidation temperature of Ni. Despite this different effect of chelating agents, the authors found an increase in thiophene HDS activity for all chelating agents [11,12].

The XPS spectra of NiMo-ED/SiO_2 model catalysts in Figure 3.6 show that indeed a major part of Ni-ED complexes decomposes at low temperatures, resulting in the sulfidation of Ni at low temperatures. However, the N 1s spectra indicate that not all ED disappears at low temperatures. A small N 1s peak at 400 eV remains visible up to temperatures above 200 ^{0}C, but has disappeared after sulfidation at 400 ^{0}C. At the same temperature the binding energy of the Ni $2p_{3/2}$ peak shifts from 853.8 eV to 854.4 eV, demonstrating that the structure of the nickel sulfide changes above 200^{0}C.

We propose the following picture. It is known that Ni complexes with more than one ED molecule [11,12]. At low temperatures most of these ED-ligands disappear and Ni sulfides partially, but remains attached to at least one ED molecule. The last ED-ligand disappears at high temperatures and releases the partially sulfided Ni. Because Mo is already completely sulfided at these temperatures, the now completely sulfided Ni is able to migrate to the MoS_2 edges, thereby forming NiMoS. The observed perseverance of the N 1s signal up to at least 200^0C, the change in binding energy of sulfidic Ni above this temperature, and the high activity of fully sulfided NiMo-ED/SiO_2 support this idea.

NiMo-EDTA/SiO_2. Ethylene diamine tetraacetic acid (EDTA), known to form very stable complexes with ions of nickel and cobalt [28], and the even more stable cyclohexane variant of this complex, CyDTA, are the most successful chelating agents with respect to stabilizing nickel against sulfidation in this study. Whereas Mo sulfidation is identical to that of Mo/SiO_2, the sulfidation of Ni is effectively retarded to temperatures above 200 ^{0}C. Hence, all Mo is present as MoS_2 when the sulfidation of Ni starts. It is therefore expected, considering the relatively low Ni/Mo ratio (i.e. 1/3), that all Ni atoms are able to migrate to the edges of the MoS_2-slabs, thereby forming a maximum amount of NiMoS phase.

The HDS activity measurements in Figure 3.8 show that the NiMo-EDTA/SiO_2 and NiMo-CyDTA/SiO_2 are indeed the most active catalysts. The activity is almost two times higher than that of NiMo-NTA/SiO_2. This is in qualitative agreement with Prins et al. [11,12], who also found that EDTA containing catalysts show higher activity than catalysts containing NTA. However, they reported a much smaller difference in HDS activity between EDTA- and NTA-containing catalysts. In a Quick EXAFS study on NiMo/SiO_2 catalysts, Cattaneo et al. [12] showed that EDTA retards the sulfidation of Ni, although Mo sulfides at higher temperatures than in our work. As a result Ni and Mo do not sulfide in separate regimes. This can explain the relatively small difference in HDS activity between NiMo-EDTA and NiMo-NTA catalysts in their study, compared to the results presented here, where Ni and Mo sulfide in separate regimes. Similarly as discussed above, it is proposed that sulfidation in porous catalysts is hindered by a slower removal of the reaction product H_2O, which is not a limiting factor in planar model catalysts.

We believe that retardation of Ni sulfidation with respect to that of Mo is the major reason for the activity enhancement observed in HDS. However, the XPS binding energies of Ni in fully sulfided catalysts from the high activity group are the same, and the XPS spectra of the least active catalysts in this category, such as calcined NiMo/SiO_2 contain little evidence for the presence of Ni in more than one state. Hence, we cannot exclude that the chelating agents have some effect on the dispersion of MoS_2 particles as well. Unfortunately, the lack of reliable methods to determine the edge dispersion of promoted sulfide particles prevents us to address this question satisfactorily.

3.5 Conclusions

XPS measurements of the rate of sulfidation of Ni and Mo in a series of differently prepared silica-supported NiMo model catalysts have been correlated with the activity of these catalysts in thiophene hydrodesulfurization (HDS). Using standard impregnation from aqueous solutions of suitable nickel and molybdenum salts produces catalysts in which nickel converts more rapidly to the sulfidic state than molybdenum does. This produces catalysts of detectable but low activity in thiophene HDS. Adding chelating ligands such as

nitrilotriacetic acid (NTA), ethylenediaminetetraacetic acid (EDTA), ethylenediamine (ED) or 1,2-cyclohexanediaminetetraacetic acid (CyDTA) stabilizes nickel against sulfidation at low temperatures, and retard sulfidation of nickel to temperatures at which an appreciable amount of molybdenum is already in the form of MoS_2. As a consequence, such systems are believed to contain a relatively large fraction of nickel in the NiMoS form, consisting of MoS_2 with Ni decorating the edges. A maximum in HDS activity is obtained for systems in which the sulfidation of nickel is retarded to temperatures where Mo is completely sulfided. Retarding the sulfidation of Ni to higher temperatures does not enhance the activity, hence the complete sulfidation of Mo preceding that of Ni is the optimum condition for NiMoS formation.

References

[1] H. Topsøe, and B.S. Clausen, *Catal. Rev.-Sci. Eng.* **26**, 395 (1984).
[2] R. Prins, V.H.J. de Beer, and G.A. Somorjai, *Catal. Rev.-Sci. Eng.* **31**, 1 (1989).
[3] H. Topsøe, B.S. Clausen, and F.E. Massoth, "Hydrotreating Catalysis", Springer-Verlag, Berlin, 1996.
[4] J.A.R. van Veen, E. Gerkema, A.M. van der Kraan, and A. Knoester, *J. Chem. Soc., Chem. Commun.* **22**, 1684 (1987).
[5] M.S. Thompson, European Patent Application 0.181.035.A2 (1986).
[6] N.-Y. Topsøe and H. Topsøe, *J. Catal.* **84**, 386 (1983).
[7] S.P.A. Louwers and R. Prins, *J. Catal.* **133**, 94 (1992).
[8] J.A.R. van Veen, H.A. Colijn, P.A.J.M. Hendriks and A.J. van Welsenes, *Fuel Proc. Technol.* **35**, 137 (1993).
[9] S.M.A.M. Bouwens, F.B.M. van Zon, M.P. van Dijk, A.M. van der Kraan, V.H.J. de Beer, J.A.R. van Veen, and D.C. Koningsberger, *J. Catal.* **146**, 375 (1994).
[10] L. Medici, and R. Prins, *J. Catal.* **163**, 38 (1996).
[11] R. Cattaneo, T. Shido, and R. Prins, *J. Catal.* **185**, 199 (1999).
[12] R. Cattaneo, Th. Weber, T. Shido, and R. Prins, *J. Catal.* **191**, 225 (2000).
[13] A.M. de Jong, V.H.J. de Beer, J.A.R. van Veen, and J.W. Niemantsverdriet, *J. Phys. Chem.* **100**, 17722 (1996).
[14] L. Coulier, V.H.J. de Beer, J.A.R. van Veen, and J.W. Niemantsverdriet, *Topics in Catal.* **13**, 99 (2000).
[15] T. Shimizu, K. Hiroshima, T. Honma, T. Mochizuki, and M. Yamada, *Catal. Today* **45**, 271 (1998).
[16] Y. Ohta, T. Shimizu, T. Honma, and M. Yamada, *Stud. Surf. Sci. Catal.* **127**, 161 (1999).
[17] E.W. Kuipers, C. Laszlo, and W. Wieldraaijer, *Catal. Lett.* **17**, 71 (1993).
[18] R.M. van Hardeveld, P.L.J. Gunter, L.J. van IJzendoorn, W. Wieldraaijer, E.W. Kuipers, and J.W. Niemantsverdriet, *Appl. Surf. Sci.* **84**, 339 (1995).
[19] A.M. de Jong, H.J. Borg, L.J. van IJzendoorn, V.G.M.F. Soudant, V.H.J. de Beer, J.A.R. van Veen, and J.W. Niemantsverdriet, *J. Phys. Chem.* **97**, 6477 (1993).
[20] P.L.J. Gunter, J.W. Niemantsverdriet, F.H. Ribeiro, and G.A. Somorjai, *Catal. Rev.-Sci. Eng.* **39**, 77 (1997).
[21] J.F. Moulder, W.F. Stickle, P.E. Sobol, and K.D. Bomben, "Handbook of XPS", Perkin Elmer Corporation, Eden Prairie, MN, 1992.

[22] J.C. Muijsers, Th. Weber, R.M. van Hardeveld, H.W. Zandbergen, and J.W. Niemantsverdriet, *J. Catal.* **157**, 698 (1995).
[23] Th. Weber, J.C. Muijsers, and J.W. Niemantsverdriet, *J. Phys. Chem.* **99**, 9194 (1995).
[24] Th. Weber, J.C. Muijsers, J.H.M.C. van Wolput, C.P.J. Verhagen, and J.W. Niemantsverdriet, *J. Phys. Chem.* **100**, 14144 (1996).
[25] G. Kishan, L. Coulier, V.H.J. de Beer, J.A.R. van Veen, and J.W. Niemantsverdriet, *J. Chem. Soc. Chem. Commun.*, 1103 (2000),
[26] B. Scheffer, J.C.M. de Jonge, P. Arnoldy, and J.A. Moulijn, *Bull. Soc. Chim. Belg.* **93**, 751 (1984).
[27] P. Arnoldy, J.A.M. van de Heijkant, G.D. de Bok, and J.A. Moulijn, *J. Catal.* **92**, 35 (1985).
[28] L.G. Silen, and A.E. Martell, Stability constants of metal-complexes vol. 2, Chemical Society, London, 1964.

4

Formation of active phases in NiW/SiO_2 hydrodesulfurization model catalysts, prepared without and with chelating agents*

Abstract

Silica-supported NiWS catalysts with a high activity for thiophene hydrodesulfurization (HDS) are obtained when chelating agents such as 1,2-cyclohexane diamine-N,N,N',N'-tetraacetic acid (CyDTA), ethylene diamine tetraacetic acid (EDTA), or nitrilo triacetic acid (NTA) are added in the impregnation stage. X-ray photoelectron spectroscopy (XPS) has been used to follow the state of Ni and W during the temperature programmed sulfidation of Ni-W model catalysts prepared with and without chelating agents on planar SiO_2 films on silicon substrates. Fully sulfided catalysts have been tested in thiophene hydrodesulfurization. The activity increases with increasing Ni content and reaches a plateau at a Ni:W atomic ratio of 0.66. In NiW catalysts prepared without additives the sulfidation of Ni precedes that of W. However, Ni sulfide formed at low temperatures changes its structure at high temperatures where WS_2 is present, as indicated by the Ni XPS binding energy, which we tentatively attribute to redispersion of sulfidic Ni over WS_2. Chelating agents stabilize Ni against sulfide formation at low temperature, the effect being strongest when CyDTA is applied. CyDTA retards the sulfidation of Ni to temperatures where all W has already been sulfided. This complete reversal in the order in which the two elements convert to sulfides is seen as the key step in preparing highly active NiWS HDS catalysts.

* This chapter was published as: G. Kishan, L. Coulier, V.H.J. de Beer, J.A.R. van Veen, and J.W. Niemantsverdriet, *Chem. Commun.* (2000) 1103; *J. Catal.* **196** (2000) 180.

4.1 Introduction

The production of low-sulfur diesel fuels is currently an important topic in oil refineries due to more stringent environmental legislation [1]. Hydrodesulfurization (HDS) of refinery streams is carried out with catalysts consisting of Mo promoted with Ni or Co, or W promoted with Ni, all in the sulfided state [2-5]. In the preparation, sulfidation of the oxidic precursors in a mixture of H_2S/H_2 or in the sulfur-containing hydrocarbon feed is an essential step. In contrast to CoMo and NiMo catalysts, W-based catalysts such as NiW are studied less frequently in literature. While NiW catalysts are very promising for deep HDS [5], more detailed knowledge more detailed knowledge about their preparation chemistry is desirable. Al_2O_3-supported NiW catalysts have received the most intention [5-13], although other supports, e.g. C and SiO_2 have also been used [14-16].

Interestingly, the sulfidation behaviour and catalytic properties of the promoted W and Mo based catalysts are clearly different. For example, the sulfidation of NiW/Al_2O_3 catalysts is much more difficult than that of $NiMo/Al_2O_3$ [6,8]. Furthermore, the optimum sulfidation degree was found to be dependent on the type of reaction for which the catalyst was used [9,11]. Reinhoudt et al. [9] showed that complete sulfidation of W resulted in the highest thiophene HDS activity, while the highest dibenzothiophene HDS activity was found when the sulfidation of W was incomplete. Several authors found that the sulfidation of oxidic W to WS_2 proceeded, as in the case of Mo [17-20], through oxysulfides and WS_3 as intermediates [6,10,21]. Due to the strong interaction of both Ni and W with the Al_2O_3-support the sulfidation mechanism of these catalysts is very complex and depends strongly on experimental conditions, e.g. metal loading, calcination temperature, and sulfidation temperature [6-11].

For CoMo or NiMo supported on Al_2O_3 or SiO_2 a fairly complete picture of the active phases exists. These consist of Co or Ni atoms on the edges of MoS_2 slabs, and are commonly referred to as CoMoS and NiMoS phases [2-4,22-28]. An EXAFS study by Louwers and Prins [14] on carbon-supported NiW catalysts provides evidence that a NiWS phase analogous to the CoMoS phase exists. Other authors also found evidence for the presence of a NiWS phase [7,9,10,21].

Addition of chelating agents such as nitrilo triacetic acid (NTA), ethylene diamine tetraacetic acid (EDTA) and 1,2-cyclohexane diamine-N,N,N',N'-tetraacetic acid (CyDTA) has a beneficial effect on the catalytic activity of CoMo, NiMo and NiW catalysts, irrespective of the support [12,13,22-29]. Work in the laboratories of Prins [23-25] and our own group [26-28] has identified retardation of Ni and Co sulfide formation as the key step in enabling the formation of the active NiMoS and CoMoS phases. Recently Shimizu et al. [12,13] also showed that chelating agents improve the (di)benzothiophene HDS activity over NiW/Al_2O_3 catalysts.

Earlier work has shown that model catalysts consisting of flat conducting substrate on top of which the active phase is deposited by spincoating is very successful to study the formation of the active phase in SiO_2-supported CoMo and NiMo hydrotreating catalysts [26-28].

In this article, we investigate the sulfidation behaviour of NiW/SiO_2 catalysts prepared without and with various chelating agents with X-ray Photoelectron Spectroscopy (XPS), and correlate the rate of sulfidation with the activity in thiophene hydrodesulfurization.

4.2 Experimental

$NiW/SiO_2/Si(100)$ model catalysts were prepared similar to the CoMo and NiMo catalysts described in more detail earlier [27,28]. Briefly, a silica model support was prepared by oxidizing a Si (100) wafer in air at 750 ^{0}C for 24 hours. After calcination the wafers were cleaned in a mixture of H_2O_2 and NH_4OH at 65 ^{0}C. The surface was rehydroxylated by boiling in water for 30 min. Next the model supports was covered with a solution of the catalyst precursors and spincoated under N_2 atmosphere at 2800 rpm [31,32]. The catalyst precursor compounds were ammonium metatungstate (Merck) and nickel nitrate ($Ni(NO_3)_2.6H_2O$). The concentration of W and Ni in the precursor solutions was adjusted to result in a loading of 6 W atoms/nm^2 and 2 Ni atoms/nm^2 after spin coating. For HDS activity studies the Ni loading was varied from 1 to 6 atoms/nm^2. After spincoating the catalysts were calcined in 20% O_2/Ar at 500 ^{0}C for 60 min at a rate of 5 ^{0}C/min.

The samples containing NTA, EDTA and CyDTA were prepared by spincoating with an ammoniacal solution, which contained the precursors of W, Ni and nitrilo triacetic acid (NTA), ethylene diamine tetraacetic acid (EDTA) or 1,2-cyclohexane diamine-N,N,N',N'-tetraacetic acid (CyDTA) (Merck) with an atomic ratio of 3:1:1, such that the amount of chelating agent was equivalent to that of Ni, as described by Van Veen et al. [22].

The model catalysts were sulfided in a mixture of 10% H_2S/H_2. The catalysts containing chelating agents were heated at a rate of 2 ^{0}C/min (other catalysts 5 ^{0}C/min) to the desired temperature and kept there for 30 min. After sulfidation, the reactor was cooled to room temperature under helium gas flow and then brought to a glovebox, where the model catalyst was mounted in a transfer vessel for transport to XPS under N_2 atmosphere.

XPS spectra were obtained by using a VG Escalab 200MK spectrometer equipped with a dual Al/Mg Kα X-ray source and a hemispherical analyzer with a five-channel detector. Measurements were recorded with constant pass energy of 20 eV. Binding energies were corrected for charging by using Si 2p peak of SiO_2 at 103.3 eV as a reference. Binding energy values thus determined are estimated to possess an accuracy of $\pm$ 0.2 eV.

Atmospheric gas-phase thiophene HDS was carried out in batch mode under standard conditions (1.5 bar, 400 ^{0}C, 4% thiophene/H_2) after presulfidation at 400 ^{0}C. For more details on the activity measurements, see [27].

4.3 Results

First we will discuss the state of Ni and W during sulfidation, as determined by XPS. Next we present the results of thiophene HDS, and correlate the catalytic activity with the relative sulfidation rates of Ni and W.

4.3.1 Sulfidation of W in W/SiO_2 and NiW/SiO_2 catalysts

Figure 4.1 shows W 4f and the S 2p XPS spectra of a W/SiO_2 model catalyst after sulfidation in a H_2S/H_2 mixture at different temperatures. It appeared that the sulfidation of W proceeded similarly in NiW/SiO_2 and in the NiW/SiO_2 catalysts prepared with chelating agents. We therefore only discuss the series of W 4f spectra in Figure 4.1. The results of the fitting of the XPS spectra are shown in Table 4.1.

The W 4f spectrum of the unsulfided W/SiO_2 catalyst shows a 4f doublet with a W $4f_{7/2}$ binding energy of 36.0 ± 0.1 eV, which is characteristic of W-oxide with an oxidation state of 6+ [30]. The small peak at 41.9 eV with FWHM of 1.9 eV is assigned to the W $5p_{3/2}$ state. In case chelating agents such as NTA, EDTA and CyDTA were applied in the preparation, the $4f_{7/2}$ binding energy was about 0.4 eV lower, indicating interaction of W with the complexing agent.

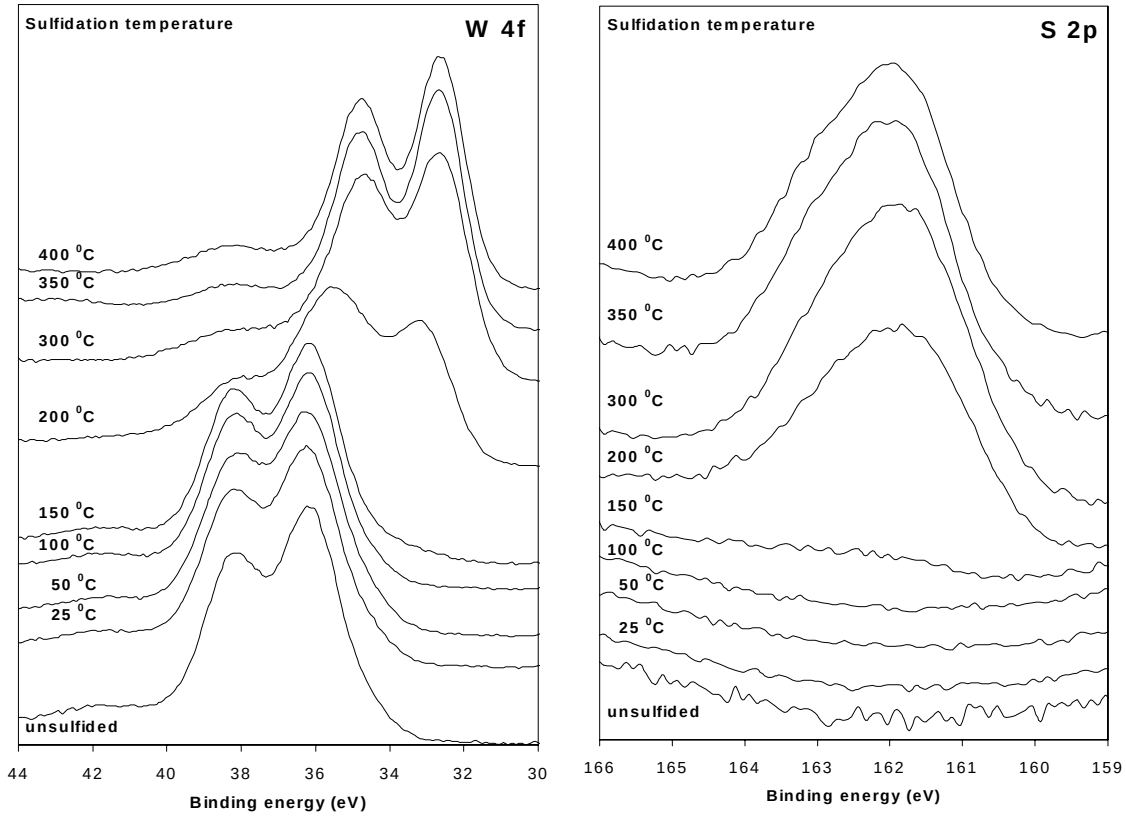

Figure 4.1 *W 4f and S 2p XPS spectra of W/SiO_2 model catalysts after stepwise sulfidation at various temperatures. The fitting results of these spectra are shown*

Fitting of the XPS spectra show that the sulfidation of W starts around 150 ^{0}C (Table 4.1), as evidenced by the appearance of a second doublet at 33.0 eV. Significant sulfidation takes place at 200 ^{0}C, where the presence of a second W 4f doublet is clearly visible in Figure 4.1. The sulfidation proceeds at higher temperatures and is almost complete at 300 ^{0}C, although Table 4.1 shows that the sulfidation is not complete. The W $4f_{7/2}$ binding energy of the W 4f doublet at high temperature, i.e. 32.6 eV, is characteristic for WS_2 [16,30]. No evidence for intermediates like oxysulfides or WS_3 was found.

The S 2p spectra confirm that the sulfidation starts at around 150 ^{0}C and is complete around 300-350 ^{0}C. The S 2p spectra can be fitted with a single doublet with S 2p binding energy of 161.8 eV, consistent with the S^{2-} type ligands present in WS_2. Table 4.1 shows the S/W_{tot} atomic ratio calculated from the XPS peak areas. The ratio increases with temperature up to 300 ^{0}C and remains constant at higher temperatures, indicating that the sulfidation is complete.

Calcination of the catalysts, variation of the W loading, nor addition of chelating agents affected the sulfidation rate of tungsten significantly.

Table 4.1 *XPS fit results of the W 4f and S 2p spectra shown in Figure 4.1, showing the sulfidation of W/SiO_2/Si(100) model catalysts as a function of temperature.*

Sulfidation temperature	W_{ox} $4f_{7/2}$ (eV)	W_{sulf} $4f_{7/2}$ (eV)	% W_{sulf}	S 2p (eV)	S/W_{tot} atomic ratio	S/W_{sulf} atomic ratio
unsulfided	36.1	-	-	-	-	-
25 ^{0}C	36.1	-	-	-	-	-
50 ^{0}C	36.0	-	-	-	-	-
100 ^{0}C	36.1	-	-	-	-	-
150 ^{0}C	35.9	33.0	5	162.3	~0.1	~2.4
200 ^{0}C	35.7	32.7	58	162.0	1.31	2.23
300 ^{0}C	35.9	32.5	91	161.7	1.94	2.13
350 ^{0}C	-	32.7	100	161.9	2.06	2.06
400 ^{0}C	-	32.6	100	161.8	2.02	2.02

4.3.2 Sulfidation of Ni in NiW/SiO_2 catalysts

Ni/SiO_2. The sulfidation of Ni/SiO_2 model catalysts was described extensively in an earlier paper [28]. It was shown that the sulfidation started already at room temperature and was complete around 100 ^{0}C. The Ni $2p_{3/2}$ binding energy of the completely sulfided catalysts, i.e. 853.8 ± 0.2 eV, corresponded well with that of Ni_3S_2. It was also shown that the addition of EDTA retarded the sulfidation of Ni to temperatures above 200 ^{0}C. However, the Ni $2p_{3/2}$ binding energy of the fully sulfided catalysts at 853.8 eV indicated that bulk nickel sulfide was present despite the retardation.

NiW/SiO_2. Figure 4.2A shows the Ni 2p XPS spectra of an uncalcined NiW/SiO_2 model catalyst recorded after sulfidation at various temperatures**.** The Ni 2p spectrum of the unsulfided catalyst exhibits a Ni $2p_{3/2}$ peak at 857.1 eV and a shake up feature at higher binding energy, which is a characteristic pattern for nickel oxide with an oxidation state of 3+ [30]. A shoulder at 854.9 eV in the spectrum of fresh NiW/SiO_2 points to the presence of hydrated oxide [30]. The Ni 2p XPS spectrum obtained for the model catalyst, upon sulfidation at room temperature exhibited an additional doublet at lower binding energy (Ni $2p_{3/2}$ ~ 854.0 eV). With increasing temperature, the intensity of this additional doublet was found to increase at the expense of the doublet with Ni $2p_{3/2}$ binding energy at 857.1 eV which disappeared completely at ~ 150 ^{0}C. The Ni 2p doublet with a Ni $2p_{3/2}$ binding energy of 854.0 eV measured after sulfidation at higher temperatures corresponds to that of bulk Ni sulfide, Ni_3S_2 [20, 29]. The Ni 2p spectrum of Ni sulfide also shows shake up features at higher binding energy, although the intensity of the peaks is less than in the case of oxidic Ni. The sulfidation of Ni in NiW/SiO_2 occurs at a somewhat higher temperature than in the case of Ni/SiO_2, as described above.

XPS binding energies of the oxidic and sulfidic contribution of both the Ni 2p and W 4f peaks and degree of sulfidation of both elements upon the various sulfidation temperatures are presented in Table 4.2. As Figure 4.2 and Table 4.2 show, the sulfidation of W starts at

around 150 ^{0}C and is complete at 350 ^{0}C, as was observed also for the W/SiO_2 catalyst in Figure 4.1, whereas that of Ni starts at room temperature and is finished at 150 ^{0}C. Hence, sulfidation of Ni 2p and W 4f occur in separated temperature regimes. Interestingly, the Ni $2p_{3/2}$ binding energy shifts gradually from 854.0 eV after sulfidation at 150 ^{0}C (characteristic of Ni_3S_2) to 854.4 eV at higher temperatures where W is completely sulfided. Such a shift has not been observed for Ni/SiO_2 with or without chelating agents. We discuss the indication of this shift in the discussion section.

Figure 4.2B shows the Ni 2p XPS spectra of the calcined silica-supported NiW catalyst after sulfiding at various temperatures. Calcination of the NiW/SiO_2 catalyst retards the sulfidation of Ni somewhat. The Ni 2p XPS spectra of this catalyst (Figure 2B) indicates that Ni sulfidation starts at room temperature but converts slower to the sulfided state than the uncalcined NiW catalyst does, as is evident if the Ni spectra after reaction at 50 ^{0}C are compared. The second doublet with Ni $2p_{3/2}$ binding energy at 854.9 eV, which contributed to a hydrated oxide, is less pronounced compared to that of the uncalcined NiW/SiO_2 catalyst in Figure 4.2A. Clearly the calcination procedure converted part of the hydrated oxide. The shift of the Ni $2p_{3/2}$ binding energy at high temperatures as described earlier is clearly visible in Figure 4.2B.

4.3.3 Sulfidation of Ni in NiW/SiO_2 catalysts prepared with chelating agents

Figure 4.2C and 4.2D illustrate the effect of NTA and EDTA on the sulfidation of Ni in NiW/SiO_2 catalysts. Clearly, the effect is to stabilize the Ni such that sulfidation occurs at higher temperatures than observed for either Ni or NiW/SiO_2 catalysts. The stabilizing effect of EDTA is stronger than that of NTA. We will discuss the effect of the even stronger chelating agent CyDTA in more detail.

Figure 4.3 shows the evolution of W, Ni, S and N in the NiW-CyDTA/SiO_2 catalyst during sulfidation in H_2S/H_2. The W 4f spectrum of the unsulfided catalysts in Figure 4.3A shows a W $4f_{7/2}$ doublet at 35.6 eV with FWHM of 2.0 which is characteristic of oxidic W in an oxidation state of 6+ [30]. The Ni 2p spectrum of the unsulfided catalyst shows the characteristic pattern of oxidic Ni with an unusually low Ni $2p_{3/2}$ binding energy of 855.4 eV, which we attribute to complexation with CyDTA. The N 1s peak around 400 eV is characteristic of the CyDTA ligand. The S 2p region shows no emission as expected.

Upon sulfidation, W is the first element to be affected, which takes place around 150 ^{0}C. The S 2p region shows the appearance of sulfur. However, Ni is not affected until temperatures of 250 ºC. Sulfidation of Ni is complete at 300 ^{0}C. Close inspection of N 1s spectra reveals that the N 1s peak disappears at above 250 ^{0}C. Hence, we conclude that sulfidation of Ni is retarded until the Ni-CyDTA complex decomposes. A similar situation occurred on NiMo/SiO_2 catalysts prepared with NTA and EDTA as the chelating agent [28].

The conversion from oxidic to sulfidic phases is reflected by the S 2p spectra (Figure 4.3C). In the spectra obtained after sulfidation at 150 ^{0}C and 200 ^{0}C, the signal results from WS_2 only, whereas from 250 ^{0}C onwards sulfided Ni contributes to the S 2p peaks. The S 2p spectra can be fitted with a doublet of S $2p_{3/2}$ binding energy of 161.8 eV, consistent with S^{2-} species [19,20,30].

The results in Figure 4.3 clearly show that addition of CyDTA in the preparation completely reverses the order in which Ni and W convert to sulfides (W first, Ni second) as compared to the standard NiW/SiO_2 catalyst, where Ni sulfidation precedes that of W.

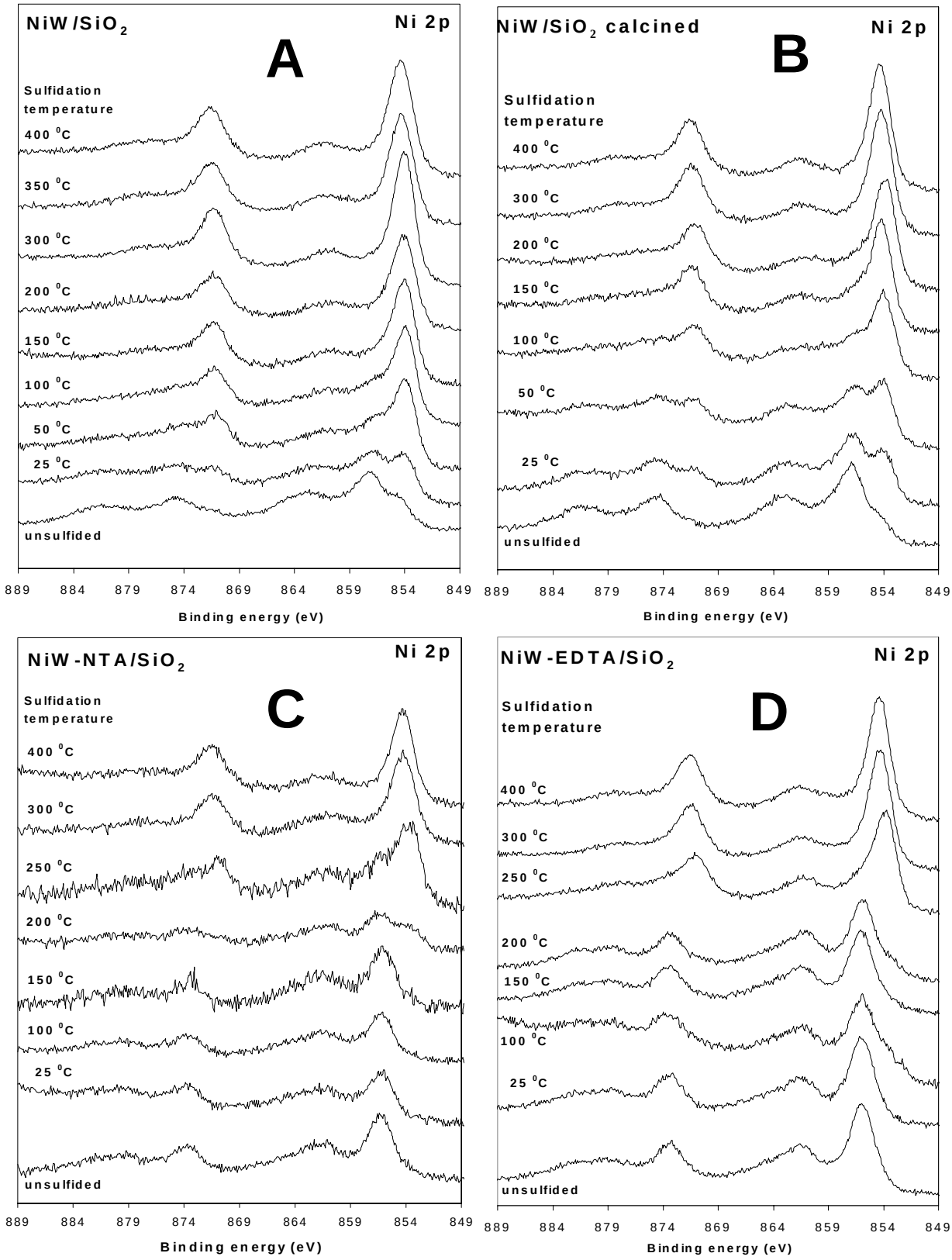

Figure 4.2 *Ni 2p XPS spectra of (A) NiW/SiO_2, (B) calcined NiW/SiO_2, (C) NiW-NTA/SiO_2, and (D) NiW-EDTA/SiO_2 model catalysts after sulfidation at various temperatures.*

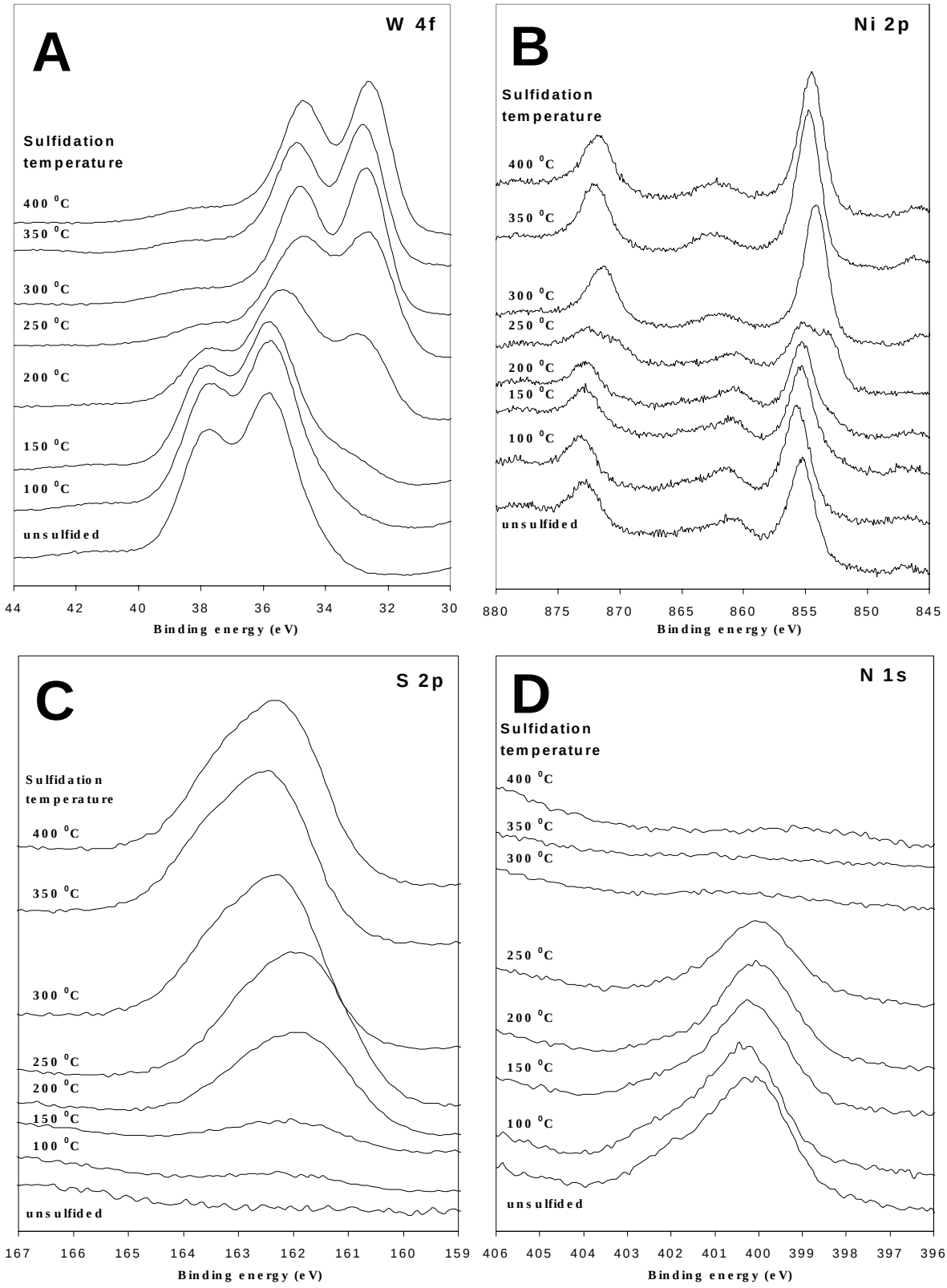

Figure 4.3 *(A) W 4f, (B) Ni 2p, (C) S 2p, and (D) N 1s XPS spectra of a NiW-CyDTA/SiO_2 model catalyst as a function of sulfidation temperature.*

Table 4.2 *XPS fit results of the W 4f and Ni 2p spectra of NiW/SiO_2 model catalysts sulfided at various temperatures.*

Sulfidation temperature	W_{ox} $4f_{7/2}$ (eV)	W_{sulf} $4f_{7/2}$ (eV)	$\%W_{sulf}$	Ni_{ox} $2p_{3/2}$ (eV)	Ni_{sulf} $2p_{3/2}$ (eV)	$\%Ni_{sulf}$
unsulfided	36.1	-	-	857.1 854.9	-	-
25 ^{0}C	36.0	-	-	856.9	854.0	46
50 ^{0}C	36.0	-	-	856.6	853.9	55
100 ^{0}C	36.0	-	-	856.4	853.9	80
150 ^{0}C	35.9	33.0	6	-	854.0	100
200 ^{0}C	35.7	33.0	54	-	854.0	100
300 ^{0}C	36.0	32.5	91	-	854.2	100
350 ^{0}C	-	32.6	100	-	854.3	100
400 ^{0}C	-	32.6	100		854.4	100

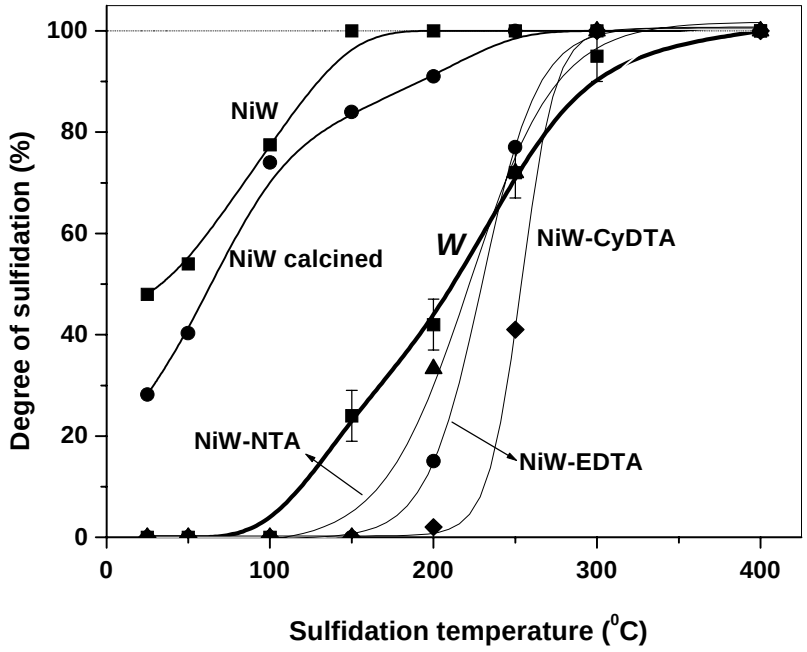

Figure 4.4 *Degree of sulfidation of Ni and W in various NiW catalysts as a function of sulfidation temperature.*

4.3.4 Comparison of the sulfidation of NiW catalysts

Figure 4.4 shows the degree of sulfidation of W and Ni for all the catalysts as a function of sulfidation temperature, as derived from the XPS spectra. Sulfidation of W in all catalysts is similar and is indicated by the heavy line in Figure 4.4. One clearly observes the retarding effect of calcination, and of the chelating agents, NTA, EDTA, and CyDTA, on the sulfidation of Ni.

Figure 4.5 shows the Ni $2p_{3/2}$ binding energy of the Ni sulfide phase versus sulfidation temperature. A nickel-only (Ni/SiO_2) catalyst, which forms sulfide at room temperature already, contains Ni with a Ni $2p_{3/2}$ binding energy of 854.0 eV, similar to that of bulk Ni_3S_2 irrespective of sulfidation temperature. The XPS spectrum of the standard NiW/SiO_2 catalyst exhibits this phase for sulfidation temperatures below 250 ^{0}C. However, all NiW catalysts sulfided at 300 ^{0}C and higher exhibit a Ni $2p_{3/2}$ binding energy that is significantly, i.e. 0.35-0.50 eV higher than that of bulk Ni_3S_2, and indicative of a different structure. As this shift in binding energy occurs at the temperatures where WS_2 forms, we believe that WS_2 accommodates the change in Ni sulfide structure.

An overview of the Ni 2p and W 4f binding energies of the fully oxidic and sulfidic (Ni)W/SiO_2 catalysts are presented in Table 4.3.

Table 4.3 *Binding energies and FWHM of Ni 2p and W 4f XPS peaks of fully oxidic and sulfidic NiW model catalysts.*

Catalyst	Ni_{ox} $2p_{3/2}$ (eV)	Ni_{sulf} $2p_{3/2}$ (eV)	W_{ox} $4f_{7/2}$ (eV)	W_{sulf} $4f_{7/2}$ (eV)
Ni/SiO_2	856.8 (3.0)	854.0 (2.4)	-	-
Ni-EDTA/SiO_2	856.1 (2.5)	853.9 (2.5)	-	-
W/SiO_2	-	-	35.9 (1.9)	32.6 (1.6)
NiW/SiO_2	857.1 (2.6) 854.9 (2.1)	854.4 (2.6)	36.1 (1.6)	32.6 (1.7)
NiW/SiO_2 calc.	856.9 (3.2)	854.4 (2.4)	36.0 (1.8)	32.6 (1.7)
NiW-NTA/SiO_2	856.0 (3.1)	854.4 (2.7)	35.6 (2.2)	32.5 (1.8)
NiW-EDTA/SiO_2	856.0 (2.7)	854.5 (2.4)	35.7 (2.2)	32.6 (1.6)
NiW-CyDTA/SiO_2	855.4 (2.4)	854.5 (2.3)	35.6 (2.0)	32.6 (1.6)

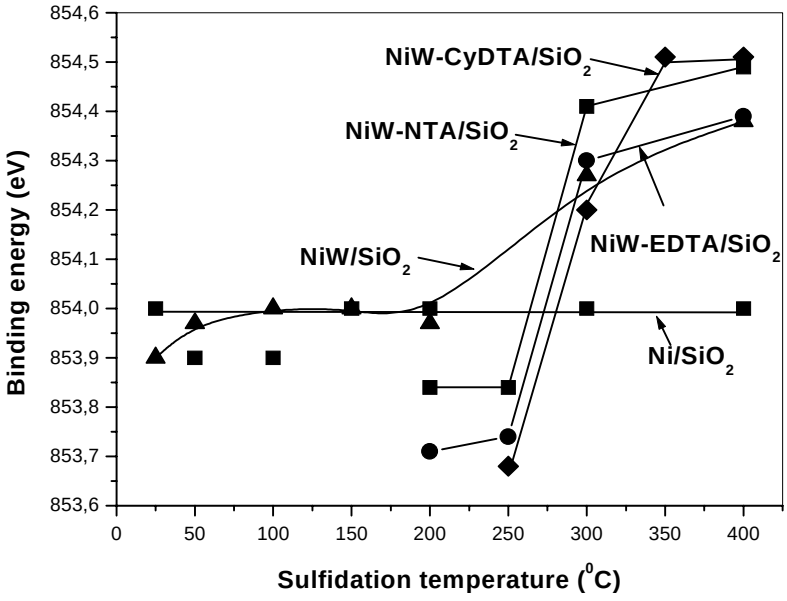

Figure 4.5 *Ni 2p binding energy of Ni sulfide in various catalysts as function of sulfidation temperature*

4.3.5 Thiophene hydrodesulfurization

All catalysts were tested on their performance in thiophene HDS. The yields are based on 5 cm^2 surface area of catalyst and have been corrected for conversion of an empty SiO_2 support in a blank experiment. These blanks showed some conversion of thiophene (0.03%) to mainly methane, ethane and propane, thought to be due to thermal decomposition of thiophene, which may be assisted by the SiO_2 support.

Figure 4.6 illustrates the promoting effect of Ni on the HDS activity of NiW/ SiO_2 and NiW-CyDTA/SiO_2 model catalysts. The activity increases with Ni loading until a Ni/W ratio of 0.66 is reached for both catalysts, after which the activity levels off. Interestingly, the optimum Ni:W atomic ratio 0.66 is equal to that reported for high surface area NiW catalysts for thiophene HDS [2,14,15].

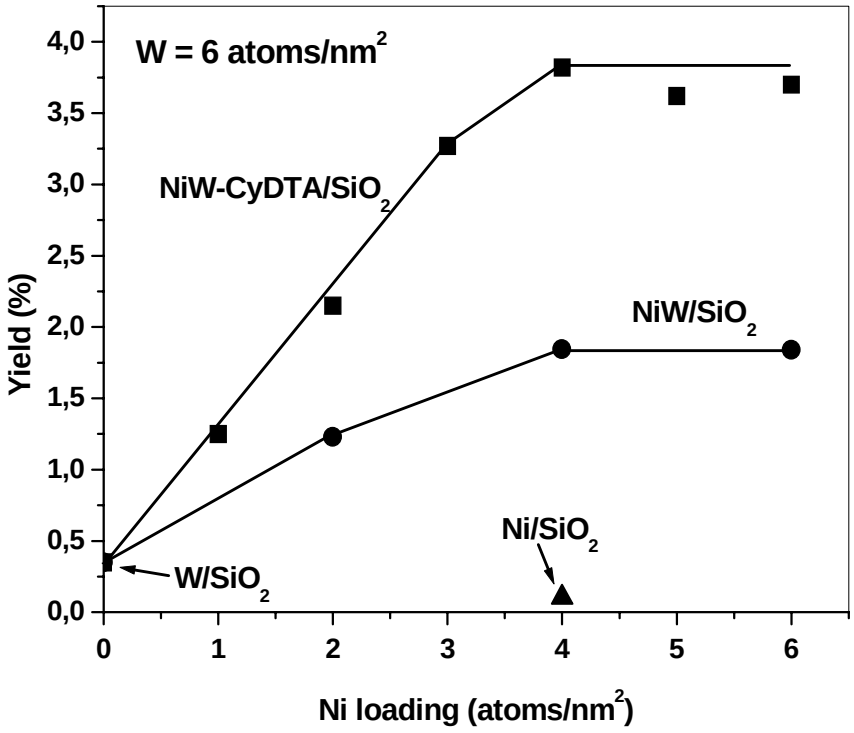

Figure 4.6 *Product yield of thiophene hydrodesulfurization at 400 ^0C for 1 h in a batch reaction over a NiW-CyDTA/SiO_2 model catalyst, as a function of Ni loading.*

Figure 4.7 compares the catalytic performance of all the NiW/SiO_2 catalysts with optimum loading of 6 W atoms/nm^2 and 4 Ni atoms/nm^2. The promotional effect of Ni on W and the increase in activity due to the presence of the chelating agents is evident.

4.4 Discussion

Promotion of W by Ni in sulfidic catalysts leads to a significant increase in catalytic activity for the hydrodesulfurization of thiophene to 1- and 2-butenes, and the promoting

effect becomes significantly higher if chelating agents such as NTA, EDTA and CyDTA are added in the impregnation stage. The activity increases with increasing Ni/W atomic ratio, and reaches a plateau at a ratio of 0.66. The maximum Ni/W ratio of 0.66 corresponds well with that found for high surface area catalysts [14,15].

An important conclusion from this work is that a clear correlation exists between the thiophene HDS activity of NiW/SiO_2 catalysts and the order in which the initially oxidic Ni and W convert into the sulfidic state during presulfidation in H_2S/H_2. This becomes immediately apparent if one compares Figure 4.7, where the catalytic performance of different NiW/SiO_2 is shown, with Figure 4.4, showing the degree of sulfidation of Ni and W versus temperature. There is a one-to-one correspondence between the extent to which sulfidation of nickel is retarded and the activity of the NiWS/SiO_2 catalyst in thiophene HDS.

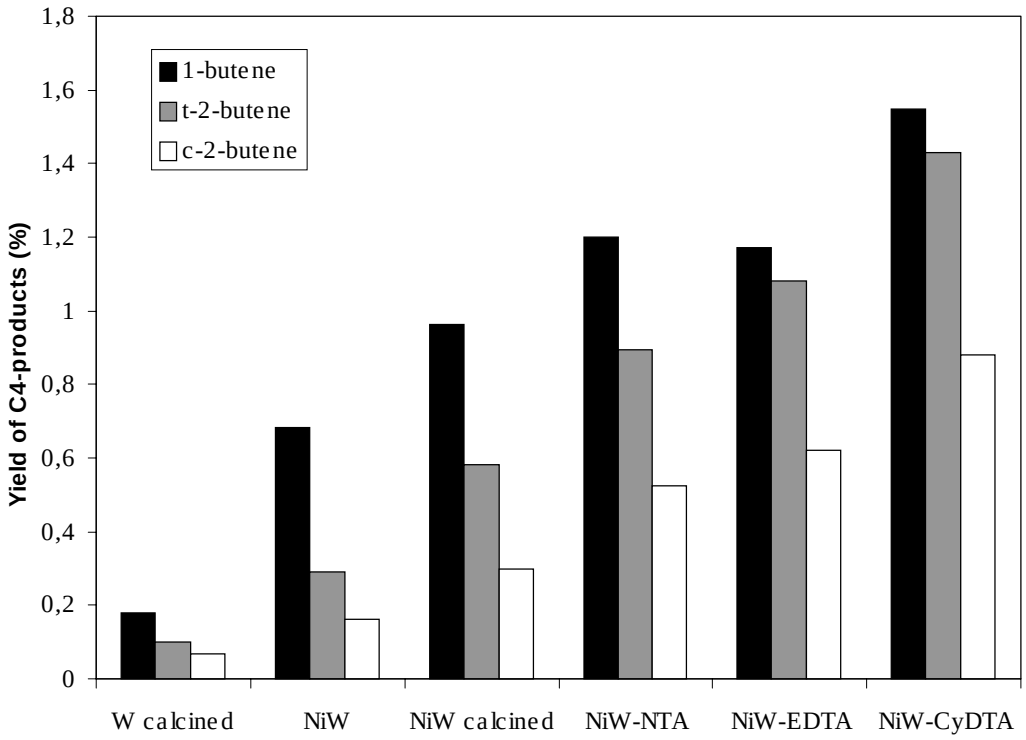

Figure 4.7 *Thiophene hydrodesulfurization over NiW/SiO_2 model catalysts prepared in different ways, showing the product distribution after 1 h of batch reaction at 400 ^{0}C.*

These findings are readily rationalized if one assumes that the optimum structure of the active phase in a sulfidic NiW/SiO_2 catalyst is the analogue of the well-known CoMoS and NiMoS phase [2-4,22-28], in which sulfidic Ni decorates the edges of WS_2 particles. Several authors found evidence for this NiWS phase [6,7,10,14]. Retarding the sulfidation of Ni by coordinating it to a sufficiently stable agent such as 1,2-cyclohexanediamine-N,N,N',N'-tetraacetic acid (CyDTA) is favorable, because the Ni is released at temperatures where WS_2 has already been formed. Of course, we cannot rule out that the chelating agents play a beneficial role with respect to the size of the WS_2 particles as well, but we believe that the stabilizing effect on the Ni is the main contributor. The detailed XPS measurements of the NiW-CyDTA/SiO_2 system in Figure 4.3 clearly illustrate this point: Ni starts to form sulfides

at the temperatures where the complex decomposes, as revealed by the intensity decrease of the N 1s spectra characteristic of the CyDTA complex.

Note that NTA was sufficiently stable to achieve the desired retardation of Co in CoMo [26,27] and Ni in NiMo [16,20] catalysts, because Mo forms sulfides at lower temperatures. As W is significantly more difficult to sulfide than Mo, chelating agents more stable than NTA such as EDTA and CyDTA are necessary to achieve the desired effect in NiWS catalysts. However, all chelating agents cause an increase in HDS activity, which was also found by Shimizu et al. [12,13]. These authors observed an increase in activity with the stability of the chelating agents NTA < EDTA < CyDTA.

Nonetheless, one cannot state that retardation of Ni sulfidation is the sole determining factor in reaching a high activity. Standard NiW catalysts, in which Ni sulfidation entirely precedes that of W, show significant HDS activity as well, at least significantly higher than that of sulfided W/SiO_2 catalyst. HDS activity tests on high surface area NiW catalysts also show this promotion effect of Ni [14,15]. The fit results in Table 4.2 give a hint why this is so. The Ni $2p_{3/2}$ binding energy of NiW/SiO_2 sulfided at low temperatures is 854.0 ± 0.2 eV, corresponding to bulk nickel sulfide, and shifts to 854.4 eV at temperatures where W is sulfided. This binding energy of 854.4 eV corresponds with that of the Ni $2p_{3/2}$ binding energy of the NiW/SiO_2 catalysts prepared with chelating agents (see Table 4.3). These catalysts showed an enhanced HDS activity and hence the Ni $2p_{3/2}$ binding energy of 854.4 eV is contributed to a highly active state of the catalysts, i.e. Ni in NiWS. This strongly suggests that the Ni_3S_2 formed at low temperature rearrange at higher temperatures. Interpreted in terms of the CoMoS structure, it is likely that the nickel redisperses over the edges of the WS_2 crystallites, as observed earlier by Reinhoudt et al. [10].

Finally, we note that all results reported here were obtained with planar, conducting model catalysts, exposing typically 5 cm^2 of surface area in the catalytic reaction. The great advantages of using these models is that their XPS spectra feature much better resolution than the spectra of high-surface area catalysts, which is particularly useful in the case of W where the W 4f doublet splitting is small.

4.5 Conclusions

For a series of differently prepared NiW supported on SiO_2 model catalysts, the rates of sulfidation have been measured by XPS and compared with the activity in thiophene hydrodesulfurization (HDS).

- Ni/SiO_2 catalysts form bulk nickel sulfide at relatively low temperatures; this catalyst is inactive in thiophene HDS.
- W/SiO_2 converts to WS_2 at significantly higher temperatures (150-350 ^{0}C); this phase shows significant activity for the HDS of thiophene at 400 ^{0}C. No evidence for oxysulfides or WS_3 as intermediates was found.
- In NiW/SiO_2 catalysts prepared by conventional impregnation Ni converts more rapidly to the sulfidic state than W. However, the Ni_3S_2 phase formed at low temperatures restructures at temperatures where WS_2 has formed as was observed by detailed XPS analysis. The resulting NiWS phase is about four times more active for thiophene HDS than WS_2.

- Optimum promotion of WS_2 by Ni is observed for Ni/W atomic ratios of 0.66. Higher Ni content does not lead to higher activity.
- Complexing to Ni with chelating agents like NTA or EDTA retards the sulfidation of Ni to higher temperatures, such that both Ni and W form sulfides in the same temperature range. This leads to higher HDS activity than measured from the standard NiW/SiO_2 catalyst.
- Complexing Ni with CyDTA retards the sulfidation of Ni where WS_2 has already formed. Nickel sulfidation starts when the CyDTA complex decomposes. As a result, nickel atoms released by the chelating agent can move to the reactive edges of the WS_2 to form a finely dispersed sulfide. This gives the highest activity for thiophene HDS. The activity is a factor 2-3 higher compared to the standard NiW catalysts.

References

[1] J. W. Gosselink, *CatTech*, **4**, 127, (1998).
[2] H. Topsøe, B.S. Clausen, and F.E. Massoth, "Hydrotreating Catalysis" Springer-Verlag, Berlin, 1996.
[3] R. Prins, V.H.J. de Beer, and G.A. Somorjai, *Catal. Rev-Sci. Eng.* **31**, 1 (1989).
[4] H. Topsøe, and B.S. Clausen, *Catal. Rev.-Sci. Eng.* **26**, 395 (1984).
[5] H.R. Reinhoudt, R. Troost, A.D. van Langeveld, S.T. Sie, J.A.R. van Veen, and J.A. Moulijn, *Fuel Proc. Technol.* **61**, 133 (1999).
[6] B. Scheffer, P.J. Mangnus, and J.A. Moulijn, *J. Catal.* **121**, 18 (1990).
[7] P.J. Mangnus, A. Bos, and J.A. Moulijn, *J. Catal.* **146**, 437 (1994).
[8] M. Breysse, M. Cattenot, T. Decamp, R. Frety, C. Gachet, M. Lacroix, C. Leclerq, L. de Mourques, J.L. Portefaix, M. Vrinat, M. Houari, J. Grimblot, S. Kasztelan, J.P. Bonnelle, S. Housni, J. Bachelier, and J.C. Duchet, *Catal. Today*. **4**, 39 (1988).
[9] H.R. Reinhoudt, A.D. van Langeveld, R. Mariscal, V.H.J. de Beer, J.A.R. van Veen, S.T. Sie, and J.A. Moulijn, *Stud. Surf. Sci. Catal.* **106**, 263 (1997).
[10] H.R. Reinhoudt, Y. van der Meer, A.M. van der Kraan, A.D. van Langeveld, and J.A. Moulijn, *Fuel. Proc. Technol.* **61**, 43 (1999).
[11] M. Breysse, J. Bachelier, J.P. Bonnelle, M. Cattenot, D. Cornet, T. Decamp, J.C. Duchet, R. Durand, P. Engelhard, R. Frety, C. Gachet, P. Geneste, J. Grimblot, C. Gueguen, S. Kasztelan, M. Lacroix, J.C. Lavalley, C. Leclerq, C. Moreau, L. de Mourques, J.L. Olive, E. Payen, J.L. Portefaix, H. Toulhoat, and M. Vrinat, *Bull. Soc. Chim. Belg.* **96**, 829 (1987).
[12] T. Shimizu, K. Hiroshima, T. Honma, T. Mochizuki, and M. Yamada, *Catal. Today* **45**, 271 (1998).
[13] Y. Ohta, T. Shimizu, T. Honma, and M. Yamada, *Stud. Surf. Sci. Catal.* **127**, 161 (1999).
[14] S.P.A. Louwers, and R. Prins, *J. Catal.* **139**, 525 (1993).
[15] Y.I. Yermakov, A.N. Startsev, and V.A. Burmistrov, *Appl. Catal.* **11**, 1 (1984).
[16] A.P. Shepelin, P.A. Zhdanov, V.A. Burmistrov, A.N. Startsev, and Y.I. Yermakov, *Appl. Catal.* **11**, 11 (1984).
[17] A.M. de Jong, H.J. Borg, L.J. van IJzendoorn, V.G.M.F. Soudant, V.H.J. de Beer, J.A.R. van Veen, and J.W. Niemantsverdriet, *J. Phys. Chem.* **97**, 6477 (1993).

[18] J.C. Muijsers, Th. Weber, R.M. van Hardeveld, H.W. Zandbergen, and J.W. Niemantsverdriet, *J. Catal.* **157**, 698 (1995).
[19] Th. Weber, J.C. Muijsers, and J.W. Niemantsverdriet, *J. Phys. Chem.* **99**, 9194 (1995).
[20] Th. Weber, J.C. Muijsers, J.H.M.C. van Wolput, C.P.J. Verhagen, and J.W. Niemantsverdriet, *J. Phys. Chem.* **100**, 14144 (1996).
[21] E. Payen, S. Kasztelan, J. Grimblot, and J.P. Bonnelle, *Catal. Today* **4**, 57 (1988).
[22] J.A.R. van Veen, E. Gerkema, A.M. van der Kraan, and A. Knoester, *J. Chem. Soc., Chem. Commun.* **22**, 1684 (1987).
[23] R. Cattaneo, T. Shido, and R. Prins, *J. Catal.* **185**, 199 (1999).
[24] L. Medici, and R. Prins, *J. Catal.* **163**, 38 (1996).
[25] R. Cattaneo, Th. Weber, T. Shido, and R. Prins, *J. Catal.* **191**, 225 (2000).
[26] A.M. de Jong, V.H.J. de Beer, J.A.R. van Veen, and J.W. Niemantsverdriet, *J. Phys. Chem.* **100**, 17722 (1996).
[27] L. Coulier, V.H.J. de Beer, J.A.R. van Veen, and J.W. Niemantsverdriet, *Topics in Catal.* **13**, 99 (2000).
[28] L. Coulier, V.H.J. de Beer, J.A.R. van Veen, and J.W. Niemantsverdriet, *J. Catal.* **197**, 26 (2001).
[29] G. Kishan, L. Coulier, V.H.J. de Beer, J.A.R. van Veen, and J.W. Niemantsverdriet, *Chem. Commun.* 1103(2000).
[30] J.F. Moulder, W.F. Stickle, P.E. Sobol, and K.D. Bomben, Handbook of XPS (Perkin Elmer Corporation, Eden Prairie, MN, 1992).
[31] E.W. Kuipers, C. Laszlo, and W. Wieldraaijer, *Catal. Lett.* **17**, 71 (1993).
[32] R.M. van Hardeveld, P.L.J. Gunter, L.J. van IJzendoorn, W. Wieldraaijer, E.W. Kuipers, and J.W. Niemantsverdriet, *Appl. Surf. Sci.* **84**, 339 (1995).

5

Promoting synergy in CoW sulfide hydrotreating catalysts by chelating agents*

Abstract

Adding chelating agents such as 1,2-cyclohexane diamine-N,N,N',N'-tetraacetic acid (CyDTA) or triethylene tetraamine hexaacetic acid (TTHA) to the aqueous solution of cobalt nitrate and ammonium metatungstate used for impregnating the silica support results in significantly enhanced activities for hydrodesulfurization of thiophene after the catalysts have been sulfided. No promotional effect of Co was found for CoW catalysts prepared by conventional method, where the sulfidation of Co precedes that of W. However, the chelating agents serve to retard the sulfidation of cobalt with respect to that of tungsten, which facilitates the formation of a phase in which Co atoms decorate the edges of WS_2, analogous to the well known CoMoS phase. The activity measurements show that using chelating agents the activity can be increased with a factor of 2.5.

* This chapter was published as: G. Kishan, L. Coulier, J.A.R. van Veen, and J.W. Niemantsverdriet, *J. Catal.* **200** (2001) 194.

5.1 Introduction

It is well known that the addition of Co and Ni to MoS_2, and of Ni to WS_2 hydrotreating catalysts significantly enhances the activity in the hydrodesulfurization of e.g. thiophene [1,2]. However, such synergy has not been observed in Co-promoted WS_2 catalysts, which is generally regarded as an unsuccessful combination. Reports on supported CoW catalysts are scarce and contradictory. Early papers on CoW systems mainly concerned unsupported $CoWS_2$ or Co impregnated on physical mixtures of WS_2 and Al_2O_3 [3,4] and comparing these systems with supported catalysts is not straightforward while the support has a large influence on the physical and catalytic properties of the active catalyst [1,2]. One of the first papers on Al_2O_3-supported CoW catalysts by Topsøe et al. [5] reported Mössbauer spectra of Co in CoW catalysts similar to those of Co in CoMo catalysts. This was evidence for the presence of a CoWS phase similar to the well-known CoMoS phase. Some recent papers on CoW/Al_2O_3 catalysts report contradictory results on the promotional effect of Co on the thiophene HDS activity on W/Al_2O_3. Suvanto et al. [6] observed an activity equal to a $CoMo/Al_2O_3$ catalyst and suggested from TPR spectra the formation of a synergetic active phase. These authors used carbonyl-precursor-based catalysts and the thiophene HDS reaction was carried out in batch mode and high pressure (10.5 bar). Vissenberg et al. [7] found for atmospheric thiophene HDS a strikingly low promotion effect of Co on W/Al_2O_3 compared to Mo/Al_2O_3, both prepared by conventional co-impregnation. Mössbauer spectroscopy showed complete sulfidation of Co at 300 K and the formation of large amounts of bulk Co-sulfide. No evidence for a highly active CoWS phase was found.

Recently, ways to increase the efficiency of promoter functionality have been reported [8], based on the generally accepted model of the CoMoS phase, in which the promoter atoms are located on the edges of the slab-structured MoS_2 phase. Key element in effective preparation routes towards CoMoS-like phases is that the transition of oxidic Co and Ni to their sulfidic state should occur after MoS_2 and WS_2 phases are formed [9-16]. Chelating agents such as nitrilo triacetic acid (NTA), ethylene diamine tetraacetic acid (EDTA) and derivatives of these molecules stabilize Ni and Co with respect to sulfide formation to temperatures where all or most of the Mo or W have converted to sulfides. These procedures enable one to prepare highly active CoMoS, NiMoS and NiWS catalysts irrespective of the support.

In this paper we will demonstrate that on conventional CoW catalysts, where Co sulfides completely before W, no synergy is observed. However, using the appropriate chelating agents to retard the sulfidation of Co with respect to that of W results in considerable enhancement of the HDS activity of CoW catalysts on silica supports.

5.2 Experimental

Catalysts were prepared on planar silica model supports. Planar silica was prepared by oxidizing a Si (100) wafer at 750 ^{0}C for 24 hours in air, cleaning it in a mixture of H_2O_2 and NH_4OH at 65 ^{0}C, and rehydroxylating the surface in boiling water for 30 min. The supports were impregnated by spincoating an aqueous solution of ammonium metatungstate (Merck), and cobalt nitrate (Merck). The concentration of W and Co in the precursor solutions was adjusted to result in a loading of 6 W atoms/nm^2 and 4 Co atoms/nm^2 after spincoating. Where desired, the chelating agents 1,2-cyclohexane diamine-N,N,N',N'-tetraacetic acid

(CyDTA; Merck) and triethylene tetraamine hexaacetic acid (TTHA; Merck) were added in an ammoniacal solutions, which contained the precursors of W, Co and CyDTA or TTHA in an atomic ratio of 6:4:4, such that the amount of chelating agent was equivalent to that of Co. Catalysts prepared without chelating agents were calcined at 500 ^{0}C for 30 min; catalysts prepared with chelating agents were used without calcination. For more details on the preparation we refer to earlier work [9,14,15].

XPS was applied to study the extent of sulfidation of catalysts as a function of temperature. Sulfidation was performed with a mixture of 10% H_2S/H_2 at a heating rate of 5 ^{0}C/min (2 ^{0}C/min for catalysts with chelating agents) to the desired temperature, after which samples were kept at that temperature for 30 min. After sulfidation, the reactor was cooled to room temperature under helium and transported to XPS under N_2 atmosphere. For details on the XPS measurements and the analysis of spectra we refer to recent publications from our laboratory on NiW/SiO_2 catalysts [9].

Model catalysts were tested in batch mode thiophene HDS under standard conditions (1.5 bar, 400 ^{0}C, 4% thiophene/H_2). Model catalysts were pre-sulfided at 400 ^{0}C for 30 min as described above. For more details, see [9,14,15].

5.3 Results and discussion

Figure 5.1 shows the Co 2p and W 4f XPS spectra for a calcined CoW/SiO_2 model catalyst sulfided at various temperatures. The Co 2p spectrum of the unsulfided catalysts shows a Co $2p_{3/2}$ at 781.9 eV and shake up features at higher binding energy, characteristic for oxidic Co [14,17]. After sulfidation at 25 ^{0}C a second Co $2p_{3/2}$ peak becomes visible at 779.0 eV, which agrees with the Co $2p_{3/2}$ binding energy of bulk Co-sulfide, i.e. Co_9S_8 [14,17]. At sulfidation temperatures of 100 ^{0}C the Co 2p doublet with Co $2p_{3/2}$ binding energy at 781.9 eV has disappeared and thus the sulfidation of Co is complete. This sulfidation behaviour corresponds well with that of Co/SiO_2 published earlier [14].

The sulfidation of W presented in Figure 5.1 proceeds similarly to that of W/SiO_2 and NiW/SiO_2 described in more detail in an earlier paper [9]. The unsulfided catalyst shows a W $4f_{7/2}$ peak at 36.0 eV which is characteristic of oxidic W in an oxidation state of 6+ [9,17]. The small peak at 42 eV is assigned to the W $5p_{5/2}$ state. The sulfidation of W starts at 150 ^{0}C, as evidenced by the appearance of second W 4f doublet at lower W $4f_{7/2}$ binding energy. WS_2 formation is characterized by the presence of a W $4f_{7/2}$ peak at 32.4 eV [9,17], clearly visible at temperatures above 150 ^{0}C. The sulfidation is complete around 300 ^{0}C. Fitting of the W 4f spectra showed no evidence for the presence of oxysulfides or WS_3 as intermediates during the sulfidation of W. The Co 2p and W 4f binding energies of the fully oxidic and sulfidic catalysts are shown in Table 5.1.

The Co 2p and W 4f spectra of $CoW\text{-}TTHA/SiO_2$ model catalysts as a function of sulfidation temperature are shown in Figure 5.2. The sulfidation of W proceeds similarly to that of W in CoW/SiO_2 (Figure 5.1). The W 4f binding energies of the fully oxidic and sulfidic catalysts with or without chelating agents are similar, as can be seen from Table 5.1. This indicates that W does not form complexes with chelating agents, which was also observed for NiW/SiO_2 model catalysts [9].

The sulfidation of Co however is greatly affected by the chelating agent. The Co 2p spectrum of the unsulfided $CoW\text{-}TTHA/SiO_2$ catalysts shows a pattern characteristic of Co in an oxidic environment, with a Co $2p_{3/2}$ peak at 781.4 eV and shake up features at higher

binding energy [14,17]. However, the Co $2p_{3/2}$ B.E. is 0.6 eV lower than that of Co in CoW/SiO_2 (see Table 5.1). This is explained by complexation of Co to TTHA, which was also observed for Ni to chelating agents like EDTA or CyDTA [9]. As shown in Figure 5.2, Co remains unsulfided to temperatures around 200 ^{0}C. Sulfidation at 250 ^{0}C shows the appearance of a second Co $2p_{3/2}$ peak at 779.5 eV. At 300 ^{0}C the doublet at 781.6 eV has disappeared and only the one at 779.4 eV remains, which means that the sulfidation of Co is complete. This temperature coincides with the complete disappearance of the N 1s signal (not shown) characteristic of the TTHA complex indicating that the decomposition of the Co-TTHA complex determines the rate of Co sulfidation.

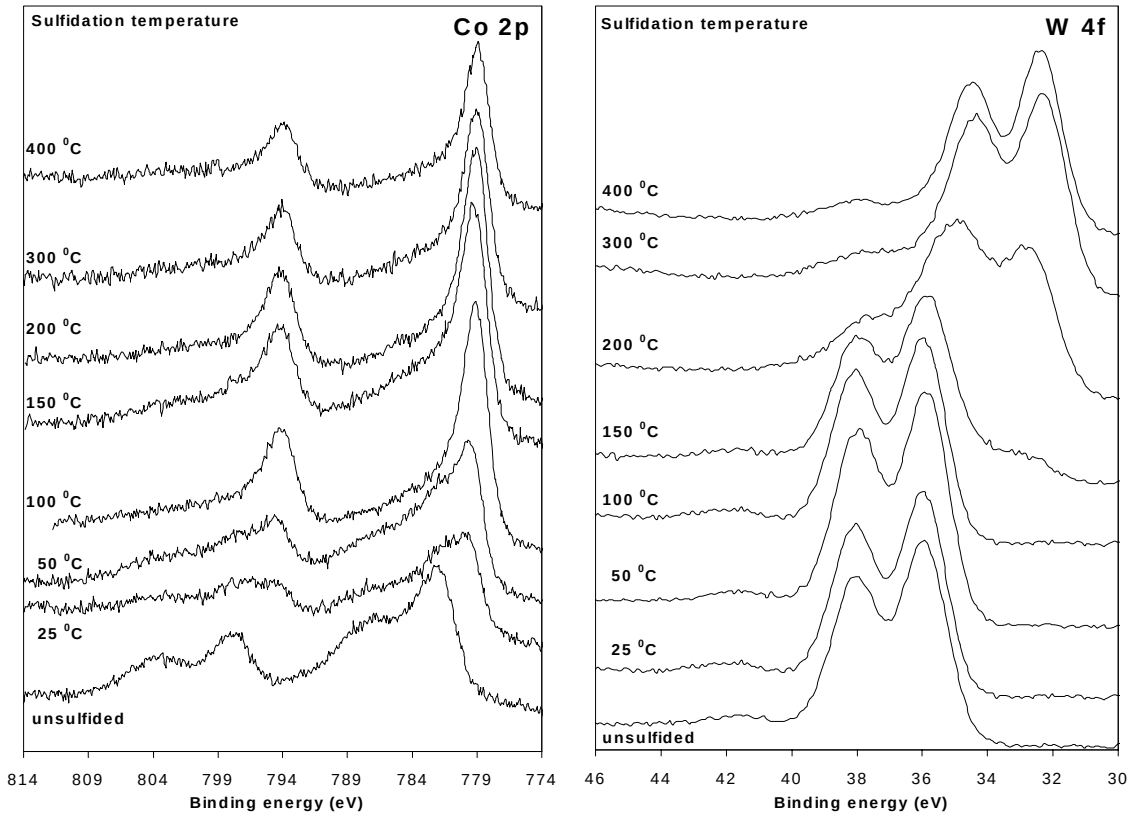

Figure 5.1 *Co 2p (left) and W 4f (right) XPS spectra of CoW/SiO_2 model catalysts sulfided at different temperatures, showing that Co and W sulfide in separate temperature regimes.*

Figure 5.3 shows the degree of sulfidation of W and Co for various CoW catalysts as a function of sulfidation temperature. The sulfidation behaviour of W in all catalysts is similar and is thus represented by the heavy line in Figure 5.4. Besides the CoW and CoW-TTHA catalysts described earlier, the sulfidation degree of CoW-NTA and CoW-CyDTA are shown. One clearly observes the retarding effect of the chelating agents on the sulfidation of Co. In the CoW catalysts the sulfidation of Co completely precedes that of W, while the chelating agents reverse this order of sulfidation, i.e. W sulfidation starts first. However, the retardation of the Co sulfidation increases in the order NTA < TTHA < CyDTA, although the differences are small.

The activity of the catalysts in thiophene hydrodesulfurization (HDS) is shown in Figure 5.4. The yields are based on 5 cm^2 surface area of catalyst and have been corrected for

conversion of an empty SiO_2 support in a blank experiment. The combination of blank SiO_2 support in the reactor has an order of magnitude lower activity than W/SiO_2, and shows mainly cracking products.

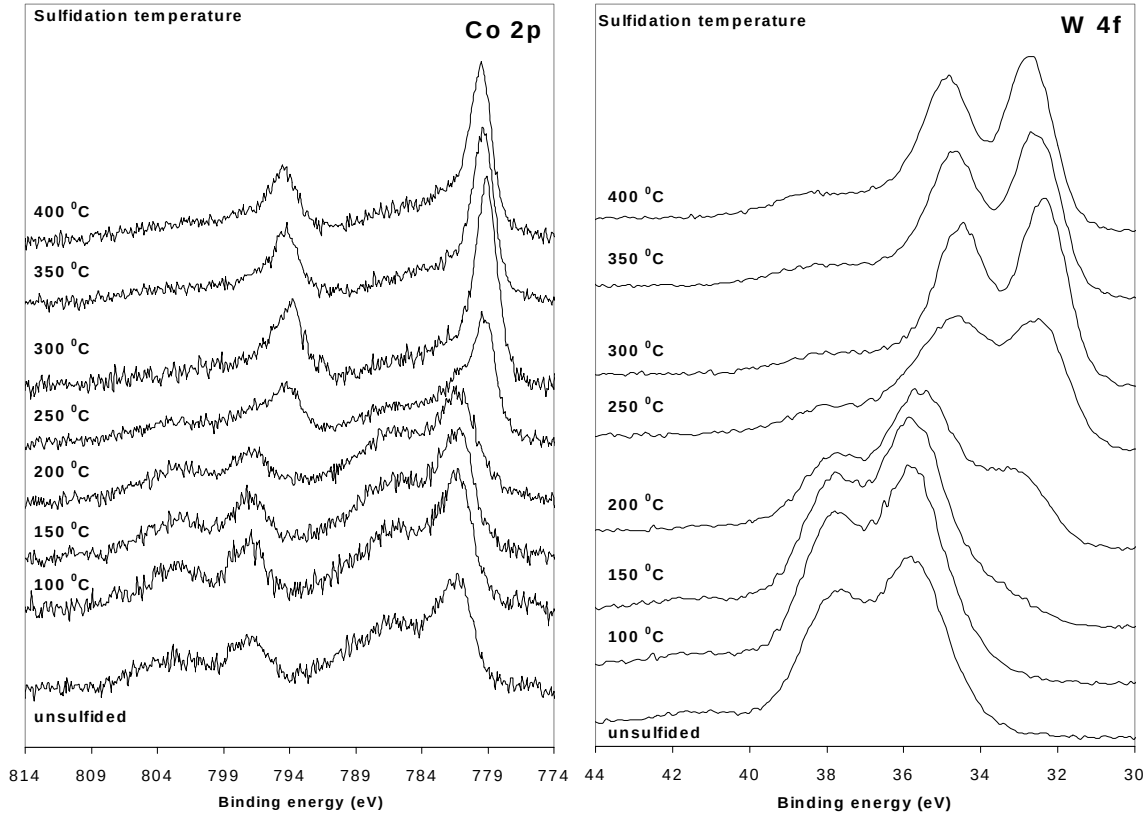

Figure 5.2 *Co 2p (left) and W 4f (right) XPS spectra of CoW-TTHA/SiO_2 model catalysts as a function of sulfidation temperature. TTHA retards the sulfidation to high temperatures, while sulfidation of W is not affected.*

Figure 5.4 shows that the lumped activity of W/SiO_2 and Co/SiO_2 is equal, hence no promotional effect of Co is observed. The XPS spectra in Figure 5.1 showed that the sulfidation of Co preceded that of W completely and hence bulk Co-sulfide formation is expected. The XPS binding energies in Table 5.1 agree with this idea. It seems that once bulk Co-sulfide is formed, Co cannot go to the edges of WS_2. This so-called redispersion to the edges of the WS_2-slabs was observed for NiW/SiO_2 catalysts resulting in a sudden change in Ni 2p binding energy at temperatures where WS_2 was formed together with a strong promotional effect of Ni on W/SiO_2 [9]. No evidence for this phenomenon was observed for CoW. Thus this confirms the notion that CoW is an unsuccessful combination for HDS reaction as was also concluded by Vissenberg et al. [7].

The addition of chelating agents clearly increases the HDS activity. NTA gives a substantial increase in activity of about 40%, while CyDTA increases the activity by 80%. The highest activity is observed with CoW-TTHA/SiO_2, which is nearly 2.4 times more active than standard CoW/SiO_2 of the same composition. The optimum Co/W ratio is 0.66, which is identical to that found for NiW catalysts [9].

Figure 5.3 shows that Co-W synergy, as measured by the increase in thiophene HDS activity, is observed when the sulfidation of Co is retarded by stabilizing Co with a chelating agent. As a result of this retardation, Co atoms released by the chelating agent can directly move to the edges of already formed WS_2 to form CoWS, a similar to CoMoS proposed by Topsøe and others [1,2]. Table 5.1 shows that for catalysts with enhanced HDS activity the Co 2p binding energy of the fully sulfided catalysts differ from the values of bulk Co-sulfide, found for CoW/SiO_2, where Co did not increased the activity. From the difference in B.E. we conclude that Co is in a different state than bulk Co-sulfide. The same difference in B.E. between low and high HDS active catalysts was found for NiW/SiO_2 [9] and $NiMo/SiO_2$ [15].

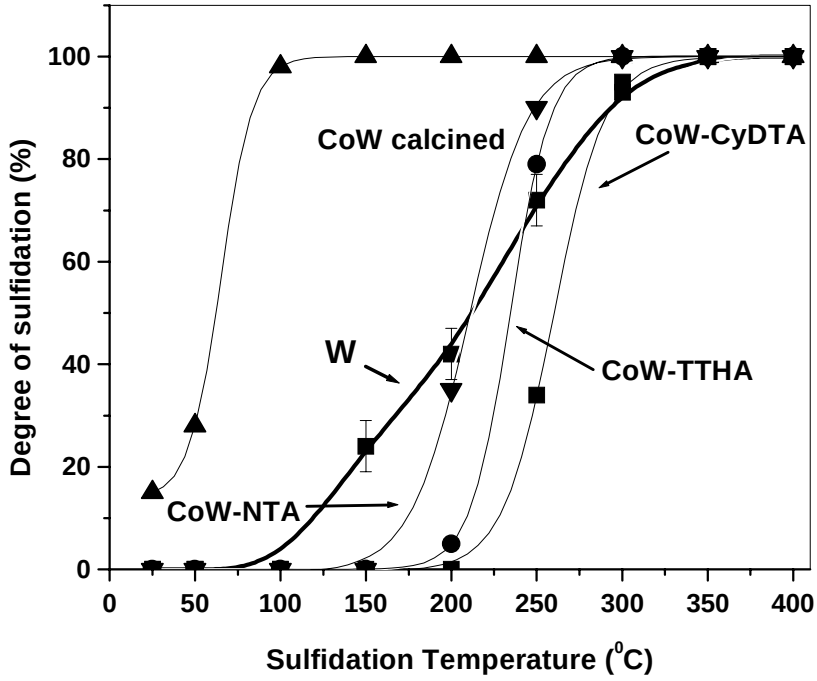

Figure 5.3 *Degree of sulfidation of Co and W in various CoW catalysts as a function of sulfidation temperature. Note that chelating agents stabilize Co against sulfide formation.*

Table 5.1 *XPS binding energies of Co 2p and W 4f doublets of fully oxidic and sulfidic CoW model catalysts.*

Catalyst	Co_{ox} $2p_{3/2}$ (eV)	Co_{sulf} $2p_{3/2}$ (eV)	W_{ox} $4f_{7/2}$ (eV)	W_{sulf} $4f_{7/2}$ (eV)
Co/SiO_2	782.3	779.1	-	-
W/SiO_2	-	-	35.9	32.6
CoW/SiO_2	782.1	779.0	35.9	32.5
$CoW\text{-}NTA/SiO_2$	781.7	779.2	35.9	32.5
$CoW\text{-}CyDTA/SiO_2$	781.6	779.4	36.0	32.7
$CoW\text{-}TTHA/SiO_2$	781.4	779.5	36.0	32.6

The effect of NTA on the HDS activity of CoW/SiO_2 is less than in the case of $CoMo/SiO_2$, as described earlier [14]. For $CoMo/SiO_2$ adding NTA increased the activity with a factor 4, while in the case of CoW only a 40% increase is observed. The difference between the two systems is the difference in sulfidation between Mo and W. In the case of Mo, adding NTA retards the sulfidation of Co to temperatures where Mo is almost completely formed, while in the case of W the degree of sulfidation of W is only 35% at this temperature. Hence, the chance that Co finds the edges of MoS_2 is larger than for WS_2.

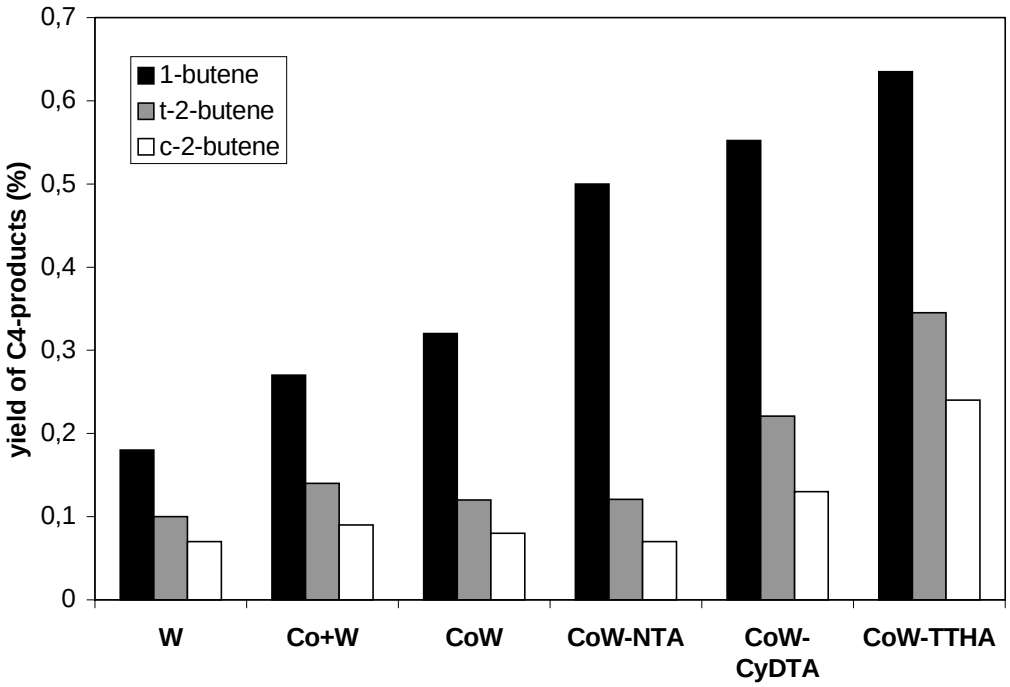

Figure 5.4 *Thiophene hydrodesulfurization over CoW model catalysts supported on silica prepared in different ways, showing the product distribution after 1 h of batch reaction at 400 ^0C.*

5.4 Conclusions

For silica-supported CoW model catalysts prepared with or without chelating agents, the rate of sulfidation of Co and W has been measured by XPS and compared with the activity in thiophene hydrodesulfurization (HDS).

- Co and W sulfide in separate temperature regimes in standard CoW/SiO_2 catalysts, which leads to the formation of bulk Co-sulfide and WS_2. This is confirmed by the XPS binding energies. No evidence for redispersion of Co after sulfidation was found.
- The CoW/SiO_2 catalysts showed no promotion effect for Co. The activity of these catalysts is equivalent to the activity of W/SiO_2 and Co/SiO_2 combined.
- Complexing of chelating agents, like NTA, CyDTA or TTHA, retards the sulfidation of Co to higher temperatures, where WS_2 has been (partially) formed. This leads to higher HDS activity compared to CoW/SiO_2. However, there exists a temperature range where Co and W sulfide simultaneously.

- The increase in activity is explained by the formation of the CoWS phase, where Co sulfide decorates the edges of WS_2-slabs. As a result of the retardation due to the chelating agents, Co atoms released by the chelating agent can directly move to the edges of already formed WS_2.

References

[1] H. Topsøe, B.S. Clausen, and F.E. Massoth, "Hydrotreating Catalysis." Springer-Verlag, Berlin, 1996.
[2] R. Prins, V.H.J. de Beer, and G.A. Somorjai, *Catal. Rev.-Sci. Eng.* **31**, 1 (1989).
[3] V.H.J. de Beer, J.G.J. Dahlman, and J.G.M. Smeets, *J. Catal.* **42**, 467 (1976).
[4] E. Furimsky, *Catal. Rev.-Sci. Eng.* **22**, 371 (1980).
[5] H. Topsøe, B.S. Clausen, R. Candia, C. Wivel, and S. Mørup, *Bull. Soc. Chim. Belg.* **90**, 1189 (1981).
[6] M. Suvanto, J. Räty, and T.A. Pakkanen, *Appl. Catal. A* **181**, 189 (1999).
[7] M.J. Vissenberg, Y. van der Meer, E.J.M. Hensen, V.H.J. de Beer, A.M. van der Kraan, R.A. van Santen, and J.A.R. van Veen, *J. Catal.* **198**, 151 (2001).
[8] J.A.R. van Veen, E. Gerkema, A.M. van der Kraan, and A. Knoester, *J. Chem. Soc., Chem. Commun.* **22**, 1684 (1987).
[9] G. Kishan, L. Coulier, V.H.J. de Beer, J.A.R. van Veen, and J.W. Niemantsverdriet, *J. Catal.* **196**, 180 (2000).
[10] R. Cattaneo, T. Shido, and R. Prins, *J. Catal.* **185**, 199 (1999).
[11] L. Medici, and R. Prins, *J. Catal.* **163**, 38 (1996).
[12] R. Cattaneo, Th. Weber, T. Shido, and R. Prins, *J. Catal.* **191**, 225 (2000).
[13] A.M. de Jong, V.H.J. de Beer, J.A.R. van Veen, and J.W. Niemantsverdriet, *J. Phys. Chem.* **100**, 17722 (1996).
[14] L. Coulier, V.H.J. de Beer, J.A.R. van Veen, and J.W. Niemantsverdriet, *Topics in Catal.* **13**, 99 (2000).
[15] L. Coulier, V.H.J. de Beer, J.A.R. van Veen, and J.W. Niemantsverdriet, *J. Catal.* **197**, 26 (2001).
[16] G. Kishan, L. Coulier, V.H.J. de Beer, J.A.R. van Veen, and J.W. Niemantsverdriet, *Chem. Commun.* 1103 (2000).

6

Influence of support-interaction on the sulfidation behaviour and hydrodesulfurization activity of Co- and Ni-promoted W/Al_2O_3 model catalysts

Abstract

The interaction of Co (or Ni) and W with the Al_2O_3-support influences the sulfidation behaviour and thiophene hydrodesulfurization (HDS) activity of CoW and NiW model catalysts. High calcination temperatures retard the sulfidation of Co, Ni and W to high temperature and lead to incomplete sulfidation. Chelating agents, like cyclohexane diamine-N,N,N',N'-tetraacetic acid (CyDTA), retard the sulfidation of Co and Ni, although the sulfidation is complete. In bimetallic catalysts, the presence of W facilitates the sulfidation of Co and Ni. It is concluded that W prevents the strong interaction of Co and Ni with the Al_2O_3-support and partially blocks the diffusion of Co and Ni into the support.

For CoW/Al_2O_3 catalysts no promotion effect is observed. During sulfidation of CoW/Al_2O_3, bulk Co-sulfide and WS_2 are formed and the HDS activity is equal to the lumped activity of Co/Al_2O_3 and W/Al_2O_3. For NiW/Al_2O_3 model catalysts a strong promotion effect of Ni is observed. Depending on the calcination temperature, the HDS activity of NiW/Al_2O_3 is a factor 5-6 higher than W/Al_2O_3. The strong promotion effect is ascribed to the formation of the NiWS phase by redispersion of pre-formed bulk Ni-sulfide to the edges of WS_2-slabs. Both the calcination and sulfidation temperature have a strong influence on the HDS activity. Incomplete sulfidation due to either high calcination temperature or low sulfidation temperature decreases the HDS activity. High sulfidation temperature and low calcination temperature leads to segregation of the NiWS phase and thus a decrease in HDS activity. NiW/Al_2O_3 containing CyDTA show the highest HDS activity. Due to the complexation of Ni with CyDTA, the sulfidation of Ni is retarded to temperatures where WS_2 is already formed, thereby forming directly NiWS.

In general, it can be concluded that for W-based catalysts, Al_2O_3 is a better support for active phase formation than SiO_2. Catalysts containing CyDTA showed the highest activity irrespective of support.

6.1 Introduction

Commonly applied catalysts for hydrotreating processes are Al_2O_3-supported Co(Ni)Mo or NiW catalysts [1]. Especially NiW/Al_2O_3 catalysts have been proven to show high activity in deep hydrodesulfurization (HDS) and hydrogenation (HYD), which is important or reducing aromatics in diesel fuel [2,3]. However, literature on W-based catalysts is less abundant compared to Mo-based catalysts.

The two systems show some similarity. For example, the sulfidation mechanism is reported to be the same, although the interaction of W with Al_2O_3 is stronger than that of Mo, leading to a different degree of sulfidation [4-6]. The promoting behaviour of Co and Ni is however different for W and Mo catalysts. Addition of Co to Mo-based catalysts and Ni to both Mo- and W-based catalysts increase the activity significantly and active phases similar to the so-called CoMoS are reported [1]. However, for CoW catalysts no promotion effect is observed [7,8]. Due to the strong interaction of W with the Al_2O_3 support, the sulfidation of W occurs at higher temperatures compared to Mo [4]. As a result Ni and Co sulfide before W and bulk Co- and Ni-sulfide is formed. In recent papers on SiO_2-supported NiW model catalysts it was shown that bulk Ni-sulfide is able to migrate to the edges of WS_2, thereby forming NiWS [9,10]. However, for CoW this was not observed, apparently bulk Co-sulfide is too stable [8]. Other authors also reported this so-called redispersion of Ni-sulfide in NiW/Al_2O_3 [5,7,11,12].

It is known that chelating agents, like nitrilo triacetic acid (NTA), increase the HDS activity irrespective of the support [13]. In the past we have shown that chelating agents, like CyDTA, increase the HDS activity of both NiW/SiO_2 and CoW/SiO_2 model catalysts [8-10]. Complexation of Co and Ni to CyDTA retards the sulfidation to temperatures where WS_2 was already partially formed and hence Co and Ni are able to move directly to the edges of WS_2 to form the active phase [8-10]. Ohta et al. [14] also found an increase in (di)benzothiophene HDS activity of NiW/Al_2O_3 catalysts using chelating agents.

In this paper we will expand our work HDS model catalysts to other supports, i.e. Al_2O_3. We will follow the sulfidation of W, CoW and NiW supported on Al_2O_3 with X-ray Photoelectron Spectroscopy (XPS) and study the influence of calcination temperature and chelating agents on the sulfidation behaviour of the various catalysts. By combining the XPS results with atmospheric gas-phase thiophene HDS activity measurements, it is possible to correlate the sulfidation behaviour with the HDS activity and study the influence of calcination and sulfidation temperature on the activity. Comparing the results with that of SiO_2-supported model catalysts will show the effect of support interaction on the formation of active phase.

6.2 Experimental

Alumina model supports were prepared in an UHV system (P~$1*10^{-7}$ mbar) by evaporation of Al in an O_2 atmosphere (P_{O2}~$1.2*10^{-3}$ mbar) on pre-cleaned Si-wafers which resulted in an Al_2O_3 layer of 5 nm. The deposition rate of the oxide layer was 0.1 nm/s. After evaporation the model supports were kept in distilled water. XPS measurements on the alumina model supports gave an Auger parameter of 1461.5 eV, which corresponds with γ-Al_2O_3. The model support was impregnated by spincoating an aqueous solution of ammonium metatungstate (Merck), and cobalt nitrate or nickel nitrate (Merck). The

concentration of W and Co (or Ni) in the precursor solutions was adjusted to result in a loading of 6 W atoms/nm^2 and 4 Co (or Ni) atoms/nm^2 after spincoating. Where desired, the chelating agents 1,2-cyclohexane diamine-N,N,N',N'-tetraacetic acid (CyDTA; Merck) was added in an ammoniacal solution, which contained the precursors of W, Co (or Ni) and CyDTA in an atomic ratio of 6:4:4, such that the amount of chelating agent was equivalent to that of Co (or Ni). Part of the catalysts prepared without chelating agents were calcined at 400 ^{0}C or 550 ^{0}C for 60 min in 20% O_2/Ar with a heating rate of 5 ^{0}C/min; catalysts prepared with chelating agents were used without calcination. One catalyst was prepared by spincoating W/Al_2O_3 calcined at 550 ^{0}C with a solution containing Co and nitrilo triacetic acid (NTA) with a Co:NTA atomic ratio of 1:1 (Co(NTA)W/Al_2O_3 calc 550 ^{0}C).

XPS was applied to study the extent of sulfidation of catalysts as a function of temperature. Sulfidation was performed with a mixture of 10% H_2S/H_2 at a heating rate of 5 ^{0}C/min (2 ^{0}C/min for catalysts with chelating agents) to the desired temperature, after which samples were kept at that temperature for 30 min. After sulfidation, the reactor was cooled to room temperature under helium and transported to XPS under N_2 atmosphere.

Model catalysts were tested in batch mode thiophene HDS under standard conditions (1.5 bar, 400 ^{0}C, 4% thiophene/H_2). Model catalysts were presulfided at 400 ^{0}C or 550 ^{0}C for 30 min as described above.

For more details the reader is referred to earlier work [10,15,16].

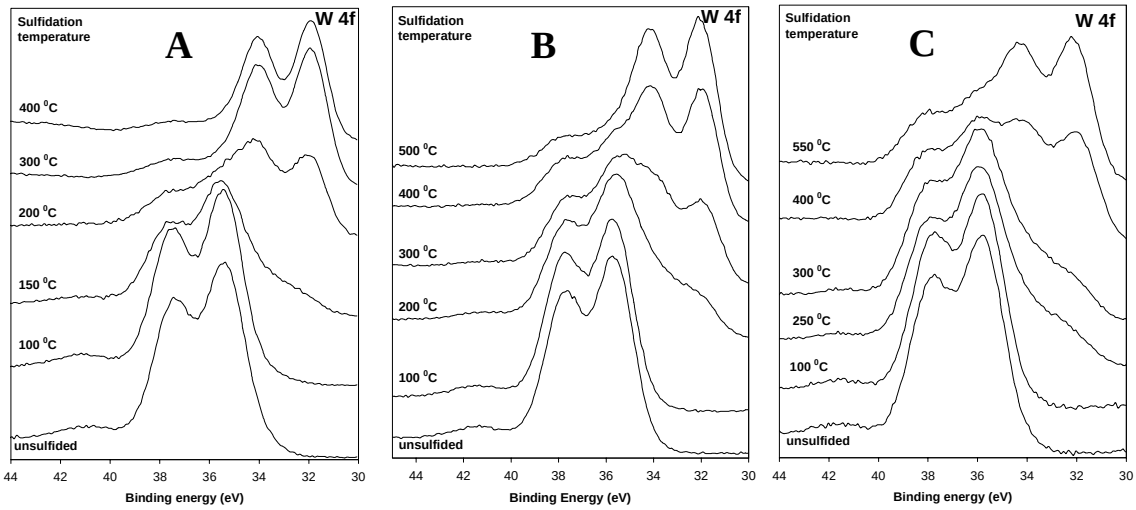

Figure 6.1 *W 4f spectra of Al_2O_3-supported W model catalysts uncalcined (A), calcined at 400 ^{0}C (B) and calcined at 550 ^{0}C sulfided at various temperatures.*

6.3 Results

W/Al_2O_3. Figure 6.1 shows the XPS spectra of W/Al_2O_3 uncalcined (A), calcined at 400 ^{0}C (B), and calcined at 550 ^{0}C (C) after sulfidation at various temperatures. The W 4f spectra of the uncalcined catalysts all show a single doublet around 35.7 eV and a W $5p_{3/2}$ peak at higher binding energy. This can be assigned to W^{6+} in an oxidic environment and corresponds well with the binding energies found by other authors for high surface area (Ni)W/Al_2O_3 catalysts [17,18] and earlier work on SiO_2-supported CoW and NiW model catalysts [8-10]. The sulfidation of W is visible from the appearance of a W 4f doublet

around 32.0 eV, corresponding with sulfided W^{4+}-species [17,18]. Comparison of the XPS spectra in Figure 6.1 indicates that the sulfidation of W/Al_2O_3 is retarded due to calcination. While for uncalcined W/Al_2O_3 the sulfidation starts at 150 ^{0}C and is complete around 250 ^{0}C, the sulfidation of the calcined catalysts is shifted to significantly higher temperatures. After calcination at 400 ^{0}C, the sulfidation starts around 200 ^{0}C and is only complete above 400 ^{0}C, while after calcination at 550 ^{0}C the sulfidation does not start until 250 ^{0}C and is still not complete at 550 ^{0}C.

Table 6.1 *XPS fit results of the sulfidation of W/Al_2O_3 as function of calcination temperature*

T_{sulf}	W/Al_2O_3 uncalc			W/Al_2O_3 calc 400 ^{0}C			W/Al_2O_3 calc 550 ^{0}C		
(^{0}C)	W_{ox} (eV)	W_{interm} (eV)	W_{sulf} (eV)	W_{ox} (eV)	W_{interm} (eV)	W_{sulf} (eV)	W_{ox} (eV)	W_{interm} (eV)	W_{sulf} (eV)
-	35.5	-	-	35.5	-	-	35.7	-	-
100	35.5	-	-	35.5	-	-	35.7	-	-
150	35.4 (0.94)	33.1 (0.06)	-	35.5	-	-	-	-	-
200	35.5 (0.36)	33.5 (0.09)	32.0 (0.55)	35.5 (0.72)	33.2 (0.21)	31.9 (0.07)	-	-	-
250	-	-	32.0	-	-	-	35.8 (0.92)	33.4 (0.08)	-
300	-	-	32.0	35.5 (0.51)	33.4 (0.18)	31.9 (0.31)	35.8 (0.85)	33.6 (0.15)	-
400	-	-	32.2	-	33.6 (0.20)	32.1 (0.80)	35.9 (0.41)	33.6 (0.13)	31.9 (0.46)
500	-	-	32.4	-	-	32.3	-	-	-
550	-	-	-	-	-	-	35.9 (0.34)	-	32.1 (0.66)

The W 4f spectra have been fitted to determine the binding energies and degree of W-sulfidation as shown in Table 6.1. The degree of WS_2 formation as a function of sulfidation temperature for the various W catalysts is shown in brackets in Table 6.1. The retarding effect of calcination can be clearly seen. For W/Al_2O_3 calcined at 550 ^{0}C a sulfidation degree of ~65% is found after sulfidation at 550 ^{0}C, while the other catalysts are completely sulfided at this temperature. All the spectra can be fitted with a W 4f doublet with W $4f_{7/2}$ B.E. at 35.7 ± 0.2 eV and one at 32.0 ± 0.2 eV, corresponding to W^{6+}-oxide and W^{4+}-sulfide species, respectively [17,18]. Due to the small difference in W $4f_{7/2}$ binding energy between WO_3 and $Al_2(WO_4)_3$ (e.g. 35.0 vs. 35.4 eV [17] and 35.5 vs. 36.1 eV [18], respectively) these species can not be excluded. For intermediate temperatures a third doublet is needed to fit the spectra. This doublet with W $4f_{7/2}$ B.E. at 33.4 ± 0.2 eV can be attributed to either oxysulfidic W^{6+}-species or WS_3, which are proposed as intermediates for the sulfidation of W [5-7,11,12,17,19-21]. These intermediate species are absent at high sulfidation temperatures, independent on the degree of sulfidation. The S 2p spectra (not shown) showed a single S 2p doublet at 161.6 eV, corresponding to S^{2-}-ligands. Analysis of the W 4f/S 2p atomic ratios show that the intermediate W-species should contain sulfur. However, there is not enough sulfur present for WS_3.

The W 4f spectra of promoted W/Al_2O_3 model catalysts do not show any differences in sulfidation behaviour. Therefore we can conclude that Co or Ni do not influence the sulfidation of W to a large extent, which we also observed for SiO_2-supported W model catalysts [8-10]. The sulfidation of W in NiWCyDTA/Al_2O_3 is identical to that of W in uncalcined W/Al_2O_3. Earlier work also showed that W does not complex to chelating agents like CyDTA [8-10], which is confirmed by Ohta et al. [14] with NMR.

Figure 6.2 shows the thiophene HDS activities after 1 h of batch reaction at 400 ^{0}C in 4% thiophene/H_2 of W/Al_2O_3 model catalysts either uncalcined or calcined at 400 ^{0}C and 550 ^{0}C. As a reference, the HDS activity of a W/SiO_2 model catalyst with the same loading is given, as reported earlier [8-10]. The latter was shown to be independent of calcination temperature. Figure 6.3 shows the influence of the sulfidation temperature on the HDS activities of various W/Al_2O_3 catalysts.

The HDS activities depend strongly on calcination temperature and sulfidation temperature. For sulfidation temperatures of 400 ^{0}C, the activity decreases with increasing calcination temperature (see Figure 6.2). The XPS spectra in Figure 6.1 showed that the sulfidation degree of W after sulfidation at 400 ^{0}C also decreases with increasing calcination temperature. Compared to W/SiO_2, which is completely sulfided at 400 ^{0}C, the activity of uncalcined W/Al_2O_3 is higher, while W/Al_2O_3 calcined at 550 ^{0}C is less active than W/SiO_2. At higher sulfidation temperatures, uncalcined W/Al_2O_3 is less active, while for the calcined W/Al_2O_3 catalysts the activity increases with increasing sulfidation temperature (Figure 6.3).

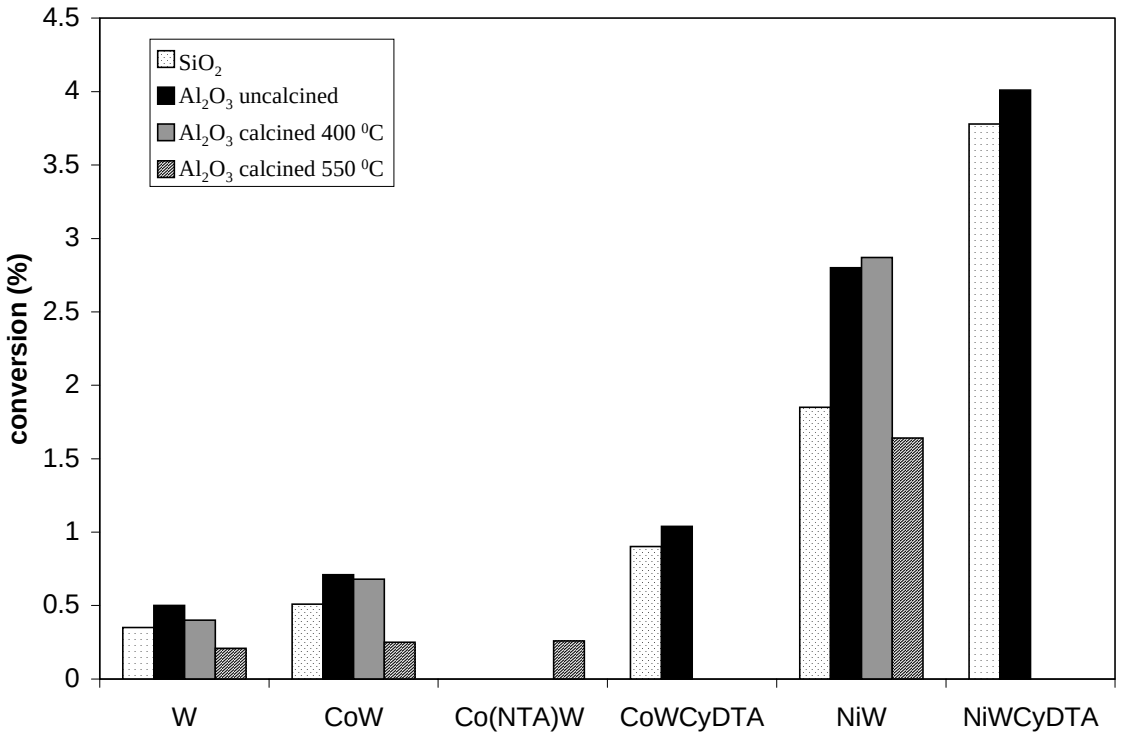

Figure 6.2 *Thiophene HDS activity of various unpromoted and promoted W/Al_2O_3 model catalysts sulfided at 400 ^{0}C. Activity expressed as conversion (%) of thiophene after 1 hour of batch reaction at 400 ^{0}C per 5 cm^2 of catalysts. For reference the HDS activities of SiO_2-supported W-based catalysts are given [8-10].*

Co(Ni)/Al_2O_3. The sulfidation of Co/Al_2O_3 and Ni/Al_2O_3 and the effect of calcination on the sulfidation are followed with XPS. Table 6.2 shows the Co 2p and Ni 2p binding energies of oxidic and sulfidic Co- and Ni-species and the degree of Co- and Ni-sulfidation at 400 ^{0}C. Figure 6.4 shows schematically the degree of Co sulfidation of various catalysts as a function of temperature. The curves in Figure 6.4 show that the sulfidation of uncalcined Co/Al_2O_3 starts at low temperatures but proceeds slowly at high temperature and complete sulfidation is only reached at 550 ^{0}C. For calcined Co/Al_2O_3 the sulfidation proceeds even more slowly. The sulfidation starts around 150 ^{0}C and is not even complete after sulfidation at 550 ^{0}C (~50%). The sulfidation of Ni/Al_2O_3 is quite similar to Co/Al_2O_3. The sulfidation of uncalcined Ni/Al_2O_3 starts at low temperatures and is complete at 400 ^{0}C (see Table 6.2). Calcination of Ni/Al_2O_3 retards the sulfidation to high temperatures and leads to incomplete sulfidation at high temperatures, i.e. 55% at 400 ^{0}C. In general, the sulfidation of Ni proceeds more easily than that of Co.

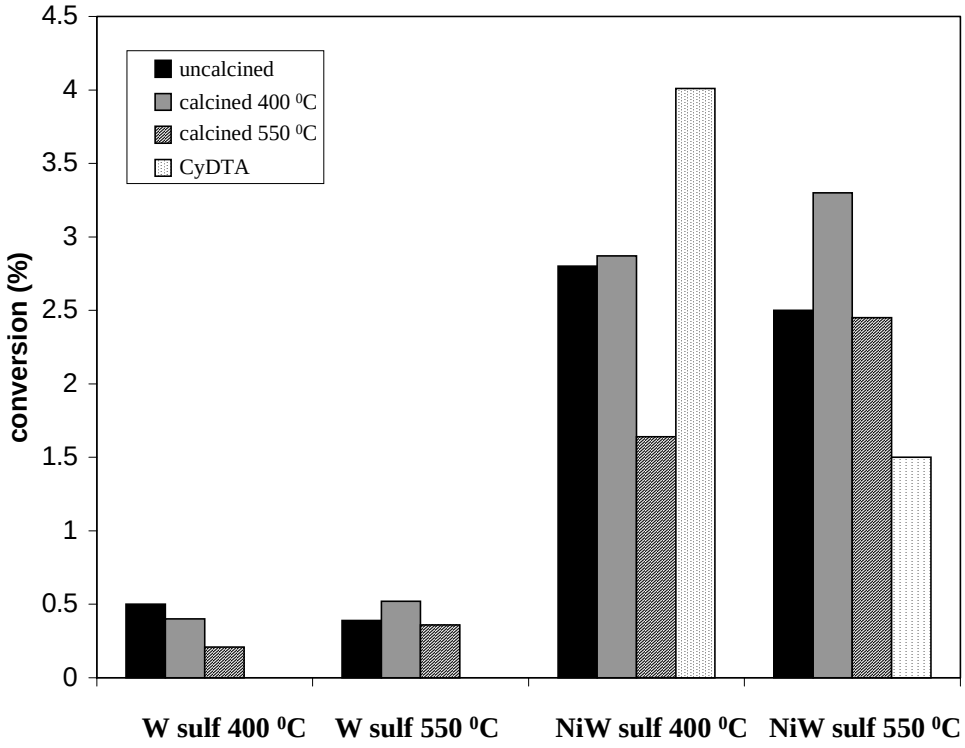

Figure 6.3 *Thiophene HDS activity of (Ni)W/Al_2O_3 model catalysts sulfided at 400 ^{0} C and 550 ^{0}C. Activity expressed as conversion (%) of thiophene after 1 hour of batch reaction at 400 ^{0}C per 5 cm^2 of catalysts.*

Table 6.2 shows that the Co $2p_{3/2}$ and Ni $2p_{3/2}$ binding energies of oxidic and sulfidic Co (or Ni) are equal for both uncalcined and calcined catalysts. The Co and Ni species at with Co $2p_{3/2}$ and Ni $2p_{3/2}$ binding energies of 782.0 eV and 856.6 eV, respectively, can be ascribed to oxidic Co and Ni [17,18,22]. The Co $2p_{3/2}$ and Ni $2p_{3/2}$ binding energy of the sulfided catalysts, respectively 778.9 eV for Co and 853.3 eV for Ni, correspond well to bulk Co- and Ni-sulfide, respectively [17,18,22].

CoW/Al_2O_3. The sulfidation of W in CoW/Al_2O_3 is identical to that of W in W/Al_2O_3, as described earlier. Figure 6.4 and Table 6.2 summarize the sulfidation behaviour of Co in the various CoW/Al_2O_3 catalysts. The Co 2p spectra could all be fitted with two Co 2p doublets, with Co $2p_{3/2}$ B.E. at 782.0 ± 0.2 eV for oxidic Co and 779.1 ± 0.2 eV for sulfidic Co [22]. Table 6.2 shows that only the Co $2p_{3/2}$ binding energy of unsulfided $CoWCyDTA/Al_2O_3$ is significantly lower, i.e. 781.1 eV, which we contribute to complexation of Co to CyDTA [8]. For the sulfided catalysts, the Co $2p_{3/2}$ binding energy of $CoWCyDTA/Al_2O_3$ is somewhat higher compared to the other catalysts, although the difference is smaller than for the oxidic catalysts.

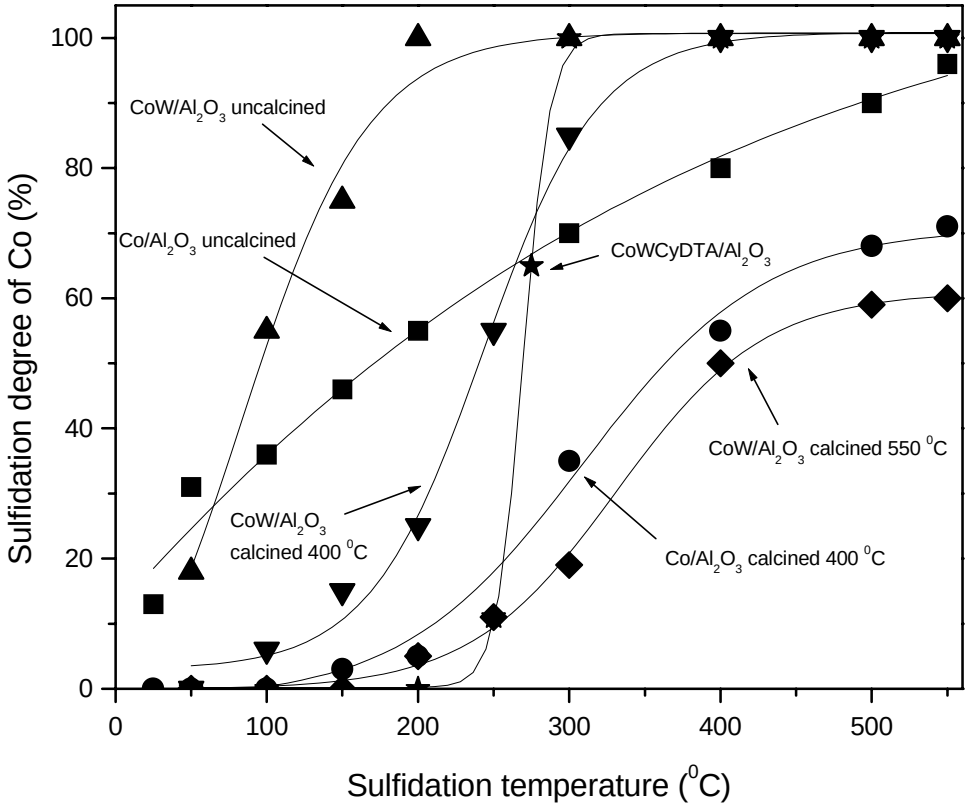

Figure 6.4 *Degree of Co sulfidation of various Co(W)/Al_2O_3 model catalysts as function of sulfidation temperature.*

Figure 6.4 shows the degree of Co sulfidation as a function of sulfidation temperature. The sulfidation of Co depends strongly on the calcination temperature, as was also observed earlier for Co/Al_2O_3. While for uncalcined CoW/Al_2O_3 the sulfidation of Co starts at room temperature and is complete at 200 ^{0}C, the sulfidation of the calcined catalysts proceeds at much higher temperature. For example, CoW/Al_2O_3 calcined at 400 ^{0}C starts to sulfide around 100 ^{0}C and is completely sulfided at 400 ^{0}C, while CoW/Al_2O_3 calcined at 550 ^{0}C is

not even completely sulfided after sulfidation at 550 ^{0}C. Interestingly the presence of W influences the sulfidation of Co. For example, Co in uncalcined Co/Al_2O_3 is only for 80% sulfided at 400 ^{0}C, while in uncalcined CoW/Al_2O_3 the sulfidation is complete at 200 ^{0}C. The same is true for the Co(W)/Al_2O_3 catalysts calcined at 400 ^{0}C (see Figure 6.4). Complexing Co to CyDTA influences the sulfidation of Co significantly. As can be seen in Figure 6.4, the sulfidation of Co starts at high temperature, i.e. 250 ^{0}C, and is complete at relatively low temperature, i.e. 300 ^{0}C. This sulfidation behaviour is similar to that of Co in CoWCyDTA/SiO_2 as reported earlier [8].

Table 6.2 *Co 2p and Ni 2p binding energies of oxidic and sulfidic Co(W)/Al_2O_3 and Ni(W)/Al_2O_3 model catalysts and degree of Co or Ni sulfidation after sulfidation at 400 ^{0}C.*

Catalyst	Co_{ox} $2p_{3/2}$ /Ni_{ox} $2p_{3/2}$ (eV)	Co_{sulf} $2p_{3/2}$ /Ni_{sulf} $2p_{3/2}$ (eV)	% CoS/NiS (T_{sulf}=400 ^{0}C)
Co uncalcined	782.0	778.9	80
Co calcined 400 ^{0}C	782.0	778.9	45
CoW uncalcined	782.0	779.1	100
CoW calcined 400 ^{0}C	781.7	778.8	100
CoW calcined 550 ^{0}C	782.0	778.8	48
CoWCyDTA	781.1	779.4	100
Ni uncalcined	856.6	853.3	100
Ni calcined 400 ^{0}C	856.5	853.3	55
NiW uncalcined	856.4	853.9	100
NiW calcined 400 ^{0}C	856.3	853.8	100
NiW calcined 550 ^{0}C	856.6	853.7	63
NiWCyDTA	855.5	854.2	100

Figure 6.2 shows the thiophene HDS activity of various (Co)W/Al_2O_3 model catalysts. For comparison the activities of SiO_2-supported CoW catalysts are also shown [8]. The most striking observation is the small promotion effect of Co. Conventional CoW catalysts are only a bit more active than W catalysts. Moreover, the lumped activity of Co/Al_2O_3 and W/Al_2O_3 is similar to the activity of CoW/Al_2O_3 and hence no synergy is observed, which we also observed for SiO_2-supported CoW catalysts [8]. However, the presence of CyDTA increases the activity considerably compared to conventional CoW catalysts for both supports, i.e. an increase with a factor 1.5 for Al_2O_3 and 1.8 for SiO_2. The activity of CoWCyDTA/Al_2O_3 is somewhat higher than CoWCyDTA/SiO_2. For the conventional catalysts the uncalcined Al_2O_3-supported catalyst shows the highest activity. Calcination at 400 ^{0}C leads to a small decrease in activity, although the activity is still higher than for CoW/SiO_2. CoW/Al_2O_3 calcined at 550 ^{0}C shows a strikingly low HDS activity. The catalyst prepared by spincoating Co-NTA on W/Al_2O_3 calcined at 550 ^{0}C, i.e. Co(NTA)W/Al_2O_3 calc 550 ^{0}C, shows the same activity

NiW/Al_2O_3. Figure 6.5 shows the Ni 2p spectra of four NiW/Al_2O_3 model catalysts as a function of sulfidation temperature, i.e. A) uncalcined NiW/Al_2O_3, B) NiW/Al_2O_3 calcined 400 ^{0}C, C) NiW/Al_2O_3 calcined 550 ^{0}C, and D) NiWCyDTA/Al_2O_3. The Ni 2p spectra all clearly show the transition of Ni from the oxidic to the sulfidic phase. At low temperatures

the Ni 2p spectra consist of a single doublet with Ni $2p_{3/2}$ B.E. around 856.4 eV with shake up features at higher temperatures, characteristic for oxidic Ni, probably Ni_2O_3 [17,18]. At high temperatures a second doublet is present around 853.8 eV with small shake up features at high sulfidation temperatures, characteristic for sulfidic Ni [17,18]. Figure 6.5 clearly shows the influence of calcination on the sulfidation of Ni. In the uncalcined catalyst Ni starts to sulfide at 50 ^{0}C and is complete around 200 ^{0}C, while for NiW/Al_2O_3 calcined at 400 ^{0}C the sulfidation starts around 100 ^{0}C and is complete around 400 ^{0}C. The sulfidation of Ni in NiW/Al_2O_3 calcined at 550 ^{0}C is retarded to even higher temperatures, i.e. sulfidation starts around 250 ^{0}C and is not even complete around 550 ^{0}C. Figure 6.5 D clearly shows the retarding effect of CyDTA on the sulfidation of Ni. The sulfidation starts around 200 ^{0}C and is completed around 300 ^{0}C, identical to NiWCyDTA/SiO_2 [9,10] and similar to CoWCyDTA as described above. In general, the sulfidation of Ni in NiW/Al_2O_3 is quite similar to that of Co in CoW/Al_2O_3 in Figure 6.4.

Table 6.2 shows the Ni $2p_{3/2}$ binding energies and the degree of Ni sulfidation of the various NiW catalysts. Comparing the degree of Ni sulfidation in Table 6.2 it is clear that W facilitates the sulfidation of Ni. For example, after sulfidation at 400 ^{0}C Ni in NiW/Al_2O_3 calcined at 400 ^{0}C is completely sulfided while for Ni in Ni/Al_2O_3 calcined at 400 ^{0}C the degree of sulfidation is only 55%. The Ni 2p spectra can all be fitted with two Ni 2p doublets, with Ni $2p_{3/2}$ binding energies of 856.4 ± 0.2 eV for oxidic Ni and 853.8 ± 0.2 eV for sulfidic Ni [17,18]. The Ni $2p_{3/2}$ binding energy of oxidic Ni in NiWCyDTA at 855.5 eV differs significantly. We contribute this to complexation of Ni to CyDTA as was also observed for SiO_2-supported CoW model catalysts [8]. The Ni $2p_{3/2}$ binding energy of oxidic Ni is equal for both Ni and NiW catalysts, while the binding energy of sulfidic Ni in NiW/Al_2O_3 is almost 0.5 eV higher compared to Ni/Al_2O_3. There is no evidence for the presence of more than two Ni species [6,12,23,24].

Table 6.3 shows the fitting results of the Ni 2p spectra of uncalcined NiW/Al_2O_3 and NiWCyDTA/Al_2O_3 as a function of sulfidation temperature. It shows that sulfidic Ni with a Ni $2p_{3/2}$ binding energy of 853.4 eV is present at 50 ^{0}C for the uncalcined NiW catalysts. This binding energy is characteristic for Ni in NiS (see Table 6.2). As the sulfidation temperature is increased the relative contribution of sulfidic Ni increases. At 300 ^{0}C, the sulfidation of Ni is complete, but the Ni $2p_{3/2}$ binding energy is shifted with 0.5 eV to 853.9 eV. The same shift is observed for the calcined NiW catalysts, although at higher temperatures. For NiWCyDTA the sulfidation of Ni starts at 200 ^{0}C and has directly a Ni $2p_{3/2}$ binding energy of 854.2 eV. Interestingly, for both catalysts the Ni $2p_{3/2}$ binding energy shifts to 853.6 eV after sulfidation at higher temperature.

Figures 6.2 shows the thiophene HDS activity of the various NiW/Al_2O_3 model catalysts sulfided at 400 ^{0}C. For comparison, the HDS activities of SiO_2-supported catalysts are also shown [9,10]. It can be seen that NiWCyDTA/Al_2O_3 shows the highest activity irrespective of the support, although NiWCyDTA/Al_2O_3 seems slightly more active than NiWCyDTA/SiO_2 .The promoting effect of Ni on the HDS activity of W/Al_2O_3 is also clearly visible. The presence of Ni increases the HDS activity with a factor 5-6, which is considerably higher compared to the promotion effect of Co. Depending on the calcination temperature, the activity of Al_2O_3-supported NiW is higher than that of SiO_2-supported NiW catalysts. While uncalcined NiW/Al_2O_3 and NiW/Al_2O_3 calcined at 400 ^{0}C is almost twice as active as NiW/SiO_2, NiW/Al_2O_3 calcined at 550 ^{0}C is slightly less active than NiW/SiO_2. As a consequence the increase in activity due to the presence of CyDTA is also different for both

supports. In the case of SiO_2-supported catalysts, CyDTA increases the activity with a factor of 2, while for Al_2O_3-supported catalysts the increase is only a factor 1.5.

Figure 6.3 shows the influence of the sulfidation temperature on the thiophene HDS activity. For catalysts sulfided at 400 ^{0}C the HDS activity increases in the order: calc 550 ^{0}C < calc 400 ^{0}C ~ uncalc < CyDTA. A higher sulfidation temperature increases the HDS activity of the calcined NiW/Al_2O_3 catalysts. While the HDS activity of uncalcined NiW/Al_2O_3 remains more or less the same at higher sulfidation temperature, the HDS activity of NiWCyDTA/Al_2O_3 decreases dramatically. As a result of the higher sulfidation temperature, the HDS activity now increases in the order: CyDTA < uncalc ~ calc 550 ^{0}C < calc 400 ^{0}C.

Table 6.3 *Ni $2p_{3/2}$ binding energies and degree of Ni sulfidation as a function of sulfidation temperature for uncalcined NiW/Al_2O_3 and NiWCyDTA/Al_2O_3.*

T_{sulf} (^{0}C)	NiW uncalcined		NiWCyDTA	
	Ni_{ox} $2p_{3/2}$ (eV)	Ni_{sulf} $2p_{3/2}$ (eV)	Ni_{ox} $2p_{3/2}$ (eV)	Ni_{sulf} $2p_{3/2}$ (eV)
-	856.4	-	855.5	-
50	856.3 (0.91)	853.4 (0.09)	855.6	-
100	856.2 (0.42)	853.5 (0.58)	855.5	-
150	856.2 (0.25)	853.5 (0.75)	-	-
200	856.3 (0.05)	853.5 (0.95)	855.6 (0.94)	853.9 (0.06)
250	-	-	855.6 (0.60)	854.1 (0.40)
300	-	853.9	-	854.2
400	-	853.9	-	854.2
550	-	853.9	-	853.6
700	-	853.5	-	853.5

6.4 Discussion

Sulfidation and HDS activity of W/Al_2O_3 model catalysts

It is known that W is much more difficult to sulfide than Mo [4,6]. However, the mechanism of sulfidation of W/Al_2O_3 has been reported to occur via W-oxysulfides and WS_3 [5-7,11,12,17,19-21], in the same way as Mo [25]. Our XPS results show the presence of a third W-species, besides oxidic W^{6+} and WS_2. From the W $4f_{7/2}$ binding energy, i.e. 33.4 eV, and the amount of sulfur present, we conclude that these species are W-oxysulfides with W probably in the 4+ or 5+ oxidation state. These species are present mainly at the start of the sulfidation where the O-S exchange has just started. Due to the strong interaction with the support, the W-O-Al linkages are much more difficult to sulfide than the W=O linkage, which can lead to S=W-O-Al oxysulfide species. The oxidic W-species that are present after sulfidation at 550 ^{0}C of W/Al_2O_3 calcined at 550 ^{0}C are very difficult to sulfide, probably due to a strong interaction with the support. Ng et al. [17] showed that $Al_2(WO_4)_3$ can only be formed during calcination at high temperatures and that these species are difficult to sulfide. Therefore it is likely that $Al_2(WO_4)_3$ is present for W/Al_2O_3 catalysts calcined at high temperatures. However, the XPS spectra can only be fit with one oxidic W^{6+}-species for all

catalysts. The binding energy of these W-species is also similar for all catalysts, hence we conclude that XPS cannot distinguish between the various W-species, which is confirmed by the binding energies of these species found in literature [17,18].

Calcination has a strong influence on both the sulfidation and the HDS activity. Our XPS results show that calcination leads to a strong interaction of W with the Al_2O_3-support, thereby retarding the sulfidation of W to higher temperatures. This results in incomplete sulfidation at high sulfidation temperature ($T \geq 400\ ^0C$). Other authors also reported incomplete sulfidation of calcined W catalysts, although the degree of sulfidation of W varies [6,7,12,19-21,24,26]. The sulfidation degree at 400 ^{0}C of 80% and 46% for W/Al_2O_3 calcined at 400 ^{0}C and 550 ^{0}C, respectively, corresponds well with those found in recent reports of Reinhoudt et al. [12] and Vissenberg et. al [7] for high surface area NiW/Al_2O_3. The HDS activity of W/Al_2O_3 sulfided at 400 ^{0}C increases in the order: calcined 550 ^{0}C < calcined 400 ^{0}C < uncalcined. Figure 6.2 shows that a higher sulfidation temperature changes the order in HDS activity significantly. The calcined W/Al_2O_3 catalysts, which have a higher degree of sulfidation due to the higher sulfidation temperature, show higher HDS activities, while the uncalcined W/Al_2O_3, which was already fully sulfided at 400 ^{0}C, shows a decrease in HDS activity. A decrease in the W 4f/Al 2p ratio (not shown) at high temperatures indicates loss of dispersion due to lateral growth of WS_2 and explains the decrease in activity. The decrease in W 4f/Al 2p ratio can also be caused by stacking of WS_2. However, stacking of WS_2 does not lead to loss of edge dispersion and would thus not lead to a decrease in HDS activity. The increase in activity for the calcined catalysts at higher sulfidation temperature is simply contributed to a higher degree of WS_2 formation. W/Al_2O_3 calcined at 550 ^{0}C has still a low degree of sulfidation at 550 ^{0}C and hence the activity is still low compared to the other catalysts.

Comparing the HDS activity at 400 ^{0}C of W/SiO_2 with W/Al_2O_3 shows that the latter has a somewhat higher HDS activity, except for W/Al_2O_3 calcined at 550 ^{0}C. This difference in HDS activity may be due to a higher dispersion of WS_2 on Al_2O_3 due to the stronger interaction with the Al_2O_3-support. The somewhat higher W 4f/Al 2p ratio of 0.05 vs. the W 4f/Si 2p ratio of 0.04 confirms this.

The presence of Co and Ni did not influence the sulfidation of W in mixed phase catalysts. Although some authors report that the sulfidation of W is enhanced by the presence of Ni [6,27], our XPS results do not support this. The use of chelating agents, like CyDTA, neither showed an influence on the sulfidation of W. The XPS binding energy of unsulfided WCyDTA/Al_2O_3 did not give evidence for complexation of W with CyDTA, which is supported by NMR measurements of Ohta et al. [14].

Sulfidation of Co(Ni)W/Al_2O_3 model catalysts

The presence of Co in CoW/Al_2O_3 and Ni in NiW/Al_2O_3 catalysts does not influence the sulfidation of W, as stated above. However, the presence of W has a large influence on the sulfidation of Co and Ni. Figure 6.4 shows that the sulfidation of Co is strongly facilitated by the presence of W. For uncalcined CoW/Al_2O_3 the sulfidation of Co is complete at 200 ^{0}C, while for uncalcined Co/Al_2O_3 the sulfidation degree is 80% at 400 ^{0}C. Catalysts calcined at 400 ^{0}C show similar behaviour, although for both catalysts the sulfidation is more difficult due to the calcination step. The XPS results in Table 6.2 show the same behaviour for Ni; the sulfidation of Ni in Ni/Al_2O_3 proceeds more difficult than that of Ni in NiW/Al_2O_3. It is

known that Co and Ni have a strong interaction with the Al_2O_3-support and can diffuse into the support during calcination [6,23,28]. The presence of W apparently prevents Co and Ni interacting with the support and hence partially inhibits the diffusion of Co and Ni into the support resulting in a higher degree of sulfidation. This effect has also been observed by Reinhoudt et al. [12] and Vissenberg et al. [7], although Scheffer et al. [6] found that W could not prevent the diffusion of Ni into the support completely and observed diffusion of Ni at high calcination temperature. The incomplete sulfidation of Co and Ni for catalysts calcined at 550 ^{0}C is in agreement with this. Comparing the results for Co and Ni, it follows that the interaction of Co with the support is stronger than for Ni and that Co diffuses more easily into the support.

Some authors explained the facilitation of the sulfidation of Co and Ni in the presence W with the presence of CoW and NiW mixed oxides, either in contact with the support or not [6,11,12,23,24,26]. $CoWO_4$ and $NiWO_4$ mixed oxides are thought to be the precursor for the active phase by some authors [26], while others found these species difficult to sulfide at low temperatures [24]. NiW mixed oxide species in contact with the support, i.e. NiWOAl, are also reported to be precursor for the active phase [6,12,23,24]. Reinhoudt et al. [12] fitted the oxidic Ni 2p spectra with two Ni 2p doublets, i.e. NiW and NiWAl mixed oxides. These authors found evidence for these species from TPS measurements and therefore used these species in their Ni 2p spectra, although the spectra did not show any visible evidence for the presence of more than one oxidic Ni-species [12]. The Ni 2p spectra in Figure 6.5 do not show visible evidence for the presence of more than one oxidic Ni species either. It is likely that the differences in oxidation state and chemical environment of the various oxidic Co- and Ni-species are very small. Hence, these species can be present but cannot be distinguished with XPS. Moreover, the sulfidation of W is not influenced by the presence of Co or Ni. This would be the case if part of W participated in CoW or NiW mixed oxides, hence we do find any evidence that CoW or NiW mixed oxide species are present in significant amounts on our model catalysts.

The sulfidation of both Co and Ni is strongly retarded due to calcination, leading to incomplete sulfidation of calcined catalysts at high sulfidation temperatures. The incomplete sulfidation of Co and Ni in CoW and NiW catalysts calcined at high temperatures indicates that W can only partially block Co and Ni and that interaction with or diffusion into the support is still possible. Especially for Co(Ni)W/Al_2O_3 calcined at 550 ^{0}C a low sulfidation degree is found. For NiW/Al_2O_3, contradictory results have been reported on the sulfidation degree of Ni. While various authors [17,19] observe complete sulfidation of Ni in calcined NiW/Al_2O_3, Moulijn and coworkers [6,11,12,24] clearly demonstrate the incomplete sulfidation of Ni in NiW/Al_2O_3 calcined at high temperatures. Differences in preparation conditions, loading, calcination temperature and sulfidation temperature can cause differences in the sulfidation degree of Ni. For example, Ng et al. [17] report the complete sulfidation of Ni in NiW/Al_2O_3 with XPS. However, their catalysts are calcined at 400 ^{0}C in He, which are relatively mild conditions for calcination and may explain the relative ease of sulfidation. Breysse et al. [19] also conclude, from XPS, the complete sulfidation of Ni in NiW/Al_2O_3. However, their XPS spectra clearly show that the sulfidation of Ni is incomplete. Our results are consistent with results on high surface area Co(Ni)W/Al_2O_3 catalysts [7,12].

We conclude that W simply prevents the interaction of Co and Ni with the support by interacting itself with the support. As a result, the sulfidation of Co and Ni proceeds more easily and diffusion of Co or Ni into the support is prevented. However, at high calcination

temperature diffusion of Co and Ni is still possible. We have no evidence for the presence of CoW or NiW mixed oxide species. In general, Co and Ni do behave similarly in promoted catalysts, i.e. the sulfidation of both Co and Ni responds in the same way to calcination. The only difference is that the sulfidation of Ni proceeds at somewhat lower temperatures compared to Co, which was also observed for Co/Al_2O_3 and Ni/Al_2O_3.

The XPS spectra of Co can all be fitted with two 2p doublets, indicating that only two Co or Ni species are present. The Co 2p doublet with Co $2p_{3/2}$ binding energy at 781.8 ± 0.2 eV is ascribed to Co-oxide. CoWCyDTA/Al_2O_3 shows a much lower Co $2p_{3/2}$ binding energy, i.e. 781.1 eV, which we ascribe to Co complexed to CyDTA, as observed earlier for CoWCyDTA/SiO_2 [8]. We could not distinguish other oxidic Co species, like $CoAl_2O_4$ or $CoWO_4$. While the latter is not likely to be present, as explained earlier, $CoAl_2O_4$ may be present after calcination at high temperatures. The incomplete sulfidation of Co for these catalysts confirms the presence of $CoAl_2O_4$, however XPS is not able to distinguish the various Co species. The Co $2p_{3/2}$ peak at 778.9 ± 0.2 eV of sulfided Co is observed for all catalysts except for CoWCyDTA/Al_2O_3 which has somewhat higher Co $2p_{3/2}$ binding energy, i.e. 779.2 eV. The Co $2p_{3/2}$ binding energy of 778.9 eV corresponds well with that of bulk Co_9S_8 [22], confirmed by the fact that for Co/Al_2O_3 the same binding energy is found.

The Ni 2p spectra can also be fit with two doublets, one with Ni $2p_{3/2}$ B.E. at 856.5 ± 0.2 eV corresponding to oxidic Ni. Due to the small differences in binding energy, it was not possible to distinguish between $NiAl_2O_4$, $Ni(OH)_2$ or Ni_2O_3 [17,18]. As explained earlier, Reinhoudt et al. [12] obtained evidence for two oxidic Ni species from TPS and therefore used two oxidic Ni species to fit the Ni 2p spectra, i.e. NiW mixed oxide at 856.2 eV and NiWAl mixed oxide at 856.9 eV. While there are no reference compounds of these species, it is difficult to know the exact binding energy. Due to the close chemical resemblance, the difference in binding energy of the two species is small. Moreover, the Ni 2p spectra of Reinhoudt et al. [12] do not show any evidence for the presence of two doublets for oxidic Ni, and could be fitted perfectly with one doublet with Ni $2p_{3/2}$ B.E. around 856.5 eV. The Ni $2p_{3/2}$ binding energy of unsulfided NiWCyDTA/Al_2O_3 is significantly lower, i.e. 855.5 eV, and is a result of complexation of Ni with CyDTA. This shows clear resemblance with CoWCyDTA/Al_2O_3 described above. Sulfided Ni species can be divided in two groups. For NiW/Al_2O_3 sulfided at low temperatures and Ni/Al_2O_3 catalysts a Ni $2p_{3/2}$ binding energy of 853.3 eV is found. This value corresponds well with bulk Ni sulfide, i.e. Ni_3S_2 [17]. However, the Ni $2p_{3/2}$ binding energy of sulfided Ni in NiW/Al_2O_3 sulfided at high temperatures, is considerably higher, i.e. 853.8 eV. It was shown that for uncalcined NiW/Al_2O_3 a shift in binding energy was observed from the value of bulk Ni-sulfide to a binding energy 0.5 eV higher. This shift in binding energy has also been observed by Reinhoudt and was ascribed to redispersion of NiS particles to WS_2-slabs [12]. It seems plausible that the shift in binding energy is a result of transformation of bulk Ni-sulfide to another sulfided Ni state. In the case of NiWCyDTA/Al_2O_3 only sulfided Ni species at 853.8 ± 0.2 eV is present and no shift is observed. Apparently, in these catalysts Ni directly goes into the high binding energy Ni-sulfide state and no bulk Ni-sulfide is formed. We will go into more detail on the possibility of redispersion in the next section. Interestingly, for both uncalcined NiW/Al_2O_3 and NiWCyDTA/Al_2O_3 the Ni $2p_{3/2}$ binding energy shifts to a lower value of 853.5 eV after sulfidation at even higher temperatures (T ~ 700 ^{0}C). This binding energy corresponds again to that of bulk Ni sulfide [17].

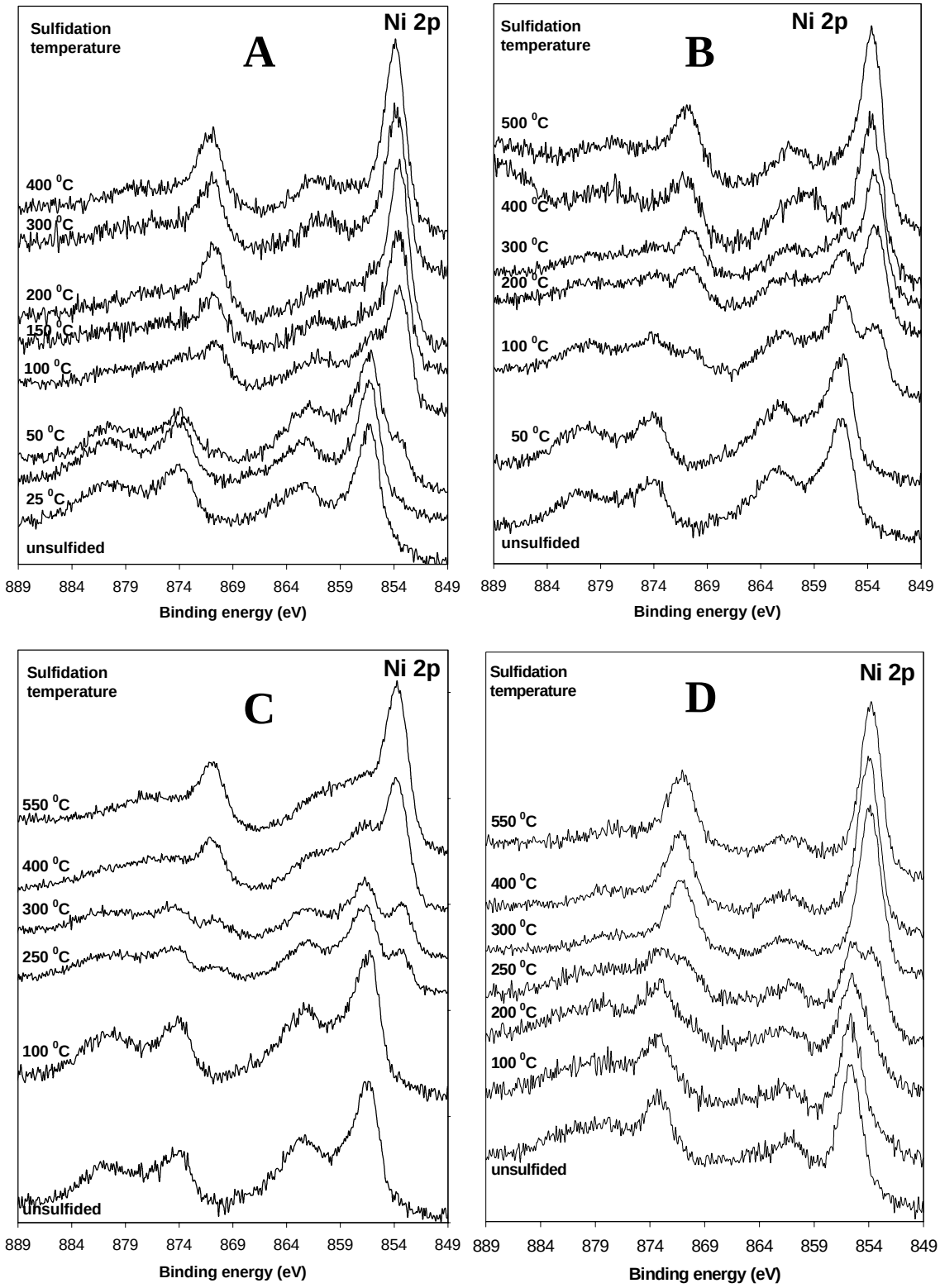

Figure 6.5 *Ni 2p XPS spectra of A) NiW/Al_2O_3 uncalcined, B) NiW/Al_2O_3 calcined at 400 ^{0}C, C) NiW/Al_2O_3 calcined at 550 ^{0}C, and D) $NiWCyDTA/Al_2O_3$ as a function of temperature.*

Sulfidation vs. HDS activity for CoW/Al_2O_3 model catalysts

In general, the activity measurements in Figure 6.2 show only a small increase in activity for CoW catalysts and a large increase for NiW catalysts compared to W catalysts. For the standard CoW catalysts the lumped activity of W/Al_2O_3 and Co/Al_2O_3 is found to be equal to that of CoW/Al_2O_3, hence no promotion effect of Co is present. This agrees well with earlier results on CoW/SiO_2 model catalysts [8] and recent reports on high surface area CoW/Al_2O_3 [7]. The binding energies confirm the presence of WS_2 and Co_9S_8 and not the active CoWS phase, similar to the well-known CoMoS phase [1,8]. Comparing the sulfidation behaviour of e.g. Co and W in uncalcined CoW/Al_2O_3, it shows that Co sulfides first to form bulk Co_9S_8 followed by sulfidation of W to WS_2. For the calcined catalysts the same is true, although both Co and W are sulfided at higher temperatures due to the calcination. Figure 6.2 also shows that the activity decreases with increasing calcination temperature. The difference between uncalcined CoW and CoW calcined at 400 ^{0}C is only small and both are more active than CoW calcined at 550 ^{0}C. The same trend is observed for W/Al_2O_3 (see also Figure 6.2). Hence, we conclude that no synergy exists for CoW/Al_2O_3 and that the HDS activity mainly is influenced by the sulfidation degree of W. This is confirmed by the difference in activity of SiO_2- and Al_2O_3-supported CoW catalysts. As was already observed for W, fully sulfided Al_2O_3-supported CoW catalysts are more active than SiO_2-supported catalysts. The difference in activity for W and CoW between the two supports is the same. From this we can conclude that the difference may be caused by a higher WS_2 dispersion on Al_2O_3 compared to SiO_2, as we concluded earlier for unpromoted W catalyst, and that Co does not play a role.

Using complexing agents, like CyDTA, increases the activity to a certain extent. Due to the complexation of Co with CyDTA, the interaction of Co with the support and diffusion into the support is prevented. Due to the stability of the complex the sulfidation of Co is retarded to high temperatures. This causes the sulfidation of Co to proceed at temperatures where W is already partially sulfided. As a result part of the Co is able to migrate to the WS_2 edges and form the CoWS phase. The somewhat lower Co $2p_{3/2}$ binding energy of sulfided CoWCyDTA/Al_2O_3 might indicate the presence of another Co phase, together with bulk Co-sulfide. This difference in binding energy between Co in bulk Co-sulfide and Co in CoWS has also been also found for SiO_2-supported CoW model catalysts [8]. Earlier papers on the effect of chelating agents show that complete separation of the sulfidation of Mo and Co or Ni result in an increase in HDS activity with a factor up to 10 [15,16]. In the case of W, the separation of sulfidation is not possible due to the more difficult sulfidation of W compared to Mo. As a result, the increase in activity due to chelating agents is not so large in the case of CoWCyDTA/SiO_2 [8] or CoWCyDTA/Al_2O_3, as can be seen in Figure 6.2. Both catalysts show an increase in activity of only 1.5-1.8 compared to standard CoW. However, the increase in activity is considerable and proves that it is possible to increase the activity by using chelating agents. The small difference in activity between CoWCyDTA supported on Al_2O_3 and SiO_2 may be attributed to a small difference in dispersion of WS_2, as was also concluded for the standard (Co)W catalysts as described above. While W is not complexed to the chelating agent, the dispersion is influenced by interaction of W with the support.

Figure 6.2 also shows that Co(NTA)W/Al_2O_3 calcined at 550 ^{0}C has the same HDS activity as CoW/Al_2O_3 calcined at 550 ^{0}C. Due to the difference in preparation between the two catalysts, Co is fully sulfided around 225 ^{0}C for Co(NTA)W/Al_2O_3 calcined at 550 ^{0}C

while the sulfidation degree of CoW/Al_2O_3 calcined at 550 ^{0}C is only 48 %. However, the different sulfidation degree has no influence on the HDS activity. Comparing the sulfidation of Co and W in Co(NTA)W/Al_2O_3 calcined at 550 ^{0}C, it can be seen that although the sulfidation of Co is retarded due to complexation with NTA, it is still completely sulfided before the sulfidation of W starts. Hence bulk Co_9S_8 and WS_2 are formed and no promotion effect is observed. This proves that the role of chelating agents is purely the retardation of the sulfidation of Co (or Ni) to temperatures where MoS_2 or WS_2 is formed. Chelating agents have thus no influence on the dispersion.

Sulfidation vs. HDS activity for NiW/Al_2O_3 model catalysts

In the case of Ni, a strong promotion effect is observed. Compared to W/Al_2O_3, the HDS activity of NiW/Al_2O_3 is a factor 5 to 6 higher, depending on calcination temperature. This promotion effect of Ni is a result of the formation of active phase, i.e. NiWS phase, during sulfidation. We therefore ascribe the Ni-sulfide species at 853.8 eV to Ni in NiWS. We reported this shift in Ni 2p binding energy during sulfidation earlier [10]. The temperature where this shift appears coincides with the complete sulfidation of WS_2 as shown in Figure 6.1. We therefore propose that at temperatures where W is completely sulfided, NiS particles redisperse and migrate to the edges of the WS_2-slabs, thereby forming NiWS. Hence, we conclude that the shift in the Ni 2p binding energy is caused by this redispersion of Ni-sulfide. The highest HDS activity is observed For NiWCyDTA/Al_2O_3. This increase in HDS activity due to the presence of chelating agents, like CyDTA, was also reported earlier for NiW/SiO_2 model catalysts [9,10] and by Ohta et al. [14] for (di)benzothiophene HDS, where an increase in activity by a factor 1.5 was observed. Complexing CyDTA to Ni retards the sulfidation of Ni to temperatures where W is already sulfided. As a result, Ni sulfides in the presence of WS_2 and is able to migrate directly to the edge of the WS_2-slabs to form NiWS. This is supported by the XPS results in Table 6.3. The fact that NiWCyDTA/Al_2O_3 is only a factor 1.3 higher in activity than standard NiW/Al_2O_3 suggests that a large part of Ni in NiW/Al_2O_3 catalysts is able to redisperse.

Calcination at high temperature decreases the activity significantly. A lower degree of sulfidation as observed with XPS leads to this lower activity. A higher sulfidation temperature increases the activity of the calcined NiW catalysts slightly, while uncalcined NiW catalysts show a somewhat lower activity. A higher sulfidation temperature has a dramatic effect on the HDS activity of NiWCyDTA/Al_2O_3. While the HDS activity is decreased by a factor 2, the Ni 2p binding energy is shifted to the value of bulk Ni sulfide as can be seen in Table 6.3. Kim et al. [26], Breysse et al. [19] and Mangnus et al. [24] reported the segregation of NiWS into WS_2 and Ni_3S_2 at high temperatures. From the decrease in HDS activity and the formation of bulk Ni-sulfide as observed form XPS, we conclude that segregation of the NiWS phase at high sulfidation temperature decreases the HDS activity of NiWCyDTA/Al_2O_3. From Table 6.3 it can be clearly seen that the active phase in NiWCyDTA/Al_2O_3 is less stable than for standard NiW/Al_2O_3. While segregation takes place at 550 ^{0}C for NiWCyDTA/Al_2O_3, the shift in binding energy to bulk Ni-sulfide takes place at 700 ^{0}C for uncalcined NiW/Al_2O_3. Calcined catalysts show a higher sulfidation degree due to higher sulfidation temperatures and this leads to an increase in HDS activity.

The influence of the support on the HDS activity of NiW catalysts is clearly visible from Figure 6.2. As was observed earlier for W and CoW, Al_2O_3-supported NiW catalysts

show a higher activity, except at high calcination temperatures where incomplete sulfidation leads to low activities for NiW/Al_2O_3. This difference in HDS activity may be due to a difference in interaction with the support. The weak interaction with SiO_2 leads generally to relatively large WS_2-slabs, while the strong interaction with the Al_2O_3 leads to more stable and well-dispersed WS_2-slabs and hence a higher activity is expected for the latter. However, the difference in HDS activity is larger compared to W and CoW catalysts. Hence, differences in WS_2 dispersion cannot be the only explanation. The dispersion of NiS can also be influenced by the interaction with the support. The size of the bulk Ni-sulfide particles may have an influence on the redispersion at high sulfidation temperature. In the case of more finely divided bulk Ni sulfide particles over the alumina support, NiS particles or atoms that migrate to more dispersed WS_2-slabs have to travel less distance than in the case of larger NiS and WS_2 particles on a silica support. This may influence the ease of redispersion, i.e. ease of active phase formation, and thus influence the HDS activity. For NiWCyDTA the difference between the two supports is very small and we can conclude that using complexing agents like CyDTA leads to highly active catalysts, irrespective of support.

6.5 Conclusions

CoW/Al_2O_3 and NiW/Al_2O_3 model catalysts are used to study the influence of calcination and sulfidation on the thiophene HDS activity. Using XPS, it is observed that the sulfidation of W, Co and Ni is strongly influenced by the calcination temperature. The sulfidation of W is retarded to high temperatures at high calcination temperatures and proceeds via W-oxysulfides as intermediate. The sulfidation of Co and Ni is also retarded by calcination but facilitated by the presence of W. It is concluded that W prevents the interaction of Co and Ni with the support and prevents partially the migration of Co and Ni into the support at high calcination temperatures.

For standard CoW catalysts no synergy is observed and bulk Co-sulfide, i.e. Co_9S_8, and WS_2 are present after sulfidation. NiW catalysts show a strong promotion effect. The HDS activity increases with a factor of 5-6, depending on the calcination temperature, compared to W/Al_2O_3. XPS shows that the formation of the active phase, i.e. NiWS, occurs by migration of NiS to the edges of WS_2-slabs, so-called redispersion. As a result of this, NiW catalysts are more active in HDS than CoW catalysts, where no redispersion is observed. High calcination temperatures decrease the HDS activity due to incomplete sulfidation. Indeed, higher sulfidation temperatures increase the sulfidation degree of calcined catalysts and thereby increased the activity to a certain extent. Chelating agents, like CyDTA, increase the HDS activity for both CoW and NiW. This can be explained by the retarding effect of the chelating agents on the sulfidation of Co and Ni. As a result Ni and Co are sulfided at temperatures where W is already (partially) sulfided and hence Co and Ni can migrate directly to the WS_2 slabs and form the active phase. However, due to overlap between the sulfidation of Co or Ni and W, not all Co or Ni could form directly the active phase. As a result the increase in activity due to the chelating agents for CoW and NiW compared to the standard CoW and NiW catalysts is small but visible. Although catalysts containing CyDTA show the highest HDS activity, high sulfidation temperatures cause a dramatic decrease in HDS activity due to instability of the NiWS phase. This instability leads to segregation of NiWS to WS_2 and bulk Ni-sulfide. Compared to standard NiW/Al_2O_3, this segregation takes place at much lower temperatures for NiWCyDTA/Al_2O_3. Using a less-

stable chelating agent, like NTA, it is shown that the role of the chelating agent is to retard the sulfidation of Co or Ni to temperatures where WS_2 is already formed only and not to influence the dispersion-

Stronger interacting supports, like Al_2O_3, result in catalysts with higher activity. Due to that strong interaction, WS_2 is more stable and better dispersed which increases the activity. Catalysts containing chelating agents are not influenced by support interaction and show high activities irrespective of support.

References

[1] H. Topsøe, B.S. Clausen, and F.E. Massoth, "Hydrotreating Catalysis." Springer-Verlag, Berlin, 1996.

[2] A. Stanislaus, and B.H. Cooper, *Catal. Rev.-Sci. Eng.* **36**, 75 (1994).

[3] H.R. Reinhoudt, Y. van der Meer, A.M. van der Kraan, A.D. van Langeveld, and J.A. Moulijn, *Fuel Processing Technol.* **61**, 133 (1999).

[4] R. Thomas, E.M. van Oers, V.H.J. de Beer, and J.A. Moulijn, *J. Catal.* **84**, 275 (1983).

[5] E. Payen, S. Kasztelan, J. Grimblot, and J.P. Bonnelle, *Catal. Today* **4**, 57 (1988).

[6] B. Scheffer, P.J. Mangnus, and J.A. Moulijn, *J. Catal.* **121**, 18 (1990).

[7] M.J. Vissenberg, Y. van der Meer, E.J.M. Hensen, V.H.J. de Beer, A.M. van der Kraan, R.A. van Santen, and J.A.R. van Veen, *J. Catal.* **198**, 151 (2001).

[8] G. Kishan, L. Coulier, J.A.R. van Veen, and J.W. Niemantsverdriet, *J. Catal.* **200**, 194, (2001).

[9] G. Kishan, L. Coulier, V.H.J. de Beer, J.A.R. van Veen, and J.W. Niemantsverdriet, *Chem. Commun.* 1103 (2000).

[10] G. Kishan, L. Coulier, V.H.J. de Beer, J.A.R. van Veen, and J.W. Niemantsverdriet, *J. Catal.* **196**, 180 (2000).

[11] H.R. Reinhoudt, Y. van der Meer, A.M. van der Kraan, A.D. van Langeveld, and J.A. Moulijn, *Fuel Processing Technol.* **61**, 43 (1999).

[12] H.R. Reinhoudt, E. Creeze, A.D. van Langeveld, P.J. Kooyman, J.A.R. van Veen, and J.A. Moulijn, *J. Catal.* **196**, 315 (2000).

[13] J.A.R. van Veen, E. Gerkema, A.M. van der Kraan, and A. Knoester, *J. Chem. Soc., Chem. Commun.* **22**, 1684 (1987).

[14] Y. Ohta, T. Shimizu, T. Honma, and M. Yamada, *Stud. Surf. Sci. Catal.* **127**, 161 (1999).

[15] L. Coulier, V.H.J. de Beer, J.A.R. van Veen, and J.W. Niemantsverdriet, *Topics in Catal.* **13**, 99 (2000).

[16] L. Coulier, V.H.J. de Beer, J.A.R. van Veen, and J.W. Niemantsverdriet, *J. Catal.* **197**, 26 (2001).

[17] K.T. Ng, and D.M. Hercules, *J. Phys. Chem.* **80**, 2094 (1976).

[18] L. Salvati Jr., L.E. Makovsky, J.M. Stencel, F.R. Brown, and D.M. Hercules, *J. Phys. Chem.* **85**, 3700 (1981).

[19] M. Breysse, J. Bachelier, J.P. Bonnelle, M. Cattenot, D. Cornet, T. Décamp, J.C. Duchet, R. Durand, P. Engelhard, R. Frety, C. Gachet, P. Geneste, J. Grimblot, C. Gueguen, S. Kasztelan, M. Lacroix, J.C. Lavalley, C. Leclercq, C. Moreau, L. de Mourgues, J.L. Olivé, E. Payen, J.L. Portefaix, H. Toulhoat, and M. Vrinat, *Bull. Soc. Chim. Belg.* **96**, 829 (1987).

[20] M. Breysse, M. Cattenot, T. Décamp, R. Frety, C. Gachet, M. Lacroix, C. Leclercq, L. de Mourgues, J.L. Portefaix, M. Vrinat, M. Houari, J. Grimblot, S. Kasztelan, J.P. Bonnelle, S. Housni, J. Bachelier, and J.C. Duchet, *Catal. Today* **4**, 39 (1988).
[21] H.R. Reinhoudt, A.D. van Langeveld, P.J. Kooyman, R.M. Stockmann, R. Prins, H.W. Zandbergen, and J.A. Moulijn, *J. Catal.* **179**, 443 (1998).
[22] I. Alstrup, I. Chorkendorff, R. Candia, B.S. Clausen, and H. Topsøe, *J. Catal.* **77**, 397 (1982).
[23] B. Scheffer, P. Molhoek, and J.A. Moulijn, *Appl. Catal.* **46**, 11 (1989).
[24] P.J. Mangnus, A. Bos, and J.A. Moulijn, *J. Catal.* **146**, 437 (1994).
[25] A.M. de Jong, H.J. Borg, L.J. van IJzendoorn, V.G.M.F. Soudant, V.H.J. de Beer, J.A.R. van Veen, and J.W. Niemantsverdriet, *J. Phys. Chem.* **97**, 6477 (1993).
[26] C.-H. Kim, W.L. Yoon, I.C. Lee, and S.I. Woo, *Appl. Catal. A.* **144**, 159 (1996).
[27] T. Kabe, W. Qian, A. Funato, Y. Okoshi, and A. Ishihara, *Phys. Chem. Chem. Phys.* **1**, 921 (1999).
[28] H. Topsøe, B.S. Clausen, R. Candia, C. Wivel, and S. Mørup, *J. Catal.* **68**, 433 (1981).

7

TiO_2-supported Mo model catalysts: Ti as promoter for thiophene HDS ?

Abstract

Flat model systems of oxidic (Ni)Mo hydrodesulfurization (HDS) catalysts, supported on a thin SiO_2, TiO_2 or Al_2O_3 layer, are used to study the influence of the support on the formation of the active phase. For Mo-based catalysts, the thiophene HDS activity increases in the order TiO_2 > Al_2O_3 >> SiO_2, while for Ni promoted Mo-catalysts the order is TiO_2 ~ Al_2O_3 >> SiO_2. XPS measurements of the sulfided TiO_2-supported catalysts show that TiO_2 is also partially sulfided. SiO_2-supported Ti(Mo) catalysts, prepared by sequential spincoating of Mo and Ti, show the same sulfidation of Ti. The HDS activity of SiO_2-supported TiMo catalysts is twice as high compared to Mo/SiO_2 and a significant increase in hydrogenation selectivity is observed.

It is concluded that Ti^{3+}-species, sulfided during heat treatment in H_2S, acts as a promoter in Mo-based catalysts in the same way as Co and Ni, although to a lesser extent. This promoter effect can explain the higher activity of Mo/TiO_2 compared to Mo/Al_2O_3. In the case of Ni-promoted catalysts, Ni acts as a promoter and the effect of Ti as promoter is absent. Hence the difference in activity between Al_2O_3- and TiO_2-supported Ni-promoted Mo catalysts disappears. Sulfided Ti–species increase the hydrogenation selectivity. The low activity of SiO_2-supported catalysts is ascribed to a lower MoS_2-dispersion due to a weaker interaction of Mo with the SiO_2 support compared to Al_2O_3 and TiO_2.

7.1 Introduction

Sulfided CoMo and NiMo catalysts are widely used for hydrotreating processes [1]. Due to environmental legislation an increasing demand is put on these hydrotreating catalysts. One way to improve these catalysts is looking at the support. The strength of the metal sulfide-support interaction has a large influence on the dispersion and morphology of the active catalysts, while the support may also influence the electronic properties of the catalyst [2,3].

Al_2O_3 is the most commonly applied support for hydrotreating catalysts, due its strong interaction with the active phase leading to highly dispersed MoS_2 [1]. However, TiO_2 [4-7] and TiO_2-Al_2O_3 [8-10] mixed oxide supports have shown promising results. For example, it was found by several authors that Mo/TiO_2 catalysts are considerably more active (factor 1.6-4.4, depending on reaction and reaction conditions) in thiophene HDS compared to Mo/Al_2O_3 [4-7,8,9,11]. More recent papers also report higher HDS activities on Mo/TiO_2 for (substituted) dibenzothiophenes [12-14]. Although there is general agreement on the superior catalytic activity of Mo/TiO_2, various explanations for this phenomenon are given. Most authors explain the difference in activity by differences in metal-support interaction, which leads to differences in e.g. dispersion [9,15,16], sulfidation [8,10,13] or morphology [5,7]. However, it still remains unclear what the real explanation is. Recent papers by Vissenberg et al. [11] and Ramirez et al. [17] concluded that differences in dispersion, sulfidability or morphology are not the cause of the difference in HDS activity between Mo/TiO_2 and Mo/Al_2O_3. These authors stated that most likely TiO_2 itself induces a synergistic effect that enhances the HDS activity [11,17]. Ramirez et al. [17] propose partial reduction or sulfidation of TiO_2 leads to Ti^{3+} species that can act as a promoter to the MoS_2 phase.

There also exists some confusion concerning the interaction of Mo with the various supports and the resulting reducibility or sulfidability of Mo. Some authors report a strong interaction of Mo with TiO_2, resulting in incomplete sulfidation at high temperatures [5,15,16,18]. However, Okamoto et al. [6] and Zhaobin et al. [8] observed that titania facilitates the sulfidation of Mo and as a result Mo is sulfided completely at 673 K. A recent paper by Vissenberg et al. [11] concluded that despite the strong Mo-TiO_2 interaction, Mo could be sulfided completely.

Another intriguing feature is the difference in promotion effect for Co- or Ni-promoted TiO_2- and Al_2O_3-supported catalysts. Ramirez et al. [5] found that $CoMo/TiO_2$ was more active in thiophene HDS than $CoMo/Al_2O_3$. However, compared to the unpromoted catalysts, the promotion effect of Co was strikingly lower for TiO_2 (factor ~3) than for Al_2O_3 (factor ~8). Ng and Gulari [4] found the same modest increase in activity of TiO_2-catalysts due to Co. Vissenberg et al. [11] found for both Co- and Ni-promoted Mo-catalysts, higher promotion factors for Al_2O_3 than for TiO_2. Due to the different values for promotion factors, some authors find promoted Mo/Al_2O_3 catalysts to be more active in HDS than promoted Mo/TiO_2 catalyst [11,19,20], while others find the opposite [5,21]. Different reactions and reaction conditions may explain these differences. The low promotion effect in the case of $CoMo/TiO_2$ catalysts supports the idea of TiO_2 acting as a promoter, as proposed by Ramirez et al. [17].

In this paper we study the thiophene HDS activity of unpromoted and Ni-promoted Mo model catalysts supported on various substrates. Combining these results with activity measurements and angle-dependent XPS on Ti-promoted Mo catalysts, we come to the

conclusion that Ti sulfides partially during sulfidation and behaves like a promoter in the same way of Co or Ni do. Furthermore, sulfided Ti-species increase the hydrogenation activity as evidenced by relatively higher amounts of butane after thiophene HDS.

7.2 Experimental

Catalysts were prepared on planar SiO_2, Al_2O_3 and TiO_2 model supports. Planar SiO_2 and Al_2O_3 model supports were prepared as described in Chapter 6. TiO_2 were prepared by evaporation of Ti in an O_2 atmosphere on a Si (100) wafer under similar conditions as Al_2O_3. The thickness of the evaporated layers is approximately 5 nm thick. The Ti 2p binding energy of the TiO_2 layer, i.e. 458.8 eV, indicated that TiO_2 was present [22]. No information on the presence of rutile or anatase could be obtained yet.

Nickel and molybdenum were applied by spincoating the model supports at 2800 rpm in N_2 with aqueous solutions of either nickel nitrate or ammonium heptamolybdate. The mixed-phase catalysts were prepared by spincoating with aqueous solutions containing Ni and Mo. The concentrations of Ni and Mo solutions were adjusted to result in a loading of 2 Ni at/nm^2 and 6 Mo at/nm^2. The dried catalysts were calcined in air at 450 ^{0}C for 30 min.

Ti-based catalysts were prepared by spincoating the substrate with an ethanol solution containing Ti(IV)-isopropoxide (98+%, Acros), resulting in a Ti loading of 2 at/nm^2. Ti-promoted Mo catalysts were prepared by subsequent spincoating of respectively Mo and Ti.

Sulfidation was carried out in a glass reactor under flow of 60 ml/min of 10% H_2S/H_2 at 1 bar. The catalysts were heated at a rate of 5 ^{0}C/min to the desired temperature and kept there for 30 min. After sulfidation the reactor was cooled to room temperature under a helium flow and brought to a glove box, where the samples were mounted in a transfer vessel for transport to the XPS under N_2 atmosphere. XPS spectra were measured on a VG Escalab 200 MK II, equipped with a standard dual source, a monochromatized Al Kα source and a five channeltron detector. Measurements were done at 20 eV pass energy. Charge correction was performed using the Al 2p peak of Al_2O_3 at 74.4 eV and the Ti 2p peak of TiO_2 at 458.8 eV as a reference [22].

Model catalysts were tested in batch mode thiophene HDS under standard conditions (1.5 bar, 400 ^{0}C, 4% thiophene/H_2). Model catalysts were presulfided at 400 ^{0}C for 30 min as described above. For more details see [23,24].

Table 7.1 *Thiophene HDS activity and promotion factors of unpromoted and Ni-promoted Mo-based model catalysts. Activity is expressed as yield of products after 1 hour of batch reaction at 400 ^{0}C in 4% thiophene/H_2.*

	Mo	NiMo	NiMo/Mo
SiO_2	0.11	1.07	9.7
Al_2O_3	0.37	2.84	7.7
TiO_2	0.6	3.2	5

7.3 Results and discussion

Table 7.1 shows the thiophene hydrodesulfurization (HDS) activity after batch reaction at 400 ^{0}C of unpromoted and Ni-promoted Mo model catalysts, supported on SiO_2, Al_2O_3 and TiO_2. The activity is expressed as total yield (%) of products per 5 cm^2 of catalysts after 1 hour of batch reaction in 4% thiophene/H_2 at 400 ^{0}C.

It can be clearly seen from Table 7.1 that for both unpromoted and promoted catalysts the activity increases in the order $SiO_2 < Al_2O_3 < TiO_2$. Unpromoted Mo/TiO_2 is almost twice as active in thiophene HDS as Mo/Al_2O_3, while for the promoted catalysts the activity is almost equal for Al_2O_3 and TiO_2. As a result the promotion factor of Ni is significantly lower for TiO_2 than for Al_2O_3, respectively a factor 5 and ~ 8 (see Table 7.1). These results are in good agreement with those of Ramirez et al. [5] and Vissenberg et al. [11] on high surface area Co(Ni)Mo catalysts. Both unpromoted and promoted SiO_2-supported catalysts show significantly lower HDS activities compared to the other two supports. As a result of the very low HDS activity of Mo/SiO_2, the increase in activity due to Ni is the largest of all supports, i.e. a factor ~ 10.

Figure 7.1 shows the Mo 3d and S 2p XPS spectra of Mo/Al_2O_3 (A,B) and of Mo/TiO_2 (C,D) calcined at 450 ^{0}C and sulfided at various temperatures in 10% H_2S/H_2. The XPS spectra of Mo/SiO_2 have been described earlier [23,25]. The sulfidation of Mo starts around 50 ^{0}C and is completed at 200 ^{0}C. Due to the weak interaction of Mo with the SiO_2-support, the sulfidation of Mo is relatively easy and large particles and low dispersion of MoS_2 can be expected. Figure 1A and 1B show that the sulfidation of Mo/Al_2O_3 is much more difficult. The sulfidation now starts around 100 ^{0}C and is only complete at 500 ^{0}C. Note that the sulfidation of Mo is incomplete at 400 ^{0}C, which is the temperature at which the HDS activity are carried out. Fitting of the Mo 3d doublets at 400 ^{0}C, shows that the major part of Mo is present as MoS_2, while still a significant part of Mo is present as Mo^{5+} species in an oxysulfidic environment (see Table 7.2). Muijsers et al. [25] also reported the presence of Mo^{5+}-oxysulfides during the sulfidation of Mo/SiO_2, although these species were already present at low sulfidation temperature and had a significantly higher Mo $3d_{5/2}$ binding energy, i.e. 231.5-232.0 eV. However, in Mo/Al_2O_3 the Mo^{5+}-species are still present at high temperatures and therefore are most probably still attached to the alumina support, thereby stabilizing the MoS_2 slabs. Due to the interaction with the support, the chemical environment of the Mo^{5+}-species is different compared to the species reported by Muijsers et al. [25], which can explain the difference in binding energy. As a result of the strong interaction with the alumina support, the MoS_2-particles are well dispersed over the support [1-3]. This explains well the difference in HDS activity between Mo/SiO_2 and Mo/Al_2O_3 as observed in Table 7.1. The S 2p spectra confirm that the sulfidation starts around 100 ^{0}C and is complete at high sulfidation temperatures. The S 2p binding energy of 161.7 eV corresponds with S^{2-}-ligands [22].

The sulfidation of Mo in Mo/TiO_2 proceeds similar to that of Mo/Al_2O_3. Figure 7.1C shows that although the sulfidation starts at a lower temperature for TiO_2 than Al_2O_3, i.e. 50 ^{0}C vs. 100 ^{0}C, for both supports the sulfidation is incomplete at 400 ^{0}C and only complete sulfidation is reached at 500 ^{0}C. As can be seen also in Table 7.2, after sulfidation at 400 ^{0}C the degree of sulfidation is 82% for Mo/TiO_2 which is almost equal to Mo/Al_2O_3, i.e. 86%. Fitting of the Mo 3d spectra shows that 82% of Mo is transformed to MoS_2. The remaining part of Mo can be fitted with a Mo 3d state with Mo $3d_{5/2}$ B.E. at 230.6 eV, which can be

assigned to Mo^{5+}-species in an oxysulfidic environment, as was also observed for Al_2O_3, as described above.

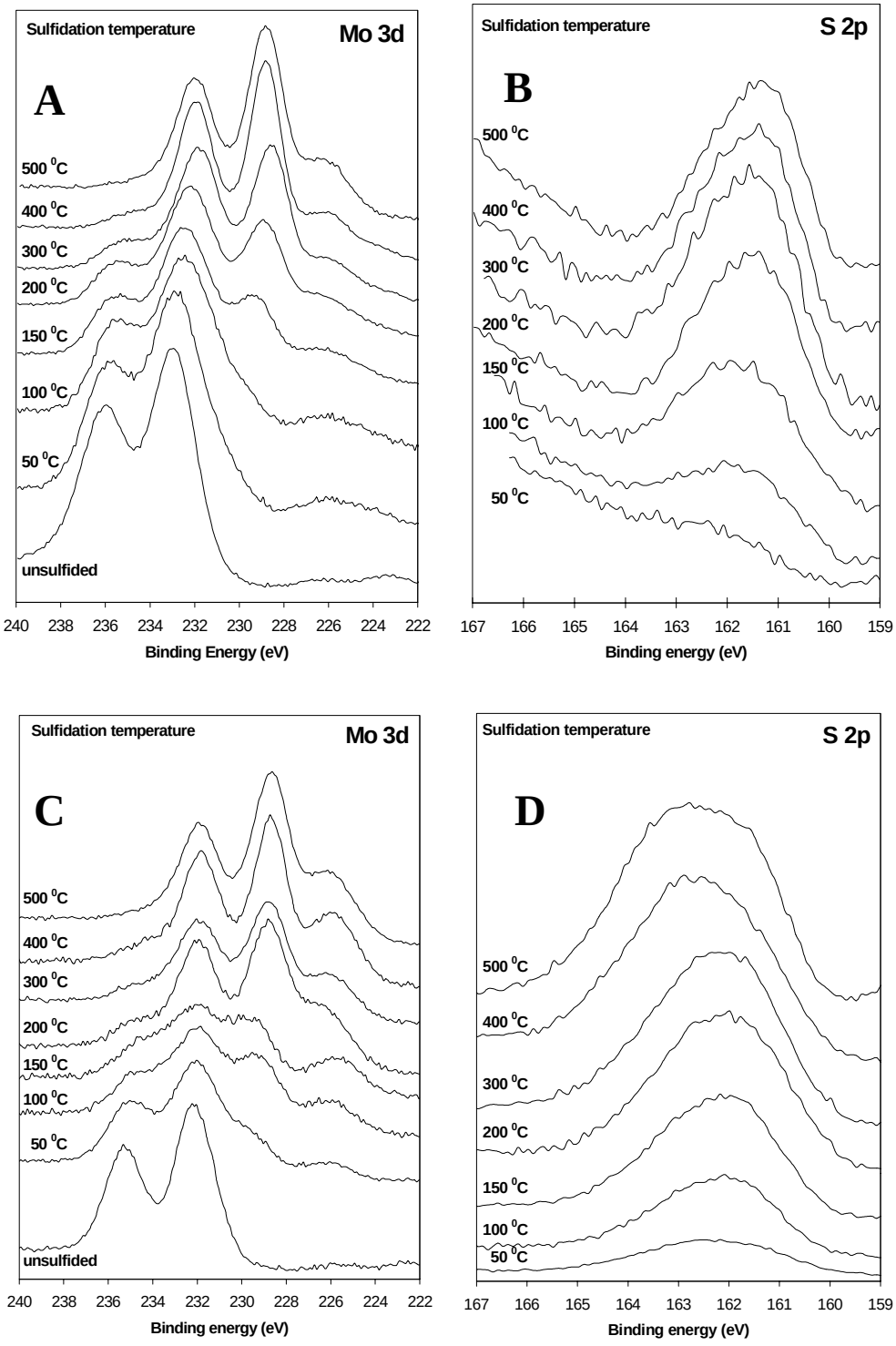

Figure 7.1 *Mo 3d and S 2p XPS spectra of Mo/Al_2O_3 (A,B) and Mo/TiO_2 (C,D) model catalysts as a function of sulfidation temperature.*

We ascribed these species earlier to Mo-species partially connected to the support. This incomplete sulfidation of Mo in Mo/TiO_2 agrees well with Ramirez et al. [5] and Leliveld et al. [15,16], who also found Mo-$O_{support}$ linkages at high sulfidation temperatures. However, other authors observed complete sulfidation of Mo [6,11]. In general, the sulfidation of Mo at higher temperatures of Mo/Al_2O_3 and Mo/TiO_2 is quite similar, from which we conclude that significant differences in dispersion are not likely. The almost equal Mo3d/Al2p and Mo3d/Ti2p atomic ratios in Table 7.2 confirm this. Hence, the difference in HDS activity can not be explained by differences in sulfidability or dispersion.

The Mo $3d_{5/2}$ binding energies of fully oxidic and sulfidic Mo do not show significant differences between the various supports (see Table 7.2). However, the S 2s and S 2p spectra of sulfided Mo/TiO_2 show some strange features. Although the position of the S 2s peaks in Figure 7.1 for the different Mo catalysts is equal at first sight, the relative contribution is significantly different. Table 7.2 shows that for Mo/SiO_2 and Mo/Al_2O_3 the absolute S 2s/Mo 3d peak ratio is ~0.25, while for Mo/TiO_2 this ratio is much higher, i.e. 0.7. The S 2p spectra in Figure 7.1 B and D and the fit results in Table 7.2 show that for Mo/TiO_2 at higher temperatures more than one sulfur species is present. Besides the S 2p peak at 161.8 eV, corresponding to S^{2-} in MoS_2 [22], a second doublet at 163.9 eV is present. These sulfur species are absent for either Mo/Al_2O_3 or Mo/SiO_2 [23] (see Figure 7.1). While the support is the only difference between the catalysts, the excess of sulfur found with XPS must be caused by the TiO_2-support.

Table 7.2 *Mo 3d and S 2p binding energies, degree of sulfidation, absolute S/Mo intensity ratios and Mo/support atomic ratios of oxidic and sulfided Mo model catalysts on various supports.*

	Mo_{ox} $3d_{5/2}$ (eV)	Mo_{sulf} $3d_{5/2}$ (eV)	S 2p (eV)	I_{S2p}/I_{Mo3d}	I_{S2s}/I_{Mo3d}	I_{Mo3d}/I_{X2p}*
Mo/SiO_2	232.8	228.9	161.8	0.40	~0.27	0.04
Mo/Al_2O_3	232.8	228.8 (86%) 230.8 (14%)	161.7	0.38	~0.25	0.13
Mo/TiO_2	232.6	228.6 (82%) 230.6 (18%)	161.8 163.6	0.9	~0.7	0.14

* X = Si, Al or Ti

Figure 7.2 shows the Ti 2p spectra of Mo/TiO_2 after different sulfidation treatments. The XPS spectra have been measured at a high angle (i.e. 60 ^{o}) between analyzer and sample, to increase the surface sensitivity [26]. The spectrum of unsulfided Mo/TiO_2 shows a single Ti 2p doublet with a Ti $2p_{3/2}$ binding energy at 458.8 eV, corresponding to TiO_2 [22]. After sulfidation at 400 ^{0}C for 30 min a small shoulder at low binding energy is visible. This shoulder is more pronounced after sulfidation at 500 ^{0}C for 2 h. For comparison, the Ti 2p spectrum of a bare TiO_2 support after sulfidation at 500 ^{0}C for 2 h is shown in Figure 7.3A. In this spectrum the extra Ti 2p doublet at lower binding energy is even more visible. The corresponding S 2p spectra of the TiO_2 support in Figure 7.3B show that after sulfidation of the bare TiO_2 support sulfur species are present around 163.4 eV, which agrees well with the extra S 2p doublet observed in Figure 7.1 and Table 7.2 for Mo/TiO_2. The extra Ti 2p doublet at high sulfidation temperature has a Ti $2p_{3/2}$ binding energy of 456.7 eV, which can be

ascribed to TiO_xS_y species possibly with a 3+ oxidation state [27]. Hence we can conclude that TiO_2 is able to sulfide partially at high temperatures. The small shoulder after sulfidation of Mo/TiO_2 at 400 ^{0}C shows that sulfidation of TiO_2 also takes place for Mo/TiO_2 catalysts used for thiophene HDS measurements (Table 7.1).

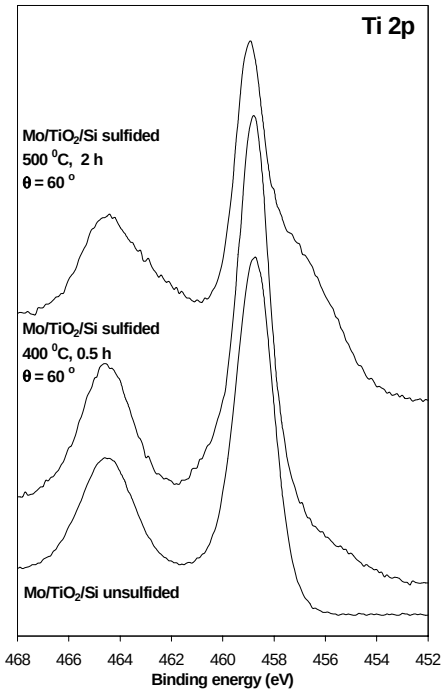

Figure 7.2 *Angle dependent Ti 2p XPS spectra of Mo/TiO_2 model catalysts sulfided at high temperatures.*

To elucidate the influence of the sulfided Ti-species on the activity of TiO_2-supported catalysts, model catalysts were prepared by spincoating Ti or TiMo from solutions onto a SiO_2 support (see Experimental section). Figure 7.3A and B show the Ti 2p and S 2p spectra of Ti/SiO_2 and $TiMo/SiO_2$ model catalysts unsulfided and sulfided at 400 ^{0}C. The Ti 2p spectra of the unsulfided catalysts show a Ti $2p_{3/2}$ peak at 458.8 eV, which can be ascribed to oxidic Ti-species [22]. It can be clearly seen that after sulfidation at 400 ^{0}C, this doublet has shifted to lower Ti $2p_{3/2}$ binding energy, i.e. 457.0 eV. The S 2p spectrum of Ti/SiO_2 sulfided at 400 ^{0}C shows two small peaks at ~161.5 and ~163.5 eV, respectively. The latter one corresponds well with the sulfur species on sulfided TiO_2 (Figure 7.3B). The S 2p spectrum of $TiMo/SiO_2$ after sulfidation shows a large peak at 161.9 eV, ascribed to S^{2-} in MoS_2, and a shoulder at higher binding energy (~163.5 eV), corresponding to sulfided Ti-species. These results agree well with that of TiO_2-supported catalysts, indicating that Ti in TiO_2 behaves similarly to Ti as a Ti-precursor in Ti-promoted Mo/SiO_2 catalysts. Note that the sulfidation of Ti is not complete at 400 ^{0}C.

Thiophene HDS activity measurements on Ti-promoted catalysts were carried out to study the influence of sulfided Ti-species on the activity of Mo-based catalysts. The results are shown in Table 7.3. The HDS activity of $TiMo/SiO_2$ is twice as high as Mo/SiO_2, showing that sulfided Ti-species have a promotional effect. Although the promotion factor is smaller compared to $NiMo/SiO_2$, the effect is significant. Ramirez et al. [17] stated that Ti^{3+} species are easily formed by reduction of Ti^{4+} under hydrogen atmosphere and are located at the surface of TiO_2. These Ti^{3+} species can easily inject electrons to the Mo 3d conduction band, which is according Harris and Chianelli [28] the requirement for MoS_2 promotion in

HDS. Note that this is in good agreement with the Bond Energy Model [29] since injections of electrons from Ti to Mo will decrease the Mo-S bond energy.

This explains also the almost equal activity for promoted catalysts: apparently Ni has more affinity for the edges of MoS_2 than Ti and thus acts as a promoter instead of Ti. The activity of Mo/TiO_2 is however a factor 3 higher compared to $TiMo/SiO_2$. This difference is probably caused by a better dispersion of MoS_2 in Mo/TiO_2 due to a stronger interaction with the support. The higher Mo3d/Ti2p atomic ratio compared to Mo3d/Si2p confirms this. The hydrogenation (HYD) selectivity, which is expressed as the ratio of n-butane/total products, in Table 7.3 shows that n-butane is only found as a product in Ti-containing catalysts. Clearly sulfided Ti-species also increase the hydrogenation selectivity.

Table 7.3 *Thiophene HDS activity of Ti-containing model catalysts and some reference catalysts. HDS is the total yield of products after 1 hour of thiophene batch reaction, HYD is the hydrogenation selectivity (n-butane/total products).*

	HDS	HYD
Mo/SiO_2	0.11	0
$TiMo/SiO_2$	0.23	0.12
$NiMo/SiO_2$	1.07	0
Mo/TiO_2	0.6	0.08

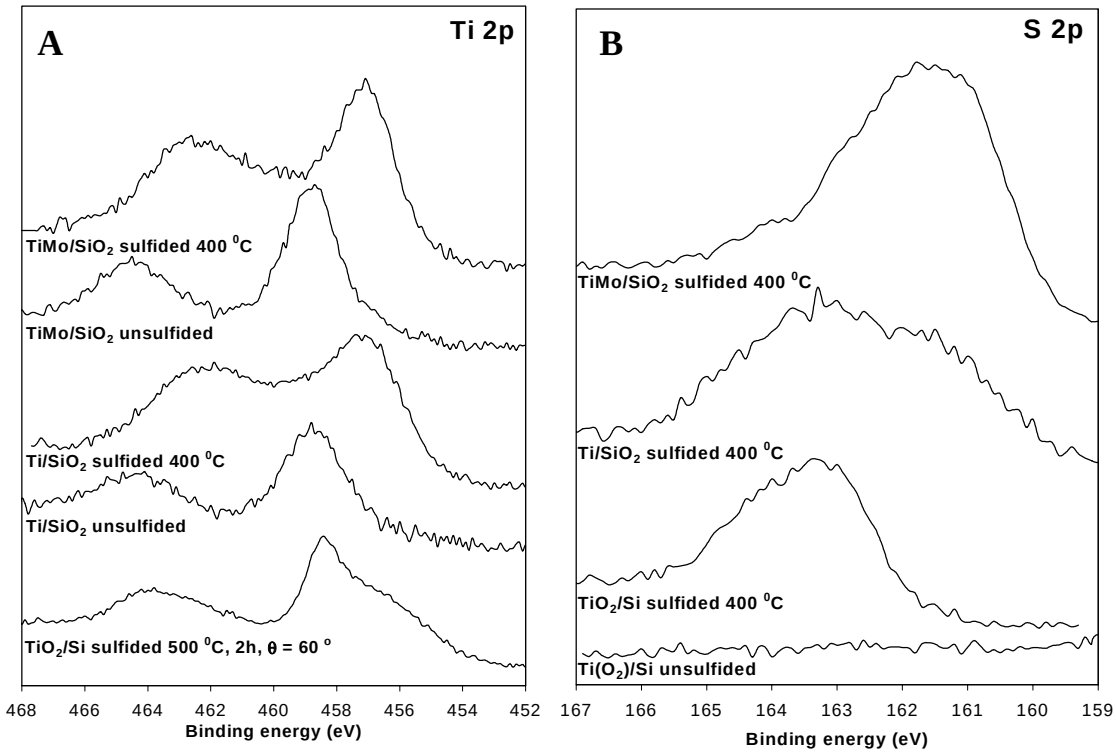

Figure 7.3 *Ti 2p (A) and S 2p (B) XPS spectra of unsulfided and sulfided Ti/SiO_2 and $TiMo/SiO_2$ model catalysts.*

7.4 Conclusions

The thiophene HDS activity of Mo/TiO_2 is twice as high as Mo/Al_2O_3, while the HDS activity of Ni-promoted Mo catalysts is almost equal. From combination of thiophene HDS measurements and angle-dependent XPS, we conclude that the difference in HDS activity of the unpromoted catalysts is due to partial sulfidation of the TiO_2-support leading to Ti^{3+} species. These species can act as a promoter in the same way as Co or Ni, although to a lesser extent. Due to the higher affinity of Co and Ni to the edge sites of MoS_2, Co and Ni acts as a promoter in promoted Mo catalyst, instead of Ti. As a result the promoter effect of Ti is absent in Ni-promoted Mo catalysts. Sulfided Ti-species also increase the hydrogenation selectivity.

Strong interaction of Mo with both TiO_2 and Al_2O_3 retards the sulfidation of Mo and leads to incomplete sulfidation at high temperatures. However, the sulfidation of Mo for both supports is similar and therefore the difference in activity could not be ascribed to differences in dispersion.

References

[1] H. Topsøe, B.S. Clausen and F.E. Massoth, "Hydrotreating Catalysis." Springer-Verlag, Berlin, 1996.
[2] F. Luck, *Bull. Soc. Chim. Belg.* **100**, 781 (1991).
[3] M. Breysse, J.L. Portefaix and M. Vrinat, *Catal. Today*. **10**, 489 (1991).
[4] K.Y.S. Ng and E. Gulari, *J. Catal.* **92**, 33 (1985).
[5] J. Ramirez, S. Fuentes, G. Diaz, M. Vrinat, M. Breysse and M. Lacroix, *Appl. Catal.* **52**, 211 (1989).
[6] Y. Okamoto, A. Maezawa and T. Imanaka, *J. Catal.* **120**, 29 (1989).
[7] K.C. Pratt, J.V. Sanders and V. Christov, *J. Catal.* **124,** 416 (1990).
[8] W. Zhaobin, X. Qin, G. Xiexian, P. Grange and B. Delmon, *Appl. Catal.* **75**, 179 (1991).
[9] J. Ramirez, L. Ruiz-Ramirez, L. Cedeno, V. Harle, M. Vrinat and M. Breysse, *Appl. Catal. A* **93**, 163 (1993).
[10] S. Damyanova, A. Spojakina and K. Jiratova, *Appl. Catal. A* **125**, 257 (1995).
[11] M.J. Vissenberg, V.H.J. de Beer and J.A.R. van Veen, Ph.D. thesis, Technical University of Eindhoven, The Netherlands, 1999, Chapter 7.
[12] C. Pophal, F. Kameda, K. Hoshino, S. Yoshinaka and K. Segawa, *Catal. Today* **39**, 21 (1997).
[13] S. Yoshinaka and K. Segawa, *Catal. Today* **45,** 293 (1998).
[14] K. Segawa and S. Satoh, in: "Hydrotreatment and Hydrocracking of Oil Fractions", B. Delmon, G.F. Froment and P. Grange (Eds.), Elsevier, Netherlands, 129 (1999).
[15] R.G. Leliveld, A.J. van Dillen, J.W. Geus and D.C. Koningsberger, *J. Catal.* **165**, 184 (1997).
[16] R.G. Leliveld, A.J. van Dillen, J.W. Geus and D.C. Koningsberger, *J. Catal.* **171**, 115 (1997).
[17] J. Ramirez, L. Cedeno and G. Busca, *J. Catal.* **184**, 59 (1999).
[18] K. Segawa and T. Soeya, *Res. Chem. Interm.* **15**, 129 (1991).
[19] G. Muralidhar, F.E. Massoth and J. Shabtai, *J. Catal.* **85**, 44 (1984).

[20] E. Olguin, M. Vrinat, L. Cedeno, J. Ramirez, M. Borque and A. Lopez-Agudo, *Appl. Catal. A* **165**, 1 (1997).
[21] M.P. Borque, A. Lopez-Agudo, E. Olguin, M. Vrinat, L. Cedeno and J. Ramirez, *Appl. Catal. A* **180**, 53 (1999).
[22] J.F. Moulder, W.F. Stickle, P.E. Stobol and K.D. Bomben, "Handbook of XPS", Perkin Elmer Corporation, Eden Prairie, MN, 1992.
[23] L. Coulier, V.H.J. de Beer, J.A.R. van Veen and J.W. Niemantsverdriet, *Topics in Catal.* **13**, 99 (2000).
[24] L. Coulier, V.H.J. de Beer, J.A.R. van Veen and J.W. Niemantsverdriet, *J. Catal.* **197**, 26 (2001).
[25] J.C. Muijsers, Th. Weber, R.M. van Hardeveld, H.W. Zandbergen and J.W. Niemantsverdriet, *J. Catal.* **157**, 698 (1995).
[26] J.W. Niemantsverdriet, "Spectroscopy in Catalysis", VCH, Weinheim, 1993.
[27] J.C. Dupin, D. Gonbeau, I. Martin-Litas, Ph. Vinatier and A. Levasseur, *Appl. Surf. Sci.* **173**, 140 (2001).
[28] S. Harris and R.R. Chianelli, *J. Catal.* **98**, 17 (1986).
[29] L.S. Byskov, B. Hammer, J.K. Nørskov, B.S. Clausen and H. Topsøe, *Catal. Lett.* **47**, 177 (1997).

8

Thiophene HDS and sulfidation behaviour of Al_2O_3- and TiO_2-supported CoMo and NiMo model catalysts: influence of the support

Abstract

The stepwise sulfidation of SiO_2-, Al_2O_3- or TiO_2-supported oxidic CoMo and NiMo hydrodesulfurization (HDS) model catalysts is followed by X-ray Photoelectron Spectroscopy (XPS). For Co(Ni)/Al_2O_3 and Co(Ni)/TiO_2 catalysts, Co and Ni can only be partially sulfided due to the strong interaction with the support. In promoted Mo-based catalysts, the presence of Mo facilitates the sulfidation of Co and Ni, thereby increasing the degree of sulfidation. It is concluded that Mo interacts with the support and hence hinders the interaction of Co and Ni with the support. The sulfidation of Mo is not influenced by the presence of Co or Ni. Calcination increases the interaction of both Co and Ni and Mo with the support. In general, the sulfidation of TiO_2- and Al_2O_3-supported catalysts proceeds in a similar way. The main difference is the reactivity of TiO_2 during sulfidation treatments. TiO_2 is able to sulfide partially and these species act as promoter. Differences in sulfidation between Co- and Ni-promoted catalysts are small, despite the somewhat slower sulfidation of Co compared to Ni.

Thiophene HDS activity measurements show that TiO_2 and Al_2O_3 are better supports for active phase formation than SiO_2. This is contributed to the strong interaction of Co, Ni and Mo with the Al_2O_3- and TiO_2-support, due to calcination, which influences both the sulfidation rate and the dispersion of the catalyst. Complexing Co, Ni and Mo to chelating agents, like ethylene diamine tetraacetic acid (EDTA), retards the sulfidation of Co and Ni, while that of Mo is facilitated due to the absence of interaction with the support. Hence, the sulfidation of Mo precedes that of Co or Ni. These catalysts show the highest HDS activity, irrespective of the support. It is concluded that TiO_2-supported catalysts show both higher HDS activity and hydrogenation (HYD) selectivity than Al_2O_3-supported catalysts. Ni is a more effective promoter than Co. The HYD selectivity increases in the order CoMo < NiMo < Mo.

8.1 Introduction

Earlier studies from our laboratory focused on the effect of chelating agents on the HDS activity of SiO_2-supported CoMo and NiMo model catalysts [1-3]. These studies showed that the key step in the formation of the active phase, i.e. CoMoS or NiMoS, was the retardation of the sulfidation of Co or Ni [1-3]. The role of the chelating agents is to form stable complexes with Co and Ni, thereby retarding the sulfidation of Co and Ni with respect to Mo [1-6]. This leads to highly active catalysts with respect to the standard $CoMo/SiO_2$ and $NiMo/SiO_2$ catalysts. The highest activity was found for catalysts containing EDTA [2,3].

Van Veen et al. [7] showed that chelating agents increase the thiophene HDS activity of high surface area CoMoNTA catalysts irrespective of support. De Jong et al. [1] reported the same for CoMoNTA model catalysts supported on flat SiO_2 and Al_2O_3. Recent studies on the influence of chelating agents on Al_2O_3-supported catalysts showed some contradictory results. While Van Veen et al. [8,9] and Bouwens et al. [10] found that $Co(Ni)MoNTA/Al_2O_3$ is twice as active as standard $(Co)NiMo/Al_2O_3$ catalysts in thiophene HDS, a recent study by Cattaneo et al. [11] showed that conventional $NiMo/Al_2O_3$ catalysts are more active in thiophene HDS than $NiMoNTA/Al_2O_3$ and equal to $NiMoEDTA/Al_2O_3$. For dibenzothiophene HDS at 3.5 MPa, there also exists some contradiction. Van Veen et al. [9] found a negative effect of NTA on the activity of $Co(Ni)Mo/Al_2O_3$ catalysts, while Ohta et al. [12,13] found a positive effect of various chelating agents on the dibenzothiophene HDS activity of $CoMo/Al_2O_3$ catalysts but no effect in the case of $NiMo/Al_2O_3$.

A main factor influencing the activity of catalysts is the dispersion and morphology, which are strongly influenced by the interaction of the active phase with the support. Al_2O_3 is the most commonly used support in industrial applications [14]. Due to the strong interaction of the metal sulfides with the alumina support a more stable catalyst with higher dispersion is present at higher temperatures [14]. However, due to this strong interaction the sulfidation behaviour of Co(Ni) and Mo is also rather complex. Another promising support is TiO_2 [15]. Several authors reported high activities for unpromoted and promoted TiO_2-supported catalysts [16-19]. There still exists some contradiction concerning the activity and structural differences of TiO_2- and Al_2O_3-supported HDS catalysts. In an earlier paper we concluded that TiO_2 is partially sulfided during sulfidation and acts as a promoter, thereby increasing the HDS activity of Mo/TiO_2 catalysts [20].

X-ray Photoelectron Spectroscopy (XPS) has been often used as a technique to follow the sulfidation of high surface area HDS catalysts (see [14] and references herein). There has been some debate on the use of XPS to study the active phase in HDS catalysts. While Bouwens et al. [10] concluded that XPS was could not be used to distinct the active phase from bulk sulfides, others concluded that they could distinguish between Co (or Ni) in bulk sulfide (e.g. Co_9S_8) and in CoMoS (or NiMoS) [21-23]. Furthermore, most studies involved the XPS spectra of fresh catalysts or catalysts sulfided at high temperatures. No studies involved the stepwise sulfidation of the catalysts to follow the sulfidation of Co (or Ni) and Mo with respect to each other.

In this paper we will systematically study the influence of the support interaction and chelating agents on the sulfidation behaviour. The sulfidation behaviour, studied with XPS, will be compared with thiophene HDS measurements. We will compare the results of CoMo and NiMo catalysts on three different supports, i.e. SiO_2, Al_2O_3 and TiO_2.

8.2 Experimental

Catalysts were prepared on planar alumina and titania model supports. Planar alumina and titania were prepared by evaporating aluminum oxide and titanium oxide, respectively, on a Si (100) wafer as described in Chapter 6 and 7. The thickness of the evaporated layers is approximately 5 nm thick.

Cobalt, nickel and molybdenum were applied by spincoating the model supports at 2800 rpm in N_2 with aqueous solutions of either cobalt nitrate, nickel nitrate or ammonium heptamolybdate. The mixed-phase catalysts were prepared by spincoating with aqueous solutions containing Co (or Ni) and Mo. The concentrations of Co (or Ni) and Mo solutions were adjusted to result in a loading of 2 Co (or Ni) at/nm^2 and 6 Mo at/nm^2. The dried catalysts were calcined in air at 450 ^{0}C for 30 min. The influence of a chelating agent was investigated by adding nitrilo acetic acid (NTA) and ethylene diamine tetraacetic acid (EDTA) to the aqueous solutions. The EDTA solutions contained atomic Co(Ni):Mo:EDTA ratios of 2:6:5, as to complex both Co and Mo. For solutions containing NTA a ratio 2:6:8 was used. For more details on the preparation we refer to earlier work [2,3,20].

Sulfidation was carried out in a glass reactor under flow of 60 ml/min of 10% H_2S/H_2 at 1 bar. The catalysts were heated at a rate of 5 ^{0}C/min (EDTA/NTA-containing samples 2^{0}C/min) to the desired temperature and kept there for 30 min. After sulfidation the reactor was cooled to room temperature under a helium flow and brought to a glove box, where the samples were mounted in a transfer vessel for transport to the XPS under N_2 atmosphere. XPS spectra were measured on a VG Escalab 200 MK II, equipped with a standard dual source, a monochromatized Al Kα source and a five channeltron detector. Measurements were done at 20 eV pass energy. Charge correction was performed using the Al 2p peak of Al_2O_3 at 74.4 eV and the Ti 2p peak of TiO_2 at 458.8 eV as a reference [24].

Model catalysts were tested in batch mode thiophene HDS under standard conditions (1.5 bar, 400 ^{0}C, 4% thiophene/H_2). Model catalysts were presulfided at 400 ^{0}C for 30 min as described above. For more details, see [2,3].

8.3 Results

8.3.1 Sulfidation of Mo in unpromoted and promoted Mo/Al_2O_3 model catalysts

The Mo 3d spectra of uncalcined and calcined Mo/Al_2O_3 have been fitted to distinct the different Mo species present as function of sulfidation temperature (see Table 8.1). Both unsulfided catalysts show a single Mo 3d doublet with Mo $3d_{5/2}$ binding energy at 232.8 eV, corresponding to oxidic Mo^{6+} [24]. Table 8.1 shows that the sulfidation of uncalcined Mo/Al_2O_3 starts at 25 ^{0}C with the presence of a second Mo doublet with Mo $3d_{5/2}$ binding energy at 231.0 eV. This doublet remains present up to 200 ^{0}C. The Mo $3d_{5/2}$ binding energy of this doublet of 229.7-231.4 eV, the relative broad FWHM of 2.7-3 eV and the presence of sulfur suggest that a variety Mo^{5+} species is present, probably in an oxysulfidic environment [25,26]. The oxidic Mo^{6+} species, i.e. Mo $3d_{5/2}$ at 232.8 eV, remains present up to temperatures of 150 ^{0}C. At temperatures above 150 ^{0}C the Mo 3d spectra can be fitted with a doublet with a Mo $3d_{5/2}$ binding energy at 228.8 eV, corresponding to MoS_2 [24]. The S 2p /Mo 3d intensity ratio (not shown) increases with increasing temperature to 1.96 at 500 ^{0}C,

which is very close to a ratio of 2 for MoS_2. The S 2p spectra can all be fitted with one doublet around 161.6 eV, characteristic for S^2-type ligands present in MoS_2 [25,26]. The sulfidation is complete at 300 ^{0}C.

The influence of calcination, thereby increasing the interaction with the support, on the sulfidation behaviour of Mo/Al_2O_3 is clearly visible in Table 8.1. The sulfidation of calcined Mo/Al_2O_3 also starts at 25 ^{0}C, with the appearance of a shoulder at lower binding energy, although less pronounced than for uncalcined Mo/Al_2O_3. The presence of sulfur is visible for T > 50 ^{0}C. The spectra at low temperatures can also be fitted with an extra Mo 3d doublet with a Mo $3d_{5/2}$ binding energy at 231.0 eV, corresponding to Mo^{5+} in an oxysulfidic environment, as described above. The Mo^{6+} species remain present up to sulfidation temperatures of 200 ^{0}C. Around 150 ^{0}C a third doublet appears with a Mo $3d_{5/2}$ binding energy around 228.8 eV, which agrees well with MoS_2. This doublet is dominant in the high temperature regime. After sulfidation at 400 ^{0}C the sulfidation is still not complete. The unsulfided Mo species at high temperature are probably in close contact with the alumina support due to the calcination step. Note that at these temperatures uncalcined Mo/Al_2O_3 is already completely sulfided, as described above. After sulfidation at 500 ^{0}C the sulfidation is complete. The S 2p/Mo 3d atomic ratio of 1.98 shows that sulfidation of Mo at high temperatures is complete.

Table 8.1 *Mo $3d_{5/2}$ XPS binding energies and relative contributions of various Mo-species during sulfidation of uncalcined and calcined Mo/Al_2O_3 as a function of temperature.*

	Mo/Al_2O_3 uncalcined			Mo/Al_2O_3 calcined		
T_{sulf} (^{0}C)	Mo^{6+} (eV)	Mo^{5+} (eV)	Mo^{4+} (eV)	Mo^{6+} (eV)	Mo^{5+} (eV)	Mo^{4+} (eV)
-	232.8	-	-	232.8	-	-
25	232.8	231.0	-	232.8	230.9	-
	(0.67)	(0.33)		(0.9)	(0.1)	
50	232.7	230.1	-	232.8	231.1	-
	(0.54)	(0.46)		(0.72)	(0.28)	
100	232.7	229.7	-	232.7	230.9	-
	(0.22)	(0.78)		(0.5)	(0.49)	
150	232.7	230.1	228.9	232.7	229.8	228.8
	(0.15)	(0.25)	(0.60)	(0.45)	(0.27)	(0.28)
200	-	231.4	228.9	232.8	231.4	228.8
		(0.06)	(0.94)	(0.2)	(0.13)	(0.67)
300	-	-	228.9	-	231.4	228.7
					(0.19)	(0.81)
400	-	-	228.9	-	230.8	228.8
					(0.14)	(0.86)
500	-	-	228.9	-	-	228.8

Earlier we reported that the sulfidation of Mo in calcined Mo/TiO_2 proceeded similarly to Mo/Al_2O_3 [20]. Although the sulfidation starts at a somewhat lower temperature, i.e. 50 ^{0}C, for both supports the sulfidation at 400 ^{0}C is incomplete and complete sulfidation is only reached at 500 ^{0}C. The Mo 3d spectra of Mo/TiO_2 can also be fitted with a maximum

of three Mo 3d doublets, one with a Mo $3d_{5/2}$ binding energy at 230.6 eV corresponding to Mo^{5+}-oxysulfides in close contact to the support. A relatively intense S 2s peak and an extra S 2p doublet around 163.5 eV were ascribed to partial sulfidation of TiO_2 [20]. The sulfidation of uncalcined Mo/TiO_2 (not shown) takes place at rather low temperature, i.e. starting at room temperature and completed around 200 ^{0}C. Hence, for Mo/TiO_2 calcination retards the sulfidation significantly, as was observed also for Mo/Al_2O_3 (see Table 8.1).

The sulfidation of Mo in promoted catalysts proceeds similar to that of unpromoted Mo catalysts, as described in this section. No influence of the presence of Co or Ni on the sulfidation behaviour of Mo is observed for both Al_2O_3- and TiO_2-promoted catalysts.

8.3.2 Sulfidation of Co (and Ni) in Co(Ni)/Al_2O_3 and Co(Ni)/TiO_2 model catalysts

The sulfidation of Co/Al_2O_3 and Ni/Al_2O_3 and the influence of calcination there upon have been described in more detail in Chapter 6 [27]. Table 8.2 shows the Co $2p_{3/2}$ and Ni $2p_{3/2}$ binding energies and the degree of sulfidation after sulfidation at 400 ^{0}C. Figure 8.1A shows the Co 2p spectra of calcined Co/Al_2O_3 as a function of sulfidation temperature. The Co 2p spectrum of unsulfided Co/Al_2O_3 shows the characteristics of oxidic Co species with a Co $2p_{3/2}$ binding energy of 782.0 eV and shake up features at higher binding energy. This binding energy corresponds well with that of $CoAl_2O_4$ or cobalt oxide [21,28]. The oxidic Co species remain visible up to sulfidation temperatures of 500 ^{0}C. This supports the presence of $CoAl_2O_4$. It is known that these species are formed by diffusion of Co into the alumina support and are very stable against sulfidation [29,30]. However, Figure 8.1A shows that part of the Co sulfides at high temperatures. At 150 ^{0}C a second doublet appears at lower binding energy, i.e. Co $2p_{3/2}$ binding energy at 778.9 eV, which corresponds well with that of bulk cobalt sulfide [21]. Analysis of the Co 2p spectra reveals that about 45% of Co is sulfided at 400 ^{0}C (see Table 8.2). Omitting the calcination step results in a strong facilitation of the Co sulfidation. For uncalcined Co/Al_2O_3 catalysts the sulfidation of Co proceeds at moderate temperatures and was complete at 500 ^{0}C [27].

Table 8.2 *Co $2p_{3/2}$ and Ni $2p_{3/2}$ XPS binding energies of oxidic and sulfided Al_2O_3- and TiO_2-supported model catalysts and degree of Co/Ni sulfidation at 400 ^{0}C.*

	Co_{ox} $2p_{3/2}$/Ni_{ox} $2p_{3/2}$ (eV)	Co_{sulf} $2p_{3/2}$ /Ni_{sulf} $2p_{3/2}$ (eV)	Sulfidation degree at 400^{0}C (%)
Co/Al_2O_3 calcined	782.0	778.9	45
Co/TiO_2 calcined	782.1	779.0	54
Ni/Al_2O_3 calcined	856.5	853.3	55
Ni/TiO_2 calcined	856.6	853.3	68
$CoMo/Al_2O_3$ calcined	782.0	779.3	75
$CoMo/TiO_2$ calcined	781.9	779.3	81
CoMoEDTA	781.4	779.6	100
$NiMo/Al_2O_3$ calcined	856.8	853.9	80
$NiMo/TiO_2$ calcined	856.6	854.0	87
NiMoEDTA	856.0	854.2	100

The results on the sulfidation of Ni/Al_2O_3 are quite similar to those of Co/Al_2O_3 [27]. Ni also shows a strong interaction with the support, although less pronounced compared to Co/Al_2O_3. For uncalcined Ni/Al_2O_3 the sulfidation of Ni was complete at 400 ^{0}C. After calcination of Ni/Al_2O_3 the sulfidation of Ni was not complete even at high temperatures. A sulfidation degree of ~55% was reached after sulfidation at 400 ^{0}C (see Table 8.2). In general, the sulfidation of Co is more difficult than that of Ni. Ni $2p_{3/2}$ binding energies of oxidic Ni species at 856.6 eV and sulfided Ni species at 853.3 eV correspond to Ni_2O_3 or $NiAl_2O_4$ [31,32] and bulk nickel sulfide [23,31].

The interaction of Co and Ni with TiO_2 is also strong. While the sulfidation of uncalcined catalysts proceeds at relatively low temperatures, calcination of the catalysts leads to incomplete sulfidation of Co and Ni at high temperatures (not shown). Binding energies of oxidic and sulfidic species in Table 8.2 indicate that the presence of Co(Ni)-oxide and bulk Co(Ni)-sulfide species, respectively, although the presence of $CoTiO_3$ or $NiTiO_3$ cannot be excluded [24]. The degree of sulfidation at 400 ^{0}C of Ni is somewhat higher compared to Co, i.e. 68% vs. 54%. Note that the sulfidation degrees are higher compared to Al_2O_3-supported catalysts (see Table 8.2).

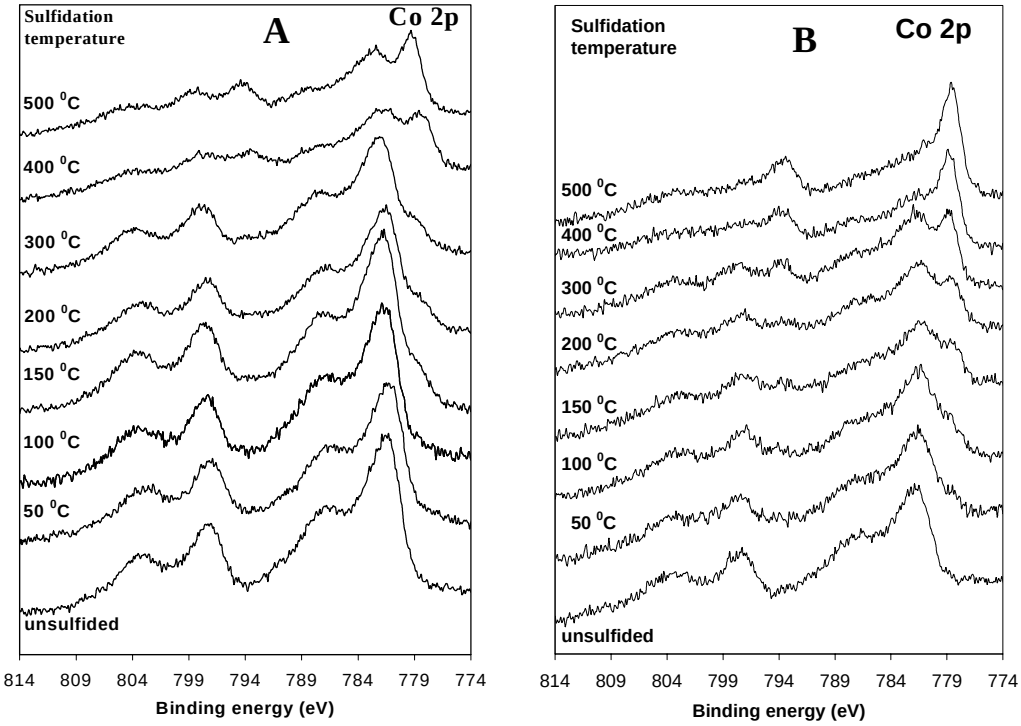

Figure 8.1 *Co 2p XPS spectra of (A) Co/Al_2O_3 calcined at 450 ^{0}C and (B) $CoMo/Al_2O_3$ calcined at 450 ^{0}C as a function of sulfidation temperature.*

8.3.3 Sulfidation of Co and Ni in Co(Ni)Mo/Al_2O_3 and Co(Ni)Mo/TiO_2 model catalysts

As stated earlier, the sulfidation of Mo is not influenced by the presence of Co or Ni. However, the opposite is not true as will be explained in this section. The sulfidation of Co

and Ni in Co/Al_2O_3 or Ni/Al_2O_3 differs greatly from that of Co or Ni in mixed phase catalysts, i.e. $Co(Ni)Mo/Al_2O_3$. The same obtains for TiO_2-supported catalysts.

Figure 8.1B shows the Co 2p spectra of calcined $CoMo/Al_2O_3$ as a function of sulfidation temperature. Table 8.2 shows the Co $2p_{3/2}$ binding energies of the oxidic and sulfidic Co species and the sulfidation degree after sulfidation at 400 ^{0}C. The Co 2p spectrum of unsulfided $CoMo/Al_2O_3$ shows a single Co 2p doublet with a Co $2p_{3/2}$ binding energy at 782.0 eV with shake up features at higher binding energy, characteristic for oxidic Co [21,28]. The Co 2p spectra at higher temperatures can all be fitted with two Co 2p doublets, i.e. oxidic Co with a Co $2p_{3/2}$ binding energy at 782.0 eV and sulfidic Co with a Co $2p_{3/2}$ binding energy at 779.3 eV. It is seen that the sulfidation starts at 100 ^{0}C and is not complete after sulfidation at 500 ^{0}C. Compared to Co/Al_2O_3, the sulfidation of Co in $CoMo/Al_2O_3$ proceeds faster. Not only does the sulfidation of $CoMo/Al_2O_3$ start at lower temperatures, the degree of sulfidation is also higher than that of Co/Al_2O_3, i.e. 75% vs. 55%, respectively (see Table 8.2). The low degree of sulfidation of calcined Co/Al_2O_3 was attributed to the strong interaction of Co with the alumina support and/or the diffusion of Co into the alumina. Clearly, the presence of Mo blocks the interaction and prevents the diffusion of Co. Table 8.2 also shows that the Co $2p_{3/2}$ binding energy of sulfided $CoMo/Al_2O_3$ is significantly lower compared to sulfided Co/Al_2O_3, i.e. 779.3 eV vs. 778.9 eV, respectively.

$NiMo/Al_2O_3$ behaves similarly as shown in Table 8.1. The degree of sulfidation is significantly higher for $NiMo/Al_2O_3$ than for Ni/Al_2O_3, i.e. 80% vs. 55%. In this case Mo also prevents Ni from interacting with the support thereby blocking the diffusion of Ni into the Al_2O_3 support to a large extent. The Ni $2p_{3/2}$ binding energies of sulfided Ni/Al_2O_3 (i.e. 853.3 eV) and $NiMo/Al_2O_3$ (i.e. 853.9 eV) also differ considerably. Figure 8.2 shows the influence of calcination on the sulfidation of Ni in $NiMo/Al_2O_3$. Shown is the degree of Ni sulfidation as a function of sulfidation temperature. It is seen that the sulfidation of Ni in uncalcined $NiMo/Al_2O_3$ starts around 50 ^{0}C and is complete at 150 ^{0}C. For calcined $NiMo/Al_2O_3$, the sulfidation of Ni is retarded to high temperatures. The sulfidation starts slowly at 100 ^{0}C and is not complete at high temperatures. After sulfidation at 500^{0}C only 80% of Ni is sulfided. Clearly calcination retards the sulfidation of Ni.

Comparing the sulfidation of Co and Ni in promoted Mo/Al_2O_3 catalysts reveals similar trends in sulfidation behaviour. For both systems calcination retards the sulfidation of Co and Ni while the presence of Mo facilitates the sulfidation. However, for both uncalcined and calcined catalysts the sulfidation of Co is a bit more difficult than that of Ni.

As described earlier for the single-phase catalysts, the interaction of Co, Ni and Mo with TiO_2 is strong and can be enhanced by calcination. Figure 8.3 shows an example of the sulfidation of a promoted TiO_2-supported catalysts, i.e. calcined $NiMo/TiO_2$. Table 8.2 shows the Co $2p_{3/2}$ and Ni $2p_{3/2}$ binding energies and the degree of sulfidation for various TiO_2-supported catalysts. The Mo 3d spectra in Figure 8.3B show that the sulfidation starts around 50 ^{0}C and is only completed after sulfidation at 500 ^{0}C. This sulfidation behaviour is identical to that of calcined Mo/TiO_2 as described in earlier paper [20]. Also visible is the relative intense S 2s peak, which was ascribed to sulfidation of the TiO_2-support [20]. The Ni 2p spectra in Figure 8.3A show that the sulfidation of Ni proceeds with a same rate as Mo. The sulfidation starts around 50 ^{0}C and is completed at 500 ^{0}C. The sulfidation degree of Ni in $NiMo/TiO_2$ at 400 ^{0}C is 87%, which is significantly higher than that of Ni/TiO_2 and also higher than that of both $NiMo/Al_2O_3$. Table 8.2 shows that in the case of TiO_2 as a support, the presence of Mo also prevents the strong interaction of Co and Ni with TiO_2, thereby

facilitating the sulfidation of Co and Ni. In general the sulfidation of Ni proceeds more easily than Co and TiO_2-supported catalysts show a higher degree of sulfidation after sulfidation at 400 ^{0}C compared to Al_2O_3. The difference in Co $2p_{3/2}$ and Ni $2p_{3/2}$ binding energy between unpromoted and promoted catalysts after sulfidation is clearly visible for both supports (see Table 8.2).

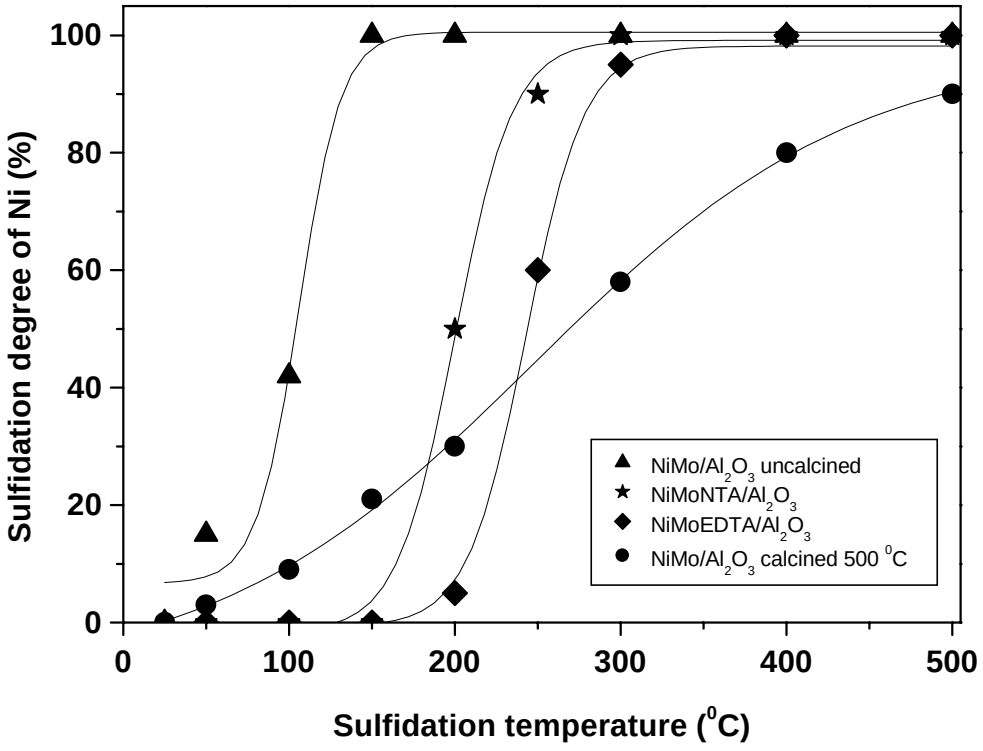

Figure 8.2 *Sulfidation degree of Ni in various Ni-promoted Al_2O_3-supported HDS catalysts as a function of sulfidation temperature.*

8.3.4 Influence of chelating agents on the sulfidation behaviour

Figure 8.2 shows the degree of sulfidation for Ni as function of sulfidation temperature for both NiMoNTA/Al_2O_3 and NiMoEDTA/Al_2O_3. Comparing the sulfidation behaviour of Ni in these catalysts with e.g. uncalcined NiMo/Al_2O_3, it is clear that the sulfidation of Ni is significantly retarded to high temperatures. EDTA retards the sulfidation of Ni to somewhat higher temperatures than NTA. For NiMoEDTA/Al_2O_3 the sulfidation starts around 200 ^{0}C and is completely sulfided at 300 ^{0}C, while for NiMoNTA/Al_2O_3 the sulfidation starts around 150 ^{0}C and is completed around 250 ^{0}C. This sulfidation behaviour is identical to that of NiMoNTA/SiO_2 and NiMoEDTA/SiO_2 [3]. However, it is strikingly different compared to calcined NiMo/Al_2O_3, where the sulfidation of Ni starts at lower temperatures and increases gradually. Moreover, the sulfidation of Ni in calcined

$NiMo/Al_2O_3$ is incomplete at high sulfidation temperatures. The sulfidation behaviour of $NiMoEDTA/TiO_2$ and $NiMoNTA/TiO_2$ is identical to that of SiO_2- and Al_2O_3-supported NiMoNTA and NiMoEDTA catalysts [3].

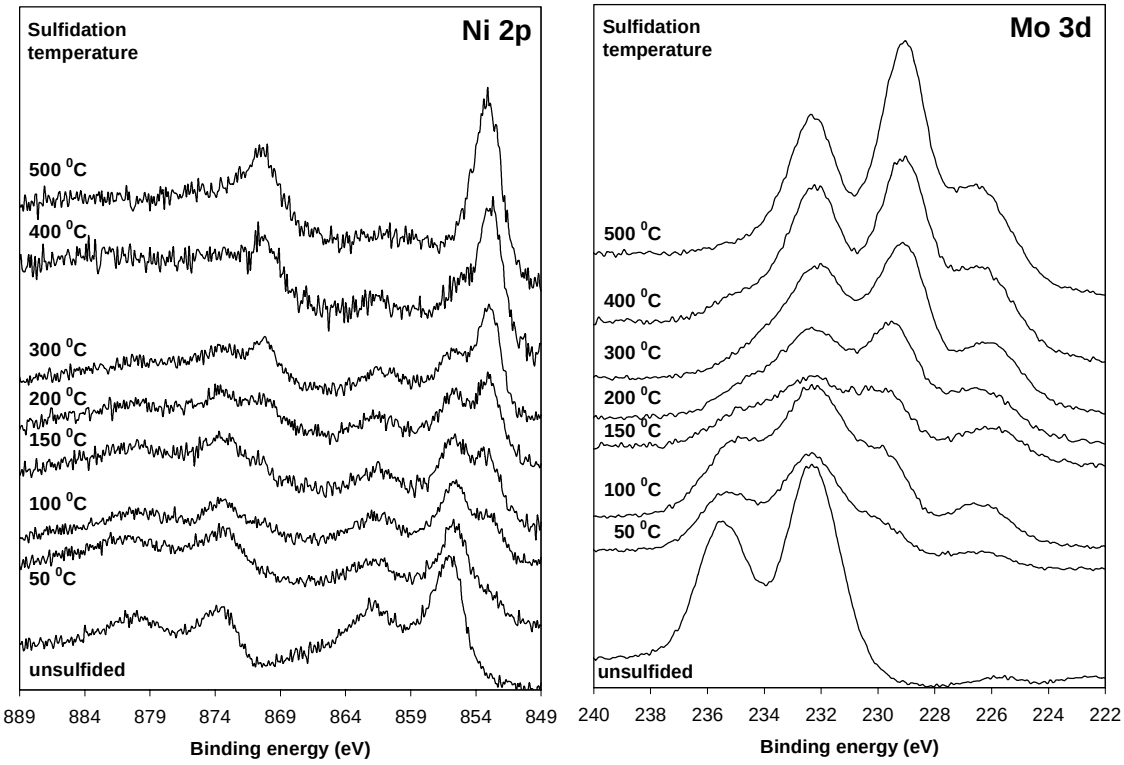

Figure 8.3 *(A) Ni 2p and (B) Mo 3d XPS spectra of a $NiMo/TiO_2$ model catalysts calcined at 450 ^{0}C after sulfidation at different temperatures.*

The sulfidation of Co in CoMoEDTA (or CoMoNTA) catalysts shows great similarity with that of NiMoEDTA (or NiMoNTA) catalysts. For these catalysts also no differences in sulfidation between different supports is observed. For more details on the influence of chelating agents on the sulfidation of Co and Ni we refer to earlier papers [1-3]. Table 8.2 shows that the binding energies of both oxidic and sulfidic Co and Ni is clearly different compared to catalysts without chelating agents, although the difference is less pronounced for the sulfided catalysts. The difference in binding energy of the oxidic species is contributed to Co and Ni complexed to NTA or EDTA [2,3].

In an earlier paper we concluded that Mo is also complexed to EDTA, thereby preventing interaction of Mo with support [2,3]. Because the decomposition of the Mo-EDTA complex occurs already at low temperature and the interaction of Mo with the support is weak, the sulfidation of Mo is fast and is completed around 150 ^{0}C [2,3].

Comparing the various catalysts containing chelating agents, it is shown that the support has no effect on the sulfidation of Co, Ni or Mo. The differences in sulfidation behaviour between Co and Ni in these catalysts are only small, both sulfide in the same temperature regime, dependent on the chelating agent used.

8.3.5 Thiophene HDS activity measurements

Figure 8.4 shows the thiophene HDS activity of various CoMo and NiMo catalysts described in this paper. The activity is expressed as the total conversion (%) per 5 cm^2 of catalyst after 1 h of batch reaction at 400 ^{0}C and 1 bar and has been corrected for blank measurements (bare alumina or titania support and empty reactor). Note that all catalysts have been calcined at 450 ^{0}C except for the catalysts containing chelating agents. For comparison the HDS activities of the corresponding SiO_2-supported catalysts are shown, as published in earlier papers [2,3].

A few observations can be made from Figure 8.4. For unpromoted catalysts, the HDS activity increases in the order $SiO_2 < Al_2O_3 < TiO_2$. While the HDS activity of Mo/TiO_2 is twice as high as Mo/Al_2O_3 the difference between Al_2O_3 and TiO_2 for promoted catalysts is almost absent. For all promoted catalysts, the HDS activity is higher compared to the Mo catalysts, indicating synergy for all systems. However, the synergy is more pronounced for Ni-promoted catalysts. The so-called promotion factor (i.e. activity Co(Ni)Mo/activity Mo) increases in the order $TiO_2 < Al_2O_3 \leq SiO_2$. Note that this order is opposite to that for the HDS activity of unpromoted catalysts. The promotion factor varies from 1.3 (for $CoMo/TiO_2$) to 6 (for $NiMo/Al_2O_3$).

Catalysts containing EDTA show the highest HDS activity for all supports. The activity is the same for all supports, although for TiO_2 the activity seems somewhat lower. As a result the promotion factor for catalysts containing chelating agents increases in the order $TiO_2 < Al_2O_3 < SiO_2$. The effect of NTA on the HDS activity depends on the support and the promoter. While for Co-promoted catalysts the presence of NTA increases the HDS activity with at least a factor 2, $NiMo/TiO_2$ is almost as active as $NiMoNTA/TiO_2$.

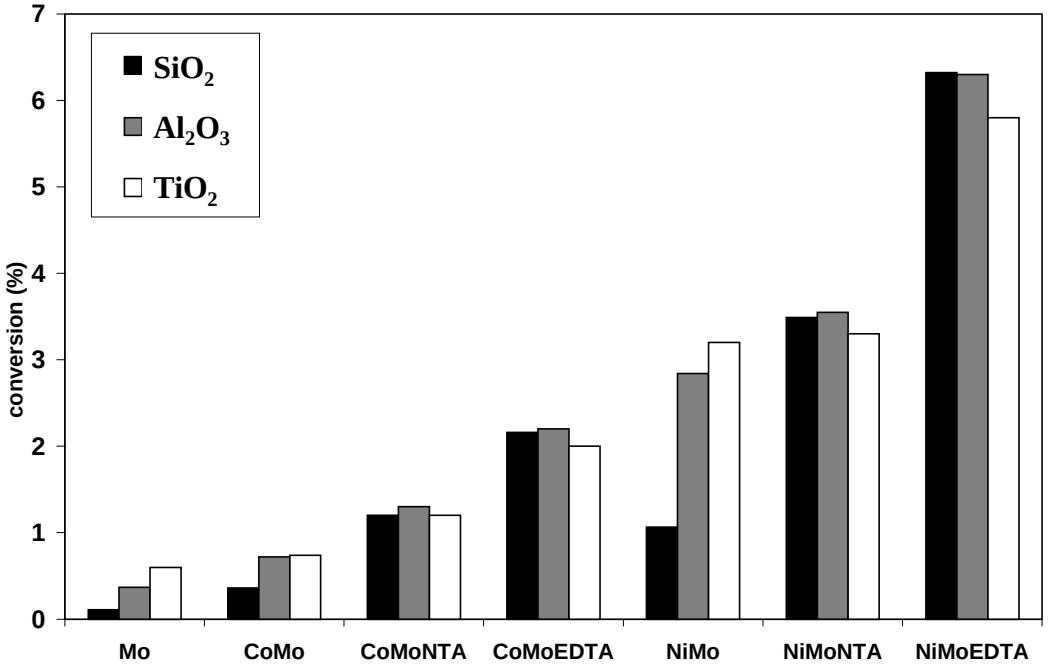

Figure 8.4 *Thiophene HDS activities of various Mo-based catalysts. The HDS activity is expressed as conversion of thiophene (%) per 5 cm^2 of model catalysts after 1 hour of batch reaction at 400 ^{0}C.*

Table 8.3 compares the HDS activity with the hydrogenation (HYD) selectivity of various model catalysts. The HYD selectivity is expressed by total n-butane production divided by total products (n-butane/total products). A few trends are visible from Table 8.3. For example, unpromoted Mo catalysts, with the lowest HDS activity, are the most active in hydrogenation. Comparing the two supports, it is clear that on TiO_2 the HYD selectivity is higher than on Al_2O_3. Although promoted catalysts are relatively less selective in hydrogenation, Table 8.3 shows that Ni-promoted catalysts are somewhat more selective towards hydrogenation compared to Co-promoted catalysts.

Table 8.3 *Thiophene HDS activity (%) and hydrogenation (HYD) selectivity of Al_2O_3- and TiO_2-supported model catalysts.*

	HDS (%)	HYD (n-butane/products)
Mo/Al_2O_3	0.37	0.04
Mo/TiO_2	0.6	0.07
$CoMo/Al_2O_3$	0.72	0.01
$CoMo/TiO_2$	0.74	0.02
$NiMo/Al_2O_3$	2.84	0.02
$NiMo/TiO_2$	3.2	0.04

8.4 Discussion

Sulfidation and HDS activity of unpromoted Mo catalysts

Table 8.1 shows the influence of the alumina support and calcination on the sulfidation of Mo. It is found that uncalcined Mo/Al_2O_3 sulfides relatively easy, although compared to Mo/SiO_2 the sulfidation is retarded to higher temperatures [2,3]. Calcination of Mo/Al_2O_3 inhibits the sulfidation even more. After sulfidation at 400 ^{0}C the sulfidation was still not complete, while a sulfidation temperature of 500 ^{0}C was necessary for complete sulfidation. Fitting of the XPS spectra shows the presence of three Mo species during sulfidation: oxidic Mo^{6+} species at 232.7 ± 0.2 eV, sulfidic Mo^{4+} species at 228.8 ± 0.2 eV, and Mo species at ~231 eV. The latter species were attributed to Mo^{5+} species, probably in an oxysulfidic environment. While the Mo $3d_{5/2}$ binding energy of these species fall in a broad range it is possible that several species are present. These Mo^{5+} have also been found on Mo/SiO_2 model catalysts [2,3,25,26], while several others also reported the presence Mo^{5+} species on high surface area Mo/Al_2O_3 with XPS [18,28,33]. These authors also found that the sulfidation of calcined Mo/Al_2O_3 is not complete after sulfidation at 400 ^{0}C. The Mo $3d_{5/2}$ binding energy of Mo^{6+} and Mo^{4+} of 232.7 eV and 228.8 eV, respectively, corresponds well with that of respectively MoO_3 and MoS_2 [21,28]. MoO_3 and $Al_2(MoO_4)_3$ can not be distinguished based on their binding energy [28]. However, the incomplete sulfidation of Mo/Al_2O_3 at 400 ^{0}C indicates that the remaining oxidic Mo-species are in close contact with the Al_2O_3-support.

Arnoldy et al. [34] proposed a mechanism of Mo sulfidation from TPS which included the formation of MoO_2 and the hydrogenation of elemental sulfur. They found no

evidence for the presence of Mo^{5+} species or MoS_3, the latter one has been observed with Quick EXAFS [11]. We found no evidence for the presence of MoO_2 or MoS_3. However, we cannot exclude these species, while it is possible that XPS is not sensitive enough to distinguish these species based on differences in binding energy, which are probably very small.

The sulfidation of Mo in Mo/TiO_2 proceeds in a similar way, as described more extensively in an earlier paper [20]. Mo has also a strong interaction with the TiO_2-support, which is intensified due to calcination. Due to this interaction, the sulfidation of Mo is slow and not complete at 400 ^{0}C. This is in good agreement with other authors who also reported the incomplete sulfidation of Mo/TiO_2 [17,35,36]. However others observed complete sulfidation of Mo/TiO_2 and conclude that the interaction of Mo with TiO_2 is weaker than that of Mo with Al_2O_3 [18,37]. Mo^{5+}-oxysulfides are proposed as intermediates for sulfidation of Mo/TiO_2 [20]. Detailed analysis of the Ti 2p and S 2p spectra lead to the conclusion that also TiO_2 sulfides partially [20]. We find no evidence for differences in sulfidation behaviour between Mo/Al_2O_3 and Mo/TiO_2 and therefore expect no large differences in morphology or dispersion of MoS_2. Earlier XPS results confirm the absence of large differences in dispersion [20]. This is in agreement with reports by Vissenberg et al. [37] and Ramirez et al. [38].

The difference in sulfidation between Mo/Al_2O_3 (or Mo/TiO_2) and Mo/SiO_2 can be explained by a difference in Mo-support interaction. It is known that e.g. the Mo-Al_2O_3 interaction is strong, and can be enhanced by calcination. Because of this interaction the sulfidation of Mo is known to be difficult compared to Mo/SiO_2, which has no strong interaction and thus easily sulfides [39-41]. As a result, a well-dispersed Mo phase is present on Al_2O_3, while already at low Mo loadings poorly spread MoO_3 crystallites are present on SiO_2 [41-43].

Comparison of the thiophene HDS activity of Mo catalysts in Figure 8.4, shows that, despite the fact the activity is low compared to the promoted catalysts, Mo/Al_2O_3 is more active than Mo/SiO_2. While the catalysts have the same Mo loading, the high activity of Mo/Al_2O_3 is totally contributed to a higher MoS_2 dispersion after sulfidation. Calcination increases the HDS activity, although slightly. The significantly higher activity of Mo/TiO_2 compared to Mo/Al_2O_3 is not ascribed to differences in dispersion, but to sulfided Ti-species, which act as a promoter and thus increase the HDS activity [20].

Order of sulfidation vs. HDS activity for promoted Mo catalysts

The Mo 3d XPS spectra of the unpromoted and promoted Mo/Al_2O_3 or Mo/TiO_2 are identical, from which we can conclude that the presence of Co or Ni has no influence on the sulfidation behaviour of Mo. Bachelier et al. [44] also found that the nature and dispersion of Mo was unaffected by the presence of Ni in the case of high surface area $NiMo/Al_2O_3$ catalysts. A TPS study of Scheffer et al. [45] on $CoMo/Al_2O_3$ revealed the same.

However, the XPS results show that the presence of Mo did influence the sulfidation of Co and Ni significantly for both Al_2O_3 and TiO_2. Compared to the sulfidation of e.g. Co and Ni in Co/Al_2O_3 and Ni/Al_2O_3 the presence of Mo facilitates the sulfidation of Co and Ni (e.g. Figure 8.1). The sulfidation degree of the calcined CoMo and NiMo catalysts is 75% for Co and 80% for Ni, respectively (Table 8.2). The sulfidation degree of calcined Co/Al_2O_3 and Ni/Al_2O_3 is much lower (45% for Co and 55% for Ni respectively). This incomplete sulfidation of Co (or Ni) in $Co(Ni)/Al_2O_3$ and $Co(Ni)Mo/Al_2O_3$ catalysts has also been

reported by others using XPS, although the extent to which the sulfidation was incomplete differed [21,28,46]. Topsøe et al. [29,30] showed with Mössbauer spectroscopy that Co could not be completely sulfided and that the unsulfided Co species were located in the alumina support. This diffusion of Co into the alumina is thought to take place during the calcination step [45,47]. TPS studies showed that the sulfidation degree of Co in $CoMo/Al_2O_3$ depends mainly on the calcination temperature [45], although the loading also plays a role. From the fact that Mo facilitates the sulfidation of Co and Ni, we conclude that Mo hampers partially the migration of Co and Ni into the alumina support. This agrees well with literature on high surface area catalysts [29,30,44,45]. We find that Ni sulfides more easily than Co, although the difference is small.

Literature on promoted Mo/TiO_2 is less abundant. Most authors report on the sulfidation and the HDS activity of Mo/TiO_2, however the sulfidation and the influence on the HDS activity of the promoters are often neglected. From the results in Table 8.2 and Figure 8.3 we can conclude that promoted Mo/TiO_2 catalysts show great similarity with Al_2O_3-supported catalysts. The presence of Mo also facilitates the sulfidation of Co and Ni. The sulfidation of Co is more difficult than that of Ni. Calcination of the promoted catalysts leads to incomplete sulfidation although the degree of sulfidation is higher compared to Al_2O_3.

For both supports the Co 2p and Ni 2p spectra can be fitted with two doublets, i.e. oxidic and sulfidic Co or Ni. It was not possible to distinguish more species. Scheffer et al. [48] showed with temperature programmed sulfidation (TPS) that up to five Co species are present in sulfided $CoMo/Al_2O_3$, while Wivel et al. [30] and Bachelier et al. [44] only found three species for Co in $CoMo/Al_2O_3$ and Ni in $NiMo/Al_2O_3$, respectively. However, the Co 2p and Ni 2p XPS spectra are rather complex, due to the shake up features, and the various possible species do not differ greatly in oxidation state and chemical environment to distinguish them with XPS. Alstrup et al. [21] showed that close inspection of the binding energy and the shape of the Co 2p spectrum could reveal the difference between Co in Co_9S_8 and in CoMoS. The authors used pure reference compounds for this, which is difficult to apply in catalysts, while more than one Co species are present in most cases [29,30,48]. Earlier we showed that it is possible to correlate the Ni 2p binding energy with the amount of active phase in SiO_2-supported NiMo model catalysts [3]. The Co $2p_{3/2}$ and Ni $2p_{3/2}$ binding energies of the sulfided catalysts listed in Table 8.2, show that there is a difference in binding energy between sulfided Co and Ni in $Co(Ni)/Al_2O_3$ and $Co(Ni)/TiO_2$, which consists mainly of bulk Co- and Ni-sulfide, and in CoMo and NiMo catalysts. The Co $2p_{3/2}$ and Ni $2p_{3/2}$ binding energies of the sulfided promoted catalysts differ from the values of bulk Co- or Ni-sulfide. While the HDS activity of e.g. Co/Al_2O_3 is below the detection limit, the activity of the promoted catalysts is significantly higher than the unpromoted catalysts. From this we conclude that the difference in binding energy represents the difference of Co (or Ni) in bulk sulfide and in the active phase, i.e. CoMoS or NiMoS. This difference in binding energy was observed earlier for SiO_2-supported model catalysts [2,3] and high surface area catalysts [21-23]. No differences in Mo $3d_{5/2}$ binding energy are observed.

The HDS activity measurements in Figure 8.4 show the promoting effect of Co and Ni on Mo-based catalysts, although the promoting effect is not the same for all catalysts. For example, Ni-promoted catalysts are clearly more active compared to Co-promoted catalysts. Although the sulfidation of Co is somewhat more difficult than that of Ni and hence the sulfidation degree is somewhat lower, the difference in sulfidation is only small (see Table

8.2) and cannot explain completely the large difference in HDS activity. However, it is known that bulk Ni-sulfide, formed at low temperatures, is able to migrate to the edges of WS_2 [27,49,50]. For Co this has not been observed [51]. It is very likely that this so-called redispersion takes also place for NiMo catalysts. If this is the case the amount of Ni in NiMoS is larger than of Co in CoMoS and this can explain the higher HDS activity for Ni-promoted catalysts.

The promotion factor, i.e. increase in HDS activity due to the presence of the promoter, is different for the various supports; it increases in the order $TiO_2 < Al_2O_3 \sim SiO_2$. This order is opposite to that of the HDS activity of Mo catalysts. Hence we conclude that the promotion factor is largely influenced by the HDS activity of the unpromoted catalysts. For example, the HDS activity of Mo/SiO_2 is very low, hence despite the lower activity of $NiMo/SiO_2$ compared to other supports, the promotion factor is high, i.e. a factor 10. On the contrary, the HDS activity of Mo/TiO_2 is relatively high, which is attributed to sulfided Ti-species acting as promoter, and as a result the promotion factor of $NiMo/TiO_2$ is only 5.

While for the unpromoted catalysts, the HDS activity increases in the order $SiO_2 < Al_2O_3 < TiO_2$, it shows that for the promoted catalysts the HDS activity of Al_2O_3- and TiO_2-supported is almost equal. This observation fits well with the similar sulfidation behaviour of these catalysts as described earlier. We already stated that the high activity of Mo/TiO_2 was caused by sulfided Ti-species acting as promoter [20]. The equal activity of promoted Mo/Al_2O_3 and Mo/TiO_2 catalysts indicate that these sulfided Ti-species do not play a significant role in promoted catalysts. Apparently, Co and Ni are more prone to act as a promoter than Ti is. We conclude that sulfided Ti-species, which acts as a promoter, causes the low promotion effect on TiO_2-supported catalysts [17].

From the hydrogenation (HYD) selectivity in Table 8.3 we can conclude that unpromoted catalysts are better catalysts for hydrogenation and that the hydrogenation selectivity is also higher on TiO_2-supports. Furthermore, Ni is a somewhat better promoter for both HDS and HYD than Co. These observations are in agreement with the idea that HDS takes place on decorated edges sites of MoS_2 while HYD is more likely to take place on 'empty' MoS_2-edges [52,53].

In general we can conclude that Al_2O_3 and TiO_2 are better supports for active phase formation in HDS than SiO_2. This is due to the interaction of Co (or Ni) and Mo with the support. We conclude that the sulfidation behaviour of these catalysts is very similar and this fits well with the equal HDS activity of Al_2O_3 and TiO_2. For SiO_2 it is known that the interaction with the support is low and hence a poor dispersion is likely [39-43]. The strong interaction of TiO_2 and Al_2O_3 leads to high dispersion and high stability of the active phase [39-43]. Furthermore, if one compares the sulfidation of Co (or Ni) with Mo on these supports, it shows that due to the retardation, as a result of the interaction with the support, Co (or Ni) sulfides at relatively high temperatures. On SiO_2-supports, Co sulfides already at low temperature and therefore Co easily forms bulk Co-sulfide, similar to Co/SiO_2 or Co/Al_2O_3. Hence, the chance that Co (or Ni) sulfides in the presence of MoS_2 and thus can form the Co(Ni)MoS phase is more likely for Al_2O_3 or TiO_2. The ability of Ni-sulfide to redisperse in the presence of MoS_2 may explain the higher HDS activities found for NiMo catalysts compared to CoMo catalysts.

Influence of chelating agents

The results in this paper on Al_2O_3 and TiO_2 show that the sulfidation behaviour of catalysts containing chelating agents is identical to that of SiO_2-supported catalysts [2,3]. This was also observed for CoMoNTA catalysts by van Veen et al. [7] and de Jong et al. [1]. Figure 8.4 shows that the HDS activity of the NTA- or EDTA-containing catalysts are also independent of the support. This is in agreement with the identical sulfidation behaviour. It is proposed that due to the complexation of Co (or Ni) and Mo with the chelating agents any interaction with the support is prevented and hence the supports act as inert substrates.

Adding chelating agents, like NTA or EDTA, retard the sulfidation of Co and Ni and prevent the interaction of Co (or Ni) and Mo with the support due to complex formation. As a result Mo is sulfided at low temperatures, followed by Co (or Ni) at higher temperatures. The sulfidation is complete at 400 ^{0}C due to the absence of interaction of the support. In the case of EDTA, the sulfidation of Co and Ni is retarded to temperatures where Mo is already completely sulfided. Hence, all Co- or Ni-sulfide particles are able to migrate to the edges of the MoS_2 and form CoMoS or NiMoS. As a result catalysts containing EDTA show high HDS activities (see Figure 8.4).

The EDTA-containing catalysts are more active than those containing NTA. This was also observed for SiO_2-supported model catalysts [2,3]. The fact that EDTA forms more stable complexes with Co and Ni, leads to a higher degree of retardation of the sulfidation of these elements. As a result, Mo is already completely sulfided at temperatures where Ni and Co are still complexed to EDTA. For NTA the complexes decompose at lower temperatures, hence the sulfidation of Co (or Ni) and Mo show some overlap and not all Co and Ni atoms are sulfided in the presence of completely sulfided Mo and can form CoMoS (or NiMoS). The difference in activity between NTA- and EDTA-containing catalysts is therefore ascribed to different amounts of active sites, i.e. CoMoS and NiMoS. As we observed earlier, Ni-promoted catalysts are more active than Co-promoted catalysts. Assuming that all Co and Ni atoms are in the CoMoS and NiMoS phase for EDTA-catalysts, it follows that Ni is intrinsically more active in thiophene HDS than Co. NiMo catalysts are found to be more active in thiophene HDS at low H_2S partial pressures than CoMo catalysts by other authors, while at higher H_2S partial pressures CoMo is more active [54-56]. While in our conditions the conversions are low, the H_2S partial pressure is low and hence the higher activity of NiMo vs. CoMo agrees well with literature [54-56].

Figure 8.4 also shows that the enhancement of the HDS activity by using chelating agents compared to the conventional promoted catalysts strongly depends on both the support and the promoter. For all supports the HDS activity of EDTA-containing catalysts is the highest and twice as high compared to NTA-containing catalysts. However, while for SiO_2-supported catalysts the activity is significantly enhanced by chelating agents, either NTA or EDTA, this is not the case for the other supports. For example, Figure 8.4 shows that NiMo/Al_2O_3 has almost the same activity as NiMoNTA/Al_2O_3 and the same is true for NiMo/TiO_2. This discrepancy may be explained in terms of CoMoS I and CoMoS II phase, as proposed by Van Veen et al. [7-9] and Bouwens et al. [10]. In these terms, CoMoNTA/Al_2O_3 catalysts, where all Co is present at the edges of fully sulfided MoS_2-slabs, i.e. CoMoS II, is twice as active as calcined CoMo/Al_2O_3, where Co is present at the edges of MoS_2 interacting with the support, i.e. CoMoS I. However, Van Veen et al. [8] reported that in the case of CoMoNTA, all Co was in the CoMoS II phase, while in our case this cannot be true because

EDTA is twice as active as NTA and we conclude from the XPS spectra that not all Co atoms are able to migrate to preformed MoS_2. Neither have we evidence that $CoMo/Al_2O_3$ or $NiMo/Al_2O_3$ contain 100% CoMoS I or NiMoS I phase. In fact, we observed that Co and Ni could not be sulfided completely. Most probably the dispersion of MoS_2 is also different for e.g. $NiMo/Al_2O_3$ and $NiMoNTA/Al_2O_3$.

Hence, we conclude that differences in sulfidation behaviour, in dispersion and differences in amounts of Co(Ni)MoS I and Co(Ni)MoS II phases, can cause differences in HDS activity between catalysts with and without chelating agents. It is not straightforward if all these possible causes do play a role. Evidence for the importance of dispersion is the lower activity we find for uncalcined $NiMo/Al_2O_3$ catalysts (not shown). For these catalysts, NTA increased the activity significantly. Calcination increases the HDS activity and makes the comparison with catalysts containing chelating agents difficult.

Van Veen et al. [7-9] and Bouwens et al. [10] found for high surface area $Co(Ni)MoNTA/Al_2O_3$ catalysts an increase in thiophene HDS activity with a factor 1.5-2 compared to calcined $Co(Ni)Mo/Al_2O_3$ but a negative effect of NTA for dibenzothiophene HDS [9]. Shimizu et al. [12-13] found a positive effect of chelating agents on the (di)benzothiophene HDS activity of CoMo catalysts but no effect in the case of NiMo. These authors also found the HDS activity of CoMo catalysts to be higher using EDTA compared to NTA, which is also visible in Figure 8.4. However, a recent study of Cattaneo et al. [11] on $NiMo/Al_2O_3$ reported contradictory results. These authors found an equal thiophene HDS activity for calcined $NiMo/Al_2O_3$ and $NiMoEDTA/Al_2O_3$ and even a lower one for $NiMoNTA/Al_2O_3$. Only small differences in preparation and pretreatment conditions distinguish the various reports. Therefore, the different HDS activity results may be caused by different amounts of chelating agents, i.e. chelating agents to complex both Co(Ni) and Mo [12,13] or only Co(Ni) [11], and different heating rates for sulfidation, i.e. 2 ^{0}C/min [7-10] vs. 6 ^{0}C/min [11]. However, the results in this paper and earlier work [2,3,27,49,51] show a consistent picture of the effect of chelating agents. Hence we can state that chelating agents do lead to highly active HDS catalysts, irrespective of support.

8.5 Conclusions

The sulfidation behaviour and thiophene hydrodesulfurization (HDS) activity of Al_2O_3- and TiO_2-supported CoMo and NiMo model catalysts is describe in this paper and the results have been compared to SiO_2-supported model catalysts, as reported in earlier publications. The main objective is to study the influence of the support on the formation of active phase. The XPS measurements show that Co and Ni have a strong interaction with the support and can diffuse into the support. This effect can be enhanced by calcination. Also Mo has a strong interaction with the alumina support and as a consequence the sulfidation is retarded to higher temperatures. In the mixed phase catalysts, i.e. CoMo and NiMo, the presence of Mo prevents the interaction of Co and Ni with the support and inhibits partially the migration of Co and Ni into the support. The sulfidation of Ni is in all cases somewhat easier than Co. The sulfidation of Mo is not influenced by the presence of Co or Ni. No evidence for Co(Ni)Mo mixed-oxide species is found. For calcined catalysts the sulfidation of Co, Ni and Mo is not complete at 400 ^{0}C. The sulfidation of TiO_2-supported catalysts show similar behaviour. However the interaction with the TiO_2-support is somewhat weaker than for Al_2O_3, which leads to a higher degree of sulfidation.

It is also shown that Al_2O_3 and TiO_2 are better supports for active phase formation than SiO_2. Due to the strong interaction with Al_2O_3 and TiO_2, MoS_2 is better dispersed which leads to a higher HDS activity. The TiO_2-support can be sulfided partially and these species are able to act as promoter. This explains the higher HDS activity of Mo/TiO_2 compared to Mo/Al_2O_3. Both Co and Ni show clearly a promotion effect for HDS, although Ni-promoted catalysts show higher HDS activities. The hydrogenation selectivity is relatively higher for unpromoted catalysts and catalysts supported on TiO_2.

In combination with earlier work we present a consistent picture of the role of chelating agents on the activity of HDS catalysts. Complexing CoMo and NiMo to chelating agents, like NTA and EDTA, retards the sulfidation of Co and Ni with respect to that of Mo, which leads to high HDS activities. While for NTA there still exists a temperature regime where both Co (or Ni) and Mo sulfide, for catalysts containing EDTA Co and Ni sulfide at temperatures where Mo is already completely sulfided. As a result catalysts containing EDTA show higher HDS activities compared to NTA. Furthermore, the HDS activities are high irrespective of support. Due to the complexation with the chelating agents the interaction with the support is prevented and Al_2O_3 and TiO_2 behave as an inert substrate in the same way as SiO_2.

References

[1] A.M. de Jong, V.H.J. de Beer, J.A.R. van Veen and J.W. Niemantsverdriet, *J. Phys. Chem.* **100**, 17722 (1996).

[2] L. Coulier, V.H.J. de Beer, J.A.R. van Veen and J.W. Niemantsverdriet, *Topics in Catal.* **13**, 99 (2000).

[3] L. Coulier, V.H.J. de Beer, J.A.R. van Veen and J.W. Niemantsverdriet, *J. Catal.* **197**, 26 (2001).

[4] L. Medici and R. Prins, *J. Catal.* **163**, 38 (1996).

[5] R. Cattaneo, T. Shido and R. Prins, *J. Catal.* **185**, 199 (1999).

[6] R. Cattaneo, Th. Weber, T. Shido and R. Prins, *J. Catal.* **191**, 225 (2000).

[7] J.A.R. van Veen, E. Gerkema, A.M. van der Kraan and A. Knoester, *J. Chem. Soc., Chem. Commun.* **22**, 1684 (1987).

[8] J.A.R. van Veen, E. Gerkema, A.M. van der Kraan, P.A.J.M. Hendriks and H. Beens, *J. Catal.* **133**, 112 (1992).

[9] J.A.R. van Veen, H.A. Colijn, P.A.J.M. Hendriks and A.J. van Welsenes, *Fuel Processing Technol.* **35**, 137 (1993).

[10] S.M.A.M. Bouwens, F.B.M. van Zon, M.P. van Dijk, A.M. van der Kraan, V.H.J. de Beer, J.A.R. van Veen and D.C. Koningsberger, *J. Catal.* **146**, 375 (1994).

[11] R. Cattaneo, F. Rota and R. Prins, *J. Catal.* **199**, 318 (2001).

[12] T. Shimizu, K. Hiroshima, T. Honma, T. Mochizuki and M. Yamada, *Catal. Today* **45**, 271 (1998).

[13] Y. Ohta, T. Shimizu, T. Honma and M. Yamada, *Stud. Surf. Sci. Catal.* **127**, 161 (1999).

[14] H. Topsøe, B.S. Clausen and F.E. Massoth, "Hydrotreating Catalysis." Springer-Verlag, Berlin, 1996.

[15] F. Luck, *Bull. Soc. Chim. Belg.* **100**, 781 (1991).

[16] K.Y.S. Ng and E. Gulari, *J. Catal.* **95**, 33 (1985).

[17] J. Ramirez, S. Fuentes, G. Diaz, M. Vrinat, M. Breysse and M. Lacroix, *Appl. Catal.* **52**, 211 (1989).
[18] Y. Okamoto, A. Maezawa and T. Imanaka, *J. Catal.* **120**, 29 (1989).
[19] K.C. Pratt, J.V. Sanders and V. Christov, *J. Catal.* **124**, 416 (1990).
[20] Chapter 7 of this thesis.
[21] I. Alstrup, I. Chorkendorff, R. Candia, B.S. Clausen and H. Topsøe, *J. Catal.* **77**, 397 (1982).
[22] J.P. Bonnelle, A. Wambeke, A. Kherbeche, R. Hubaut, L. Jalowiecki, S. Kasztelan and J. Grimblot, in: "Advances in Hydrotreating Catalysts", M. Occelli, and R. Chianelli (Eds.), Elsevier, Amsterdam, 123 (1989).
[23] S. Houssenbay, S. Kasztelan, H. Toulhoat, J.P. Bonnelle and J. Grimblot, *J. Phys. Chem.* **93**, 7176 (1989).
[24] J.F. Moulder, W.F. Stickle, P.E. Stobol and K.D. Bombden, in "Handbook of XPS", Perkin-Elmer, Eden Prairie, USA, 1992.
[25] A.M. de Jong, H.J. Borg, L.J. van IJzendoorn, V.G.M.F. Soudant, V.H.J. de Beer, J.A.R. van Veen and J.W. Niemantsverdriet, *J. Phys. Chem.* **97**, 6477 (1993).
[26] J.C. Muijsers, Th. Weber, R.M. van Hardeveld, H.W. Zandbergen and J.W. Niemantsverdriet, *J. Catal.* **157**, 698 (1995).
[27] Chapter 6 of this thesis.
[28] T.A. Patterson, J.C. Carver, D.E. Leyden and D.M. Hercules, *J. Phys. Chem.* **80**, 1700 (1976).
[29] H. Topsøe, B.S. Clausen, R. Candia, C. Wivel and S. Mørup, *J. Catal.* **68,** 433 (1981).
[30] C. Wivel, R. Candia, B.S. Clausen, S. Mørup and H. Topsøe, *J. Catal.* **68**, 453 (1981).
[31] K.T. Ng and D.M. Hercules, *J. Phys. Chem.* **80**, 2094 (1976).
[32] L. Salvati Jr., L.E. Makovsky, J.M. Stencel, F.R. Brown and D.M. Hercules, *J. Phys. Chem.* **85**, 3700 (1981).
[33] C.P. Li and D.M. Hercules, *J. Phys. Chem.* **88**, 456 (1984).
[34] P. Arnoldy, J.A.M. van den Heijkant, G.D. de Bok and J.A. Moulijn, *J. Catal.* **92**, 35 (1985).
[35] R.G. Leliveld, A.J. van Dillen, J.W. Geus and D.C. Koningsberger, *J. Catal.* **165**, 184 (1997).
[36] R.G. Leliveld, A.J. van Dillen, J.W. Geus and D.C. Koningsberger, *J. Catal.* **171**, 115 (1997).
[37] M.J. Vissenberg, Ph.D. thesis, Eindhoven University of Technology, The Netherlands, 1999, chapter 7.
[38] J. Ramirez, L. Cedeno and G. Busca, *J. Catal.* **184**, 59 (1999).
[39] R. Thomas, E.M. van Oers, V.H.J. de Beer and J.A. Moulijn, *J. Catal.* **84**, 275 (1983).
[40] B. Scheffer, P. Arnoldy and J.A. Moulijn, *J. Catal.* **112**, 516 (1988).
[41] C.V. Caceres, J.L.G. Fierro, J. Lazaro, A. Lopez Agudo and J. Soria, *J. Catal.* **122**, 113 (1990).
[42] F.E. Massoth, G. Muralidhar and J. Shabtai, *J. Catal.* **85**, 53 (1984).
[43] N.K. Nag, *J. Phys. Chem.* **91**, 2324 (1987).
[44] J. Bachelier, J.C. Duchet and D. Cornet, *J. Catal.* **87**, 292 (1984).
[45] B. Scheffer, J.C.M. de Jonge, P. Arnoldy and J.A. Moulijn, *Bull. Soc. Chim. Belg.* **93**, 751 (1984).

[46] J. Grimblot, P. Dufresne, L. Gengembre and J.P. Bonnelle, *Bull. Soc. Chim. Belg.* **90**, 1261 (1981).
[47] P. Arnoldy, J.L. de Booys, B. Scheffer and J.A. Moulijn, *J. Catal.* **96**, 122 (1983).
[48] B. Scheffer, E.M. van Oers, P. Arnoldy, V.H.J. de Beer and J.A. Moulijn, *Appl. Catal.* **25**, 303 (1986).
[49] G. Kishan, L. Coulier, V.H.J. de Beer, J.A.R. van Veen and J.W. Niemantsverdriet, *J. Catal.* **196**, 180 (2000).
[50] H.R. Reinhoudt, E. Creeze, A.D. van Langeveld, P.J. Kooyman, J.A.R. van Veen and J.A. Moulijn, *J. Catal.* **196**, 315 (2000).
[51] G. Kishan, L. Coulier, J.A.R. van Veen and J.W. Niemantsverdriet, *J. Catal.* **200**, 194 (2001).
[52] R. Candia, O. Sørenson, J. Villadsen, N.-Y. Topsøe, B.S. Clausen and H. Topsøe, *Bull. Soc. Chim. Belg.* **93**, 763 (1984).
[53] H. Topsoe, R. Candia, N.-Y. Topsoe and B.S. Clausen, *Bull. Soc. Chim. Belg.* **93**, 783 (1984).
[54] S. Kasahara, T. Shimizu and M. Yamada, *Catal. Today* **35**, 59 (1997).
[55] E. Lecrenay, K. Sakanishi and I. Mochida, *Catal. Today* **39**, 13 (1997).
[56] E.J.M. Hensen, PhD-thesis, Eindhoven University of Technology, The Netherlands, 2000, Chapter 8.

9

Thiophene hydrodesulfurization: comparison of activities and kinetics on HDS model catalysts

Abstract

Thiophene hydrodesulfurization (HDS) activity measurements have been carried out on flat model systems of sulfidic HDS catalysts. A comparison of thiophene HDS activity of the four possible promoted systems on two different supports are shown. Comparing the thiophene HDS activity of various catalysts, it was concluded that intrinsically Ni is a better promoter than Co for both MoS_2 and WS_2. The promotion effect of Co and Ni was observed for all catalysts, except for the CoW combination. Chelating agents can increase the HDS activity for all systems, irrespective of support. The strongest enhancement due to chelating agents is found for Mo-based catalysts. However, these catalysts are very sensitive to deactivation at too high sulfidation temperatures. In general the thiophene HDS activity decreases in the order: NiMo ≥ NiW > CoMo > CoW ≥ W ~ Mo. The hydrogenation of butenes to butane is relatively higher for unpromoted catalysts, while W shows higher hydrogenation activity than Mo. Al_2O_3 is a better support for both HDS and hydrogenation than SiO_2.

Kinetic experiments over a broad temperature range (T-200-500 ^{0}C) show Volcano-behaviour for various catalysts, with a maximum in activity between 375-400 ^{0}C. Although this behaviour cannot be fully explained yet, it is concluded that a two-site reaction mechanism, where thiophene adsorbs on one site, in competition with H_2S, and hydrogen on a different site, can explain this Volcano-behaviour. The resulting negative value for the apparent activation energy (E_{act}^{app}) at high temperatures is only possible if the activation energy of the rate limiting step (E_{act}^{rds}) is exceeded by the adsorption energies of the adsorbed species in the rate determining step at high temperature (i.e. low coverages).

9.1 Introduction

As explained earlier in Chapter 1, commonly used catalysts for hydrotreating processes are Al_2O_3-supported metal sulfide catalysts. In industry CoMo sulfide catalysts are the preferred combination for hydrodesulfurization (HDS) reactions, while NiMo sulfide catalysts show better performance in hydrodenitrogenation (HDN) and hydrogenation (HYD) [1-4]. NiW sulfide catalysts have shown to be very promising in deep HDS, aromatic HYD and cracking [2-5]. CoW sulfide catalysts are not used due to their low activity for all reactions [3]. While literature confirms some of these trends, several contradictory results have been reported. For example, in most studies $NiMo/Al_2O_3$ is reported to be a better catalyst or at least equally active for HDS than $CoMo/Al_2O_3$, for both thiophene HDS and (substituted) benzothiophenes [e.g. 5-11].

Despite the enormous amount of literature on hydrotreating catalysts, only a few studies deal with the comparison of the activities of catalysts containing Mo and W promoted by Co and Ni on different supports [12,13]. Most authors study only one or two combinations in great detail and due to the large amounts of variables in preparation- (e.g. metal loading), pretreatment- (e.g. reduction- or sulfidation-mixture and temperature) and reaction-conditions (e.g. reacting molecule, temperature or pressure) it is difficult to compare the various results. Moreover, the various ways in which the reaction rate is expressed makes it even more difficult to compare the various catalysts.

Thiophene HDS is a standard test reaction for HDS. Although this is one of the simplest reactions there is still debate on both the kinetics and the mechanism of this reaction. Although there is agreement that the surface reaction between thiophene and hydrogen is the rate-determining step, both the mode of thiophene and hydrogen adsorption is still unclear. Another debate concerns the (inhibiting) role of H_2S.

A recent report by Leliveld et al. [14] proposes the presence of two kinds of active site for HDS, one at low and another at high temperature. It was already demonstrated that thiophene HDS and the subsequent hydrogenation to butane take place at different sites [15,16]. All these complicating factors are the cause that up to now no satisfying kinetic expression has been found to describe the thiophene HDS reaction over a broad temperature range. Most kinetic studies only focus on a particular catalyst and only a small temperature and pressure range is used. Especially high temperatures are troublesome for standard catalysts due to internal- and external-diffusion limitations.

In previous studies we studied the sulfidation of various HDS model catalysts on different supports with X-ray Photoelectron Spectroscopy (XPS) [17,18]. By combining these results with thiophene HDS activity measurements we were able to study the influence of e.g. chelating agents and metal-support interaction on the formation of the active phase.

In this chapter we will first compare the thiophene HDS activities of all HDS model catalysts supported on flat SiO_2 and Al_2O_3 model supports. We look at the influence of sulfidation temperature, chelating agents and support on the HDS activity of the various catalysts. Due to the non-porous structure of our model catalysts, internal- or external-diffusion limitations do not play a role. This allows us to measure the HDS activity over a broad temperature range. We will use this to study the kinetics of the thiophene reaction of various catalysts. The conclusion of this chapter is that our model catalyst approach can be very useful in the future for both kinetic and mechanistic research in hydrotreating reactions.

9.2 Experimental

For details on the preparation of the model catalysts we refer to earlier work [19,20]. Summarizing, the model catalysts consist of planar SiO_2 and Al_2O_3 supports. Subsequently, these model supports were spincoated at 2800 rpm in N_2 with aqueous solutions containing the required precursors (i.e. Co, Ni, Mo and/or W). The concentrations of Co(Ni) and Mo(W) solutions were adjusted to result in the required (2 or 4 Co(Ni) at/nm^2 and 6 Mo(W) at/nm^2). Catalysts containing chelating agents were prepared by spincoating a solution containing both the required precursors and the chelating agent, as described by Van Veen et al. [21]. Part of the catalysts were calcined in 20% O_2/Ar for 30 min with 5 ^{0}C/min to the desired temperature.

Thiophene HDS activity measurements were carried out at atmospheric pressure in 4% thiophene/H_2. The catalysts were presulfided in 10% H_2S/H_2 at a heating rate of 5 ^{0}C/min (chelating agents 2 ^{0}C/min) to the desired temperature and kept there for 30 min. For the standard activity measurements the reaction temperature was 400 ^{0}C and reaction was carried out in batch mode. In the batch mode, after sulfidation the reactor was flushed with 4% thiophene/H_2 for 5 min. After that the reactor was closed and the reaction time started. After 1 hour a sample was taken from the reactor with a syringe and the products were analyzed by GC. The activity is expressed as total conversion of thiophene (%) after 1 hour of batch reaction per 5 cm^2 of catalysts and corrected for blank measurements.

For the kinetic measurements, the same procedure as described above was carried out. However, after reaction at a certain temperature the reactor was flushed with 4% thiophene/H_2 and cooled down or heated up to the next temperature.

Flow measurements were carried out in a flow of 100 Nml/min of 4% thiophene/H_2 and samples were taken with an automatic GC-sampler. While the conversions were low (<1 %), the reaction rate could be calculated using a differential packed-bed reactor.

9.3 Results

9.3.1 Comparison of the HDS activity and hydrogenation (HYD) selectivity

Figure 9.1 shows the thiophene HDS activity of SiO_2-supported CoMo, NiMo, CoW and NiW model catalysts sulfided at 400 ^{0}C as a function of Co(Ni)/Mo(W) atomic ratio. For the Ni-promoted catalysts the presence of Ni increases the HDS activity significantly, while for Co-promoted catalysts the enhancement is less. Especially for CoW/SiO_2 the effect of Co on the HDS activity is marginally. In fact, in an earlier paper we showed that the lumped activity of W/SiO_2 and Co/SiO_2 is equal to the activity of CoW/SiO_2 [22]. For all other catalysts the HDS activity increases with increasing Co(Ni)/Mo(W) atomic ratio. Interestingly, the optimum ratio for Mo-based catalysts is 0.33 while for W-based catalysts the optimum ratio is 0.66. Due to different optimum Co(Ni)/Mo(W) ratios one should be careful when comparing activities between catalysts. For ratios of 0.33 the HDS activity increases in the order CoMo ~ CoW < NiMo ~ NiW, while for a ratio of 0.66 the order is CoMo < CoW < NiMo < NiW. In the following we only compare the HDS activities of catalysts with optimum Co(Ni/Mo(W) ratios.

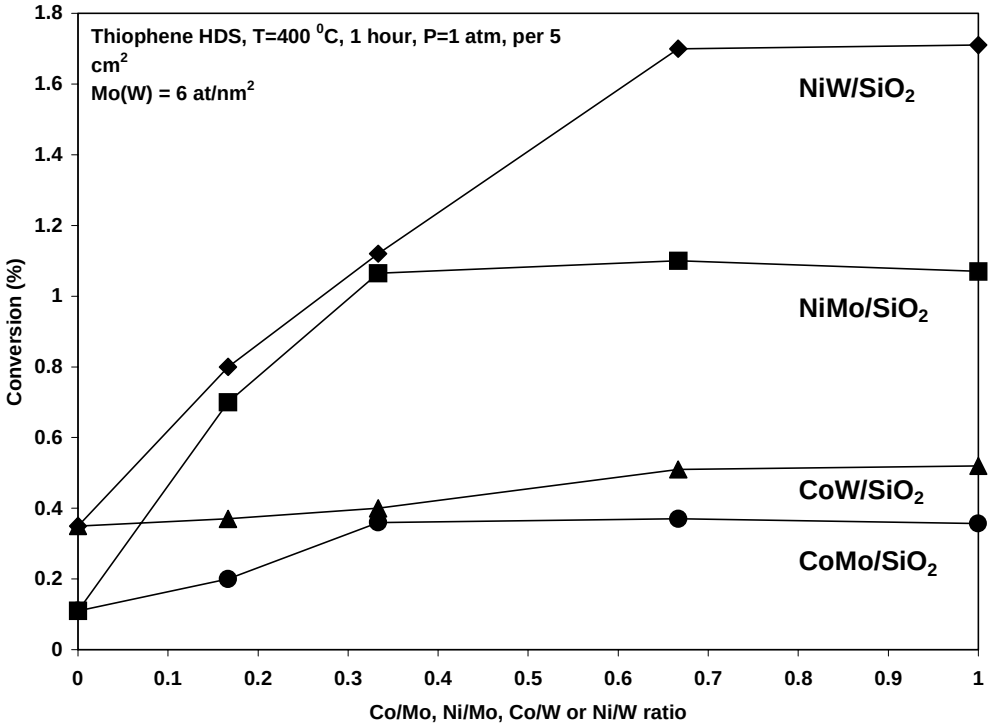

Figure 9.1 *Thiophene HDS activity of SiO_2-supported model catalysts as a function of promoter loading.*

The promotion factors, i.e. activity of promoted catalysts divided by that of the unpromoted catalysts (Mo or W), for the catalysts with optimum ratios are shown in Table 9.1. The promotion factor increases in the order CoW < CoMo < NiW < NiMo. The HDS activity increases, however, in the order CoMo < CoW < NiMo < NiW (see Figure 9.1). This difference between activity and promotion effect is mainly due to the strikingly low activity of Mo/SiO_2 compared to W/SiO_2. As a result the promotion effect of Co or Ni on Mo/SiO_2 is large although the total activity is still lower than that of W-based catalysts.

The thiophene HDS activity after 1 hour of batch reaction at 400 ^{0}C of various HDS model catalysts supported on SiO_2 and Al_2O_3, the latter either uncalcined or calcined at 400 ^{0}C, with optimum Co(Ni)/Mo(W) ratio and sulfided at 400 ^{0}C are shown in Figure 9.2. The activity is expressed as conversion (%) of thiophene after 1 hour per 5 cm^2 of catalysts. For catalysts containing CyDTA, the amount of chelating agents is adjusted to complex both Co(Ni) and Mo. W did not form complexes with CyDTA. A few observations can be made from Figure 9.2. First, Ni-promoted catalysts show higher activity than Co-promoted catalysts. Furthermore, Al_2O_3-supported catalysts show higher HDS activities compared to SiO_2-supported catalysts, except for catalysts containing CyDTA, that show equal HDS activity for Al_2O_3- and SiO_2-supports. For the standard catalysts the HDS activity increases in the order CoMo ~ CoW < NiMo ≤ NiW. However for catalysts containing CyDTA, the HDS activity increases in the order CoWCyDTA < CoMoCyDTA < NiWCyDTA < NiMoCyDTA. For all catalysts the CyDTA-containing catalysts show the highest HDS activity.

Table 9.1 *Promotion factors of SiO_2- and Al_2O_3-supported Mo- and W-based HDS model catalysts.*

	CoW	CoWCyDTA	NiW	NiWCyDTA
SiO_2	1.5	2.6	5.3	10.8
Al_2O_3	1.7	2.6	7.3	10.0

	CoMo	CoMoCyDTA	NiMo	NiMoCyDTA
SiO_2	3.3	20.5	9.7	60.0
Al_2O_3	2.0	6.0	7.7	17.9

Table 9.1 shows the promotion factors of SiO_2- and Al_2O_3-supported catalysts with and without CyDTA. The presence of CyDTA especially increases the activity of SiO_2-supported Mo-based catalysts. This can be also observed from Table 9.2, that shows the enhancement of HDS activity due to the presence of CyDTA, i.e. activity of catalysts with CyDTA divided by the activity of catalysts without CyDTA. The table shows that CyDTA increases the activity of Mo-based catalysts supported on SiO_2 with a factor 6, while for W-based catalysts an increase with only a factor 2 is observed. As stated earlier, the activity of Mo/SiO_2 is very low. As a result the promotion factors of $CoMoCyDTA/SiO_2$ and $NiMoCyDTA/SiO_2$ are very high, i.e. 20 and 60 respectively.

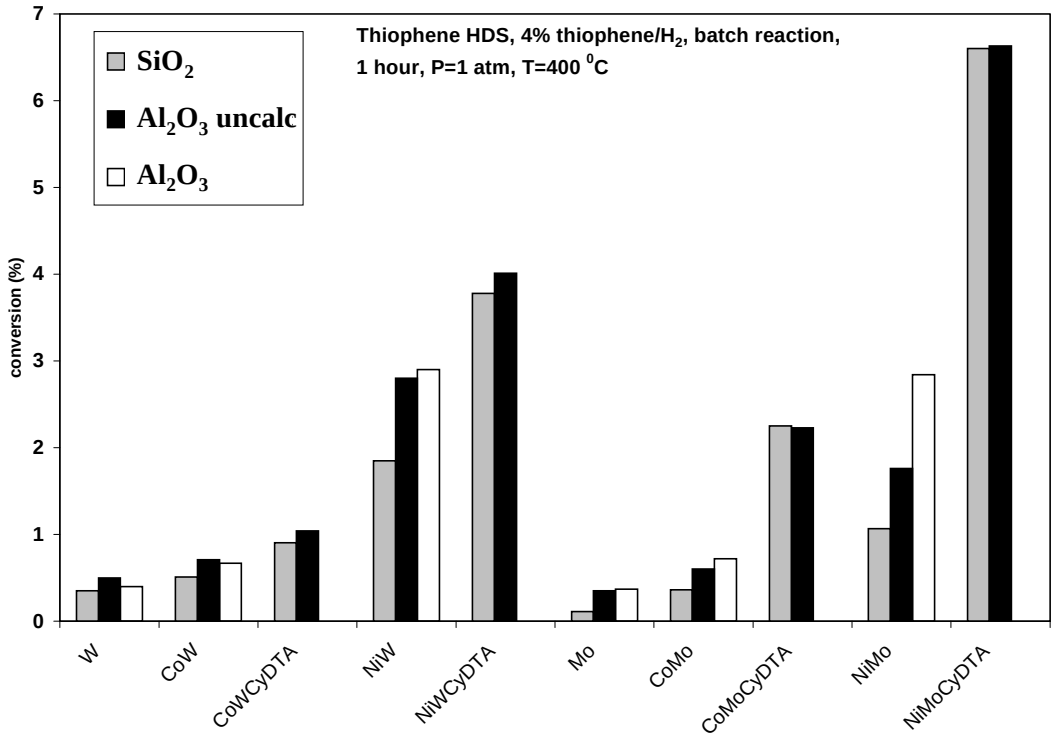

Figure 9.2 *Comparison of the thiophene HDS activity of various SiO_2- and Al_2O_3-supported model catalysts presulfided at 400 ^{0}C.*

Table 9.2 *Enhancement of HDS activity due to CyDTA for different HDS model catalysts.*

	CoWCyDTA	NiWCyDTA	CoMoCyDTA	NiMoCyDTA
SiO_2	1.8	2.0	6.3	6.2
Al_2O_3	1.6	1.4	3.1	2.3

Al_2O_3-based catalysts prepared without CyDTA show generally higher HDS activities than SiO_2-supported catalysts. Although for W and CoW the difference is only small between the two supports, Al_2O_3-supported Mo, CoMo, NiMo and NiW catalysts are around twice as active as their SiO_2-supported counterparts (see Figure 9.2). As a result the promotion factors also differ between SiO_2- and Al_2O_3-supported catalysts. For example, due to the higher activity of Al_2O_3-supported catalysts and the fact that catalysts containing CyDTA show high activities irrespective of support, the enhancement of HDS activity due to the presence of CyDTA, as shown in Table 9.2, is significantly lower than for SiO_2-supported catalysts. The same is observed for the promotion factors in Table 9.1. Especially due to the relatively high activity of Mo/Al_2O_3 the promotion factors of Mo-based catalysts are much lower.

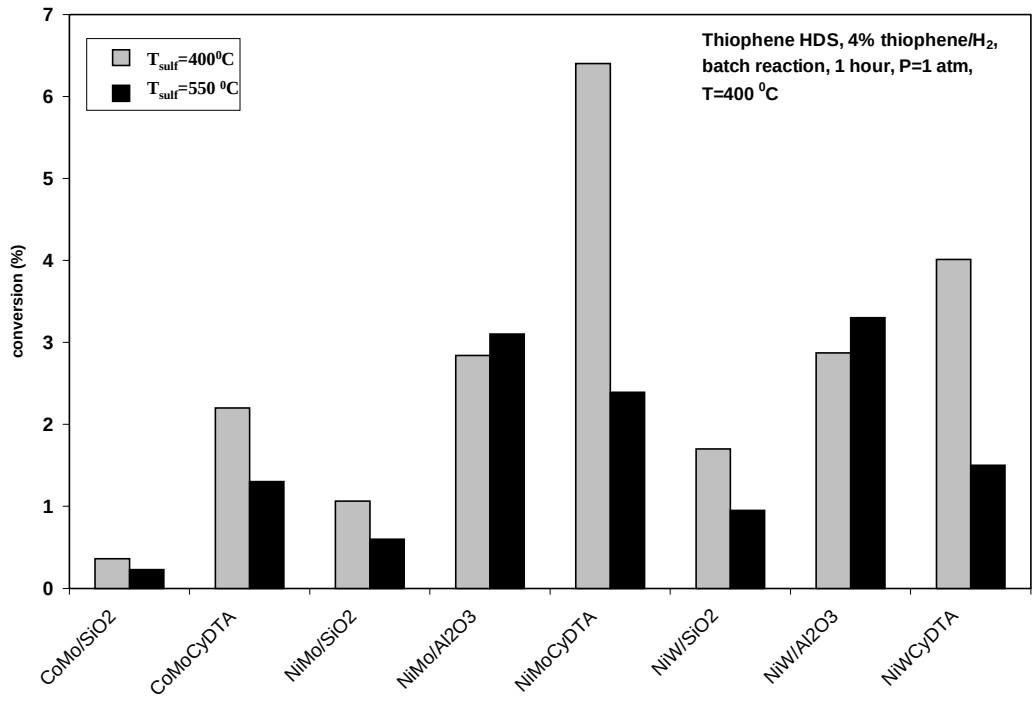

Figure 9.3 *Influence of the sulfidation temperature on the thiophene HDS activity at 400 ^0C of different HDS model catalysts.*

The influence of calcination on the HDS activity of Al_2O_3-supported catalysts is also shown in Figure 9.2. For W and CoW catalysts the activity slightly decreases due to calcination, while NiW show slightly higher HDS activity. Calcination increases the HDS activity of $NiMo/Al_2O_3$ by a factor 2 and a smaller increase for Mo and CoMo catalysts.

Table 9.3 *HDS activity and hydrogenation (HYD) selectivity of various Al_2O_3-supported HDS model catalysts.*

	HDS (%)	HYD (n-butane/products)
W	0.4	0.09
NiW	2.9	0.03
NiWCyDTA	4.01	0.02
Mo	0.37	0.04
CoMo	0.72	0.01
NiMo	2.84	0.02
NiMoCyDTA	6.63	0.01

The hydrogenation (HYD) selectivity, expressed as yield of n-butane divided by total yield of C_4-products, of various Al_2O_3-supported catalysts are shown in Table 9.3, together with the HDS activity of these catalysts. While the conversions in our activity experiments are low, i.e. <7 %, the amount of n-butane is also very low. For SiO_2-supported catalysts n-butane is sometimes present, but only in trace amounts. Table 9.3 shows that hydrogenation to butane is more facile on unpromoted catalysts, while W-based catalysts are also more active in hydrogenation than Mo-based catalysts. CyDTA-containing catalysts show somewhat lower hydrogenation selectivity and the same accounts for Co-promoted catalysts compared to Ni-promoted catalysts.

The influence of sulfidation temperature on the thiophene HDS activity is shown in Figure 9.3. It is seen that a higher sulfidation temperature has a dramatic influence on the trends in activity. Both SiO_2-supported catalysts and catalysts containing CyDTA show a strong decrease in activity for high sulfidation temperatures. Especially CyDTA-containing catalysts show a dramatic decrease in activity. However, Al_2O_3-supported catalysts show a small increase in activity at higher sulfidation temperatures. As a result, at higher sulfidation temperatures CyDTA-containing catalysts are no longer the most active catalysts and thus the positive effect of using chelating agents to increase the HDS activity is disappeared.

9.3.2 Kinetics of thiophene HDS: temperature dependence

As described in the experimental section, kinetic measurements are carried out in a broad temperature range, i.e. 200-500 ^{0}C. The HDS activities of the catalysts at a certain reaction temperature are expressed as conversion of thiophene per 1 hour of batch reaction per 5 cm^2 of catalysts. The main products are 1-butene, c-2-butene, t-2-butene and traces of n-butane. The catalysts are first sulfided to the desired temperature and then exposed to the thiophene/H_2 mixture at various temperatures.

Due to the absence of pores, internal diffusion limitations do not play a role. Calculating the so-called Damköhler number (Da) for our reaction conditions and assuming a first order reaction a value of Da ~ $4 \cdot 10^{-4}$ indicates that external (=film) diffusion from the bulk phase to the catalysts surface does also not play a role in our kinetic experiments [23]. Hence we can conclude that we are looking at intrinsic kinetics.

An example of such a kinetic experiment is shown in Figure 9.4. In this figure the conversion is plotted against the reaction temperature for two catalysts, i.e. NiMo/SiO_2

sulfided at 400 ^{0}C and 500 ^{0}C, respectively. As can be seen the conversion for $NiMo/SiO_2$ sulfided at 500 ^{0}C is near to zero around 200 ^{0}C and increases strongly at higher temperatures. The activity goes through a maximum around 400 ^{0}C and decreases gradually at higher temperatures. This curve, which has the characteristics of a Volcano-curve, was proposed by Sabatier for heterogeneous catalytic reactions. The reaction temperatures are taken in random order and no hysteresis is observed. $NiMo/SiO_2$ sulfided at 400 ^{0}C shows a total different behaviour. Starting the reaction at 200 ^{0}C, after sulfidation at 400 ^{0}C, the activity increases up to a temperature of 400 ^{0}C and then decreases rapidly at high temperatures. Going back to lower temperatures a different trend is observed: the activity decreases slowly but gradually to zero around 250 ^{0}C. A clear hysteresis is thus observed in this case.

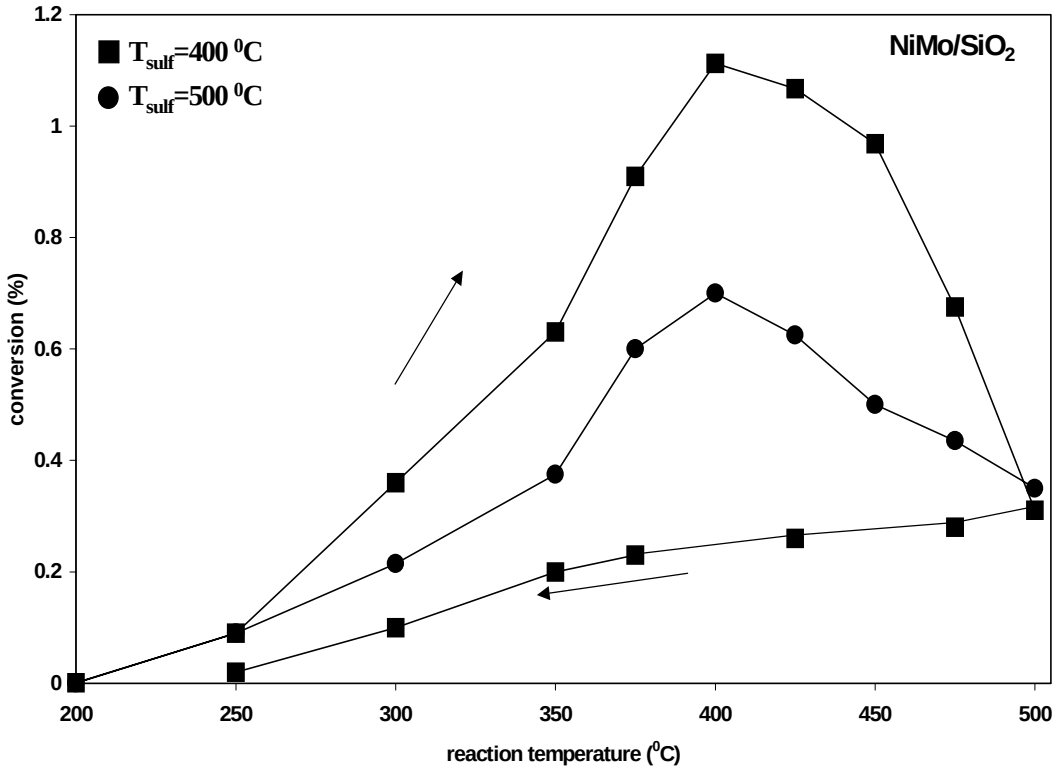

Figure 9.4 *Thiophene HDS activity of $NiMo/SiO_2$ as a function of reaction temperature for different sulfidation temperatures.*

Figure 9.5 shows the same activity-temperature plots as Figure 9.4, but now for three different catalysts, i.e. $CoMo/SiO_2$, $NiMo/SiO_2$ and NiW/SiO_2, all sulfided at 500 ^{0}C. Although the activity increases in the order $CoMo/SiO_2 < NiMo/SiO_2 < NiW/SiO_2$, the same activity trend as function of temperature is observed as described above for NiMo. For all catalysts the maximum lies around 400 ^{0}C. Due to the relatively large steps in temperature, it not possible to find the exact temperature where the maximum in activity is. Note that the curves as observed in Figure 9.5 are only present if after sulfidation at 500 ^{0}C, the catalysts are first subjected to thiophene HDS at 500 ^{0}C and then at lower temperatures. Thus, Volcano-curve behaviour is observed only after a stabilization period at the highest temperature but is present irrespective of catalyst composition. Catalysts containing chelating

agents show deviating behaviour (not shown). If these catalysts are sulfided at 400 ^{0}C the activity vs. temperature plot shows behaviour similar to that in Figure 9.4 and 9.5 up to temperatures of 400 ^{0}C. However, sulfidation at higher temperatures leads to a large decrease in activity, as observed in Figure 9.3, and activity measurements at other temperatures show irregular and irreproducible behaviour.

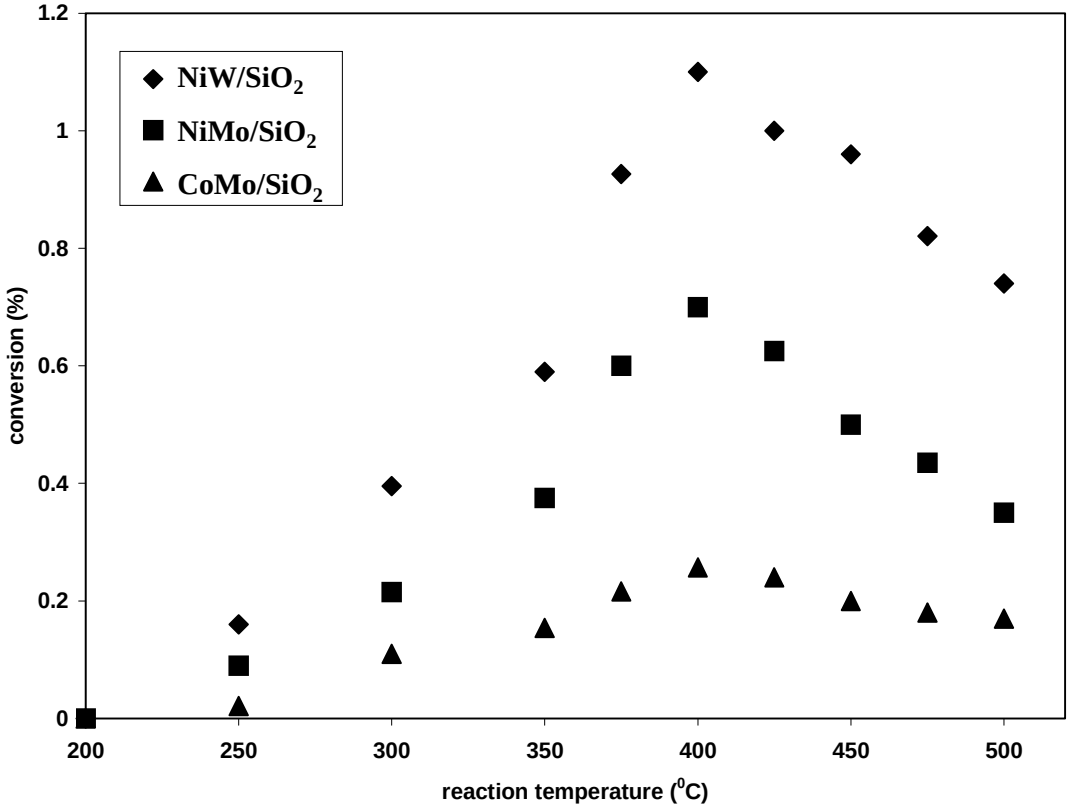

Figure 9.5 *Volcano-curves of $CoMo/SiO_2$, $NiMo/SiO_2$ and NiW/SiO_2 model catalysts, presulfided at 500 ^{0}C, for the thiophene HDS reaction.*

Table 9.4 *Activation energies (in kJ/mol) from Arrhenius plots of various HDS model catalysts.*

	T_{sulf} (^{0}C)	E_{act}^{app} (kJ/mol) 200-300 ^{0}C	E_{act}^{app} (kJ/mol) 300-400 ^{0}C
$CoMo/SiO_2$	400	90	30
$CoMo/SiO_2$	500	85	27
$CoMoEDTA/SiO_2$	400	114	49
$NiMo/SiO_2$	400	114	32
$NiMo/SiO_2$	500	109	34
$NiMoEDTA/SiO_2$	400	130	72
NiW/SiO_2	400	118	44
NiW/SiO_2	500	111	29

From the activity vs. temperature plots it is possible to construct Arrhenius plots. Assuming a Langmuir-Hinshelwood model for the thiophene reaction and pseudo-first order in thiophene, one can plot for a differential reactor ln r vs. 1/T and obtain curves with slopes of $-E_a/R$. Figure 9.6 shows the Arrhenius plots for two model catalysts, i.e. $CoMo/SiO_2$ and $CoMoEDTA/SiO_2$, from 200 to 400 ^{0}C. The figure shows the same trend for both catalysts: a slow decrease for low values of 1/T followed by a sharp decrease around 0.0018 K^{-1} or 275 ^{0}C. This change in slope is clearly demonstrated by the values of E_{act}^{app} in Figure 9.6. At high values of 1/T (i.e. low temperatures) E_{act}^{app} is 90 and 114 kJ/mol for $CoMo/SiO_2$ and $CoMoEDTA/SiO_2$, respectively, while at low values of 1/T (i.e. high temperatures) E_a is 30 and 49 kJ/mol, respectively. Note that E_{act}^{app} represents the *apparent* activation energy and not the activation energy of the rate-determining step (E_{act}^{rds}). Table 9.4 shows the kinetic parameters of other catalysts studied. In general, catalysts showing high activity have high values for E_{act}^{app}. At high reaction temperatures, where the conversion decreased with increasing temperature as shown in Figure 9.4 and 9.5, the plot of ln r and 1/T leads to negative values of E_{act}^{app}. In the discussion we try to explain this Volcano-behaviour.

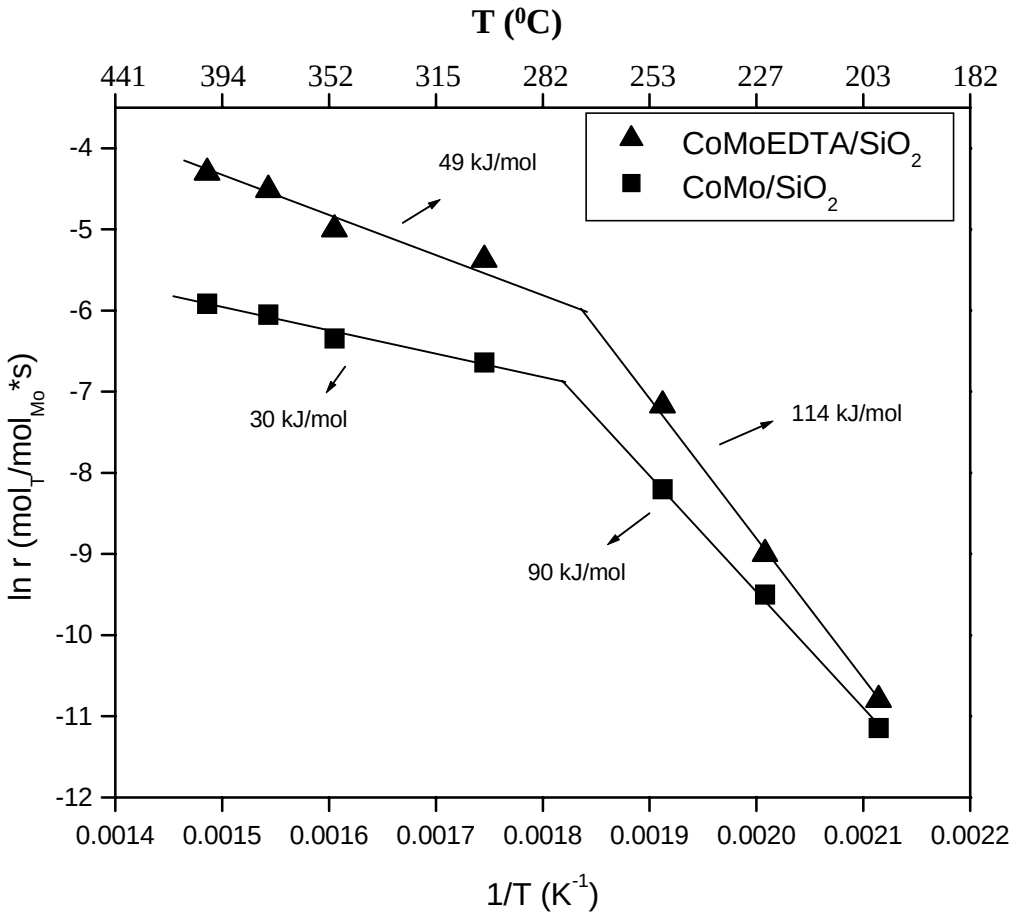

Figure 9.6 *Arrhenius plots for two $CoMo/SiO_2$ catalysts sulfided at 400 ^{0}C.*

9.4 Discussion

On the promotional effect in HDS catalysts

We have presented an overview of thiophene HDS activities of Co- and Ni-promoted Mo and W catalysts supported on different supports. All catalysts are prepared and pretreated in the same way and thus can be compared straightforward.

Figure 9.1 shows that the promotion effect is different for Mo- and W-based catalysts. While for Mo-based catalysts the optimum Co(Ni)/Mo atomic ratio is 0.33, this ratio is significantly higher for W-based catalysts, i.e. 0.66. The same is observed for other supports. These results correspond well with reports by Scheffer et al. [24] and Vissenberg et al. [13] on high surface area catalysts. The lateral dimensions of MoS_2 and WS_2 slabs will not differ very much, hence the difference in optimum promoter amount is not due to higher promoter capacity of WS_2 compared MoS_2. If all Co or Ni atoms would sit on the edges of either MoS_2 or WS_2, a ratio of 0.33 would be almost enough to fill all edge positions [2]. We ascribe the different promoter amounts to a higher affinity of Co and Ni atoms to sit on the edges of MoS_2 than on WS_2. This means that it more difficult to put promoter atoms on the edges of WS_2 and a larger amount is necessary to make sure that some of the atoms sit on the edges of WS_2.

The support has a strong effect on the HDS activity (see Figure 9.2). In general, Al_2O_3-supported catalysts show higher HDS activities than SiO_2-supported catalysts, while calcination at 400 ^{0}C increases the HDS activity for all promoted catalysts except CoW. In earlier papers we concluded that both TiO_2 and Al_2O_3 show strong interactions with Co, Ni, Mo and W [17,18]. This strong interaction could be enhanced by calcination. Due to the strong interaction with these supports the dispersion higher and the sulfidation rate slower compared to SiO_2. However, SiO_2 shows only weak interactions and hence sulfidation is fast and sintering is much more likely on these systems. The effect of the support on the HDS activity corresponds well with results of Muralidhar et al. [25] and Medici et al. [26] who also find significantly higher HDS activities for Al_2O_3-supported catalysts compared to SiO_2-supported catalysts. However, earlier reports by Konings et al. [27] and Yermakov et al. [28] reported equal activity for Al_2O_3- and SiO_2-supported NiMo and NiW catalysts. The effect of calcination on the HDS activity of W-based catalysts is confirmed by others [13,29]. Our results show a clear and consistent picture and hence we conclude that Al_2O_3 is a better support for active phase formation than SiO_2 for CoMo, NiMo and NiW catalysts and that calcination at 400 ^{0}C increases the HDS activity to a certain extent.

The influence of support interaction becomes even more distinct at higher sulfidation temperatures as can be seen in Figure 9.3. The thiophene HDS activity of SiO_2-supported catalysts decreases with almost a factor 2 after sulfidation at 550 ^{0}C, while the HDS activity of Al_2O_3-supported catalysts increases slightly after sulfidation at high temperature. We explain the loss of activity for SiO_2-supported catalysts by loss of dispersion due to segregation of the active phase at high sulfidation temperature due to a weak support interaction. This in contrast with for Al_2O_3-supported catalysts which have a strong interaction with the support and even show a small increase in activity after sulfidation at high temperature.

The interaction with the support has also a strong influence on the order in HDS activity. For example, the HDS activity for SiO_2-supported catalysts increases in the order

Mo < W < CoMo < CoW < NiMo < NiW, while for calcined Al_2O_3-supported catalysts the HDS activity increases in the order Mo ~ W < CoW ≤ CoMo < NiMo ~ NiW (see Figure 9.2). Higher sulfidation temperatures do not change this pattern (see Figure 9.3). This order in activity is at first sight totally different from that of commercial catalysts for HDS. Generally, CoMo is the preferred catalyst for HDS followed by NiMo and NiW, respectively [3,4]. However, in industrial applications reactions are carried out at high pressure and in liquid phase and this can easily explain the differences. For thiophene HDS contradictory results are reported [7,11,24,27,28]. Difference in preparation conditions and metal loadings may explain the contradictory results. However, we conclude that our model catalysts, which are all prepared in the same way and have the same Mo or W loading, give a consistent picture for both SiO_2- and Al_2O_3-supported catalysts and the differences can be explained by XPS results as reported in earlier papers [17,18].

The results in Table 9.3 showed besides the HDS activity also the hydrogenation (HYD) selectivity for the hydrogenation of butenes to butane. We can conclude from this that Ni is also a better promoter for HYD, although unpromoted catalysts show relatively the highest HYD selectivity. Furthermore, W-based catalysts show higher HYD selectivity than Mo-based catalysts. From the absence of butane as product for SiO_2-supported catalysts we can also conclude that Al_2O_3 is a better support for both HDS and HYD.

In earlier papers we described extensively the beneficial influence of chelating agents on the sulfidation and HDS activity of HDS model catalysts [19,20]. It is seen in Figure 9.2 that CyDTA increases the HDS activity for all catalysts and the activity is equal for SiO_2- and Al_2O_3-supported catalysts. The latter was also concluded in an earlier paper where also TiO_2-supported catalysts showed equal activity [18]. We explain this by the complexation of both Co (or Ni) and Mo to the chelating agents thereby preventing any interaction with the support. The support acts thus as an inert substrate and hence there is no difference in activity between the different supports. We reported earlier that the key step in active phase formation is the retardation of the sulfidation of Co and Ni to temperature where Mo and W are already completely sulfided. For Mo-based catalysts this was possible but due to the slow sulfidation of W complete separation of the sulfidation of Co or Ni and W was not possible and hence the chance of Co and Ni to sulfide in the presence of WS_2 is smaller than for Mo-catalysts [22,31]. This explains the larger enhancement of HDS activity for Mo-based catalysts containing CyDTA compared to W-based catalysts, as observed in Table 9.2. As a result of the difference in increase of activity due to CyDTA, the HDS activity now increases in the order: CoW < CoMo < NiW < NiMo.

The conclusion that chelating agents, like CyDTA, increase the HDS activity of all promoted SiO_2- and Al_2O_3-supported catalysts only holds for low sulfidation temperatures. Figure 9.3 shows that higher sulfidation temperatures, i.e. 550 ^{0}C, leads to a dramatic decrease in HDS activity for all catalysts containing CyDTA, irrespective of support. As a result, these catalysts do not show the highest activity. We observed this effect earlier for NiWCyDTA/Al_2O_3, where we concluded from XPS that segregation of the active phase takes place at high sulfidation temperature [17]. It is also observed that catalysts containing chelating agents are very sensitive to calcination [10]. Hence we have to adjust our conclusion by stating that although catalysts containing chelating agents show the highest HDS activity for all systems, irrespective of support, these catalysts are very sensitive to e.g. high sulfidation temperatures, which leads to segregation of the active phase.

Comparing the HDS activities of the various catalysts, it is concluded that Ni-promoted catalysts show higher thiophene HDS activities than Co-promoted catalysts (see Figure 9.2). This effect can also be clearly seen from the promotion factors in Table 9.1. This is in contradiction with commercial applications where Co is the preferred promoter [1-4], although in HDS literature several groups report the superiority of Ni as a promoter for thiophene HDS [6,10,11,24]. However, it is also reported that Ni is more susceptible to inhibition by H_2S than Co and thus CoMo is more active at high H_2S partial pressures [8,9,30]. However, in standard reaction conditions used in literature the H_2S partial pressures are low, as in our case, while for commercial applications these values are much higher. Furthermore, in industrial applications reactions are carried out at high pressures and in the liquid phase. These different conditions can explain the superiority of Co as promoter in industrial HDS catalysts.

However, it is still unclear whether this is due to differences in intrinsic activity or different amounts of promoter in the active phase. We have shown in an earlier paper that for e.g. CoMoEDTA and NiMoEDTA catalysts it was possible to sulfide Mo completely before Co or Ni [18,20]. For CyDTA the same effect is observed. From this order in sulfidation we concluded that all Co and Ni atoms sulfide in the presence of MoS_2 and hence Co and Ni are able to find the edges of MoS_2 thereby forming CoMoS or NiMoS. As a result these catalysts should contain 100% CoMoS and NiMoS. If this is true than the activity results in Figure 9.2 imply that Ni is an intrinsically better promoter than Co under the present conditions.

Thiophene HDS kinetics: Volcano-curve behaviour

The kinetic experiments in Figure 9.4 and 9.5 show a maximum in the thiophene HDS activity as function of reaction temperature. As explained earlier, reversible This is observed only for conventionally prepared catalysts sulfided at 500 ^{0}C and if the first activity measurement was done at 500 ^{0}C. From this we conclude that the catalyst needs a stabilization period at high temperatures before the kinetic experiments can be carried out without any structural rearrangement. This behaviour is observed for various catalysts, i.e. NiW, NiMo and CoMo, showing the similarity of these systems. The temperature where the maximum in activity is found is roughly between 375-400 ^{0}C. Activity data at smaller temperature intervals are necessary to find the exact optimum temperature and to see if the three systems in Figure 9.5 show exactly the same behaviour. The data in Figure 9.5 have been carried out in random order and all catalysts have been sulfided at 500 ^{0}C and reacted at 500 ^{0}C first. Hence we exclude thermal sintering or changes in dispersion being the cause of the trend in HDS activity as function of temperature.

The curve in Figure 9.5 can be seen as a Volcano-curve, although normally a Volcano-curve is plotted as reaction rate vs. heat of adsorption of the majority reacting intermediate. However both can be explained by Sabatier's principle. At low temperatures the surface is completely covered with adsorbed species, i.e. thiophene and hydrogen. These species are strongly bonded and hence the reaction rate is low. With increasing temperature the reaction between the surface species becomes more likely and thus the reaction rate increases. However at high temperatures it is difficult for species to adsorb, hence the surface is almost empty. As a result the reaction rate decreases again. Thus there is an optimum situation for which the reaction rate reaches a maximum.

Only one report is known in literature where kinetic measurements are carried out at high temperatures. Leliveld et al. [14] studied the thiophene HDS reaction on porous $CoMo/Al_2O_3$. These authors found an increase in HDS activity for temperatures up to 350 ^{0}C. At somewhat higher temperatures a local maximum was observed but at even higher temperatures the activity increased again up to 500 ^{0}C. Descending temperatures showed a hysteresis and no maximum was observed. The increase in HDS activity at high temperatures was explained by a second type of active site [14]. This is in clear contrast to the results shown in this chapter. However, we have no explanation at this moment for these contradictory results.

Figure 9.4 shows very different behaviour for catalysts sulfided at 400 ^{0}C. After initial sulfidation at 400 ^{0}C the HDS activity increases with increasing temperature from 200 to 400 ^{0}C. At higher temperatures the activity decreases sharply. This sharp decrease in activity is attributed to structural differences of the catalysts, while the catalysts has not been pretreated to temperatures higher than 400 ^{0}C in these experiments. The most remarkable observation is the trend in activity with descending temperatures. This shows no maximum in activity. One would expect that despite some sintering due to the high reaction temperatures, the activity should show an optimum in activity with decreasing temperature, be it at lower conversion. At this moment we cannot explain this behaviour. Note that this is the result of only one measurement and more measurements have to be carried out to exclude any experimental errors.

Most kinetic studies use a rather small temperature range and only one type of catalyst. Usually low temperatures, i.e. up to 400 ^{0}C, are used for these kinetic studies in order to exclude internal and external diffusion limitations and to obtain the activation energy of the rate determining step (E_{act}^{rds}). From these studies it is more or less clear that a kinetic expression can be derived taking the surface reaction between adsorbed thiophene and adsorbed hydrogen as the rate-determining step, competition between adsorbed thiophene and H_2S at one site and adsorbed hydrogen on another site. Note that some authors claim that also S removal can be the rate-determining step [32,33]. However, Kasztelan [34] concluded that a Volcano curve could only be obtained when the surface reaction is the rate-determining step involving two sites. The reaction rate (r) can then be expressed as, according to Lee and Butt [35] and Massoth [36]:

$$r = k \frac{K_T \cdot p_T}{(1 + K_T \cdot p_T + K_S \cdot p_S)} \cdot \frac{K_H \cdot p_H}{(1 + K_H \cdot p_H)} \tag{9.1}$$

Neglecting the (inhibiting) effect of H_2S because of the very low conversions and thus the very low H_2S partial pressure, the expression is even more simplified:

$$r = k \frac{K_T K_H p_T p_H}{(1 + K_T p_T)(1 + K_H p_H)} \tag{9.2}$$

with:

k:	the reaction rate constant
K_T,K_H,K_S:	the adsorption constant of thiophene (T), hydrogen (H) and H_2S (S)
p_T,p_H,p_S:	partial pressure of thiophene, hydrogen and H_2S

When k has Arrhenius-type behaviour and can be considered independent of surface coverage one can calculate the apparent activation energy by:

$$E_{act}^{app} = -R_g \cdot \frac{\partial \ln r}{\partial T^{-1}} = E_{act}^{rds} + (1-\Theta_T^{\#}) \cdot \Delta H_{ads}^{T} + (1-\Theta_H^{*}) \cdot \Delta H_{ads}^{H} \qquad (9.3)$$

with:

E_{act}^{app}:	apparent activation energy
R_g:	gas constant
T:	temperature
E_{act}^{rds}:	activation energy rate determining step
Θ_T:	surface coverage by thiophene on site #
ΔH_{ads}^{T}:	heat of adsorption of thiophene
Θ_H:	surface coverage by hydrogen on site *
ΔH_{ads}^{H}:	heat of adsorption of hydrogen

At low temperatures, the coverages of both thiophene and hydrogen are high ($\theta \sim 1$) and hence the apparent activation energy equals the activation energy of the rate determining step. However at high temperatures, the coverages are very low ($\theta \sim 0$). As a result the apparent activation energy (E_{act}^{app}) equals:

$$E_{act}^{app} = E_{act}^{rds} + \Delta H_{ads}^{T} + \Delta H_{ads}^{H} \qquad (9.4)$$

In this case the value of E_{act}^{app} depends not only on the true activation energy (E_{act}^{rds}) but also on the adsorption energy of thiophene (ΔH_T) and hydrogen (ΔH_H). This coverage dependence of the apparent activation energy explains the decrease in E_{act}^{app} with increasing temperature (θ: $1 \rightarrow 0$) as observed in Figure 9.6 and Table 9.4. This behaviour has also been observed for high surface area catalysts [14,33,37].

The absence of reliable values for activation energies and especially adsorption constants makes it very difficult to justify the Arrhenius plots with the model described above. Because apparent activation energies are highly temperature dependent it is difficult to compare the different values reported in literature [14,33]. However, heats of adsorption are not temperature dependent and should therefore be constant. Despite this a broad range of values have been reported for the heats of adsorption of e.g. thiophene and hydrogen deduced from both experiments and theory. For example, Lee and Butt [35] find a heat of adsorption for thiophene of -50 kJ/mol while Satterfield and Roberts [38] report a value of about -75 to -100 kJ/mol. Theoretical values calculated by Neurock and van Santen [32] vary between -62 and -137 kJ/mol. This demonstrates clearly the inconsistency of the kinetic parameters reported in the literature.

However, equation (9.3) and (9.4) can explain Arrhenius plots as shown in Figure 9.6. Note that when a catalyst shows a Volcano-curve, as a result the Arrhenius plots continue at lower values of 1/T (i.e. higher T) with a negative slope. In this temperature regime the apparent activation energy has thus a negative value. The decrease in activity at high temperature implies a negative slope in the Arrhenius plots and hence a negative value for

E_{act}^{app} (see Figure 9.6). From equation (9.4) it follows that a negative value for E_{act}^{app} is only possible if $-(\Delta H_T+\Delta H_H) > E_{act}^{rds}$. This was already proposed by Leglise et al. [39]. Taking the kinetic parameters of Leglise et al. [39] it is possible to obtain a negative value for E_{act}^{app} at high reaction temperatures. However the enormous spreading of kinetic parameters in literature implies that one should be careful drawing conclusions based on these parameters. Note that in the above the role of H_2S is neglected and a simplified empirical kinetic expression is used. Further research is necessary to get more precise information, on e.g. the reaction orders of the various reactants, in order to obtain the kinetic expression of thiophene HDS based on elementary steps.

9.5 Conclusions

For the first time a complete comparison of the thiophene HDS activity of all four known systems, i.e. CoMo, NiMo, NiW and CoW, supported on two supports, i.e. SiO_2 and Al_2O_3, is reported. From this comparison we conclude that Ni is intrinsically a better promoter than Co for thiophene HDS under the present reaction conditions. The optimum promoter loading is different for Mo- and W-based catalysts. For Mo-based catalysts an optimum activity if found for Co(Ni)/Mo ratio of 1/3 while for W-based catalysts the optimum ratio is 2/3. The CoW system did not show a promoter effect, while for the other systems a significant enhancement in activity is observed due to the presence of a promoter. The thiophene HDS activity decreases in general in the order: NiMo ≥ NiW > CoMo > CoW ≥ W ~ Mo. Al_2O_3 is a better support for both HDS and hydrogenation of butenes to butane. Unpromoted catalysts show higher hydrogenation activity, while W-based catalysts are more active in hydrogenation than Mo-based catalysts. While SiO_2-supported catalysts deactivate at high sulfidation temperatures due to sintering, Al_2O_3-supported catalysts show equal or even higher HDS activities at higher sulfidation temperatures due to the strong interaction of the active phase with the support.

CyDTA increase the HDS activity for all systems and supports. As a result catalysts prepared with CyDTA show the highest HDS activity. However, these catalysts deactivate severely at high sulfidation temperatures.

It is shown that flat, non-porous model catalysts can be used for intrinsic kinetic studies. Kinetic experiments are carried out over a broad temperature range, i.e. T 200-500 ^{0}C. For thiophene HDS Volcano-curves are observed for the HDS activity as function of the reaction temperature, with an optimum activity around 375-400 ^{0}C. This behaviour is observed for different catalysts, and is very dependent on the pretreatment conditions. Arrhenius plots of the Volcano curves imply that at high temperatures the apparent activation energy has a negative value. We give a possible explanation for this behaviour on the basis of a two-site reaction mechanism, where thiophene adsorbs on one site and hydrogen on a different site and the role of H_2S is neglected at low conversions. A negative value for the apparent activation energy is then possible if the activation energy of the rate limiting step is exceeded by the heats of adsorption of thiophene and hydrogen.

Although further research is necessary to confirm and explain the work presented in this chapter, it shows that non-porous model catalysts can be excellently used for kinetic and mechanistic studies in the future.

References

[1] T.F. Kellet, A.F. Sartor and C.A. Trevino, *Hydrocarbon Processing*, May 1980, 139.
[2] H. Topsøe, B.S. Clausen, and F.E. Massoth, "Hydrotreating Catalysis." Springer-Verlag, Berlin, 1996.
[3] P. Grange and X. Vanhaeren, *Catal. Today* **36**, 375 (1997).
[4] E. Furimsky, *Appl. Catal. A* **171**, 177 (1998).
[5] H.R. Reinhoudt, R. Troost, A.D. van Langeveld, S.T. Sie, J.A.R. van Veen and J.A. Moulijn, *Fuel Processing Technol.* **61**, 133 (1999).
[6] H. Topsøe, B.S. Clausen, N.-Y. Topsøe and E. Pedersen, *Ind. Eng. Chem. Fundam.* **25**, 25 (1986).
[7] S.-K. Ihm, S.-J. Moon and H.-J. Choi, *Ind. Eng. Chem. Res.* **29**, 1147 (1990).
[8] S. Kasahara, T. Shimizu and M. Yamada, *Catal. Today* **35**, 59 (1997).
[9] E. Lecrenay, K. Sakanishi and I. Mochida, *Catal. Today* **39**, 13 (1997).
[10] W.R.A.M. Robinson, J.A.R. van Veen, V.H.J. de Beer and R.A. van Santen, *Fuel Processing Technol.* **61**, 89 (1999).
[11] M.J. Vissenberg, Ph.D. thesis, Eindhoven University of Technology, The Netherlands, 1999, Chapter 7.
[12] E. Furimsky, *Catal. Rev.-Sci. Eng.* **22**, 371 (1980).
[13] M.J. Vissenberg, Y. van der Meer, E.J.M. Hensen, V.H.J. de Beer, A.M. van der Kraan, R.A. van Santen, and J.A.R. van Veen, *J. Catal.* **198**, 151 (2001).
[14] R.G. Leliveld, A.J. van Dillen, J.W. Geus and D.C. Koningsberger, *J. Catal.* **175**, 108 (1998).
[15] R. Candia, O. Sørenson, J. Villadsen, N.-Y. Topsøe, B.S. Clausen and H. Topsøe, *Bull. Soc. Chim. Belg.* **93**, 763 (1984).
[16] H. Topsoe, R. Candia, N.-Y. Topsoe and B.S. Clausen, *Bull. Soc. Chim. Belg.* **93**, 783 (1984).
[17] This thesis, Chapter 6.
[18] This thesis, Chapter 8.
[19] L. Coulier, V.H.J. de Beer, J.A.R. van Veen and J.W. Niemantsverdriet, *Topics in Catal.* **13**, 99 (2000).
[20] L. Coulier, V.H.J. de Beer, J.A.R. van Veen and J.W. Niemantsverdriet, *J. Catal.* **197**, 26 (2001).
[21] J.A.R. van Veen, E. Gerkema, A.M. van der Kraan and A. Knoester, *J. Chem. Soc., Chem. Commun.* **22**, 1684 (1987).
[22] G. Kishan, L. Coulier, J.A.R. van Veen, and J.W. Niemantsverdriet, *J. Catal.* **199**, (2001).
[23] H. Scott Fogler, "Elements of Chemical Reaction Engineering", 3rd Ed., Prentice Hall PTR, London, 1999.
[24] B. Scheffer, Ph.D. thesis, University of Amsterdam, The Netherlands, 1988, appendix.
[25] G. Muralidhar, F.E. Massoth and J. Shabtai, *J. Catal.* **85**, 44 (1984).
[26] L. Medici and R. Prins, *J. Catal.* **163**, 38 (1996).
[27] A.J.A. Konings, W.L.J. Brentjens, D.C. Koningsberger and V.H.J. de Beer, *J. Catal.* **67**, 145 (1981).
[28] Y.I. Yermakov, A.N. Startsev and V.A. Burmistrov, *Appl. Catal.* **11**, 1 (1984).

[29] H.R. Reinhoudt, Y. van der Meer, A.M. van der Kraan, A.D. van Langeveld, and J.A. Moulijn, *Fuel Processing Technol.* **61**, 43 (1999).
[30] E.J.M. Hensen, PhD-thesis, Eindhoven University of Technology, The Netherlands, 2000, Chapter 8.
[31] G. Kishan, L. Coulier, V.H.J. de Beer, J.A.R. van Veen, and J.W. Niemantsverdriet, *J. Catal.* **196**, 180 (2000).
[32] M. Neurock and R.A. van Santen, *J. Am. Chem. Soc*. **116**, 4427 (1994).
[33] E.J.M. Hensen, M.J. Vissenberg, V.H.J. de Beer, J.A.R. van Veen and R.A. van Santen, *J. Catal.* **163**, 429 (1996).
[34] S. Kasztelan, *Appl. Catal. A* **83**, L1 (1992).
[35] H.C. Lee and J.B. Butt, *J. Catal.* **49**, 320 (1977).
[36] F.E. Massoth, *J. Catal.* **47**, 316 (1977).
[37] A.N. Startsev, S.A. Shkuropat and E.N. Bogdanets, *Kinetics and Catalysis* **35**, 258 (1994).
[38] C.N. Satterfield and G.W. Roberts, *AIChE Journal* **14**, 159 (1968).
[39] J. Leglise, J. van Gestel and J.-C. Duchet, *Symp. Adv. Hydrotreating Catalysts, ACS, Washington,* **533** (1994).

10

Summary, Conclusions and Recommendations

In this part we will firstly summarize the contents of this thesis in general terms and compare the general conclusions we made with the objectives stated at the beginning of this thesis. The main subjects will be the contribution of our work to the use of model catalysts in catalysis research and the contribution to the hydrotreating catalysis research. Secondly the conclusions of the various chapters will be listed and compared with each other. The final part will deal with recommendations for future work considering hydrotreating (model) catalysts and the use of model catalysts in general. Some explorative experiments, with new techniques, will be presented, that open the door to some new fields in both hydrotreating and model catalyst research. The main themes for future work are kinetics and mechanisms in hydrotreating catalysis, particle size and distribution in hydrotreating catalysts, new characterization techniques for model catalysts and preparative aspects of catalysts.

10.1 Summary

10.1.1 Model catalysts

Preparation of realistic model catalysts

The main objective of this thesis was the preparation and application of realistic models of hydrotreating catalysts. These model catalysts consisted in our case of thin layers of oxide (e.g. Al_2O_3, SiO_2 and TiO_2) on a Si-wafer on top of which the precursors were deposited. The main differences between our model catalyst approach and the majority of model catalysts used in literature, are the way of deposition of precursors and the fact that we studied these precursors in the oxidic and sulfidic form. The latter is quite exceptional while model catalysts used in literature often consist of metal particles (e.g. Pt, Rh or Pd) on an oxidic substrate [1]. These metal particles are mostly deposited by evaporation in vacuum. In our case we use the so-called spincoating technique to prepare our model catalysts [2,3]. This wet chemical technique has shown to mimic the impregnation technique used for high surface area catalysts [2,3]. It is clear that this wet chemical technique which is carried out under the same experimental conditions as the impregnation technique is much more realistic than

evaporation of metals in vacuum. Especially the chemistry of precursor compounds with the support, which has a large influence on the dispersion of the active phase, is completely absent in the case of evaporation of metals in vacuum.

The deposition of precursors on supports is only the first step in the preparation of catalysts. Pretreatment like calcination, reduction or sulfidation is necessary to convert the precursor into the active state. To prepare realistic model catalysts it is thus necessary to pretreat the model catalysts under conditions similar to high surface area catalysts. In our case both the calcination and the sulfidation treatment are carried out in the same equipment as high surface area catalysts. Moreover, the conditions used for calcination and sulfidation are identical to that of high surface area catalysts, as was shown in Chapter 1. Combining this with the spincoating technique for depositing the precursors we conclude that we prepare our model catalysts as realistically as possible.

As mentioned earlier, commonly used model catalysts consist of metal particles on an oxidic substrate [1]. Despite the relevance of these catalysts, for e.g. automotive exhaust catalysis, and the substantial contribution these model catalysts have made to catalysis research, many other catalysts consist of oxides or sulfides. These catalysts are generally complex due to the structure of the active phase where defects play an important role. It is maybe due to this that literature on oxidic or sulfidic model catalysts is less abundant, while research on oxidic or sulfidic model catalysts prepared under realistic conditions is particularly rare [1].

However, a good model of a catalyst should also show comparable catalytic activity. We have clearly shown that the various model catalysts used in this thesis do show representative catalytic activity in the hydrodesulfurization (HDS) of thiophene, a reaction often used as a test reaction for hydrotreating reactions. Not only do the trends in HDS activity reflect that of high surface area catalysts, also the product distribution is similar. Calculating the HDS activity as moles of thiophene reacted per mole Mo per second shows activities in the same order of magnitude for model catalysts and high surface area catalysts (see Table 10.1) [4].

Table 10.1 *Model vs. porous catalysts: HDS activity of Al_2O_3-supported catalysts at 400 ^0C.*

	Model catalysts	Porous catalysts [4]
	R (mol_T/mol_{Mo}*h)	R (mol_T/mol_{Mo}*h)
Mo/Al_2O_3	6.8	3.9
$CoMo/Al_2O_3$	13.2	18.4
$NiMo/Al_2O_3$	52.2	31.5

We thus conclude that we are able to prepare realistic models of hydrotreating catalysts. All preparation and pretreatment conditions are similar to that of the porous hydrotreating catalysts and our model catalysts show representative activity for the hydrodesulfurization of thiophene.

Using the advantages of model catalysts

As already mentioned in Chapter 1, using flat model catalysts has several advantages. The first advantage is the presence of a conducting substrate that reduces charging problems

associated with isolators like porous silica or alumina. As a result of this charging the spectra in electron-spectroscopy shift to higher energy and the peaks become broader resulting in lower resolution [5]. In Chapter 2 to 8 we have used X-ray Photoelectron Spectroscopy (XPS) to study the sulfidation of our model catalysts. Due to the conducting substrate our XPS spectra show only minor charging and the resolution is good. Moreover, using model catalysts for XPS measurements has an extra advantage. For example, the preparation of a model catalyst by spincoating takes minutes, while impregnation and drying of porous catalysts takes much longer. Furthermore, sample preparation for XPS measurements is far easier for model catalysts than for porous catalysts. The XPS measurements described in this thesis carried out with porous catalysts would have taken much more time.

To use the advantage of the conducting substrate it is important to have only a thin oxide layer on top of it. This thin oxide layer is used as a model support (i.e. SiO_2). Because the support is only about 5 nm thick, chemical changes can be much more easily observed than for porous bulk supports. A good example was shown in Chapter 7 where the role of TiO_2 on the HDS activity of Mo-based catalysts was studied. Owing to the small thickness of the TiO_2 layer and the surface sensitivity of XPS we were able to see the partial sulfidation of TiO_2 and we could conclude that sulfided TiO_2 species act as a promoter and thereby increase the HDS activity. Such an observation would be difficult to make for bulk TiO_2 samples.

Another main advantage of using model catalysts is the absence of pores. This means that internal (= pore) diffusion limitation is absent. If one can exclude external (= film) diffusion limitation it is possible to study intrinsic kinetics. Chapter 9 showed a good example of using model catalysts for kinetic studies, where we studied the thiophene HDS kinetics on different catalysts over a broad temperature range. This approach seems to be very promising for the future. However, a disadvantage is of course the low surface area of our model catalysts leading to low conversions. As a result we measure the HDS activities of our model catalysts in batch mode. The ultimate would be to measure the activity in flow mode. This is possible as demonstrated in Chapter 10 for the catalysts with the highest activity, i.e. NiMoEDTA/SiO_2. The conversions were indeed very low and it was impossible to measure in flow mode for less active catalysts. It is thus necessary for the future to develop a way to improve the sensitivity of the analysis method. We will go in more detail on how to do this in the last section of this chapter.

Another important aspect of the absence of pores in our model catalysts, is the efficient removal of H_2O during sulfidation as described in Chapter 3. As a result the sulfidation speeds up compared to high surface area catalysts where higher partial H_2O pressures in the pores slow down the rate of sulfidation.

In conclusion, we state that we have used our realistic hydrotreating model catalysts in such a way as to profit from the advantages of using model catalysts consisting of a thin layer of oxide on a conducting non-porous substrate.

10.1.2 Hydrodesulfurization (HDS) catalysis

Sulfidation vs. thiophene HDS activity on SiO_2-supported HDS catalysts

The first part of this thesis focused on the sulfidation of hydrotreating catalysts characterized with XPS. The sulfidation behaviour was correlated with the thiophene HDS activity of the various catalysts. In Chapter 2 to 5 only SiO_2-supported catalysts were studied.

The four different systems, i.e. CoMo, NiMo, CoW and NiW, showed great similarity although some striking differences were observed as well.

In Chapter 2 the formation of the so-called CoMoS phase was studied for $CoMo/SiO_2$ catalysts. It was shown that the key step in the formation of the CoMoS phase is the retardation of the sulfidation of Co. Chelating agents like nitrilo triacetic acid (NTA) form stable complexes with Co thereby retarding the sulfidation of Co to temperatures where Mo is already partially sulfided. These are beneficial circumstances for CoMoS formation. In contrast, the sulfidation of Co/SiO_2 occurs at low temperatures and hence bulk Co-sulfide is formed. Mo/SiO_2 sulfides at moderately temperatures and forms MoS_2. In conventional $CoMo/SiO_2$ the sulfidation of Co is slightly retarded and this was attributed to a Co-Mo interaction. However, despite this interaction the sulfidation of Co still precedes that of Mo and hence the chance of formation of CoMoS is small, resulting in catalysts with lower HDS activity.

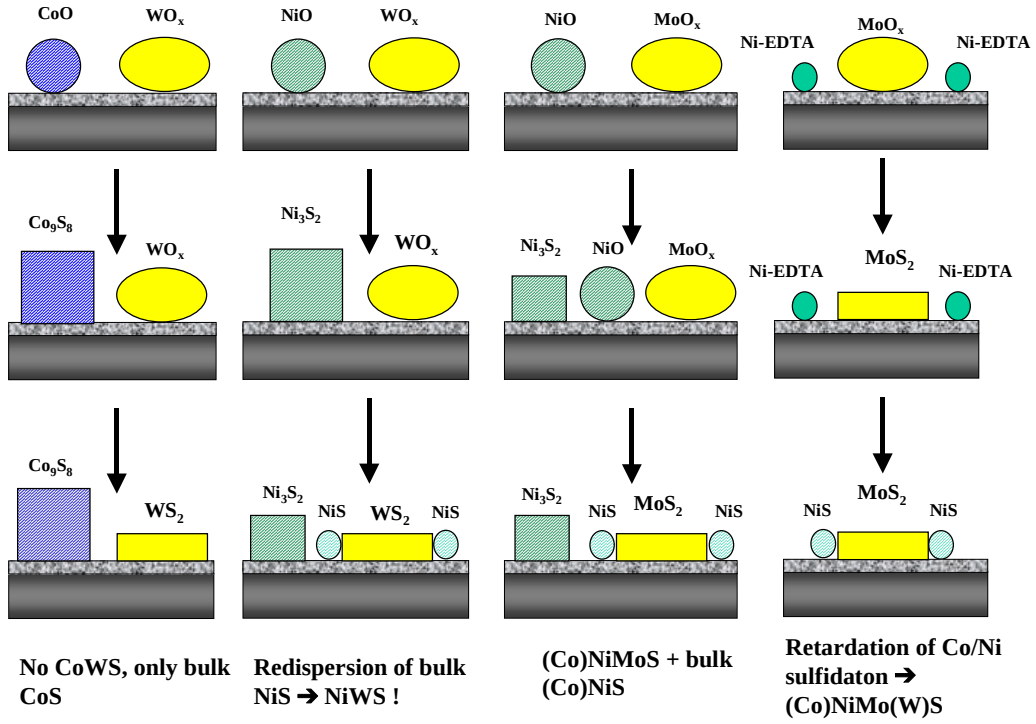

Figure 10.1 *Schematic overview of the formation of the active phase on the various catalysts studied in this thesis.*

$NiMo/SiO_2$ catalysts were studied in Chapter 3. These catalysts showed much similarity with $CoMo/SiO_2$. For these catalysts the key step in the formation of the NiMoS phase was the retardation of the sulfidation of Ni. The use of chelating agents also had a positive influence on the HDS activity of Ni-promoted catalysts. By using more stable complexes, like ethylene diamine tetraacetic acid (EDTA), it was possible sulfide Ni in the presence of completely sulfided Mo. This optimum in order of sulfidation resulted in catalysts with the highest HDS activity. Complexes with even higher stability, like 1,2-cyclohexane diamine tetraacetic acid (CyDTA), retarded the sulfidation of Ni to even higher temperature but showed the same activity as EDTA, hence an optimum is reached when the sulfidation of Mo completely precedes that of Ni. Using these chelating agents the HDS

activity could be increased with a factor of 6. From the XPS binding energies the complexation of Ni to the chelating agents could be observed. Furthermore the binding energies of the fully sulfided catalysts showed a significant difference between Ni in bulk Ni-sulfide and Ni in NiMoS.

Chapter 4 and 5 focused on the formation of the active phase in W-based catalysts. The sulfidation of W was shown to be much more difficult compared to Mo. As a result Ni and Co sulfided completely before W. For CoW/SiO_2 this resulted in the formation of two separate phase, i.e. bulk Co-sulfide and WS_2. These catalysts showed HDS activities equal to the lumped activity of W/SiO_2 and Co/SiO_2. Hence no promotion effect of Co was observed. For NiW/SiO_2 we observed from XPS that at first instance bulk Ni-sulfide is formed. However, at temperatures where WS_2 was formed a sudden shift in Ni 2p binding energy was observed. From this shift in binding energy from bulk Ni-sulfide to Ni in NiWS and the high activity of NiW/SiO_2 it was concluded that Ni-sulfide (partially) migrates to the edges of WS_2-slabs thereby forming the NiWS phase. This mechanism of active phase formation was not encountered for the other systems. The use of chelating agents increased the HDS activity of both CoW/SiO_2 and NiW/SiO_2. Due to the slow sulfidation of W, very stable complexes, like CyDTA or triethylene tetraamine hexaacetic acid (TTHA) were necessary to significantly enhance the HDS activity. Despite these stable complexes it was not possible to separate the sulfidation of Co or Ni and W completely, hence we anticipate that the activity is not yet at its theoretical maximum. As a result chelating agents increased the activity with only a factor of 2 to 3, which is significant but less compared to Mo-based catalysts. XPS could also be used here to distinguish between bulk Ni- or Co-sulfides and Co and Ni in CoWS and NiWS, respectively. An overview of the various phenomena observed during sulfidation on the four different catalysts is shown in Figure 10.1.

The influence of support interaction on the sulfidation and thiophene HDS activity

In Chapter 6 and 8 the influence of different supports, like Al_2O_3 and TiO_2, on the sulfidation and thiophene HDS activity was studied for different catalysts. In general, these supports showed strong interactions with Co, Ni, Mo and W. The strong interaction could be increased by calcination. As a result of this the sulfidation of Co, Ni, Mo and W was slower compared to SiO_2-supported catalysts.

In Chapter 6 it was found that for W-based catalysts supported on Al_2O_3 high calcination temperatures retarded the sulfidation of Co, Ni and W to high temperatures and lead to incomplete sulfidation. Chelating agents, like CyDTA, retarded also the sulfidation of Co and Ni but lead to complete sulfidation at 400 ^{0}C. In mixed oxide catalysts W prevented the interaction of Co and Ni with the Al_2O_3 support and partially blocked the diffusion of Co and Ni into the support. The same was observed for Mo-based catalysts on Al_2O_3 and TiO_2 in Chapter 8. As a result the sulfidation of Co and Ni is facilitated.

For CoW/Al_2O_3 no promotion effect was observed, similarly as for CoW/SiO_2. NiW/Al_2O_3 showed a strong promotion effect and redispersion of Ni-sulfide to WS_2-slabs was observed from XPS. The redispersion of Ni-sulfide was only observed for NiW catalysts. For Co-promoted catalysts no evidence for redispersion was observed. We cannot exclude the possibility of redispersion for NiMo catalysts. However, in the case of NiW catalysts, the sulfidation of Ni precedes completely that of W while in the case of NiMo some overlap exists. Because of the complete separation of Ni and W sulfidation we could observe the

redispersion of Ni-sulfide in this case. The HDS activity could be increased using chelating agents, e.g. CyDTA. It was concluded that for conventional catalysts Al_2O_3 is a better support for active phase formation. However, catalysts containing chelating agents showed the highest HDS activity, irrespective of support. The HDS activity was strongly influenced by both sulfidation and calcination temperature. A combination of high calcination temperature and low sulfidation temperature lead to incomplete sulfidation and thus a lower HDS activity. However, a combination of high sulfidation temperature and low calcination temperature lead to segregation of the NiWS phase and thus a decrease in HDS activity. The segregation effect was largest for catalysts containing chelating agents. Furthermore it was concluded that the effect of chelating agents is the retardation of the sulfidation of Co and Ni and not a dispersion effect.

Chapter 8 clearly showed the influence of other supports, e.g. Al_2O_3 and TiO_2, on the HDS activity of Mo-based catalysts was studied. It was concluded that both Al_2O_3 and TiO_2 are better supports for active phase formation than SiO_2. This was contributed to the strong interaction of Co, Ni and Mo with Al_2O_3 and TiO_2, due to calcination, which influenced both the sulfidation rate and dispersion of the active phase. TiO_2-supported catalysts showed both higher HDS and hydrogenation activity. Ni was a more effective promoter than Co. Chelating agents, like EDTA, increased the HDS activity for all supports and lead to catalysts with the highest activity irrespective of support. It was concluded that due to the complexation of both Co (or Ni) and Mo by EDTA, any interaction with the support is prohibited and hence the support acts as an inert substrate. Therefore the HDS activity is equal for all supported catalysts that where prepared with chelating agent.

The low activity of SiO_2-supported catalysts was ascribed to a lower MoS_2 dispersion due to a weaker interaction of Mo with SiO_2 support compared to Al_2O_3 and TiO_2.

The role of TiO_2 in HDS

Chapter 7 revealed the role of TiO_2 in HDS catalysts. For unpromoted Mo catalysts, the thiophene HDS activity increased in the order $TiO_2 > Al_2O_3 >> SiO_2$, while for Ni-promoted catalysts the order was $TiO_2 \sim Al_2O_3 >> SiO_2$. Detailed angle-dependent XPS measurements showed that TiO_2 sulfided partially during sulfidation. HDS activity measurements of Ti-promoted Mo catalysts showed a significant increase in HDS activity compared to Mo catalysts. From this it was concluded that sulfided Ti^{3+}-species act as a promoter in the same way as Co and Ni, although less effective. This explains the high HDS activity of Mo/TiO_2 compared to Mo/Al_2O_3. For Co- or Ni-promoted Mo catalysts the differences in activity between the two supports were small. Apparently Ti only acts as a promoter in the absence of Co and Ni. Sulfided Ti-species also increased the hydrogenation activity.

Comparing the HDS activity and kinetics of thiophene HDS

In the last chapter we focused on the thiophene HDS reaction. The first part showed a comparison of the thiophene HDS activities of all catalysts used in this thesis. Such a comparison between the various systems on different supports is lacking in the literature on HDS. It was concluded that for our experimental conditions Ni is an intrinsically more effective promoter than Co. For all systems a promotion effect was observed, except for

CoW. Chelating agents could increase the activity for all catalysts. The strongest effect of chelating agents was observed for Mo-based catalysts. These catalysts were however very sensitive to high sulfidation temperatures. The hydrogenation of butenes to butane was relatively higher for unpromoted catalysts, while W showed higher hydrogenation activity than Mo. The activity for HDS and the hydrogenation selectivity decreased in the order $TiO_2 \geq Al_2O_3 > SiO_2$. In general the HDS activity decreased in the order NiW ≥ NiMo > CoMo > CoW ≥ W ~ Mo

The kinetic measurements over a broad temperature range (T=200-500 ^{0}C) showed Volcano-plot behaviour for the first time for this reaction. A maximum in activity around 375-400 ^{0}C was observed for CoMo, NiMo and NiW catalysts supported on SiO_2. Although this behaviour could not be explained completely, it was concluded that a two-site mechanism, where thiophene adsorbs on one site, in competition with H_2S, and hydrogen on a different site, could explain this Volcano-behaviour. Arrhenius plots resulted in activation energies at low temperatures similar to that of high surface area catalysts. For high temperatures negative (apparent) activation energies were found due to the Volcano-behaviour. This negative value is only possible if the activation energy of the rate limiting step is exceeded by the adsorption energies of adsorbed species like thiophene or hydrogen. Future experiments and modeling are necessary to elucidate the mechanism and kinetic expression for thiophene HDS that can explain the Volcano-like behaviour.

10.2 General conclusions

In the previous section an overview of the conclusions of the various chapters was given. In this section we will summarize the general conclusions which result from the work presented in this thesis:

- Realistic models of hydrotreating catalysts can be prepared using spincoating impregnation and preparative conditions similar to those employed for high surface area catalysts.
- These model catalysts show representative activity in the hydrodesulfurization of thiophene, which is an often-used model reaction for hydrodesulfurization of crude oil.
- X-ray Photoelectron Spectroscopy (XPS) in combination with a conducting model system is a very useful technique to study the transition of oxides to sulfides. Detailed fitting of the XPS spectra can distinguish between Co and Ni in bulk sulfides and in the active phase. Phenomena like redispersion and segregation of the active phase can also be clearly followed with XPS. Model catalysts are especially useful for XPS due to the low surface charging and the consequently high resolution of the XPS spectra.
- We have studied the sulfidation and HDS activity of the four known systems, e.g. CoMo, NiMo, NiW and CoW, on three different supports, i.e. SiO_2, Al_2O_3 and TiO_2, thus providing a rather complete systematic overview of these related systems.
- The advantages of model catalysts have been exploited successfully in this work. The use of thin oxide films made it possible to observe the sulfidation of TiO_2 and to conclude the role of sulfided TiO_2 as promoter.
- Due to the absence of pores we were able to study the intrinsic kinetics of thiophene HDS. For the first time Volcano-like behaviour was found for thiophene HDS as a

function of temperature. This approach seems fruitful for future kinetic and mechanistic studies using model catalysts.

10.3 Outlook

10.3.1 Kinetic and mechanistic studies

Chapter 9 has shown that model catalysts can be applied successfully for kinetic studies. The big advantage of model catalysts is the absence of pores which means that internal (= pore) diffusion does not play a role. If one can avoid external (= film) diffusion it is possible to measure intrinsic kinetics over a broad temperature range. Another advantage of the absence of pores is the fact that the chance of readsorption of e.g. intermediates is small. As a result the chance of finding intermediates of catalytic reactions using model catalysts is much higher than for porous catalysts.

Although we think that this approach can be used for almost every catalytic system and reaction, we will now focus on hydrotreating catalysis. In this thesis we only studied the kinetics of thiophene HDS as a function of temperature. Varying partial pressures of thiophene, hydrogen and hydrogen sulfide is of course the next step. The resulting orders of the different reactants and products will give additional information concerning the kinetics. Hopefully the experiments and additional modeling will reveal the true kinetics of thiophene HDS. The main problem is the low surface area and thus the low conversion of our model catalysts.

So far thiophene HDS activity measurements were always carried out in batch mode. This is done because the conversion levels obtained for model catalysts are very low due to the low surface area and hence the low amount of active material. Recently we tried to do our reactions in flow mode under the same conditions as in batch mode. The only difference is that the amount of catalyst in flow mode is twice as high as in batch mode and analysis is carried out with an automatic GC sampler. In order to explore whether this method works, we tested the most active HDS catalyst, i.e. NiMoEDTA/SiO_2.

Table 10.2 *Batch vs. flow HDS activity measurements for NiMoEDTA/SiO_2 sulfided at 400 ^0C.*

T_r (^{0}C)	Batch		Flow	
	X (%)	r (mol_T/mol_{Mo}*h)	X (%)	r (mol_T/mol_{Mo}*h)
300	0.7	29.9	0.005	27.7
325	1.0	41.8	0.009	44.6
350	2.5	99.7	0.025	119.9
375	5.0	192.6	0.030	138.2
400	6.3	232.6	0.059	259.2

Table 10.2 shows for NiMoEDTA/SiO_2 the conversion and subsequent reaction rate of thiophene HDS at various temperatures for both batch and flow mode measurements. While the conversion levels of the two reaction modes are of course different, the reaction rate expressed in moles of thiophene per mole Mo per second are very similar. Furthermore,

the HDS activity increases from 300 to 400 ^{0}C for both reaction modes. It was however not possible to go to lower temperatures in flow mode or to study catalysts with lower activities. In these cases the conversions fall below the detection limit of the GC. These results show that batch experiments on model catalysts are good representatives for the standard flow measurements on high surface area catalysts. The flow measurements are very important for the future to study intermediates in mechanistic studies as will be discussed more explicitly in one of the following sections.

Although we are able to measure the HDS activity in flow mode this was only possible for the catalysts with the highest HDS activity, viz. NiMoEDTA/SiO_2. For less active catalysts the conversions were too low to obtain accurate kinetic data. For future measurements it is thus necessary to either increase the total conversion by e.g. increase the amount of catalyst or decrease the flow rate or increase the GC sensitivity. Increasing the amount of catalyst and decreasing the flow rate is of course possible but only to a certain extent. The sensitivity of GC can be increased by using multicapillary GC columns produced by Stylacats Ltd. These GC columns show increasingly higher sensitivities.

Other hydrotreating reactions like hydrodeoxygenation (HDO), hydrogenation (HYD), hydrocracking or hydrodenitrogenation (HDN) are also candidates to study with model catalysts in the future. The only restriction is that the current equipment is at present only suitable for reactions in the gas phase and at low pressures (~ 1 atm).

For mechanistic studies short contact times are necessary. A combination of fast flow rates and the absence of pores should be successful to observe intermediates in thiophene HDS at high temperatures and low pressures, like dihydrothiophenes (DHT). These species are proposed as intermediates but are only visible at low reaction temperatures on high surface area catalysts when hydrogenation is thermodynamically favorable [6].

10.3.2 Towards particle size and distribution

The ultimate goal in comparing activities of different catalysts and studying the intrinsic kinetics and activities of active sites is to express the activity as a turnover frequency (e.g. atoms of thiophene per active site per second). To achieve this one has to know the amount of active sites on a catalyst. One disadvantage of the work presented in this thesis is the fact that we have not obtained direct information on particle size and distribution. As a result we cannot unambiguously exclude dispersion effects. Although XPS can give some evidence of the presence or absence of dispersion effects it is necessary to have some direct evidence. One way to do this is imaging of the active phase with e.g. transmission electron microscopy (TEM). This technique is able to give at least the number and lateral dimensions of the particles. By statistical analysis it is possible to calculate, in the case of HDS catalysts, the size of the MoS_2 slabs and thus the maximum amount of Co or Ni atoms that can sit on the edges of these slabs. These atoms are believed to be the active sites in HDS reactions [7]. Figure 10.2 shows an example of a TEM picture of one of our model catalysts. This catalyst consist of a Si-wafer where on certain spots the Si has been chemically etched and only a thin SiO_2 layer remains which is transparent both for the eye and for the electron microscope. The catalysts is prepared in the same way as described in this thesis and is transferred to the electron microscope after sulfidation without air exposure.

Visible in Figure 10.2 are the Mo atoms (black lines). A single black line corresponds to one MoS_2 slab consisting of one row of Mo atoms (visible) and two rows of sulfur atoms (not visible). If one looks at the lateral dimensions in Figure 10.2 it is clear that the lengths of the slabs is about 4 nm and that both single and multiple slabs are visible. These features correspond well with dimensions of high surface area catalysts. However, the problem of making TEM images of model catalysts is the high fragility of the thin layer of SiO_2 that is necessary for these measurements. Careful preparation and transport of these model catalysts in the future should make it possible to obtain reliable TEM pictures of hydrotreating model catalysts in this way.

Other techniques that may be useful to obtain information on particle size and distribution are Low Energy Ion Scattering (LEIS) and Atomic Force Microscopy (AFM). While LEIS can give information on surface coverage of e.g. MoS_2 on the support, from AFM the number and height of particles can be obtained. A combination of these two techniques can thus reveal the particle size and distribution for a sample if the metal loading is known.

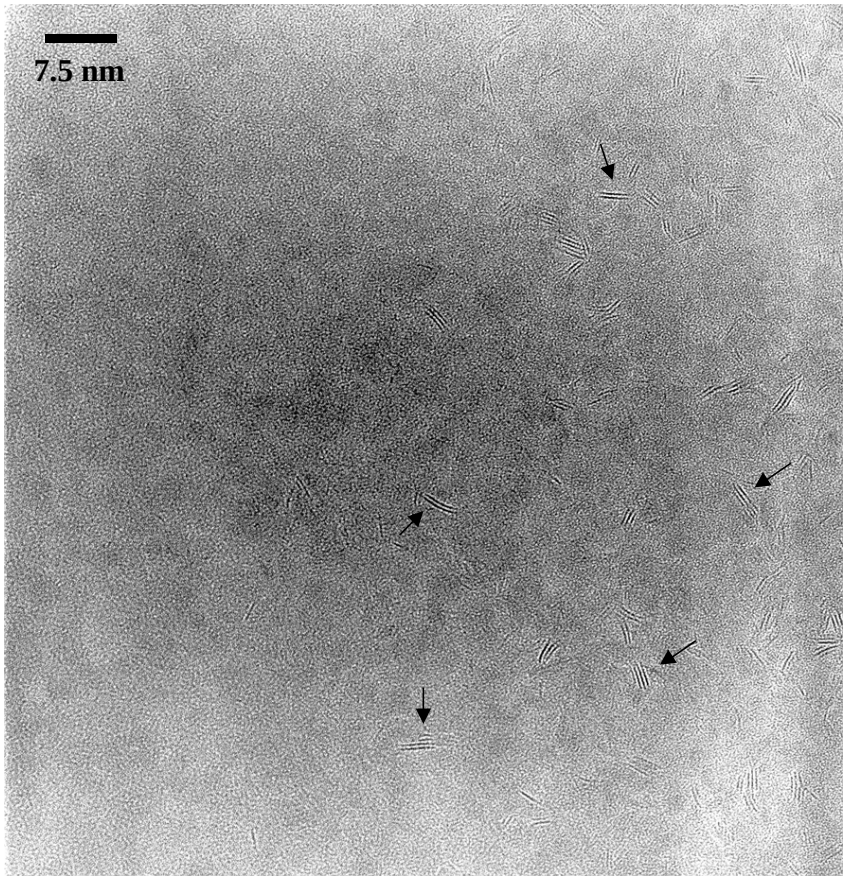

Figure 10.2 *TEM picture of a Mo/SiO_2 model catalyst sulfided at 400 ^{0}C.*

10.3.3 Characterization of model catalysts

In this thesis XPS was the main characterization technique. However, more characterization techniques are required to compete with high surface area catalysts. Different

vacuum techniques have already been applied on model catalysts, e.g. RAIRS, EELS, AES [1]. The main disadvantage of these techniques is the fact that samples must be heated and cooled and that the measurements are carried out at low pressure. Therefore model catalysts prepared by evaporation of metals on a substrate are used for these techniques.

Figure 10.3 shows ultra violet-Raman spectra of various model catalysts. The advantage of UV-Raman is the absence of fluorescence of the material, which is a significant problem in standard Raman spectra. Due to this surface sensitiveness of UV-Raman we were able to obtain UV-Raman spectra of our model catalysts despite the low amount of material, e.g. Mo or W, present. The different peaks in Figure 10.3 can all be explained in terms of (hydrated) Mo-O and W-O compounds. Raman spectroscopy is a very useful technique for metal-oxygen or metal-sulfur vibrations, like Mo-O, Mo-S, W-O or W-S [5]. Information can be obtained on the presence of different Mo or W structures. An additional advantage is the possibility of in-situ measurements. Adsorbed species do not interfere significantly with the signals from the gas phase, enabling studies under reaction conditions.

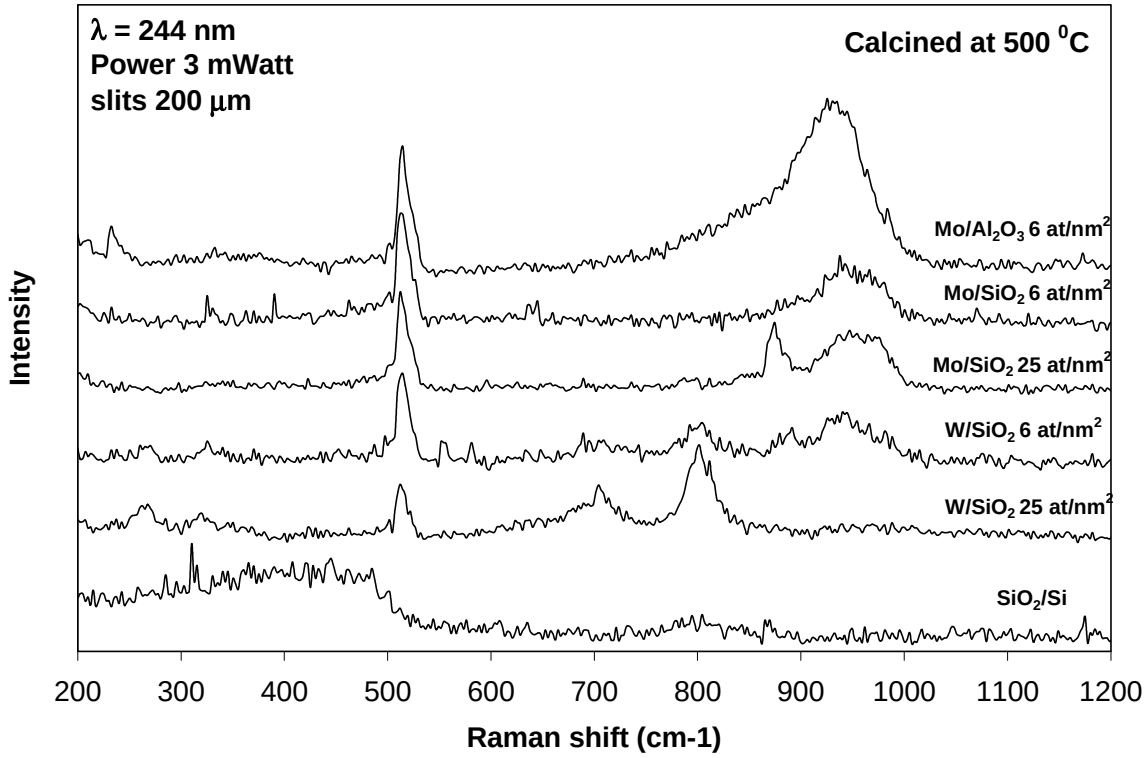

Figure 10.3 *UV-Raman spectra of various oxidic model catalysts.*

Although UV-Raman can be used for all kinds of catalysts, especially hydrotreating catalysts are very useful because they usually contain Mo or W. Important subjects which can be studied using hydrotreating model catalysts are the influence of pH and calcination on the structure of the oxidic and sulfidic catalysts. It is known that ammoniacal preparation of HDS catalysts result in higher activity than catalysts prepared with neutral solutions, however a clear explanation has not been given yet. Another interesting subject is the influence of additives like P or F on the structure of HDS catalysts. It is known that these additives

increase the HDS activity [7]. The use of model catalysts is extra interesting for this because the flat model support can be seen as a pore wall and thus one can directly see what the influence of various treatments or additives is on the structure of the support.

Finally, we conclude that the research presented in this thesis is one of the first examples of application of realistic model catalysts in catalysis research. Especially the advantages of using model catalysts have been used successfully and it was shown that this approach looks very promising for the future.

References

[1] P.L.J. Gunter, J.W. Niemantsverdriet, F.H. Ribeiro and G.A. Somorjai, *Catal. Rev.-Sci. Eng.* **39**, 77 (1997).
[2] E.W. Kuipers, C. Laszlo and W. Wieldraaijer, *Catal. Lett.* **17**, 71 (1993).
[3] R.M. van Hardeveld, P.L.J. Gunter, L.J. van IJzendoorn, W. Wieldraaijer, E.W. Kuipers and J.W. Niemantsverdriet, *Appl. Surf. Sci.* **84**, 339 (1995).
[4] M.J. Vissenberg, Ph.D. thesis, Eindhoven University of Technology, The Netherlands, 1999.
[5] J.W. Niemantsverdriet, “Spectroscopy in Catalysis: An Introduction”, VCH, Weinheim, 1993.
[6] E.J.M. Hensen, M.J. Vissenberg, V.H.J. de Beer, J.A.R. van Veen and R.A. van Santen, *J. Catal.* **163**, 429 (1996).
[7] H. Topsøe, B.S. Clausen, and F.E. Massoth, “Hydrotreating Catalysis.” Springer-Verlag, Berlin, 1996.

Samenvatting

Het verminderen van zwavelhoudende verbindingen in brandstoffen is een van de maatregelen om de milieuvervuiling aan te pakken. Wanneer deze stoffen in de brandstoffen komen en verbrand worden in bijv. de automotor, dan vormt zich SO_2 wat zwavelzuur kan vormen met water en een van de veroorzakers van zure regen is. Ten opzichte van ongeveer tien jaar geleden is de hoeveelheid zwavelhoudende verbindingen in brandstoffen al sterk gereduceerd. Als gevolg van deze reductie is het zure regen probleem, vooral in westerse landen, al bijna opgelost. Echter, de zwavelverbindingen hebben nog een groot nadeel. De katalysator in auto's die ervoor zorgen dat er o.a. minder CO en NO in de atmosfeer komen, wordt vergiftigd door deze zwavelverbindingen. Dit leidt tot een grotere uitstoot van schadelijke stoffen. Het is daarom noodzakelijk dat ook de laatste restjes zwavelhoudende verbindingen uit de brandstoffen verdwijnen. Om dit te bewerkstelligen zijn zeer actieve ontzwavelings katalysatoren nodig.

De doelstellingen van dit proefschrift zijn de bereiding en toepassing van realistische ontzwavelings modelkatalysatoren. De industriële katalysator voor ontzwaveling van ruwe olie bestaat in het algemeen uit MoS_2 deeltjes op een hoog oppervlakkige drager, b.v. Al_2O_3. Co of Ni atomen die op de rand van de MoS_2 deeltjes gaan zitten, de zogenaamde CoMoS fase, wordt gezien als de actieve fase voor deze katalysator. Co en Ni nemen hier de rol van promoter aan. De model katalysatoren die worden gebruikt in dit proefschrift bestaan uit een dunne oxide laag, b.v. SiO_2 of Al_2O_3, op een Si-wafer, representatief voor een model drager, waarop de precursors worden afgezet met behulp van spincoating impregnatie. De bereiding en voorbehandeling van de modelkatalysatoren gebeurd onder vergelijkbare omstandigheden vergeleken met industriële katalysatoren en ook de katalytische activiteit van de model katalysatoren in het ontzwavelen van thiofeen, een veelgebruikt molecuul wat model staat voor zwavelhoudende verbindngen in ruwe olie, is representatief. Hieruit kunnen we concluderen dat we in staat zijn realistische ontzwavelings modelkatalysatoren te kunnen bereiden.

Het gebruik van vlakke model katalysatoren heeft een aantal voordelen ten opzichte van poreuze katalysatoren. Een van de voordelen is de aanwezigheid van een geleidend substraat. Door de aanwezigheid van een geleidend substraat is de kans op oplading sterk gereduceerd. Isolatoren, zoals alumina en silica dragers, zorgen voor grote opladingsproblemen voor poreuze katalysatoren. Deze oplading veroorzaakt het opschuiven van spectra in bijvoorbeeld electronen spectroscopie en het breder worden van de pieken waardoor de resolutie lager wordt. Model katalysatoren met een geleidend substraat, waarbij opladingsproblemen dus sterk gereduceerd zijn, zijn daarom ideaal voor bijvoorbeeld X-ray Photoelectron Spectrscopy (XPS). In dit proefschrift laten we zien dat XPS in combinatie met een geleidend model systeem een goede techniek is om de overgang van oxides naar sulfides te bestuderen. Door het gedetailleerd fitten van de XPS spectra van ingezwavelde katalysatoren bij verschillende temperaturen kunnen we onderscheid maken tussen Co en Ni in bulk sulfides en in de actieve fase. Ook verschijnselen als redispersie en segregatie kunnen worden gevolgd met XPS.

Het combineren van het inzwavelgedrag, bestudeerd met XPS, en katalytische activiteit voor de ontzwaveling van thiofeen, levert een aantal interessant conclusies op omtrent de vorming van de actieve fase in deze katalysatoren. De vier mogelijke combinaties,

d.w.z. CoMo, NiMo, CoW en NiW, vertonen veel overeenkomsten alhoewel er ook een aantal grote verschillen zijn. Voor alle systemen geldt dat de volgorde van inzwavelen de belangrijke stap in de vorming van de actieve fase is. Wanneer Mo of W eerder inzwavelen dan Co of Ni dan leidt dat tot een verhoging van de activiteit. Onder normale omstandigheden zwavelen Co en Ni in bij lage temperaturen en vormen daarbij stabiele bulk sulfides, terwijl Mo en W pas bij hogere temperatuur inzwavelen. Organische moleculen zoals NTA vormen stabiele complexen met Co en Ni waardoor het inzwavelen van Co en Ni wordt vetraagd tot hogere temperaturen. Soortgelijke moleculen zoals EDTA en CyDTA vormen zulke sterke complexen met Co en Ni, dat Mo eerst volledig inzwavelt en daarna pas Co en Ni. Aangezien dit leidt tot katalysatoren met een maximale activiteit concluderen we dat dit de ideale omstandigheden voor de vorming van de actieve fase. Het inzwavelen van Co en Ni gebeurt nu in de aanwezigheid van MoS_2 en Co en Ni kunnen makkelijk op de randen van de MoS_2 deeltjes gaan zitten, in plaats van bulk sulfides te vormen. Doordat het inzwavelen van W bij hogere temperatuur plaatsvindt vergeleken met Mo, zijn er stabielere complexen nodig. Het is echter niet mogelijk om W volledig in te zwavelen voordat Co en Ni dat doen. Als gevolg hiervan is de verhoging van de activiteit door het gebruik van complexen hoger voor Mo dan voor W. Voor NiW katalysatoren is gebleken dat bulk Ni sulfide kan redispergeren in de aanwezigheid van WS_2. Dit wil zeggen dat Ni atomen vanuit de bulk sulfide kunnen migreren naar de randen van de WS_2 deeltjes en daarbij de actieve fase vormen. Als gevolg van het gebruik van complexen kan de activiteit van sommige katalysatoren verhoogd worden met een factor 5 tot 6. Terwijl voor alle andere systemen een duidelijk promoter effect van Co en Ni zichtbaar is, blijkt CoW een slechte combinatie te zijn en geen promoter effect te vertonen. Slechts het gebruik van zeer stabiele complexen verhoogt de activiteit van CoW katalysatoren enigzins.

De invloed van het gebruik van complexen op de activiteit is onafhankelijk van de drager. Voor zowel silica, titania en alumina wordt dezelfde activiteit gevonden voor katalysatoren waarbij complexen worden gebruikt. Deze katalysatoren hebben ook altijd de hoogste activiteit. In deze gevallen gedraagt de drager zich als een inert substraat en speelt interactie van de precursors met de drager een ondergeschikte rol. De drager heeft echter wel veel invloed op het inzwavelgedrag en de activteit van katalysatoren zonder complexen. Vooral de sterke interactie van Co-, Ni-, Mo- en W-oxides met alumina en titania hebben een grote invloed. Door deze sterke interactie wordt het inzwavelen vertraagd en wordt de dispersie van MoS_2 en WS_2 over de drager ook beter ten opzichte van silica. Dit effect kan versterkt worden door de katalysatoren te calcineren voor het inzwavelen. Over het algemeen hebben alumina- en titania-gedragen katalysatoren een hogere ontzwavelingsactiviteit vergeleken met silica-gedragen katalysator, terwijl Ni een intrinsiek betere promoter is dan Co. Hoge inzwaveltemperaturen leiden tot segregatie van de actieve fase, d.w.z. het uiteenvallen van de actieve fase in bijv. bulk Ni sulfide en WS_2. Vooral de katalysatoren waarbij complexen worden gebruikt zijn instabiel bij hoge inzwaveltemperaturen en verliezen hun hoge activiteit.

We hebben in dit proefschrift het inzwavelgedrag en de katalytische activiteit van vier verschillende systemen op drie verschillende dragers bestudeerd. Dit resulteert in een redelijk compleet en systematisch overzicht. Zo'n overzicht ontbreekt in de literatuur en is dus een goed voorbeeld hoe modelkatalysatoren kunnen bijdragen aan onderzoek in de ontzwavelingskatalyse.

Door gebruik te maken van het feit dat onze dragers uit een dunne laag bestaan (~ 5 nm) zijn we in staat de rol van titania in ontzwavelings reacties te bestuderen. In combinatie met XPS, kunnen we concluderen dat ook titania gedeeltelijk inzwavelt en dat deze Ti-sulfide deeltjes zich gedragen als promoter net zoals Co en Ni. Dit verklaart de hoge ontzwavelingsactiviteit van Mo/TiO_2 ten opzichte van Mo/Al_2O_3. Ook de hydrogeneringsactiveit wordt verhoogd door deze Ti-sulfide deeltjes. In aanwezigheid van Co of Ni wordt de rol van Ti als promoter overgenomen door Co of Ni en verdwijnt het verschil in activiteit tussen alumina- en titania-gedragen katalysatoren.

Het gebruik van vlakke modelkatalysatoren heeft ook voordelen voor het doen van kinetische metingen. Door de afwezigheid van poriën speelt interne diffusie geen rol. Ook kan externe diffusie limitering verwaarloosd worden. Dit betekent dat men met deze systemen intrinsieke kinetiek kan bestuderen over een groot temperatuur bereik. Door het ontbreken van poriën is ook de kans op readsorptie klein en lijken deze systemen ideaal voor het bestuderen mechanismen en intermediairen.

Dit proefschrift geeft tot slot een voorproefje van het gebruik van model katalysatoren voor kinetische studies. De thiofeen ontzwavelingsactiviteit, gemeten over een groot temperatuur bereik (T=200-500 ^{0}C), laat voor het eerst een Vulkaan-curve te zien voor verschillende katalysatoren met een maximum in de activiteit rond 375-400 ^{0}C. Meer metingen zijn nodig om tot een kinetische uitdrukking te komen die dit gedrag volledig kan verklaren. Arrhenius-plots van deze kinetische metingen resulteren in activeringsenergiën bij lage temperatuur (T<400 ^{0}C) die goed overeenkomen met de literatuurwaarden voor industriële katalysatoren. Door het Vulkaan-gedrag is de activeringsenergie bij hoge temperatuur negatief. Alhoewel dit op het eerste moment onmogelijk lijkt is het toch verklaarbaar. Voor een simpel reactiemodel waarbij de snelheidsbepalende stap de reactie tussen geadsorbeerd thiophene (op site 1) en geadsorbeerd waterstof (op site 2) is krijgt men uit de Arrhenius vergelijking dat bij hoge temperatuur de gemeten activeringsenergie negatief kan zijn als de absolute waarde van activeringsenergie van de snelheidsbepalende stap kleiner is dan de som van de adsorptie warmtes van thiophene en waterstof. Literatuurwaarden voor adsorptie warmtes tonen aan dat dit in principe mogelijk is.

Tenslotte concluderen we dat we in staat zijn realistische model katalysatoren te maken en dat we de voordelen van deze modelsystemen hebben gebruikt om een bijdrage te leveren aan de ontzwavelingskatalyse. Deze benadering is zeker geschikt voor toekomstig katalytisch onderzoek, waarbij voornamelijk op het gebied van kinetiek en mechanisme veel eer valt te behalen. Niet alleen voor ontzwavelingskatalyse maar voor vele andere katalytisch systemen kan deze methode nieuwe inzichten geven.

Publications

Modeling supported catalysts in surface science
L. Coulier, J.W. Niemantsverdriet and F.H. Ribeiro, *Cattech* **5** (1999) 81

Surface chemical characterization
L. Coulier and J.W. Niemantsverdriet, in: 'Encyclopedia of Chemical Physics en Physical Chemistry', in press.

On the formation of cobalt-molybdenum sulfides in silica-supported hydrotreating model catalysts,
L. Coulier, V.H.J. de Beer, J.A.R. van Veen and J.W. Niemantsverdriet, *Topics in Catal.* **13** (2000) 99.

Correlation between hydrodesulfurization activity and order of Ni and Mo sulfidation in planar silica-supported NiMo catalysts: the influence of chelating agents
L. Coulier, V.H.J. de Beer, J.A.R. van Veen and J.W. Niemantsverdriet, *J. Catal.* **197** (2001) 26.

Preparation of highly active NiW hydrotreating model catalysts with 1,2-cyclohexanediamine-N,N,N',N'-tetraacetic acid (CyDTA) as a chelating agent
G. Kishan, L. Coulier, V.H.J. de Beer, J.A.R. van Veen and J.W. Niemantsverdriet, Chem. Commun. (2000) 1103.

Sulfidation and thiophene hydrodesulfurization activity of nickel and tungsten sulfide model catalysts, prepared without and with chelating agents
G. Kishan, L. Coulier, V.H.J. de Beer, J.A.R. van Veen and J.W. Niemantsverdriet, J. Catal. **196** (2000) 180.

Promoting synergy in CoW sulfide hydrotreating catalysts by chelating agents
G. Kishan, L. Coulier, J.A.R. van Veen and J.W. Niemantsverdriet, *J. Catal.* **200** (2001) 194.

Surface science models for CoMo hydrodesulfurization catalysts: influence of the support on hydrodesulfurization activity
L. Coulier, G. Kishan, J.A.R. van Veen and J.W. Niemantsverdriet, *J. Vac. Sci. Technol. A* **19** (2001) 1510.

Extreme surface sensitivity of UV-Raman spectroscopy applied to molybdenum oxide model catalysts
B.L. Mojet, L. Coulier, J. van Grondelle, J.W. Niemantsverdriet and R.A. van Santen, J. Raman Spectr., *submitted.*

Influence of the support-interaction on the sulfidation behaviour and hydrodesulfurization activity of Co- and Ni-promoted W/Al_2O_3 model catalysts
L. Coulier, G. Kishan, J.A.R. van Veen and J.W. Niemantsverdriet, to be submitted.

TiO_2-supported Mo model catalysts: Ti as promoter for thiophene HDS ?
L. Coulier, J.A.R. van Veen and J.W. Niemantsverdriet, to be submitted.

Comparison of the thiophene HDS of Al_2O_3- and TiO_2-supported CoMo and NiMo and NiW model catalysts: influence of the support and chelating agents
L. Coulier, J.A.R. van Veen and J.W. Niemantsverdriet, to be submitted.

Kinetics of thiophene hydrodesulfurization on HDS model catalyst
L. Coulier, J.A.R. van Veen and J.W. Niemantsverdriet, to be submitted.

Dankwoord

Zo dat was het dan. Na vier jaar (hard) werken is het gedaan. Ik niet mag klagen daar alles redelijk van een leien dakje ging en goede herinneringen zullen de overhand hebben als ik oud ben. Maar helaas, niet dat alles ging even makkelijk. Er zijn toch twee dingen die genoemd moeten worden die niet zo vlotjes gingen. Ten eerste het aanvragen van het doctoraal examen om de felbegeerde Ir. titel binnen te halen. Normaal gesproken is dit een formaliteit maar ik heb er zo'n drie maanden over gedaan! Want als aio-4 een Ir. opleiding doen, kan dat? Het blijkt dan toch weer dat mensen die eens iets anders (en extra's) doen dan anderen en zich dus buiten de normale paden begeven hiervoor zeker beloond worden. Of is het een beloning dat ik drie identiteitsnummers met bijbehorende pincode en twee cijferlijsten heb, waarvan één met alleen maar vrijstellingen die weer verwijzen naar de andere cijferlijst. Geen goede reclame voor een universiteit!

Ook de perikelen rondom de overgang van het zwavellab van San naar dieter Vogt ging niet ideaal. Ik weet niet hoeveel vergaderingen er zijn geweest en wie er allemaal bij waren, maar de mensen die er rechtstreeks mee te maken hadden in ider geval niet. Het bleek in ieder geval zeer moeilijk om afspraken te maken (of zich eraan te houden). Dit heeft niet alleen mij geirriteerd! Uiteindelijk zijn het de 'gewone' mensen geweest die gezorgd hebben dat ik zonder al te veel hinder door ben kunnen gaan met mijn onderzoek. Laat dit een wijze les zijn!

Dan nu het dankwoord. Als drs. en van boven de rivieren naar Eindhoven om te promoveren, da's een hele overgang. Maar ik kwam, zag en overwon! Dat deed ik natuurlijk niet alleen. Daarom dank aan de volgende personen. Ten eerste mijn twee promotoren, Hans en Rob, respectievelijk de man met de doorlopende reisverzekering en de man met 'de lach'. Beste Hans, ik weet nu de waarde van een onderzoeksvoorstel. Erg bedankt voor de hulp als het nodig was (gelukkig niet vaak), het lezen van artikelen en hoofdstukken, het gunstige financiële klimaat, de reisjes (Palm Springs!), hulp bij praatjes en posters (posterprijs!) en het aannemen van goeie/leuke mensen. En nu maar een goeie opvolger zien te vinden!

Rob, bedankt voor jouw industriële kijk op zaken en de daarbij horende relativering van wetenschappelijk onderzoek. Het was zeker nuttig om een echte expert erbij te hebben. Nu weet ik dat HDS onderzoek ondanks alles nog steeds één grote gatenkaas is. Ook bedankt voor het proberen te ondergraven van mijn theoriën/conclusies en het lezen van alle artikelen en hoofdstukken.

Ofcourse many thanks to Gurram Kishan. Without you my thesis would not contain as many pages as it has now. Thanks to you we now have a rather complete overview of the various HDS catalysts. It was nice working with you. Thanks again and good luck in India. Don't be afraid: Hans won't shoot you!

Dan natuurlijk ook dank aan de Opper zwavelnees San de B. en zijn lakeien Emile H. (Oost West, Zuid best!) en Marcel V. (de meubelmaker). Zonder jullie hulp en apparatuur was mijn proefschrift onmogelijk geworden. Ook jullie werk/proefschriften hebben mij zeer geholpen. Het is soms wel eenzaam om de enige nog te zijn die stinkt!

Ook veel dank aan de handige mensen in de groep: Tiny, Joop, Wout en Peter (hoewel handig?). Ik dacht altijd dat ik maar één linker hand had, maar door jullie weet ik beter. Tiny bedankt voor alle herstelwerkzaamheden (succes met de glovebox!), het zal wel

rustig zijn zonder jou luide kritiek! Joop, erg bedankt voor de hulp bij het verhuizen van de zwavelapparatuur naar ‘jouw’ lab. Ik heb toch maar mooi twee opstellingen (professorisch) in één zuurkast gekregen en dat beetje H_2S wat de lucht ingaat, ach……. Ik hoop dat je dankzij mij je Nederlands weer een beetje hebt kunnen oefenen. Wout het was fijn om bij jou even te mogen slaan. Je weet waar de rekening van de ferrules naar toe moeten. En dan Peter, tsja, wat moet ik daarop zeggen: Vielen dank für alles! Het introduceren van XPS, spincoaten, het fitten en het eindeloos ophouden van werkbesprekingen etc. Ik ben toch altijd blij geweest dat ik niet op jou kamer zat (sorry Tiny!). Success met je ultimatieve experimenten en het STW voorstel.

Ik vond het erg prettig om andere technieken dan XPS te verkennen, daarvoor mijn dank aan Barabara Mojet (Raman), Patricia Kooyman (TEM), Arie Knoester en Hidde Brongersma (LEIS), Ton Kuiper (TEM wafers) en Joachim Loos en later D. Daan voor de AFM metingen. Niet alles is nog gelukt maar volgens mij komt dat nog wel! Voor de ‘kinetiek’ berekeningen wil ik nog bedanken Jaap Schouten en Mart de Croon.

Ik overwon niet alleen door te promoveren maar ook door de Ir. titel te behalen. Hiervoor wil ik vooral Jan Meuldijk bedanken die dit toch allemaal in goede banen heeft geleid.

Ik heb echter niet alleen maar gewerkt! Daarom wil ik mijn naaste collega’s bedanken voor de verschillende ontspannende zaken. Vooral de scheldkannonades van mijn kamergenoot Marco van H. zijn onvergetelijk en ook de (soms sporadische) aanwezigheid van Wouter van G. werd geapprecieerd. Binnenkort mag je Jimmy en de Sirtaki zo hard draaien als je wil! Tiny (de Master of D****), Peter, Ralf, Sander, Eero, Daniël, Armando, de researchstagiaires (in bijzonder Waldo Beek, Peppie en Kokki) en afstudeerders in onze groep (in bijzonder Marc Jacobs) bedankt voor de hartenjaag sessies, dagelijks geleuter, FORT bezoekjes, AOR bezoekjes, zuipavondjes etc. Dat had ik zeker nodig! Hierbij moet ik natuurlijk ook de (ex)-metaalmannen Pieter, Frank en Darek voor hun bijdrage aan de hartenjaag sessies, ondanks jullie chronische gebuk (maar dat zal wel metaalmoeheid zijn).

Ook de overige collega’s van de vakgroep wil ik bedanken voor de koffie-sessies, vrijdagmiddag borrel, FORT, AOR, congresbezoekjes. Dit wil niet zeggen dat alle collega’s hiervoor in aanmerking komen. Zeker de laaste jaren werd het aantal mensen dat aanwezig was bij de koffie en meeging naar het FORT of de AOR steeds kleiner. Een slechte ontwikkeling!! Dus dank aan de trouwe mensen! De toekomst ziet er echter wat rooskleuriger uit door de komst van de Vogt groep en zijn jonge honden. Ook de ‘oude’ en ‘nieuwe’ secretaresses bedankt voor hun hulp als het nodig was.

Nu een stapje naar boven de rivieren. Dank aan Emile en Mark voor alle niet aan werk gerelateerde zaken. Misschien dat ik de achterstand op jullie snel inloop (auto, mobieltje, ‘echte’ baan). Emile, als je net zoveel tijd in je huis had gestoken als in vrouwen dan was het al af geweest. Mark, alhoewel ik me een tijdje zorgen heb gemaakt om je in de tijd dat je als brabantse vrijgezelle jongen zonder vaste woonplaats rondzwierf in de grote stad, ben ik toch blij dat je nu je schaap(jes) op het droge hebt. Erik en Tommy worden natuurlijk ook bedankt voor de gezelligheid maar verdienen een extra vermelding voor hun (bijna) tevergeefse inspanning om mijn heerschappij op de squash-baan te doen omverwerpen. Heeze zegt jullie allebei wel wat. De ‘homies’ uit Zuid-Oost Mr. J. Wind en Berry mogen niet missen natuurlijk. Na al die jaren en totaal verschillende carrieres (en woonplaatsen) nog steeds regelmatig contact. Houen zo! Dat plan met die pillen en poeders staat nog steeds wat mij betreft!

In tegenstelling tot de meeste andere proefschriften bedank ik mijn familie als laatste en terecht vind ik! Dat wil niet zeggen dat ik geen dank verschuldigd ben aan Minne. Al die jaren met mij kunnen uithouden, da's knap, blijven volhouden. Danzij jou heb ik de leegte die ontstond tijdens het afronden van mijn proefschrift kunnen vullen met klussen. Ik denk dat ik al één linker hand kwijt ben. Het wordt nu tijd om te genieten van 'ons' huis! Voor mij zit het er op, nu jij nog…

Dan volgt nu het geslacht Coulier: mijn vader en moeder wil ik erg bedanken voor mijn opvoeding, alle (financiele) steun, de hulp bij verhuizingen en de weekendjes Deventer. Hierdoor hebben jullie de eerste Dr. in de familie voortgebracht! En de afspraak wat betreft dat huisje op Aruba staat nog steeds. Ook de overige familie (zus, Wim, opa, oma) wil ik bedanken voor alles. Vivian en Wim, aan jullie de taak om de tweede Dr. voort te brengen?
Nou Opa, ik hoop dat ik de naam Coulier een beetje hoog heb kunnen houden, meer kan ik niet doen want Prof. zal ik nooit worden!

De universitaire/wetenschappelijke wereld zeg ik vaarwel. Ik heb erg veel geleerd in die vier jaar. Ik wil dit in een paar woorden omschrijven: jaknikkers (zie voorkant), hielenlikkers, handen…..(censuur), vriendjespolitiek, beter een verre vriend dan een goede buur, goh weer diezelfde man met hetzelfde praatje, bio-inspired, nano, combinatorial, brak, meuk en alle Limburgers heten Sjeng!

Maar verder was het wel leuk!

Curriculum Vitae

Ik werd geboren op 10 juli 1974 in Deventer. Het VWO diploma werd behaald aan het Alexander Hegius Scholengemeenschap te Deventer in 1992. Daarna werd begonnen met de studie Scheikunde aan de Universiteit van Utrecht. Naast twee bijvakken, met als onderwerpen halfgeleiderchemie en katalyse, werd het afstudeeronderzoek in de vakgroep Heterogene Katalyse, werkgroep Oppervlakte onderzoek gedaan. Onder begeleiding van Dr. E. Voogt, Dr. O.L.J. Gijzeman en Prof. Ir. J.W. Geus werd de adsorptie en oxidatie van CO op Pd/SiO_2 model katalysatoren bestudeerd met behulp van ellipsometrie. Het doctoraal examen werd afgelegd (met genoegen) in augustus 1997.

Aansluitend werd begonnen met het promotieonderzoek aan de Technische Universiteit in Eindhoven in de vakgroep Anorganische Chemie en Katalyse onder begeleiding van Prof. Dr. J.W. Niemantsverdriet en Prof. Dr. J.A.R. van Veen. Tegelijkertijd werd begonnen met de studie Chemische Technologie aan de Technische Universiteit in Eindhoven. Het doctoraal examen werd in december 2000 afgelegd. In oktober 2001 werd het in dit proefschrift beschreven onderzoek afgerond.